frontiers in

NANOCATALYSIS SCIENCE

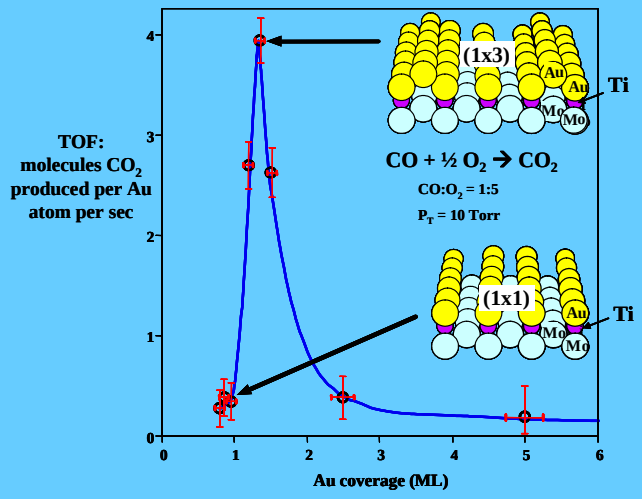

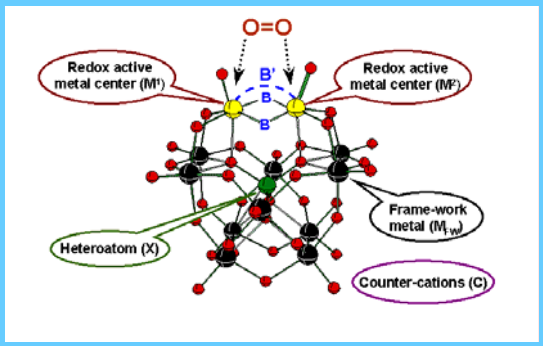

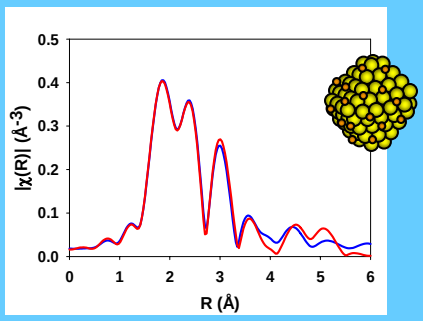

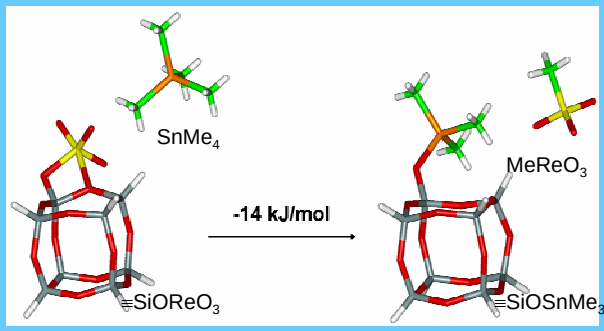

Meeting of the **Catalysis and Chemical Transformations Program**

Chemical Sciences, Geosciences and Biosciences Division

Office of Basic Energy Sciences, U.S. Department of Energy

Rockville, MD ____ **May 18-21, 2005**

frontiers in

NANOCATALYSIS SCIENCE

***Meeting of the* Catalysis and Chemical Transformations Program**

Chemical Sciences, Geosciences and Biosciences Division
Office of Basic Energy Sciences, U.S. Department of Energy

Rockville, MD –— May 18-21, 2005

Cover figures (clockwise): see abstracts for (i) D.W. Goodman et al., (ii) D. Musaev, et al., (iii) S. Scott et al., (iv) J. Yang, et al. Background: see M.G. White et al.

This document describes activities performed under contract number DE-AC05-00OR22750 between the U.S. Department of Energy and Oak Ridge Associated Universities.

FOREWORD

This meeting of the Catalysis and Chemical Transformations Program is sponsored by the Division of Chemical Sciences, Geosciences and Biosciences, Office of Basic Energy Sciences (OBES), U.S. Department of Energy. It is being held on May 18-21, 2005, at the Doubletree Hotel, Rockville, MD. The purposes of this meeting are to discuss the recent advances in nano science and catalysis science; to foster exchange of ideas and cooperation among participants; and to discuss the new opportunities for catalysis and chemical transformations at the interfaces with other disciplines, including materials science, biosciences, theory, modeling and simulation, and advanced instrumentation.

Catalysis activities within OBES emphasize fundamental research aimed at understanding and controlling the chemical reactivity of fluid and condensed matter. The long-term goal of this research is to discover the fundamental principles and develop the techniques to predict structure-reactivity relations. Such knowledge, integrated with advances in nanostructure synthesis, will help us to control chemical reactions along desired pathways. Ultimately, this new knowledge will result in chemical and materials processes to efficiently convert fossil and renewable resources, or to generate, convert and store energy, with minimum impact to our environment.

Special thanks go to our invited speakers, who will expose us to recent advances in their fields, and to the program investigators and their students, postdocs, and collaborators, for their dedication to the continuous success and visibility of the OBES Catalysis and Chemical Transformations Program. We also thank the Oak Ridge Institute of Science and Education staff, Ms. Sophia Kitts, Ms. Rachel Smith and Ms. Kellye Sliger, for the logistical support and the compilation of this volume. We are also indebted to the session moderators for accepting to help on such a short notice.

John Gordon and Raul Miranda
Chemical Sciences, Geosciences and Biosciences Division
Office of Basic Energy Sciences
U.S. Department of Energy

NANOCATALYSIS MEETING OVERVIEW
Catalysis and Chemical Transformations Contractors' Meeting
May 18 – 21, 2005 Doubletree Hotel, Rockville, MD

Time	Wednesday, May 18	Thursday, May 19	Friday, May 20	Saturday, May 21
7 a.m.		**Continental breakfast** *Plaza 1*	**Continental breakfast** *Plaza 1*	**Continental breakfast** *Plaza 1*
8 a.m.		**Workshop overview**		
8:30 a.m.		**Session A:** **Building blocks, ligand design and functionalization** *Plaza 2-3*	**Session C:** **Surfaces and interfaces under reaction** *Plaza 2-3*	**Session F:** **Principles of rational design of nanocatalysts** *Plaza 2 -3*
9 a.m.				
10 a.m.				
11 a.m.				**Discussion: grand challenges in nanocatalysis science**
noon		**Discussion** *Plaza 2-3*	**Discussion** *Plaza 2-3*	**Box lunch** *Discussion continues* *Plaza 2-3*
12:30		**Lunch buffet** *Plaza 1*	**Lunch buffet** *Plaza 1*	
1 p.m.				**Meeting adjourns at 1:00 p.m.**
2 p.m.		**Session B:** **Clusters, supramolecules and biomolecules—free and confined in pores and on surfaces** *Plaza 2-3*	**Session D:** **Oxide Structures and oxide-oxide superstructures under reaction** *Plaza 2-3*	
3 p.m.				
4 p.m.				
5 p.m.				
5:30 p.m.	**Registration** *Regency Foyer* **Poster set-up** *Regency and Randolph* **Dinner buffet** *Plaza 1*	**Discussion** *Plaza 2-3*	**Discussion** *Plaza 2-3*	
6 p.m.		**Dinner buffet** *Plaza 1*	**Dinner buffet** *Executive Dining Room*	
7 p.m.			**Session E:** **Nanocatalysis and advanced instrumentation — university, national lab, industry cooperation** *Executive Dining Room*	
7:30	**Poster session** *Regency and Randolph*	**Poster session** *Regency and Randolph*		
8 p.m.				
9 p.m.				
10 p.m.				

NANOCATALYSIS SCIENCE

Catalysis and Chemical Transformations Contractors' Meeting
May 18-21, 2005 – Doubletree Hotel, Rockville, MD

AGENDA

Poster presentations – Regency Room and Randolph Room
Oral presentations – Plaza Ballroom

Wednesday, May 18		
5:00 p.m.	Regency Room - Registration, poster set-up	
5:30 – 8:00 p.m.	Plaza Ballroom – Informal reception, cash bar, no-host dinner	
7:30-10.00 p.m.	Poster Session - All posters - (Continues on Thursday)	

Thursday, May 19		
7:30 a.m.	Coffee	
8.00 a.m.	Plaza Ballroom - Workshop Overview	
Session A: Building blocks, ligand design and functionalization Moderator: **John Gordon**		
8:30-9:20	Invited Speaker – **Seth Brown**	*Electronic Symmetry and Dissymetry in Catalyst Design*
9:20-9:30	Break	
9:30-12:00	**Craig Hill**	*Principles of Selective O2-Based Oxidation by Optimal (Binuclear) Catalytic Sites*
	Jeffrey Long	*Cluster-Expanded Solids: A Strategy for Assembling Functional Porous Materials*
	Marek Pruski/Victor Lin	*Selective and Efficient Catalysis in 3-D Controlled Environments*
	Christopher Jones	*Basic Principles that Govern the Interaction of Organometallic Catalysts with Supports - The Science of Immobilized Molecular Catalysts*
	Colin Nuckolls	*Synthesis, Directed Assembly, and Local Probe Measurements of Dipolar, Organic Nanostructures*
	Susannah Scott	*Design of heterogeneous catalysts for the low temperature metathesis of unfunctionalized and functionalized olefins*
12:00-12:20	Discussion	
12:30-1:30 p.m.	Lunch – Plaza 1	
Session B: Clusters, supramolecules and biomolecules—free and confined in pores and on surfaces Moderator: **Richard Finke**		
2:00-2:50 p.m.	Invited Speaker – **Matt Francis**	*Synthetically Modified Viral Capsids: Building Blocks for Nanoscale Materials*
2:50-3:00 p.m.	Break	
3:00-5:30 p.m.	**Bruce Gates**	*The Role of Cations in Supported Metal Nanocluster Catalysts*
	Mekki Bayachou	*Electron transfer, Oxygen Activation, and NO Biosynthesis: An Integrative Electrochemical, Biochemical, and Computational Approach*
	John Shelnutt	*Growth of Metal and Semiconductor Nanostructures Using Localized Photocatalysts*

	James Haw	*Supported Molecular Catalysts: Synthesis, In-Situ Characterization and Performance*
	Steven Overbury	*Nanocatalysts: Synthesis, Properties, and Mechanisms*
	Daniel Resasco	*Controlling Structural Characteristics of Single-Walled Carbon Nanotubes (SWNT) by Tailoring Catalyst Composition and Synthesis Conditions*
5:30-5:50 p.m.	Discussion	
6:00-7:30 p.m.	Dinner – Plaza 1	
7:30-10:00 p.m.	Poster Session - All posters - (Ends on Friday)	

Friday, May 20 **Note:** Posters must be removed before 4 p.m.

Session C: Surfaces and interfaces under reaction
Moderator: **Andrew Gellman**

8:00-8:30 a.m.	Coffee	
8:30-9:20 a.m.	Invited Speaker – **William Schneider**	*Environmental Catalysis at the Interface of Metals and Metal Oxides*
9:20-9:30 a.m.	Break	
9:30-12:00	**C. Buddie Mullins**	*The Surface Chemistry of Size-Controlled Oxide-Supported Ir Nanoclusters*
	Michael G. White	*Catalysis on the Nanoscale: Preparation, Characterization and Reactivity of Metal-Based Nanostructures*
	Tony Heinz	*Controlling Structural, Electronic and Energy Flow Dynamics of Catalytic Processes through Tailored Nanostructures*
	Gary Haller	*Nanopore Radius Of Curvature Effect On Catalysis And Catalytic Particle Formation*
	Gabor Somorjai	*Nanoscience and Nanoparticles for 100% Selective Catalytic Reactions*
	Francisco Zaera	*Molecular Level Design of Chiral Heterogeneous Catalysts*
12:00-12:20	Discussion	
12:30-1:30 p.m.	Lunch	

Session D: Oxide structures and oxide-oxide superstructures under reaction
Moderator: **Mark Barteau**

2:00-2:50 p.m.	Invited Speaker – **Ulrike Diebold**	*Surface Science Investigations of Titanium Dioxide: Relevant for Photocatalysis?*
2:50-3:00 p.m.	Break	
3:00-5:30 p.m.	**Charles Peden**	*Early Transition Metal Oxides as Catalysts: Crossing Scales from Clusters to Single Crystals to Functioning Materials*
	Michael Henderson	*Controlling the Thermal and Non-Thermal Reactivities of Metal Oxide Structures Through Nanoscaling*
	Raul Lobo	*Photocatalytic Activity of Microporous Titanium-Silicate ETS-10*
	Robert Davis	*Structure and Function of Supported Base Catalysts*
	Jeffrey Brinker	*Novel Transport Behaviors of Porous and Composite Nanostructures*
	Steven Suib	*Microporous and Mesoporous Nanosized Transition Metal Oxides: Preparation, Characterization and Applications*

5:30-5:50 p.m.	Discussion	
6:00-7:00 p.m.	Dinner – Plaza 1	

Session E: Nanocatalysis and advanced instrumentation — University, National Lab, Industry cooperation
Moderator: **John Gordon**

7:00-8:00 p.m.	**Judith Yang**	*Synthesis, Charge Transfer, Three-Dimensional Structural Characterization, and ab initio Simulations of Ligand-Stabilized and Supported Metal Nanoparticles*
	Simon Bare	*X-Ray Facilities – Successful Collaborations*

Saturday, May 21

Session F: Principles of rational design of nanocatalysts
Moderator: **Francisco Zaera**

8:00-8:30 a.m.	Coffee	
8:30-11:00 a.m.	**Nicholas Delgass**	*Catalyst Design by Discovery Informatics*
	D. Wayne Goodman	*Toward an Understanding of Catalysis by Supported Metal Nanoclusters*
	Mark Barteau	*From First Principles Design to Realization of Bimetallic Catalysts for Enhanced Selectivity*
	Jingguang Chen	*Structure-Property Relationship in Metal Carbides and Bimetallic Alloys*
	James Dumesic	*Fundamental Studies of the Reforming of Oxygenated Compounds over Supported Metal Catalysts*
	Peter Stair	*Nanostructured Membrane Catalysis*

11:00-1:00 p.m. **Discussion: Grand Challenges in Nanocatalysis Science-**
Topics:
A: Rational design of building blocks, ligands, pores, and reactive interfaces
B: Nanostructure synthesis and functionalization—synthesis characterization
C: Mechanisms and *operando* characterization of reactions catalyzed by nanostructures
D: Biomimetics—local bonding, secondary and long-range interactions—confinement—structural dynamics
E: Research infrastructure—facilities for rapid synthesis, *in-situ* characterization, chemical and structural imaging, and for theory, simulation and informatics.
F: Emerging opportunities for energy- and materials-synthesis related catalysis, photocatalysis and electrocatalysis
G: Summary of grand challenges in nanocatalysis science

12:00 p.m.	Working Lunch – Discussion continues
1:00 pm.	Meeting Adjourn

POSTER PRESENTATIONS
Session: Wednesday and Thursday, 7:30-10:00 pm

J.W. Ager III	*In Situ UV-Raman and FTIR Spectroscopies: Studies of 3-D nanostructured catalysts*
Craig Barnes	*Nanostructured Metal Oxide Catalysts via Building Block Syntheses*
Mekki Bayachou	2 posters: *Electrocatalytic Microsensors for Separate Monitoring of Nitric Oxide and Peroxynitrite on NOS-modified Electrodes*
J.M. Caruthers	*Development of a Computer-Aided Discovery Environment for Catalysis Design*
Richard Crooks	*From First Principles Design to Realization of Bimetallic Catalysts for Ultrahigh Selectivity*
Larry Curtiss	*Quantum Chemical Study of Mechanisms for Oxidative Dehydrogenation of Propane on Vanadium Oxide*
Sheng Dai	*Synthesis of Au catalysts on Nanostructured Supports*
W.N. Delgass	*Catalyst Design by Discovery Informatics*
Ulrike Diebold	*The influence of oxygen composition on the surface functionality of SnO2(101)*
Michel Dupuis	*Charge Transport in Metal Oxides: Theoretical Studies*
Dave Dixon	*Computational Catalysis: Transition Metal Oxide Clusters*
Zdenek Dohnálek	*Supported Transition Metal Oxides: Chemical Physics Aspects of Their Growth and Reactivity*
Richard Finke	*Nanocluster Catalysts Formation and Stabilization Fundamental Studies*
Heinz Frei	*Catalyst Characterization through Time-Resolved FT-IR Monitoring under Reaction Conditions*
Anatoly Frenkel	*EXAFS and XANES studies of 3D structure and metal-ligand charge transfer of ligand-stabilized and supported metal nanoparticles*
Andrew J. Gellman	Templated Chiral Surfaces for Enantioselective Adsorption
Valentin Gogonea	*Electrostatic coupling Hamiltonian for hybrid quantum mechanical molecular mechanics calculations*
D. Wayne Goodman	*Structure-function relationships in Pd-Au catalysts*

Maciek Gutowski	*Computational Catalysis: Density Functional Study of WO_3(001)*
James F. Haw	*NMR and Computational Studies of Solid Acidity*
Michael Henderson	*Photocatalysis on a Model TiO2 surface: Acetone on Rutile TiO2(110)*
Enrique Iglesia	*Early Transition Metal Oxides as Catalysts: 'Single-site' Synthesis, Atomic Connectivity, and Reaction Mechanisms*
Ping Liu	*Density Functional Studies of Metcar Nanoparticles as Hydrodesulfurization Catalysts*
Peter Ludovice	*Molecular Modeling of Inorganic and Polymer Supports for Molecular Catalysts*
Andrew Maverick	*Guest Exchange in a Nanoporous Fe-Ag System*
Andrew Maverick	*Inorganic-Organic Molecules and Solids with Nanometer-Sized Pores*
Manos Mavrikakis	Alloy Catalysts Designed from First-Principles
James Muckerman	*First-Principles Study of Ti-Catalyzed Hydrogen Chemisorption on an Al Surface: A Critical First Step for Reversible Hydrogen Storage in NaAlH4*
David Mullins	*Surface Chemistry Related to Heterogeneous Catalysis*
Ralph Nuzzo	*Probing the Effects of Surface Oxygen on Al2O3-Supported Platinum Nanoparticles*
Talat Rahman	*On factors influencing diffusion and reaction of molecules on nanostructured surfaces*
John J. Rehr	Towards an Understanding of the Re/alumina Catalysts: Theory, Simulations, and X-ray Spectroscopy Experiment
José A. Rodriguez	*In situ Time-resolved Characterization of Cu-CeO_2 Nanocatalysts during the Water Gas Shift Reaction*
David Sherrill	*Theoretical Investigations in Transition-Metal Catalysis*
Lawrence Sita	*Ferrocene-Based Nanoelectronics*
Larry Sneddon	*New Chemical Routes to Nanostructured Advanced Ceramic Materials via Metal Catalyzed Syntheses and Polymerization Reactions of Alkenylpolyboranes*
Peter Stair	*Atomic Level Control of Nanostructured Membranes for Catalysis*
Steven Suib	*Magnetic Route to Measure the Average Oxidation State of Mixed-Valent Manganese in Manganese Oxide Octahedral Molecular Sieves (OMS)*

Table of Contents

Session C: Surfaces and Interfaces under Reaction

Session D: Oxide Structures and Oxide-Oxide Superstructures under Reaction

Session E: Nanocatalysis and Advanced Instrumentation — University, National Lab, Industry Cooperation

Session F: Principles of Rational Design of Nanocatalysts

Poster Presentations

Session A:

Building Blocks, Ligand Design and Functionalization

Electronic Symmetry and Dissymmetry in Catalyst Design

Seth Brown
Department of Chemistry and Biochemistry
University of Notre Dame
Notre Dame, IN 46556

Our recent efforts to design water-stable titanium(IV) complexes for use as "green" catalysts have led us to make several observations about electronic effects in catalysis. The first observation is that tuning the relative donor strengths of the ligands *trans* to the substrate can have dramatic and predictable effects on reactions involving two-point substrate binding. This has been analyzed quantitatively in proton-coupled ligand substitution reactions. The second observation is that dissymmetry in bonding alone, without steric effects or other nonbonding interactions, can be a useful source of chiral induction. This novel use of electronic dissymmetry has been demonstrated in chiral recognition, and prospects for applying it in catalysis will be discussed.

DE-FG02-03ER15461 **C.L. Hill**

CATALYSIS SCIENCE INITIATIVE: Principles of Selective O_2-Based Oxidation by Optimal (Binuclear) Catalytic Sites

PIs: Djamaladdin G. Musaev, Craig L. Hill, Keiji Morokuma
Postdocs Yurii Geletti, Bogdan Botar, Travis Anderson, Nelya Okun, Yan Wang
Students: Zhen Luo, Alexander D. Hillesheim, Lyuba A. Khavrutskii, Jongwoo Han, and Xikui Fang
Collaborators: J. Poblet, and A. Müller

Affiliations: Emory University, Department of Chemistry
dmusaev@emory.edu, chill@emory.edu, morokuma@emory.edu
phone: 404-727-2382, 404-727-6611, 404-727-2180

Goals:

The goal of this project is to develop combined experimental and theoretical approach to enable molecular-level understanding of the mechanisms of selective (non-radical), reductant-free, O_2-based oxidation of organic substrates catalyzed by polyoxometalates (POMs) with di-metal active sites, virtually the only synthetic compounds capable of this chemistry. The objectives of this integrated effort has entailed clarification of the structural, solution and catalytic properties of one of the few purported catalysts for selective O_2-based oxidations of organic substrates, the polyoxometalate (POM) of formula γ-$M^1M^2(OH)_2X(M_{FW})_{10}O_{38}^{n-}$, where M_{FW} = Mo and W; M^1 and M^2 = Fe, Ru, Mn, Cu, Co, Mo and W, and X = B, P, Si, Al, Co and Zn.

DOE Interest:

The proposed research addresses the selective (non-radical) oxidation of organic substrates by O_2 catalyzed by bimetal centers. The design and realization of catalysts capable of such transformations remains a monumental challenge and has occupied some of the most capable investigators for years. This application addresses key issues in depth on metal oxide cluster anions (polyoxometalates or "POMs") substituted with two adjacent d-electron-containing redox-active metals not only for their practical and scientific relevance, but also because they provide a foundation for developing and exploring broadly applicable principles for designing synthetic catalysts and understanding the biological processes (such as those catalyzed by MMO and RNR).

Research Plan:

This grant targets a deeper understanding of the structural, electronic and dynamic factors underlying the design of catalysts for selective reductant-free O_2 oxidations. It aims to establish the factors that control reactivity of the catalysis of selective (non-radical) oxidation of organic substrates by O_2 (or air) without the requirement of other agents including a sacrificial reductant.

To address the high expectations and goals of this program we proposed a highly integrated experimental and computational approach. The actual composite experimental-theoretical approach is illustrated in Figure 1 using gamma-$(M^1M^2OH_2)_2X(M_{FW})_{10}O_{38}^{n-}$ (M^1M^2**1**) as the POM. The other two prototype POMs capable of such catalysis, Ru_2**2** and Fe_3**3**/CNP are amenable to the same experimental alterations and computational approaches as (M^1M^2**1**). Thus for simplicity, this proposal focuses on M^1M^2**1** with the understanding that protocols applicable to this POM are are also very likely applicable to the others. We proposed to systematically alter many key structural components of M^1M^2**1**, while all the other structural components are kept

constant. For each POM, the most simultaneously insightful experimental and theoretical parameters will be determined.

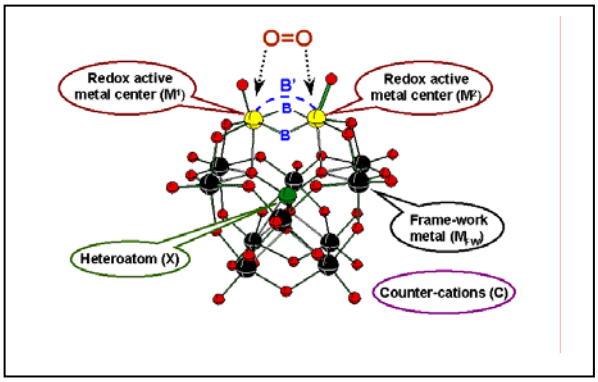

Figure 1. Graphical overview of the central integrated experimental-computational thrust of the program as exemplified by one of the 3 multi-component POM catalysts, gamma-$(M^1M^2OH_2)_2(H_2O)XW_{10}O_{38}^{6-}$ (**1**). All the following key parameters impacting reactivity can and will be altered and the consequences will be addressed experimentally and computationally. Parameters**:** $\mathbf{M^1}$ and $\mathbf{M^2}$ = Fe, Mn, Cu, Co, Ru, Cr, etc.; **B** = O, OH; **B'** = acetate, etc.; $\mathbf{M_{FW}}$ = W and/or Mo; **X** = P, Si, Al, Zn, B, Co, etc.; **C** = Li^+, Na^+, K^+, R_4N^+, biological cations, chiral cations, etc.

The single biggest determinant of reactivity will likely be the d-electron-containing metals M^1 and M^2. The identity of both the in-plane (oxo or hydroxo) and/or other ligands bridging M^1 and M^2 (B and B', respectively) will be dictated to some extent by the identity of M^1 and M^2. At the same time, these ligands can also be altered systematically because the four bonds to M^1 and M^2 from the gamma-Keggin POM unit are chelating and fairly robust. The main "framework" metals of the POM (M_{FW}) can likely be varied, too. Finally, heteroatoms X and the counterions C can certainly be altered.

In addition to these compositional parameters the redox potentials and characteristic reactivity of each POM will be determined. The catalytic activity of the POMs for oxygenation of the important model substrates cyclohexene, cyclohexane, tetrahydrothiophene and/or *p*-chlorophenol will be rapidly assessed. Key steps and reactions we propose to study are: binding of dioxygen to the ($M^1_{red}M^2_{red}$) subunit; reactions of the resultant oxygen adduct, $(M^1M^2)(O_2)$, with select substrates; O-O bond cleavage to form the reactive intermediates $(M^1M^2)(O)_2$; and reactions of these species with select substrates.

We plan to establish the detailed mechanisms of these processes not only because this information will be of considerable fundamental value and insight in its own right, but also to provide the reliable information needed to interpret the results from the sophisticated computational assessments of the these mechanisms we propose to carry out in parallel with the experimental work.

Although we will mainly use the density functional and hybrid ONIOM methods in these studies, we also plan to develop a new hybrid ONIOM approach containing the promising self-consistent Charge-Density functional tight binding (SCC-DFTB, or SDFTB for simplicity) method as a low-level method. This method has been shown to be 2-3 orders of magnitude faster than hybrid DFT and provides better agreement with experiment than the full DFT method. However, it has never been applied to transition metal complexes. In order to apply this promising method to the targeted POMs in the current proposal, we plan to develop the DFTB parameters for the Mo, W, Fe, Ru, Mn, Cu, Co, Ni, and Zn atoms, which are essential for our studies.

Recent Progress:

Comprehensive studies of olefin epoxidation in organic solvents by O_2 catalyzed by [γ-$SiFe_2W_{10}O_{38}(H_2O)_2]^{6-}$ (**1**) (the system recently reported by Mizuno et al) showed that this

catalytic epoxidation chemistry proceeds predominantly *via* the radical-chain autoxidation. The intact POM is only minimally involved. As a consequence, the focus of our research was shifted to aqueous solutions.

Attempts to grow crystals of $[\gamma\text{-}SiFe_2W_{10}O_{38}(H_2O)_2]^{6-}$ (**1**) from aqueous solutions resulted in isolation of several new multi-iron-containing POMs, which are possible by-products or intermediates in the synthesis of **1** itself. For example, a new iron(III) tungstosilicate derivative, $K_7[(CH_3)_2(NH_2)]_8[(\gamma\text{-}SiW_{10}O_{36})_3Fe_6(OH)_9(H_2O)_6]\cdot 31H_2O$ (**2**) was isolated and comprehensively characterized. Polyanion **2** can be viewed as trigonal (trilobal) arrangement of three $\{\gamma\text{-}SiW_{10}\}$ polyanion units connected by an electrophilic $[Fe_6(OH)_9(H_2O)_6]^{9+}$ central core. In contrast to **1**, the iron atoms of the Fe_2 centers are no longer bonded to the oxygens of the internal heteroatom (Si in this case). The presence of this "out-of-pocket" $\{SiW_{10}M_2\}$ structural motif has only been observed in a dichromium(III) γ-derivative. The trimeric like complex, **1**, isomerizes to different di-iron-containing POMs depending on the experimental conditions. For example, a new $[\beta(3,12)\text{-}SiFe_2W_{10}O_{36}(OH)_2(H_2O)Cl]^{5-}$ (**3**) Keggin POM has been synthesized and thoroughly characterized (the numbers 3 and 12 indicate the positions of Fe-centers according to IUPAC numbering scheme). This POM appears to be the first metal substituted β-Keggin anion that is disorder-free in the solid state.

The catalytic activity in aerobic epoxidation (organic solutions) and in 2-mercaptoethanol oxidation (aqueous solutions) of all synthesized compounds was investigated. None of the compounds noted above were active in epoxidation and only **2** was active in thiol oxidation. The reaction kinetics of 2-mercaptoethanol oxidation were studied and revealed, among other noteworthy features, that the catalytically active species forms during the isomerization of **2**.

The computational effort has lead to validation of DFT and proposed geometrical models for the $\gamma\text{-}M_2$-substituted and the unprotonated lacunary POMs. The proposed "full" and "medium" models of $\gamma\text{-}M_2$-substituted POMs and the DFT method were applied to the Fe, Ru, Tc, Mo and Rh derivatives, $[(SiO_4)M_2(OH)_2W_{10}O_{32}]^{4-}$, as well as to $[(XO_4)Ru_2(OH)_2W_{10}O_{32}]^{4-}$, where X = Al, Si, P and S. For these POMs, except M = Mo, the "closed" isomer is energetically more favorable than "open" one. The M-M interaction is strong only for M = Mo and Ru. The computational data clearly show that nature of the heteroatom X in the di-Ru substituted $\tilde{\gamma}$Keggin POMs, $[(X^{n+}O_4)Ru_2(OH)_2(M_{FW})_{10}O_{32}]^{(8-n)-}$, for $X = Al^{III}$ (**4**), Si^{IV} (**5**), P^{V} (**6**) and S^{VI} (**7**), where M_{FW} = Mo and W, is crucial in defining the lower-lying electronic states of the system, which, in its turn, likely impact reactivity significantly. For the electropositive $X = Al^{III}$ (**4**), the ground state is $^1A_1$, while for the more electronegative $X = S^{VI}$ (**7**) the ground state is the high-spin $^7B_1$ state. Thus, the heteroatom X can be "internal switch" for defining the ground electronic states and, consequently, the reactivity of the $\gamma\text{-}M_2$-Keggin POMs. Interestingly, in M_{FW} = Mo-systems, the dependence of the energy gap between the high-spin and low-spin states from the nature of X is less pronounced than in M_{FW} = W-systems. For purposes of experimental verification the computationally predicted $\tilde{\gamma}[(SiO_4)Ru_2(OH)_2(OH_2)_2W_{10}O_{32}]^{4-}$ has been prepared and characterized.

The Computational investigations of the structure of "$\gamma\text{-}[(SiO_4)W_{10}O_{32}H_4]^{4-}$" indicates it is "$\gamma\text{-}[(SiO_4)W_{10}O_{28}(OH)_4]^{4-}$" (four terminal hydroxo ligands) and not "$\gamma\text{-}[(SiO_4)W_{10}O_{30}(H_2O)_2]^{4-}$" (with two terminal aqua ligands) as proposed previously. The asymmetry in the observed *and* calculated W-OH bonds derives from $O^1H^{1\cdots}O^2H^2$ and $O^4H^{4\cdots}O^3H^3$ hydrogen bonds.

Publications

1. Musaev, D. G.; Geletti, Yu. V.; Hill, C. L.; Morokuma, K. "*Computational Modeling of Di-Transition-Metal-Substituted γ-Keggin Polyoxometalate Anions. Structural Refinement of the Protonated Divacant Lacunary Silicodecatungstate" Inorg. Chem* **2004**, 43, 7702-7708

2. Quinonero, D.; Morokuma, K.; Khavrutskii, L. A.; Botar, B.; Geletti, Yu. V.; Hill, C. L.; Musaev, D. G. "*The role of the central atom in structure and reactivity of polyoxometalates with adjacent d-electron metal sites. Computational and experimental study of γ-*$[(X^{n+}O_4)Ru_2(OH)_2W_{10}O_{32}]^{(8-n)-}$*, X =* Al^{III}*,* Si^{IV}*,* P^{V} *and* S^{VI}*." J. Am. Chem. Soc.,* **2005**, submitted.

3. Quinonero, D.; Morokuma, K.; Hill, C. L.; Musaev, D. G. " A Density Functional Study of Geometry and Electronic Structure of *γ-*$[(SiO_4)M_2(OH)_2W_{10}O_{32}]^{4-}$*, where M = Mo, Tc, Ru and Rh." Inorg. Chem.* **2005**, will be submitted shortly.

4. Wang, Y.; Morokuma, K.; Hill, C. L.; Musaev, D. G. "*Similarities and Differences in the electronic and geometrical structures of γ-*$[(X^{n+}O_4)Ru_2(OH)_2(M_{FW})_{10}O_{32}]^{(8-n)-}$ *for* M_{FW} *= Mo and W, where X =* Al^{III}*,* Si^{IV}*,* P^{V} *and* S^{VI}*: The Theoretical Studies." Inorg. Chem.* **2005**, will be submitted shortly.

5. Botar, B.; Geletii, Yu. V.; Hill, C. L.; Musaev, D. G.; Morokuma, K.; Weinstock, I. A. "*Diiron-Substituted Polyoxometalates: Synthesis, Structure and Catalytic Activity,"* 13th International Congress on Catalysis, 11-16 July 2004, Paris, France, Book of Abstracts1, page 253.

6. Botar, B.; Geletii, Yu. V.; Kögerler, P.; Musaev, D, G.; Morokuma, K.; Weinstock, I. A.; Hill, C. L. "*Asymmetric terminal ligation on substituted sites in a single Keggin anion,*" *Dalton Trans.* **2005**, (will be submitted shortly).

Cluster-Expanded Solids: A Strategy for Assembling Functional Porous Materials

Postdoctoral Associate:	Stéphane A. Baudron
Graduate Students:	Laurance G. Beauvais, Miriam V. Bennett, Louise A. Berben, Nathan R. M. Crawford, Allan G. Hee, Eric G. Tulsky, Eric J. Welch
Undergraduate Students:	Mary Faia, Alex Fois, Shaun Wong, Chun Liang Yu
Collaborators:	P. Batail (U. Angiers), R. G. Bergman (UC Berkeley), S. E. Hayes (Washington U.), H. Park (Harvard U.)
Contact:	J. R. Long, Dept. of Chemistry, University of California, Berkeley, CA 94720-1460; phone: (510) 642-0860; e-mail: web page: alchemy.cchem.berkeley.edu

Goal

The intention of the research is to explore the use of molecular cluster precursors in the assembly of microporous coordination solids that function as sieves, sensors, or catalysts.

Recent Progress

Cyano-Bridged Frameworks Incorporating Mixed-Metal Clusters. Reactions of the face-capped octahedral clusters $[Re_5OsSe_8Cl_6]^{3-}$ and $[Re_4Os_2Se_8Cl_6]^{2-}$ with NaCN in a melt of $NaNO_3$ afford the cyano-terminated clusters $[Re_5OsSe_8(CN)_6]^{3-}$ and $[Re_4Os_2Se_8(CN)_6]^{2-}$. The former species reacts with $[Ni(H_2O)_6]^{2+}$ in aqueous solution to yield the cluster-expanded Prussian blue analogue $Ni_3[Re_5OsSe_8(CN)_6]_2 \cdot 33H_2O$. In addition, these clusters can be reduced by one electron to give the first 25-electron clusters of their type. As demonstrated with the synthesis and characterization of $\{Re_4Os_2Se_8[CNCu(Me_6tren)]_6\}^{9+}$, the reduced diosmium cluster is capable of engaging in ferromagnetic exchange interactions, indicating its potential utility in the synthesis of a microporous magnet.

Cyano-Bridged Frameworks Incorporating $[Zr_6BCl_{12}]^{2+}$ Cluster Cores. The reaction between $[Zr_6BCl_{18}]^{4-}$ and $[Cr(CN)_6]^{3-}$ in aqueous solution, leads to the immediate precipitation of the cluster-expanded Prussian blue analogue $(Et_4N)[Zr_6BCl_{12}][Cr(CN)_6] \cdot Et_4NCl \cdot 3H_2O$. The cubic Prussian blue type structure of this compound was confirmed via Rietveld profile analysis of X-ray powder diffraction data, and magnetization measurements reveal the onset of long-range magnetic ordering at 2 K.

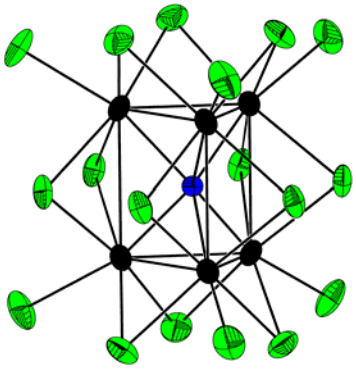

$[W_6NCl_{18}]^{2-}$

Trigonal Prismatic Cluster Building Units. Simultaneous reduction of WCl_6 and CCl_4 with bismuth metal at 450 °C, leads, upon work-up, to the carbon-centered trigonal prismatic cluster $[W_6CCl_{18}]^{2-}$. Cyclic voltammetry experiments performed on solutions containing this cluster show that it possesses five chemically-accessible redox states. Related reactions incorporating NaN_3 in place of CCl_4 led to the analogous nitrogen-centered cluster $[W_6NCl_{18}]^{2-}$, enabling access to even more reduced electron counts. Substitution of the outer chloride ligands in clusters of this type has led to species such as $[W_6CCl_{12}(CF_6SO_3)_6]^{3-}$, $[W_6CCl_{12}(CN)_6]^{3-}$, and $[W_6CCl_{12}(py)_6]^{2+}$, with significant variation in the associated electrochemical behavior.

New Metal-Chalcogen Cluster Building Units. Evaporation of binary transition metal chalcogenides and cocondensation of the vapor with PEt_3 has led to a range of new metal-chalcogen clusters. For example, evaporation of Cu_2Se enables isolation of $[Cu_{26}Se_{13}(PEt_3)_{14}]$ and $[Cu_{70}Se_{35}(PEt_3)_{21}]$, containing surface-ligated fragments of the original solid.

Prussian Blue Analogues Incorporating $[Co(CN)_5]^{3-}$. The reaction between $[Co(H_2O)_6]^{2+}$ and the square pyramidal complex $[Co(CN)_5]^{3-}$ in deoxygenated water yields the Prussian blue analogue $Co_3[Co(CN)_5]_2{\cdot}8H_2O$, containing a high concentration of lattice vacancies. Upon dehydration, the compound retains crystallinity and exhibits a Type I dinitrogen sorption isotherm, characteristic of a microporous solid. Magnetic measurements showed it to behave as a ferrimagnet with an ordering temperature of 48 K, which is reduced to 38 K in the dehydrated solid. This is the first truly microporous material shown to exhibit magnetic hysteresis.

New Cyanomolybdate Building Units. Octahedral coordination of molybdenum(III) was achieved by limiting the amount of cyanide available upon complex formation. Reaction of $Mo(CF_3SO_3)_3$ with LiCN in DMF affords $Li_3[Mo(CN)_6]{\cdot}6DMF$, featuring the previously unknown octahedral complex $[Mo(CN)_6]^{3-}$. Further restricting the available cyanide in a reaction between $Mo(CF_3SO_3)_3$ and $(Et_4N)CN$ in DMF, followed by recrystallization from DMF/MeOH, yields $(Et_4N)_5[Mo_2(CN)_{11}]{\cdot}2DMF{\cdot}2MeOH$.

New Cyanorhenate Building Units. Reaction of $(Bu_4N)CN$ with $[ReCl_6]^{2-}$ in acetonitrile affords yellow $(Bu_4N)_3[Re(CN)_7]$, featuring the pentagonal bipyramidal complex $[Re(CN)_7]^{3-}$. In aqueous solution, this compound reacts with Mn^{2+} ions to generate the porous, and potentially photomagnetic, three-dimensional solid [*fac*-$Mn(H_2O)_3$][*cis*-$Mn(H_2O)_2$][$Re(CN)_7$]$\cdot 3H_2O$. Addition of KIO_4 to the reaction solution, originally intended to prevent reduction of the rhenium during solid formation, instead yields white $(Bu_4N)_3[Re(CN)_8]$, featuring the square antiprismatic complex $[Re(CN)_8]^{3-}$.

Homoleptic Trimethylsilylacetylide Complexes. Reactions between simple transition metal salts and $LiCCSiMe_3$ have been shown to generate three new octahedral complexes: $[Cr(CCSiMe_3)_6]^{3-}$, $[Fe(CCSiMe_3)_6]^{4-}$, and $[Co(CCSiMe_3)_6]^{3-}$. Characterization of these molecules has enabled us to establish the ligand field strength of trimethylsilylacetylide as lying just below methyl in the spectrochemical series.

DOE Interest

The new microporous materials resulting from these studies may be of utility in a range of applications, including molecular sieving, detection of volatile organic compounds, ion exchange, and homogeneous catalysis.

Future Plans

Synthesis of a Microporous Magnet. Our efforts to produce molecular cluster building units capable of delivering strong magnetic coupling with surrounding metal ions will continue. The goal here is to generate solids with ordering temperatures at or above room temperature for use in performing magnetic separations (e.g., for the noncryogenic separation of dioxygen from dinitrogen). New targets of particular interest here include the clusters $[Gd_6CCl_{18}]^{9-}$, $[Re_{6-n}Mo_nQ_8(CN)_6]^{(4+n)-}$, $[M_6Q_8(CN)_6]^{n-}$ (M = Cr, Fe, Co), $[W_6CCl_{12}(CN)_6]^{3-}$, and $[B_6(CN)_6]^{1-}$. Relatedly, dioxygen-binding experiments will be carried out on porous phases incorporating $[Co(CN)_5]^{3-}$.

Homogeneous Catalysis in Cluster-Expanded Prussian Blue Type Solids. Attempts will be made to exploit the coordinatively-unsaturated metal sites within dehydrated cluster-expanded Prussian blue solids for homogeneous catalysis.

Characterization of Photomagnetic Solids. The photomagnetic properties of porous solids incorporating $[Re(CN)_7]^{3-}$ and $[Re(CN)_8]^{3-}$ will be further characterized, with the intention of developing potential sensing applications.

Synthesis of Acetylenediide-Bridged Solids. The new trimethylsilylacetylide complexes obtained recently will be used in coupling reactions intended to produce unprecedented frameworks featuring acetylendiide bridges.

Publications (2003-2005)

1. "New Cyanometalate Building Units: Synthesis and Characterization of $[Re(CN)_7]^{3-}$ and $[Re(CN)_8]^{3-}$" Bennett, M. V.; Long, J. R. *J. Am. Chem. Soc.* **2003**, *125*, 2394-2395.

2. "New Routes to Transition Metal-Carbido Species: Synthesis and Characterization of the Carbon-Centered Trigonal Prismatic Clusters $[W_6CCl_{18}]^{n-}$ (n = 1, 2, 3)" Welch, E. J.; Crawford, N. R. M.; Bergman, R. G.; Long, J. R. *J. Am. Chem. Soc.* **2003**, *125*, 11464-11465.

3. "Cluster-to-Metal Magnetic Coupling: Synthesis and Characterization of 25-Electron $[Re_{6-n}Os_nSe_8(CN)_6]^{(5-n)-}$ (n = 1, 2) Clusters and $\{Re_{6-n}Os_nSe_8[CNCu(Me_6tren)]_6\}^{9+}$ (n = 0, 1, 2) Assemblies" Tulsky, E. G.; Crawford, N. R. M.; Baudron, S. A.; Batail, P.; Long, J. R. *J. Am. Chem. Soc.* **2003**, *125*, 15543-15553.

4. "Atomlike Building Units of Adjustable Character: Solid State and Solution Routes to Manipulating Hexanuclear Transition Metal Chalcohalide Clusters" Welch, E. J.; Long, J. R. *Prog. Inorg. Chem.* **2005**, *54*, 1-45.

5. "Synthesis and Characterization of the Nitrogen-Centered Trigonal Prismatic Clusters $[W_6NCl_{18}]^{n-}$ (n = 1, 2, 3)" Welch, E. J.; Yu, C. L.; Crawford, N. R. M.; Long, J. R. *Angew. Chem., Int. Ed.* **2005**, *44*, in press.

6. "Homoleptic Trimethylsilylacetylide Complexes of Chromium(III), Iron(II), and Cobalt(III): Syntheses, Structures, and Ligand Field Parameters" Berben, L. A.; Long, J. R. *J. Am. Chem. Soc.*, submitted.

7. "Determination of ^{77}Se-^{77}Se and ^{77}Se-^{13}C *J*-Coupling Parameters for the C_{4v}-Symmetry Selenocyanide Cluster $[Re_5OsSe_8(CN)_6]^{3-}$" Ramaswamy, K.; Tulsky, E. G.; Kao, L.-F.; Long, J. R.; Hayes, S. E. *Inorg. Chem.*, submitted.

Selective and Efficient Catalysis in 3-D Controlled Environments

Graduate Students and Postdocs: H.-T. Chen, S. Huh, K. Lemma, D.R. Radu, J. Trebosc
Collaborators: A. Bakac, J.W. Wiench

Ames Laboratory and Department of Chemistry, Iowa State University, Ames, IA 50011-3111
vsylin@iastate.edu, mpruski@iastate.edu

Goal

Develop and characterize multifunctionalized mesoporous silica materials with well-defined pore/particle morphology and surface properties for heterogenization of single-site catalysts, and study the selectivity, reactivity and kinetics of these catalytic systems.

Recent Progress

(**1**) We have utilized the recently developed synthetic method[1-6] of multifunctionalization of mesoporous supports to test the feasibility of the major research goals of this project.

(**a**) We have demonstrated that the reaction selectivity of mesoporous catalysts can be controlled by using the novel concept of *gatekeepers*.[3-5] Specifically, we prepared a series of bifunctionalized mesoporous silica nanosphere-based (MSN) catalysts for nitroaldol (Henry) reaction.[3] In these catalysts, a common 3-[2-(2-aminoethylamino)ethylamino]propyl (AEP) primary group served as a catalyst, while three different secondary groups, ureidopropyl (UDP), mercaptopropyl (MP), and allyl (AL) functionalities, were incorporated as gatekeepers to control the reaction selectivity as depicted in **Figure 1**.[3] We demonstrated that the selectivity of these bifunctionalized MSN catalysts could be systematically tuned simply by varying the polarity and hydrophobicity of the gatekeepers. In a separate study, we demonstrated a unique "sieving"

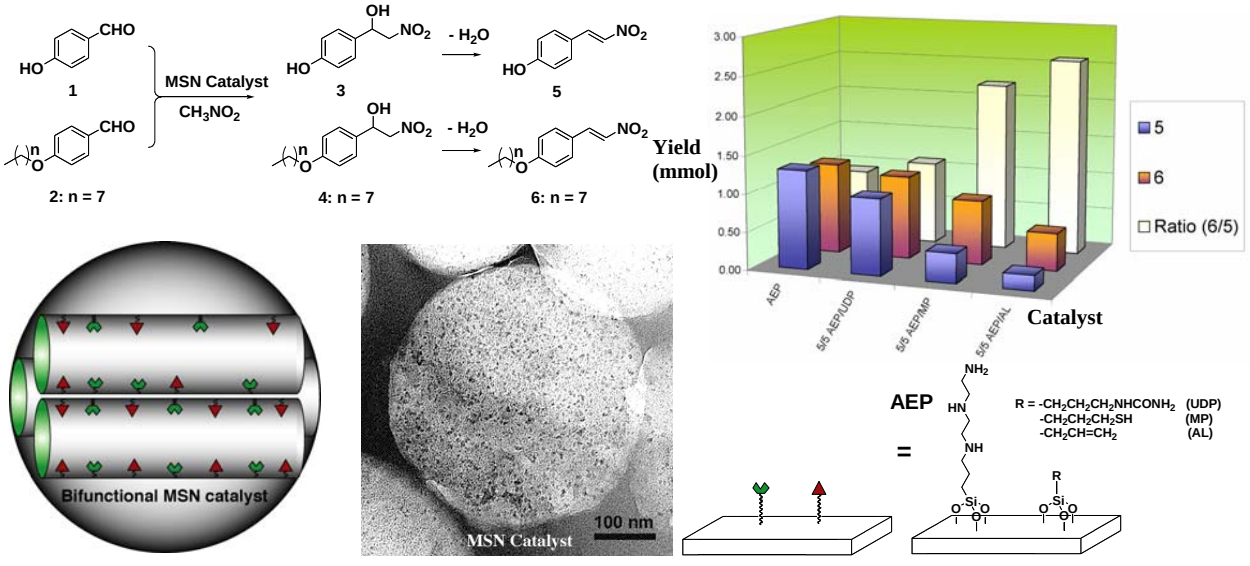

Figure 1. Bifunctionalized mesoporous silica nanosphere (MSN) catalyst for competitive nitroaldol reaction and the transmission micrograph of the bifunctional MSN material.[3]

effect of the poly(lactic acid) layer that was covalently attached to the exterior surface of mesoporous silica nanospheres.[4] By utilizing this layer as a gatekeeper, we investigated the molecular recognition events between several structurally similar neurotransmitters, i.e., dopamine, tyrosine, and glutamic acid and a pore surface-anchored *o*-phthalic hemithioacetal (OPTA) group.[4]

(**b**) We reported a new cooperative catalytic system[5] comprised of a series of bifunctionalized mesoporous silica nanosphere (MSN) materials with various relative concentrations of a general acid, ureidopropyl (UDP) group, and a base, 3-[2-(2-aminoethylamino)ethylamino]propyl (AEP) group. As depicted in **Figure 2**, three bifunctional AEP/UDP-MSN catalysts with the initial molar ratio of the organoalkoxysilane precursors, AEP/UDP = 2/8, 5/5, and 8/2, were synthesized via our previously reported cocondensation method.[1,2] The syntheses and characterizations of the monofunctionalized MSNs with either AEP or UDP functionality were also reported.[2] As shown in **Figure 3**, these AEP/UDP-MSN bifunctional materials were employed as catalysts for aldol, Henry and cyanosilylation reactions.[5] We have demonstrated that the general acid group, UDP, could cooperatively activate substrates with the base group, AEP, in catalyzing these reactions that involve

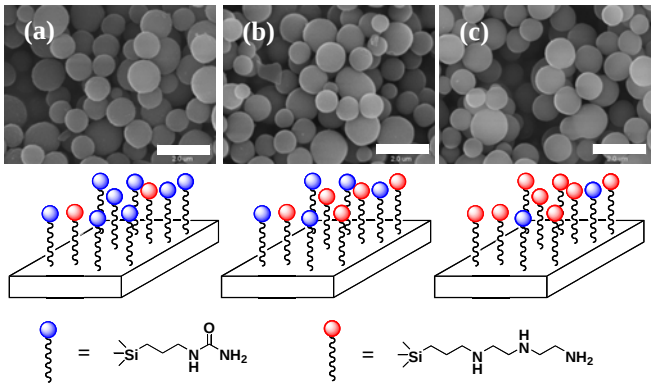

Figure 2. Scanning electron micrographs (SEM, above) and schematic drawings (below) of the bifunctional MSNs: **(a)** 2/8 AEP/UDP-MSN, **(b)** 5/5 AEP/UDP-MSN and **(c)** 8/2 AEP/UDP-MSN. Scale bar = 2.0 μm.[5]

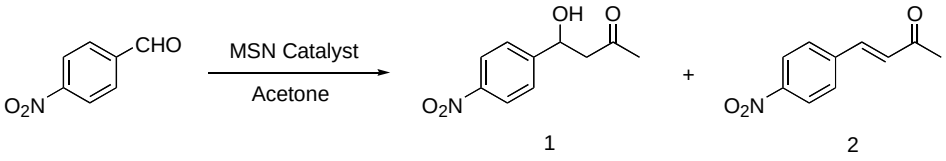

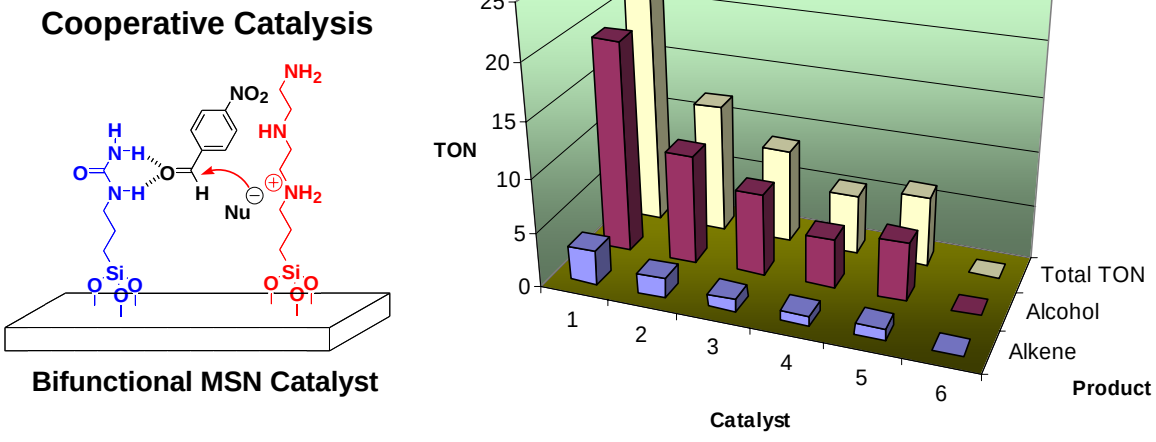

Figure 3. Turnover numbers (TONs) for the aldol reaction: 2/8 AEP/UDP-MSN (1), 5/5 AEP/UDP-MSN (2), 8/2 AEP/UDP-MSN (3), AEP-MSN (4), physical mixture of AEP-MSN and UDP-MSN (5) and UDP-MSN (6). Product alcohol is 1 and alkene is 2.[5]

carbonyl activation (**Figure 3**).[5] By fine-tuning the relative concentrations and proper spatial arrangements of different cooperative functional groups, we were able to regulate the turnover numbers of these important reactions.

(**c**) A mesoporous silica-supported uranyl material ($U_{aq}O_2^{2+}$-silica) was prepared by a co-condensation method.[9] Our approach involved an $I^-M^+S^-$ scheme, where the electrostatic interaction between the anionic inorganic precursor (I^-), surfactant (S^-), and the cationic mediator (M^+) provided the basis for the stability of the composite material. The synthesis was carried out under acidic conditions, where the anionic SDS (sodium dodecyl sulfate) provided the template for the uranyl cation and silicate to condense. Excitation with visible or near-UV light of aqueous suspensions of $U_{aq}O_2^{2+}$-silica generated an excited state that decays with $k_0 = 1.5 \times 10^4$ s^{-1}. The reaction of the excited state with aliphatic alcohols exhibited kinetic saturation and concentration-dependent kinetic isotope effects. For 2-PrOH, the value of k_{C3H7OH}/k_{C3D7OH} decreased from 2.0 at low alcohol concentrations to 1.0 in the saturation regime at high alcohol concentrations. Taken together, the data describe a kinetic system controlled by chemical reaction at one extreme and diffusion at the other. At low [alcohol], the second-order rate constants for the reaction of silica-$*U_{aq}O_2^{2+}$ with methanol, 2-propanol, 2-butanol, and 2-pentanol are comparable to the rate constants obtained for these alcohols in homogeneous aqueous solutions containing H_3PO_4. Under slow steady-state photolysis in O_2-saturated suspensions, $U_{aq}O_2^{2+}$-silica acts as a photocatalyst for the oxidation of alcohols with O_2.

(**2**) We used a variety of solid state NMR methods to characterize the MCM supports before and after functionalization, to study the structure and absolute/relative concentration of various moieties in the mesopores, and to determine their spatial distribution and orientation with respect to the surface.[1-5,7,8] In addition, two extensive investigations of MSN silicas were carried out in order to develop and/or adapt the solid state NMR methods that are specifically dedicated to the studies of functionalized surfaces.[7,8]

(**a**) We have demonstrated that the ^{1}H NMR measurements performed under MAS rates of up to 45 kHz provided high-quality resolution and excellent means for implementing various homo- and heteronuclear two-dimensional methods to the studies of MSN materials.[7] By applying ultrafast ^{1}H MAS, the ^{1}H-^{1}H homonuclear correlation (double quantum, exchange and RFDR) and ^{1}H-^{29}Si heteronuclear correlation (HETCOR) NMR methods could be used to examine the surface of *non-functionalized* MCM-41-type MSNs prepared under low surfactant concentration. The surface species, which included weakly adsorbed water, silanol groups and the residual surfactant (CTAB) molecules, were precisely quantified and characterized. Water was hydrogen bonded to the silanol groups, all of which were involved in such bonds under ambient humidity. Specific structures involving these SiOH-$(H_2O)_n$ species were proposed for various stages of thermal treatment, which included

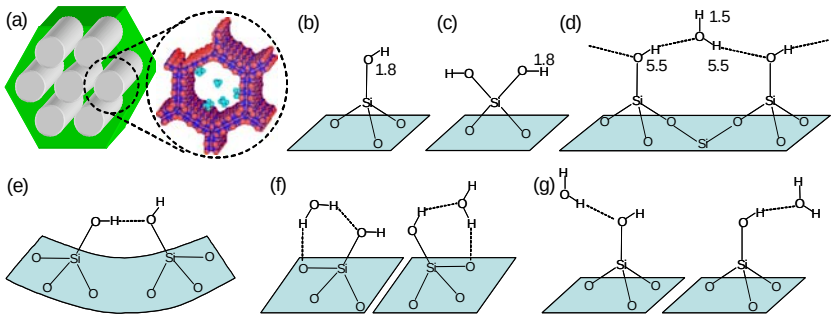

Figure 4. Schematic representation of cylindrical mesopores of MCM-41 nanoparticles (a), single silanol groups (b), geminal silanol groups (c), and the structures involving both the silanol groups and water on the pore surface described in reference 7 (d-g).[7]

dehydration, dehydroxylation and subsequent rehydration (**Figure 4**). The study also showed that the CTAB molecules which remained in the pores after the acid extraction assumed prone positions along the pores, with the tailgroup being most mobile.

(**b**) The fast MAS approach proved very profitable on the *functionalized* silica surfaces, especially in HETCOR NMR spectroscopy involving protons and low-gamma nuclei.[8] In the case of ^{1}H-^{13}C and HETCOR NMR, the spectra of surface functional groups on silica could be obtained without the isotopic enrichment using small (less than 10 μL) sample volumes. In ^{1}H-^{29}Si HETCOR NMR spectroscopy, a sensitivity gain of more than *one order of magnitude* has been achieved by incorporating the CPMG train of π pulses into the standard HETCOR pulse sequence. The ^{1}H-^{13}C and ^{1}H-^{29}Si HETCOR methods provided detailed characterization of the surface of MSN silicas functionalized with allyltrimethoxysilane (≡$SiCH_2CHCH_2$) in the absence of templating molecules (**Figure 5**). Similar methods are being currently applied in the studies of surfaces functionalized with more complex molecules. Access to smaller surfaces and/or lower molecular concentrations can be gained by using isotopically enriched samples.

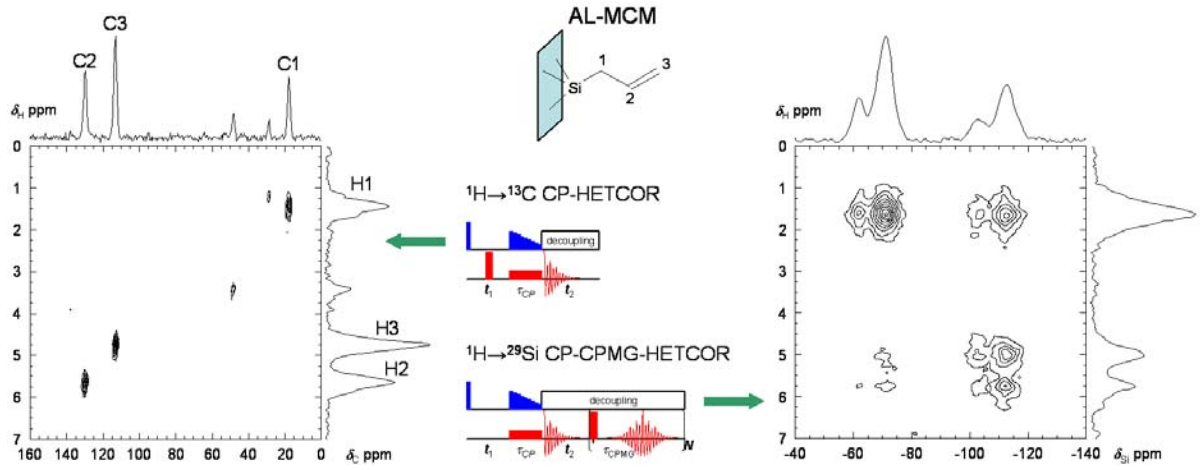

Figure 5. Two-dimensional heteronuclear ^{1}H→^{13}C (left) and ^{1}H→^{29}Si (right) correlation spectra of an allyl group (-CH_2-CH=CH_2) covalently bound to the pore walls of a MCM-41 type silica material taken using schemes shown in the middle of the figure.[8]

DOE Interest

Developing catalytic systems that can coherently unite the best features of the homogeneous and heterogeneous areas of catalysis has been a key interest of the DOE. By controlling the structure, reactivity and morphology of the mesoporous solid support and its interaction with the active sites, these studies provide truly unique opportunities for the design of a new generation of highly efficient and selective catalysts. This research can also provide new fundamental knowledge about catalysis in general by deconvoluting the key factors that affect selectivity, reactivity and kinetics.

Future Plans

- *Influence of the mesopore environment on catalyst selectivity and activity.*[10] Our ability to anchor two types of groups on mesopore walls allows us to tether not only the catalyst but also other functional moieties. The influence of these auxiliary groups will be directed

toward achieving various catalyst functions, such as enantioselectivity. These studies will use the concept of gatekeepers, which will be tested in the development of catalysts for the stereochemically controlled polymerization, selective hydrolysis, etc.

- *Cooperative catalysis inside mesopores.* To study how various functional groups could synergistically catalyze a reaction in a 3-D controlled environment, we will functionalize the surface of mesopores with two to three different types of catalytically active moieties and vary the relative ratio and spatial distribution of these functionalities. As a proof of principle, functional groups that can serve as general acid and base will be introduced to study the selective carbon-carbon bond formation in, for example, aldol, Diels-Alder, and hetero-Diels-Alder (HDA) reactions that involve carbonyl activation.
- *Control of the orientation and activity of tethered transition metal complex catalysts.* In order to understand the activity and selectivity of metal complex catalysts tethered on the walls of mesopores, we will characterize and control the location and the exact structure of the tethered catalysts on the surface.
- *Catalyst characterization*. Solid state NMR techniques will be further developed to better characterize the catalytic surfaces, especially to probe the spatial organization of the surface species and to provide key dynamic information about catalysts that will be prepared and tested during the next stages of this research. We will focus on further exploitation of J-spectroscopy, ^{1}H-^{1}H multiple quantum NMR methods and the CPMG-based schemes for enhancing the sensitivity.
- *Theory, modeling and simulation of transport and reaction in mesopores.* Theoretical and computational tools will be developed to allow analysis of electronic structure and dynamics for the complex silica surface + functional group + reactant + solvent systems. Second, statistical mechanical models will be proposed for the relevant many-particle transport and reaction processes in silica nanopore geometries, ideally utilizing energetic and dynamic information from the above electronic structure studies.

Publications (2003-present)

1. S. Huh, J.W. Wiench, J.-C. Yoo, M. Pruski, and V.S.-Y. Lin, "Organic Functionalization and Morphology Control of Mesoporous Silica Materials via a Co-condensation Synthesis Method", *Chem. Mater.* **2003**, *15*, 4247-4256.
2. S. Huh, J.W. Wiench, B.G. Trewyn, S. Song, M. Pruski, and V.S.-Y. Lin, "Tuning of Particle Morphology and Pore Properties in Mesoporous Silicas with Multiple Organic Functional Groups", *Chem. Comm. (Cambridge, U.K.)*, **2003**, *18*, 2364-2365.
3. S. Huh, H.-T. Chen, J.W. Wiench, M. Pruski, and V.S.-Y. Lin, "Controlling the Selectivity of Competitive Nitroaldol Condensation by Using a Bifunctionalized Mesoporous Silica Nanosphere-Based Catalytic System", *J. Am. Chem. Soc.*, **2004**, *126*, 1010-1011.
4. D.R. Radu, C.-Y. Lai, J.W. Wiench, M. Pruski, and V.S.-Y. Lin, "Gatekeeping Layer Effect: A Poly(lactic acid)-coated Mesoporous Silica Nanosphere-Based Fluorescence Sensor for Detection of Amino-Containing Neurotransmitters", *J. Am. Chem. Soc.*, **2004**, *126*, 1640-1641.

5. S. Huh, H.-T. Chen, J.W. Wiench, M. Pruski, and V.S.-Y. Lin, "Cooperative Catalysis by General Acid and Base Bifunctionalized Mesoporous Silica Nanosphere Catalysts", *Angew. Chem. Int. Ed.* **2005**, *44*, 1826-1830.
6. D.R. Radu, C.-Y. Lai, J. Huang, and V.S.-Y. Lin, "Fine-tuning the Degree of Organic Functionalization of Mesoporous Silica Nanosphere Materials via an Interfacially Designed Co-condensation Method", *Chem. Comm. (Cambridge, U.K.)*, **2005**, *10*, 1264-1266.
7. J. Trebosc, J.W. Wiench, S. Huh, V.S.-Y. Lin, and M. Pruski, "Solid state NMR study of MCM-41-type mesoporous silica nanospheres", *J. Am. Chem. Soc.*, **2005**, *127*, 3057-3068.
8. J. Trebosc, J.W. Wiench, S. Huh, V.S.-Y. Lin, and M. Pruski, "Studies of Organically Functionalized Mesoporous Silicas Using Heteronuclear Solid State Correlation NMR Spectroscopy under Fast Magic Angle Spinning", *J. Am. Chem. Soc.*, **2005** submitted.
9. J.A. Nieweg, K. Lemma, V.S.-Y. Lin, and A. Bakac, "Mesoporous Silica-Supported Uranyl: Synthesis and Photoreactivity", Inorg. Chem., **2005** submitted.
10. H.-T. Chen, S. Huh, J.W. Wiench, M. Pruski and V.S.-Y. Lin, "Dialkylaminopyridine-functionalized Mesoporous Silica Nanosphere as a Highly Stable Heterogeneous Nucleophilic Catalyst", *J. Am. Chem. Soc.*, **2005**, submitted.

DE-FG02-03ER15459 **Christopher W. Jones (GT)**
DE-FG02-03ER15460 **Robert J. Davis (UVA)**

***CATALYSIS SCIENCE INITIATIVE*: Basic Principles that Govern the Interaction of Organometallic Catalysts with Supports - The Science of Immobilized Molecular Catalysts**

Additional PIs: Marcus Weck, C. David Sherrill, Peter Ludovice (GT);
Post-docs: Kunquan Yu, Michael Holbach, Xiaolai Zheng, Nam Phan, Chandrashekhar Sonwane (GT); Yaying Ji (UVA)
Students: William Sommer, John Richardson (NSF Fellow), John Sears, Andrew Swann, Rebecca Shiels (NSF Fellow); Surbhi Jain (UVA)

School of Chemical & Biomolecular Engineering
Georgia Institute of Technology
Atlanta, GA 30332
cjones@chbe.gatech.edu

Department of Chemical Engineering
University of Virginia
Charlottesville, VA
rjd4f@virginia.edu

Goals:

Immobilized organometallic catalysts, in principle, can give high rates and selectivities like homogeneous catalysts with the ease of separation enjoyed by heterogeneous catalysts. However, the science of immobilized organometallics has not been developed because the field lies at the interface between the homogeneous and heterogeneous catalysis communities. By assembling an interdisciplinary research team that can probe all aspects of immobilized organometallic catalyst design, the entire reacting system can be considered, where the transition metal complex, the complex-support interface and the properties of the support can all be considered simultaneously from both experimental and theoretical points of view. In particular, our approach combines catalyst synthesis by design, classical and quantum modeling, *in-situ* characterization and classical kinetics and poisoning studies to allow for a thorough understanding of the catalytic systems. Metal pincer complexes for carbon-carbon bond formations and dehydrogenations as well as metal salen complexes for oxidations and kinetic resolutions are immobilized on polymeric, silica and gold supports. Using these two model ligand systems, the fundamental principles that can be used to understand and design future classes of immobilized organometallic catalysts will be elucidated.

DOE Interest

The work performed in this program elucidates fundamental principles important in the design of immobilized molecular catalysts. These catalysts have the potential of being highly active and selective while being easy to separate for the reaction medium. All of these aspects provide a substantial energy advantage in chemical processing. In addition to establishing basic catalyst design principles, the specific ligand systems being studied are widely applicable to a variety of important catalytic processes including carbon-carbon bond formations, production of olefins and hydrogen from alkanes, and oxidations.

Research Plan

The systematic study of two important ligand systems, salens and pincers, immobilized on different supports is being carried out through a combination of experimental studies and application of both classical and quantum modeling. Although there are many reports of

immobilized molecular catalysts in the literature, there are no long term, detailed studies of immobilized ligand systems and as a result the field is still largely empirically driven. By studying a few immobilized systems using an array of experimental and computational techniques, we will develop basic principles that can be used to guide catalyst design.

Carbon-carbon bond forming reactions such as Heck and Suzuki couplings are critical methods used for the conversion of aromatic molecules. Pd pincer complexes were identified in the literature as attractive, stable organometallic complexes that are active for both of these reactions. Furthermore, other authors reported the immobilization of these complexes on silica and polymer supports, although no detailed catalytic studies were carried out. Thus, this metal-ligand combination was identified as a candidate for our multifaceted analysis. Pd pincer complexes with SCS and PCP coordination of the metal atom were developed on both soluble polymeric (Weck) and insoluble silica and resin supports (Jones). These catalysts are being evaluated in Heck reactions via classical kinetic and poisoning studies (Jones and Weck) and via *in-situ* spectroscopic analysis (Davis). The impact of immobilization on the electronic structure and reactivity of the metal complex is being probed computationally using quantum methods (Sherrill).

Building on the expertise in pincer complexes developed studying the Pd pincer system, immobilized Ir-PCP pincer analogues are also being developed for alkane dehydrogenation reactions. This research path resulted directly from discussions with Alan Goldman at the 2004 DOE Catalysis Science Contractor's Meeting, highlighting the utility of such meetings.

An important component of the research effort is developing an understanding of the influence of support structure on catalytic properties. To this end, both the silica and polymeric supports are being studies via classical modeling. Realistic models of hexagonal mesoporous silica materials such as SBA-15 and MCM-41 are being developed, and the dynamics and accessibility of tethered metal complexes are then probed (Ludovice). Ultimately, correlations between the accessibility of the metal complexes and the experimentally observed turnover frequencies (TOFs) will be used to establish and understanding of the role of the tethered ligand-support interface.

In parallel with the studies of the pincer system, Co and Mn salens are being evaluated. Whereas the pincer system represented a relatively new ligand system, the salen system is well-studied and significant literature exists on both homogeneous and immobilized salen catalysts. This gives a wealth of data in addition to our own that may prove useful in the development of our basic principles for immobilized metal complex catalyst design. New synthetic protocols to prepare asymmetric salen ligands with a variety of support tethers are being developed. The complexes are again supported on a several substrates, including poly(norbornene), linear and cross-linked poly(styrene), hexagonal mesoporous silica, and gold nanoparticles (Weck and Jones). The Mn systems are evaluated in the asymmetric epoxidation of olefins and the Co systems in the hydrolytic kinetic resolution of epoxides. In parallel, classical models of salen ligands tethered within hexagonal mesoporous silica and onto side-chains of ring-opened poly(norbornene) are being developed (Ludovice). Quantum computational studies again help generate an understanding of the electronic structure and reactivity of the tethered complexes (Sherrill), while *in-situ* characterization allows for probing the active catalyst under reaction conditions (Davis).

A final system of interest is Pd complexes bound by N-heterocyclic carbene ligands. This represents an alternate ligand system for carbon-carbon bond coupling reactions.

Recent Progress

Pincer Systems: At the outset of this project, we focused our attention on the studies of Pd SCS and PCP pincer systems in the Heck reaction of iodobenzene and n-butyl acrylate. Several literature reports indicated that these complexes represented stable species in Heck reactions and reports of polymer (*J. Am. Chem. Soc.* **1999**, *121*, 9531; *Chem. Commun.* **2004**, 42; *J. Am. Chem. Soc.* **2001**, *123*, 11105; *J. Am. Chem. Soc.* **2000**, *122*, 9058) and silica-supported (*J. Mol. Catal. A.* **2003**, 201, 23) recoverable, recyclable catalysts were known. However, early-on in our studies of these systems, it was apparent that the supported complexes were not stable under reaction conditions. Systematic studies of the immobilized complexes via classical kinetic and catalyst poisoning studies indicated that these complexes decomposed under reaction conditions to liberate soluble Pd(0) catalytic species [1,2]. By combining these results with quantum calculations, continuous reactor studies and in-situ XAS investigations, we were able to unequivocally prove that the pincer complexes decompose under reaction conditions and we were able to offer a possible mechanism of complex leaching [3]. The hypothetical mechanism involved the complex in an "arm-off" state that was stabilized by coordination of the base triethylamine, followed by hydride elimination to yield the Pd(II) monohydride complex and a quaternary ammonium species. Reductive elimination of the hydride and the pincer ligand via hydrogen-transfer from the Pd-bound hydride to the Pd-bound carbon of the aryl group of the pincer could result in the formation of a non-metallated pincer complex and the leaching of a molecular Pd-species. This mechanism was supported by several experimental observations, including the observation of multiple types phosphorous species in the ^{31}P NMR spectra of the pincer complexes exposed to triethylamine and the verification of the existence of the quaternary ammonium species via mass spectrometry. Furthermore, quantum mechanical calculations clearly supported the experimental observations with favorable energetics for the arm-off configuration of metallated pincer catalysts using organic nitrogen-containing bases.

In parallel with the studies of the Pd pincer system, we also investigated the behavior of silica supported Pd nanoparticles in the Heck reaction in an effort to elucidate the nature of a potentially common catalytic species that may result from both systems. Kinetic and poisoning studies in a batch reactor along with long-term stability tests using a continuous flow, packed bed reactor supported the hypothesis that these systems also are unstable and leach soluble catalytic species in the presence of aryl iodides [8]. Careful analysis of literature data in conjunction with our new data supports the hypothesis that there may be a common soluble, molecular Pd(0) species that is responsible for all Heck reactions of aryl iodides, regardless of the starting Pd precatalyst used. Additional studies along these lines are underway.

Salen System: Over the last twelve months, efforts have focused on developing immobilized, asymmetric salen complexes on a number of supports. Despite a large number of reports of attempts to immobilize Jacobsen's salen catalysts, highly active and selective, *recyclable* salen systems have not been fully realized to date. In most studies, the activities and selectivities of the supported catalysts were significantly lower than their homogeneous counterparts. There are a wide variety of hypotheses about why they do not behave as well as the homogeneous analogue. Hypotheses include a lack of rotational or translational degrees of freedom, or inaccessibility of the catalytically active sites to the substrates. Furthermore, in previous studies,

the recyclability of the supported catalysts turned out to be a major challenge. Often, the catalytic activities and/or selectivities drop significantly when the catalysts were reused, However, to date, no detailed studies have conclusively shown what the cause of the poor performance is and what potential catalyst designs can alleviate these problems.

We focused our efforts on a novel strategy to immobilize salen ligands on a wide variety of supports. Our strategy follows the following criteria: (i) the supported catalyst should resemble the optimized salen ligand sphere developed by Jacobsen as closely as possible, (ii) the salen ligand should be attached to the support via a *single* linker to minimize local steric restrictions, (iii) the catalyst loading should be easily controllable (sufficiently low to maximize site isolation of the catalytic centers and thus minimize the possibility of forming the inactive oxo-bridged dimmers, or sufficiently high to give good catalyst loadings), and (iv) the morphology of the supports should ensure free accessibility to all active sites. To minimize steric interactions and to optimize accessibility we employed *mono*-functionalized salen cores attached via a single site to the poly(norbornene) or poly(styrene) backbone for all studies. For the attachment of the ligand to the different supports, chemically inert C-C bond linkages via a rigid phenylene-acetylene or biphenyl linker have been employed. Poly(norbornene), poly(styrene), insoluble cross-linked poly(styrene) beads, as well as mesoporous silica solids have been employed as supports. The preferential immobilization method is to first prepare the homogeneous, metallated complex and then tether it to a support via controlled polymerization (norbornene or styrene) or via grafting (mesoporous silica). Both Co and Mn complexes have been prepared.

The poly(norbornene) supported Mn salen catalysts are as active and selective as the original Jacobsen small molecule analogue and are the most active and selective supported catalyst system reported to date [6]. Using styrene, methyl styrene or 1,2-dihydronaphthalene as substrate, epoxidations were quantitative within minutes with outstanding selectivities that are on par with the unsupported Jacobsen catalyst (for example 88 % *ee* for the original Jacobsen catalyst *vs*. 83% *ee for the poly(norbornene) supported one*). Furthermore, the cobalt version of the poly(norbornene) supported salen catalyst is highly active in the hydrolytic kinetic resolution of epoxides with ee above 99.9% within minutes. Finally, the Co catalysts *can be recycled and reused with equivalent activities and selectivities*.

The soluble as well as insoluble poly(styrene) supported Co salen complexes are also outstanding catalysts for the hydrolytic kinetic resolution of epoxides [7]. Using a novel ligand synthesis and straight-forward polymerization techniques, we were not only able to synthesize supported Co-salen homopolymers but also copolymers containing between 10-50% Co-salen complex per repeat unit. These copolymers will allow us to study the effect of catalyst density on the catalyst activity as well as potential decomposition pathways (for example it has been suggested that the main decomposition pathway of Mn-salen complexes is via the formation of bimetallic dimers. Using the newly synthesized copolymers, we will be able to test this hypothesis).

Molecular Modeling of Tethered Complexes: A key hypothesis of this work is that for polymer-supported metal complex catalysts, reaction rates will correlate well with the accessibility of the active sites. Accessibility will be dictated to a large degree by the conformation of the polymer chains in solution. We hypothesize that poly(norbornene) will adopt a conformation in solution that will lead to highly accessible side chains that contain catalyst sites. To this end, we have

developed the necessary simulation protocols to allow us to build the first model of poly(norbornene) in solution (Ludovice, Weck). We have modified the commercial program from the Chemical Computing Group to correctly execute an efficient symplectic molecular dynamics algorithm for our simulations [9]. We are now using this program to develop a long-range Rotational Isomeric States (RIS) model for various configurations of poly(norbornene) (Ludovice, Weck). A survey of the literature indicated that reasonable models for hexagonal mesoporous silica that would allow for the modeling of metal complex catalysts tethered within the mesopores of the support do not exist. Hence, new models for the structure of hexagonal mesoporous silicas such as MCM-41 and SBA-15 were developed (Ludovice, Jones) and validated via comparisons of simulated surface areas, pore volumes, wide and small angle X-ray diffraction patterns, and adsorption isotherms with experimental results [4, 5]. With these models in hand, the dynamics of metal complex catalysts such as salens and pincers can be modeled and the experimentally determined TOFs can be correlated with metal complex accessibility and dynamics.

Quantum Calculations: As noted above, integration of experimental studies and quantum calculations directly led to a proposed mechanism of decomposition of Pd pincer complexes during Heck chemistry (Sherrill). Additionally, substantial work has been completed characterizing the Mn salen system as well, and our studies indicate that this system has an unusually rich and intricate electronic structure, which may not be accurately modeled by entry-level *ab initio* quantum methods [10]. Using convergent wavefunction-based methods, we are obtaining the first definitively converged theoretical results for this important system. We have already discovered the existence of some artifactual, unstable wavefunctions at the Hartree-Fock level, which we hypothesize may account for some otherwise unexplained discrepancies in previous theoretical investigations. We have also discovered that there are several additional, previously-uncharacterized low-lying excited electronic states which may influence reaction mechanisms involving the Mn salen complex.

Synergy of the Research Team

Thus far, the team members involved in this project have been able to closely coordinate their efforts. Researchers in the Weck and Jones groups meet together weekly to coordinate catalyst design activities. All GT researchers meet monthly, with each researcher presenting an update on their current progress and soliciting feedback from team members. Conference calls involving GT and Virginia researchers take place quarterly. The PI from Virginia (Davis) has visited GT and GT researchers have visited Virginia (Jones). This summer, students from Virginia will visit GT. It is noteworthy that 6 of the 10 publications in print or in preparation have contributions from multiple research groups.

Summary

- Pd pincer complexes have been unequivocally shown to decompose under Heck conditions to give soluble Pd catalytic species that are akin to those produced from Pd on silica (Jones, Weck, Sherrill, Davis)
- New asymmetric ligands were designed and immobilized on various polymer supports. Immobilized Mn and Co catalysts derived from these ligands are catalytically equal or superior to all known supported salen catalysts in regard catalytic rates and *ee*'s in olefin epoxidation reactions and epoxide kinetic resolutions. The Co catalysts are fully recyclable, based on preliminary studies. Characterization of the supported Mn systems

via quantum calculations has elucidated several unique subtleties regarding the electronic structure of these complexes (Weck, Jones, Sherrill).

- New models for mesoporous silicas MCM-41 and SBA-15 have been developed that are suitable for studies of tethered catalysts within the pore systems. These models represent the most realistic models of these materials reported to date (Ludovice, Jones).

Publications (papers in preparation defined as those to be submitted by June 30)

1. "Silica-Tethered Pd-SCS-Pincer Complexes: Evidence for Precatalyst Decomposition to Form Soluble Catalytic Species in Heck Chemistry." K. Yu, W. Sommer, M. Weck and C. W. Jones, *Journal of Catalysis*, **2004**, 226, 101-110.

2. "Evidence that SCS Pincer Pd(II) Complexes are only Precatalysts in Heck Catalysis and the Implications for Recycle and Reuse." K. Yu, W. Sommer, J. Richardson, M. Weck and C. W. Jones, *Advanced Synthesis and Catalysis*, **2005**, 347, 161-171.

3. "Investigations into the Stability of Immobilized Pd^{II} Pincer Complexes During Heck Catalysis." W. Sommer, K. Yu, J. S. Sears, Y. Ji, X. Zheng, R. J. Davis, C. D. Sherrill, C. W. Jones and M. Weck, *Organometallics*, **2005**, in revision.

4. "A Model for the Structure of MCM-41 Incorporating Surface Roughness." C. Sonwane, C. W. Jones and P. J. Ludovice, *Journal of Physical Chemistry B.* **2005**, submitted.

5. "Modeling Microporosity in SBA-15" C. Sonwane, J. Richardson, C. W. Jones and P. J. Ludovice manuscript in preparation.

6. "Synthesis and Application of Poly(norbornene)-Supported Monofunctionalized Salen Complexes" M. Holbach and M. Weck, manuscript in preparation.

7. "Recoverable, Recycleable Immobilized Co-Salen for the Hydrolytic Kinetic Resolution of Racemic Epoxide" X. Zheng, M. Holbach, C. W. Jones, and M. Weck, manuscript in preparation.

8. "Factors that Influence Metal Leaching from Supported Pd Catalysts used in the Heck Reaction." Y. Ji, S, Jain and R. J. Davis, manuscript in preparation.

9. "The Importance of Symplectic MD Algorithms in the Dynamics of Cyclopentane" A. Swann, P.J. Mucha and P.J. Ludovice, manuscript in preparation.

10. "On the Challenging Electronic Structure of Mn(salen): Wavefunction Instabilities, Nondynamical Correlation, and Low-lying Electronic States," J. S. Sears and C. D. Sherrill, manuscript in preparation.

DE-FG02-01ER15264 **Colin Nuckolls**

Synthesis, Directed Assembly, and Local Probe Measurements of Dipolar, Organic Nanostructures

Students: Chaya Ben-Porat, George Tulevski, Mark Bushey, Dr. Thuc-Quyen Nguyen, and Dana Horoszewski
Collaborators: Louis Brus (Columbia), Michael Steigerwald (Columbia), Irving Herman (Columbia), and Shalom Wind (Columbia)
Contact: C. Nuckolls, Columbia University, Department of Chemistry, mail code 3130, New York, NY 10027. phone (212) 854 6289; Email: cn37@columbia.edu
Web page: nuckolls@chem.columbia.edu

Goal

To develop methods to grow individual wires that are attached to metal surfaces and measure their properties locally. Two approaches are explored: (1) Using weak forces such as hydrogen bonding or electrostatic attraction to direct assembly of individual stacks of molecules; (2) To use catalyst sites that are integrated into metal electrodes to grow individual molecular wires.

Recent Progress

(1) Self-Assembly Directed by Hydrogen Bonds:

The research program applies organic synthesis and self-assembly to create nanoscale materials. It focuses on self-assembly of complex aromatic molecules at interfaces because this allows electronic and polar properties to be investigated on molecular length-scales. The design principle uses steric crowding to force the recognition groups—amides—out of the aromatic ring-plane and into a conformation that would allow intermolecular hydrogen bonds to form allowing a synergy between hydrogen bonds and π-to-π interactions to emerge.

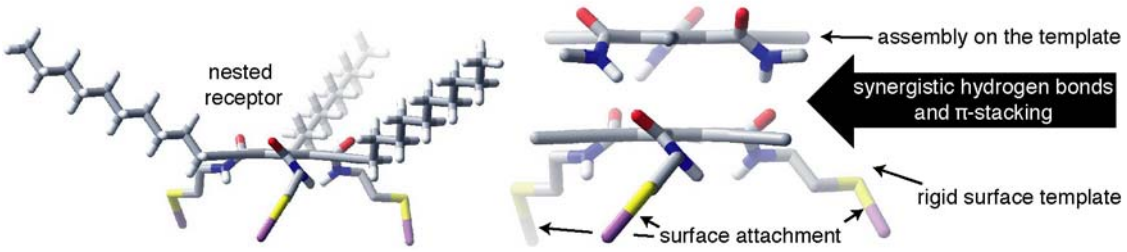

Figure 1. Molecular model showing the side-view of the model when bound to surface showing the nested receptor site (red: oxygen, grey: carbon, blue: nitrogen, yellow: sulfur, and purple: gold atom). (b) A noncovalent dimeric stack attached to a gold surface. The hydrogen atoms and the substituents on the alkynes have been removed.

We show that crowded aromatics could be attached to surfaces and can act as a surface template for the stacking of aromatic molecules in a defined direction. Recently we found that such a template can be made by attaching surface active groups for metals like the thiols (in Figure 1) onto the side arm of the trisamide core. These molecules have interesting assembly characteristics at the interfaces of metals. These surface templates orient the column growth perpendicular to the surface.

The results of the electrostatic self-assembly study are shown in Figure 2. The AFM micrographs show gold electrodes on a silicon substrate spaced by ca. 3µm. The electrodes are labeled 1-4 in Figure 2. The molecules were drop cast from solution into the gap while a 10 V/µm field was applied between electrode 1 and 2. Figure 2 reveals bundles of strands grown in the direction of the electric field lines. In Figure 2c, growth process was terminated before the strands could reach the counter electrode showing that the strands grow from the negative to the positive electrode.

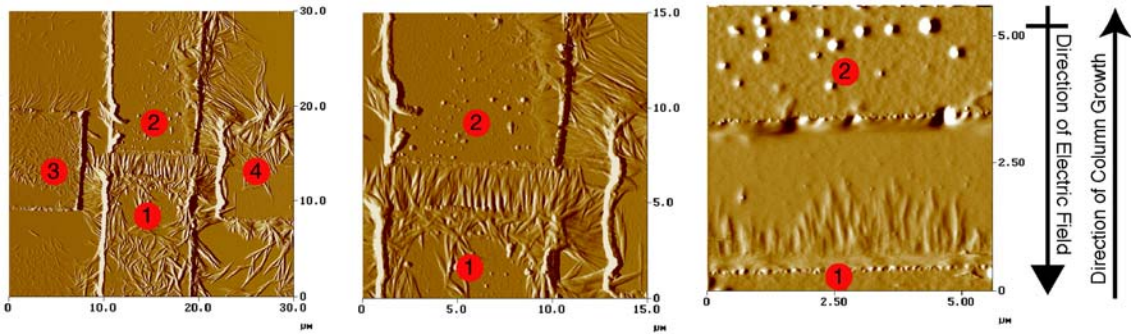

Figure 2. AFM micrographs detailing the assembly of strands with electric fields. The numbers indicate the four different electrodes deposited by e-beam lithography to have 3 µm spacing. The bias was applied between electrode 1 and 2.

(2) Individual Catalyst Sites for Molecular Wire Growth

Increasingly the DOE project is working toward catalytic methods to growth molecular wires that are structurally and electronically contacted to metal surfaces. We recently found that carbene precursors such as diazoalkanes react with clean ruthenium surfaces to yield monolayers of carbenes on metal surfaces. We are interested in using these methods to grow molecular scale wires through the ring opening reactions shown below in Figure 3.

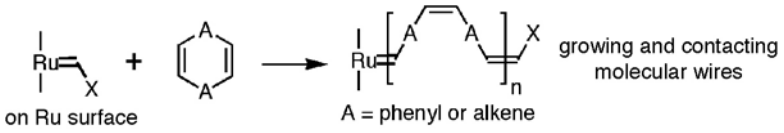

Figure 3. A scheme to grow molecular wires from individual catalyst sites on a ruthenium surface.

We have recently shown that these surfaces are able to initiate the olfefin metathesis reaction. The system investigated is shown in Figure 4 below. Monolayers can be generated through reaction with the appropriate diazoalkanes and then interconverted by reaction with olefins. We can detect the products of the surface reactions with IR, XPS, and scanned probe measurements as well as the byproducts of the reaction by GC/MS (shown in Figure 4).

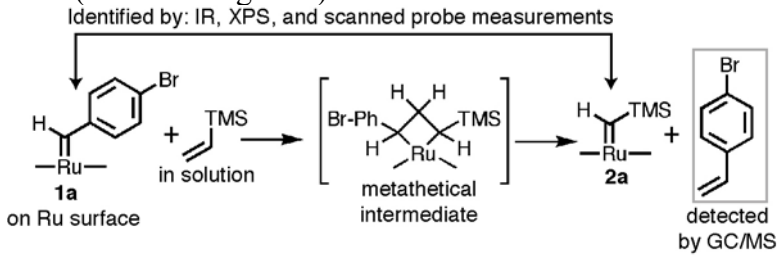

Figure 4. A surface metathesis reaction.

DOE Interest

These studies are significant because they could provide a deeper understanding of how polar properties emerge and propagate on the nanoscale. Moreover, these columnar structures provide a mechanism to convert electrical energy to mechanical energy at extremely small length-scales. For the electrical measurements, the potential outcomes for these experiments are unprecedented, providing a deeper understanding of how charge is delocalized in low dimensional organic nanostructures and as a general method to use catalysis to create molecular electronics devices.

Future Plans

Our future plans are in measuring the conductivity of the wires grown in situ from the ruthenium surfaces through ring opening metathesis polymerization. We also intend to measure properties of individual columns of molecules assembled at interfaces.

Publications

(1) "STM Imaging of Self-Assembled Helical Nanostructures", T.-Q. Nguyen, R. Martel, A. Carlsen, P. Avouris, M. L. Bushey, L. E. Brus, and C. Nuckolls, *in preparation*.

(2) "Organization of Acenes with a Cruciform Assembly Motif", Q. Miao, X. Chi, S. Xiao, R. Zeiss, M. Lefenfeld, C. Kloc, T. Siegrist, M. Steigerwald, and C. Nuckolls, *submitted.*

(3) "A Catalytic Path to Ohmic Contact in Metal-Molecule Junctions", G. S. Tulevski, M. B. Myers, M. Hybertsen, M. Steigerwald, and C. Nuckolls, *submitted.*

(4) "Electric Fields on Oxidized Silicon Surfaces: Static Polarization of PbSe Nanocrystals", C. Ben-Porat, O. Cherniavskaya, L. Brus and K.-S. Cho and C. B. Murray, *J. Phys. Chem. B.*, *accepted for publication.*

(5) "Large Dipole Moments in One Dimensional Organic Nanostructures Composed of Substituted Arenes as Measured by Dielectric Impedance Spectroscopy", J. H. Dickerson, M. L. Bushey, S. Banerjee, T.-Q. Nguyen, C. Nuckolls, and I. P. Herman, *submitted.*

(6) "Molecular Interactions in One-Dimensional Organic Nanostructures", T.-Q. Nguyen, R. Martel, P. Avouris, M. L. Bushey, C. Nuckolls, and L. Brus, *J. Am. Chem. Soc.,* **2004**, *126*, 5234-5442.

(7) "Dimeric π-stacks on Gold using Three Dimensional Lock-and-Key Receptors," G. S. Tulevski, M. L. Bushey, J. L. Kosky, S. J. Toshihiro-Ruter, and C. Nuckolls, *Angew. Chem. Int. Ed.,* **2004**, *43*, 1836–1839..

(8) "Using Hydrogen Bonds to Direct the Assembly of Crowded Aromatics," M. L. Bushey, T.-Q. Nguyen, W. Zhang, D. Horoszewski, and C. Nuckolls, *Angew. Chem., Int. Ed.*, **2004**, *43*. 5446-5453.

(9) "Synthesis, Assembly, and Thin Film Transistors of Dihydrodiazapentacene—an Isostructural Motif for Pentacene," Q. Miao, T.-Q. Nguyen, T. Someya, G. B. Blanchet, and C. Nuckolls, *J. Am. Chem. Soc.* **2003**, *125*, 10284–10287.

(10) "A Defined Secondary Structure in Covalently-Linked Overcrowded Aromatics," W. Zhang, D. Horoszewski, J. Decatur, and C. Nuckolls, *J. Am. Chem. Soc.* **2003**, *125*, 4870–4873.

(11) "Synthesis, Self-Assembly, and Electro-optic Switching of One-Dimensional Nanostructures from New Crowded Aromatic," M. L. Bushey, T.-Q. Nguyen, and C. Nuckolls, *J. Am. Chem. Soc.* **2003**, *125*, 8264–8269.

DE-FG02-03ER15467 **Susannah Scott**

CATALYSIS SCIENCE INITIATIVE: **Design of heterogeneous catalysts for the low temperature metathesis of unfunctionalized and functionalized olefins**

Co-PIs: Bradley Chmelka, Juergen Eckert
Graduate students: Anthony Moses, Heather Leifeste, Christina Raab
Postdoctoral fellows: Naseem Ramsayhe, Swarup Chattopadhyay
Collaborators: Robert Maughon (Dow Chemical), Francis Timmers (Dow Chemical)

Department of Chemical Engineering
University of California
Santa Barbara CA 93106-5080
sscott@engineering.ucsb.edu

Goals:

Olefin metathesis is a powerful method for forming new C=C bonds. However, the full potential of heterogeneous metathesis catalysts has yet to be exploited, because supported metal oxides show low rates of activation and rapid deactivation. A major goal of this project is to create fundamental knowledge about how carbene active sites spontaneously form from inorganic and organometallic precursors, and how they are deactivated. This knowledge will be used to design catalysts with increased metathesis activity, better long-term stability and higher functional group tolerance.

DOE Interest:

Supported perrhenate catalysts are of particular interest for olefin metathesis, because they are active at much lower temperatures and are more functional group-tolerant than either Mo- or W-based catalysts. These properties make them potentially useful in liquid phase reactions involving biorenewable feedstocks, such as seed oils, provided major issues of rapid deactivation and poor regenerability can be overcome.

Research Plan:

Tetraalkytin activators confer functional group tolerance on supported perrhenate catalysts, yet prevent reactivation due to deposition of SnO_2 during calcination. The origin of the tin promotion effect is not known. Identifying key features of the Re-Sn interaction will aid us in designing catalysts that use alternate promoters. We hypothesized that $SnMe_4$ reacts with supported perrhenate to generate *in situ* a small amount of methylrhenium trioxide, a functional-group-tolerant olefin metathesis catalyst. Using organometallic synthesis, selective isotopic labeling, surface spectroscopies and DFT calculations, we aim to investigate reactions between the organometallic components of these supported catalysts.

The mechanisms by which methyltrioxorhenium catalyzes the epoxidation of olefins and the olefination of aldehydes are now fairly well-understood. In contrast, the origin of its reactivity in olefin metathesis has received much less attention. It is known that activation by a Lewis acidic solid (*e.g.*, silica-alumina, niobia) is required. Understanding the nature of $MeReO_3$-support interaction is the first step towards

explaining how solid oxides induce metathesis activity. In particular, we are interested in exploring whether the methyl ligand is the origin of the carbene active site, or whether olefin oxidation at the oxo ligands generates a carbene ligand *in situ*. This insight will allow us to design other rhenium coordination environments to increase the fraction of sites that become active.

Probing the activity and selectivity of supported $MeReO_3$- and perrhenate-based solid catalysts through product analysis, kinetic studies and kinetic modeling leads to an appreciation of the complexity of the reaction manifold, and in particular, side-reactions leading to deactivation.

Recent Progress:

Relevance of $MeReO_3$ to supported perrhenate catalysts.

Deposition of volatile $MeReO_3$ (Aldrich) onto amorphous silica-alumina (Davicat 3113, 5.7 wt.% Al, 450 m^2/g) is readily achieved at room temperature either from the vapor phase or from toluene solution. In each case, chemisorption is rapid and irreversible: the grafted material is stable to washing with fresh solvent and to prolonged evacuation ($\leq 10^{-4}$ Torr). The solid is either a deep yellow color (for hydrated silica-alumina) or brown (for silica-alumina calcined and fully dehydrated at 450°C). $MeReO_3$ does not chemisorb onto silica, which lacks Lewis acidity.

DFT calculations on a silisesquioxane model system support our hypothesis that SnR_4 causes the displacement of supported perrhenates to yield $MeReO_3$, Figure 1. Experimentally, exposure of silica-supported perrhenate to a solution of $SnMe_4$ led no color change (as expected) but the formation of soluble, colorless methylrhenium(VII), detected by ^1H NMR. Exposure of a silica-alumina-supported perrhenate to $^{13}MeSn^nBu_3$ at room temperature induced a color change from white to brown and the appearance of a new ^{13}C CP/MAS signal at 33 ppm, both characteristic of $MeReO_3$ grafted onto silica-alumina. Reaction of SnR_4 with surface hydroxyl sites, accompanied by evolution of alkane, also occurs spontaneously at room temperature, accounting for the apparent need for excess SnR_4 to activate supported perrhenates.

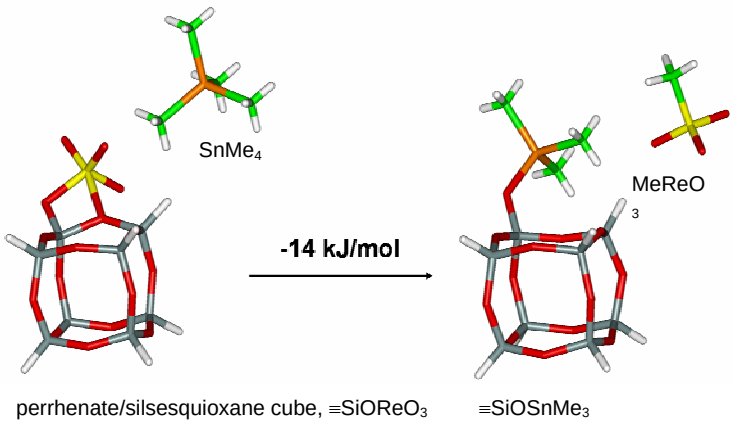

Figure 1. Calculated reaction energy for $SnMe_4$ interacting with perrhenate attached to a silsesquioxane cube, as a model for silica, showing the formation of $MeReO_3$. Re (yellow), Sn (orange), Si (grey), O (red), C (green) and H (white).

Nature of the interaction between $MeReO_3$ and amorphous silica-alumina.

Possible structures for grafted $MeReO_3$ were investigated by DFT. An Al-substituted silsequioxane was selected to model the latent Lewis acidity of silica-alumina.

An all-Si silsequioxane monosilanol was modified by replacing one SiH corner with an Al atom and a capping water molecule to establish tetrahedral geometry at Al, Figure 2.

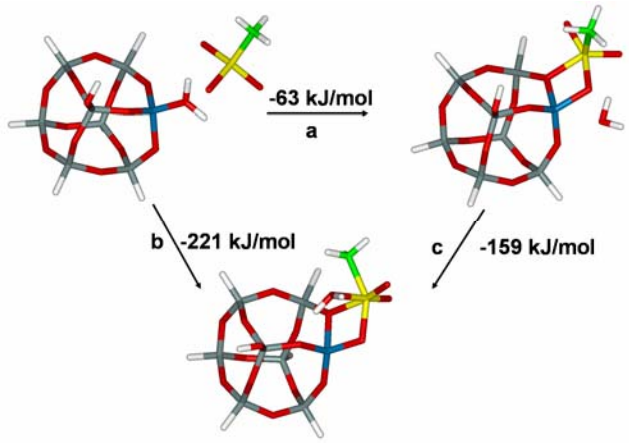

Figure 2. Calculated reaction energies for $MeReO_3$ interacting with an aluminosilsesquioxane cube, as a model for silica-alumina: (a) displacement of water bound at the Al site (blue) by $MeReO_3$; (b) adsorption of $MeReO_3$ onto the cube, with migration of water from Al to Re; (c) adsorption of water onto grafted $MeReO_3$.

Possible grafting modes we considered include interactions of the Re atom with the silanol oxygen or any of the bridging oxygens of the cube, hydrogen-bonding of the silanol to $MeReO_3$ and interactions with the latent Lewis acid site. The lowest energy geometry found for $MeReO_3$ grafted to the alumino-silsesquioxane cube is shown in Figure 2, with calculated bond distances summarized in Table 1. The cube model shows a clear preference (-63 kJ/mol) for binding $MeReO_3$ rather than water at the Al site. In the water-free site, repre-senting the structure of $MeReO_3$ grafted onto fully dehydrated silica-alumina, one of the oxygen atoms of $MeReO_3$ binds to Al, at an Al-O distance of 1.80 Å. Substantial lengthening of the Re=O bond, from 1.71 to 1.80 Å, suggests a reduction in its bond order. This Lewis acid-base interaction is accompanied by a second interaction between Re and an adjacent, bridging oxygen (SiOAl). Changes in the Mulliken charges indicate charge transfer to the oxygen interacting with Al from the other oxo ligands and the methyl carbon. There is a slight lengthening of the Re-C bond, relative to the calculated and observed structures for molecular $MeReO_3$. The grafted $MeReO_3$ exhibits a high affinity for the displaced water molecule (-159 kJ/mol), partly explaining the attenuation of metathesis activity by humidity.

Experimental evidence for the nature of $MeReO_3$ binding to the surface was established by analysis of the EXAFS recorded at the Re L_{III} edge. The spectrum of $MeReO_3$ adsorbed on calcined silica-alumina is shown in Figure 3. A feature visible in

Table 1. Comparison of bond distances (Å) for molecular $MeReO_3$ and $MeReO_3$ grafted onto dehydrated silica-alumina

path	*N*	$MeReO_3$		$MeReO_3/SiO_2$-Al_2O_3	
		lit[a]	calc[b]	calc[b]	obs[c]
Re=O	2	1.71	1.71	1.69, 1.72	1.69 (0.0012)
Re=O	1	1.71	1.71	1.80	1.79 (0.0016)
Re-C	1	2.06	2.07	2.09	2.07 (0.0012)
Re-$O_{support}$	1	-		2.07	2.13 (0.0056)
Re-Al	1	-		2.93	3.06 (0.0054)

[a]Obtained by gas phase electron diffraction.[1] [b]DFT calculation. [c]Obtained by EXAFS curve-fitting, with coordination numbers fixed at integers. The Debye-Waller factors σ^2 (Å^2) are shown in parentheses. The inner potential energy (E_0) and global amplitude reduction factor (S_0^2) were fixed at 0 and 1, respectively.

the unphase-corrected *R*-space at ca. 2.7 Å, not present in the EXAFS of polycrystalline $MeReO_3$, is attributed to scattering of the photoelectron wave by an atom Y of the support. This feature indicates a highly specific Re···Y interaction.

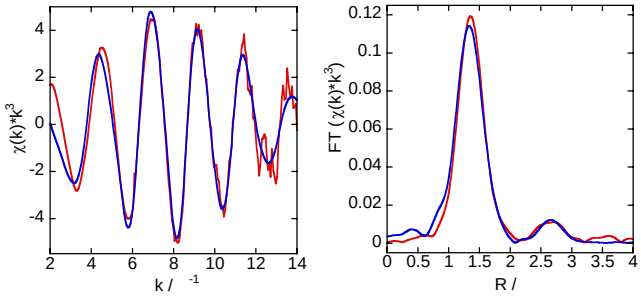

Figure 3. EXAFS data (red) in k^3-weighted *k*-space (left) and *R*-space (unphase-corrected, right), for $MeReO_3$ adsorbed on calcined, fully dehydrated silica-alumina (5.7 wt.% Al, 1.3 wt.% Re). Parameters for the curve-fit (blue) are given in Table 1. Residual = 21.

The curve-fit for a model containing one C shell (*N*=1), one O shell (*N*=3) and one Al shell (*N*=1) to the EXAFS data gave unreasonably small Debye-Waller factors (ca. $1x10^{-4}$ $Å^2$), suggesting the presence of an additional scatterer. Including another Re-O scattering path increased the Debye-Waller factors to values comparable to those calculated for molecular $MeReO_3$. Replacing the Y=Al shell by Si, Re, or an additional oxygen shell resulted in poorer fits to both the FT magnitude and its imaginary component. Allowing the three oxo ligand paths to vary independently resulted in a better fit, leaving two Re=O distances essentially unperturbed and one Re=O substantially longer. When coordination numbers for this fit were allowed to vary, they produced integer values for all scatterers, within the error of the EXAFS technique. In order to reduce the number of correlated parameters, coordination numbers were therefore fixed at integer values; for each path, the distance (*R*) and Debye-Waller factor (σ^2) were refined sequentially refined. The curve-fit and parameters for this model are shown in Figure 3 and Table 1, respectively.

Agreement between the calculated structure of grafted $MeReO_3$ and the EXAFS curve-fit parameters in the first three shells (*i.e.*, the oxo and methyl ligands) is striking. The shells representing support interactions, $Re\text{-}O_{support}$ and Re-Al, appear at slightly longer distances in the EXAFS than in the cube model. This is understandable if the fixed SiOAl angles of the cube differ from those in the average silica-alumina surface structure.

Evidence for support-induced tautomerization of grafted $MeReO_3$.

Our experimental and computational results suggest that chemisorption of $MeReO_3$ onto silica-alumina occurs preferentially at Lewis acidic Al sites, leading to dramatic elongation of a Re=O bond whose increased basicity should promote tautomerization. Unsupported $MeReO_3$ does not catalyze olefin metathesis in the solid state or in solution, since the tautomer $CH_2{=}ReO_2(OH)$ is 108 kJ/mol higher in energy.

When CD_3ReO_3 is grafted onto unlabeled silica-alumina, peaks appear at positions consistent with vibrations of a CD_3 group. However, new vibrational modes appear almost immediately, Figure 4. A broad band at 2650 cm^{-1} and a narrow band at 2757 cm^{-1}, attributed to

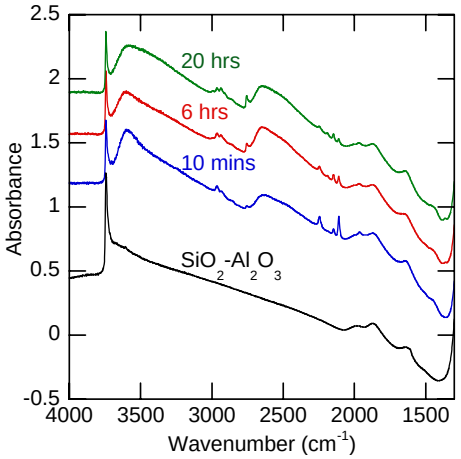

Figure 4. In situ FTIR spectra for CD_3ReO_3 deposited onto SiO_2-Al_2O_3.

ν(SiO-D) modes, increase in intensity with time. Thus deuterium from the methyl group is readily incorporated into the exchangeable proton pool of the surface hydroxyls. Simultaneously, ν(C-H) bands characteristic of surface methyl groups appear and their intensities increase with time, while the intensities of the ν(C-D) bands decrease. Both ν(C-H) and ν(C-D) regions contain additional vibrational modes consistent with lower symmetry in the methyl group as a result of partial deuteration.

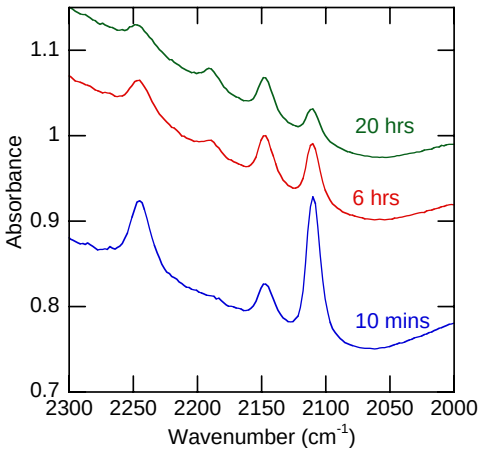

Figure 5. Detail of C-D stretching region for CD_3ReO_3 on SiO_2-Al_2O_3.

Figure 5 shows the changes in the ν(C-D) region as the H/D exchange progresses. The peaks that are initially present at 2245 and 2110 cm^{-1} are assigned to $\nu_{as}(CD_3)$ and $\nu_s(CD_3)$, respectively, due to their similarity to the spectrum of CD_3ReO_3. In addition, new bands appear, first at 2147 cm^{-1}, and later at 2190 cm^{-1}. By comparison to the IR spectrum of CD_2HTiCl_3, the former is assigned to the $\nu_s(CD_2)$ mode of a (CHD_2) isotopomer; the $\nu_{as}(CD_2)$ mode is likely not resolved from $\nu_{as}(CD_3)$. The slower-forming band at 2190 cm^{-1} is assigned to the isolated ν(CD) mode of the CH_2D isotopomer. In the ν(C-H) region, new modes first appear at 2964 and 2935 cm^{-1}. The former is assigned to the isolated ν(CH) mode of the CD_2H isotopomer. The intensity of this band decreases with time as the band at 2935 cm^{-1} grows stronger; it is attributed to the $\nu_s(CH_2)$ mode of a (CH_2D) isotopomer. Bands at 2993 and 2905 cm^{-1} are the last to appear. Their frequencies are identical to the $\nu_{as}(CH_3)$ and $\nu_s(CH_3)$ modes of grafted CH_3ReO_3. Thus the IR spectrum supports the evolution of the surface methyl groups from CD_3 to CD_2H to CH_2D and, finally, to CH_3. Facile H/D exchange into the methyl ligand implies the ready formation of the methylene tautomer, Scheme 1.

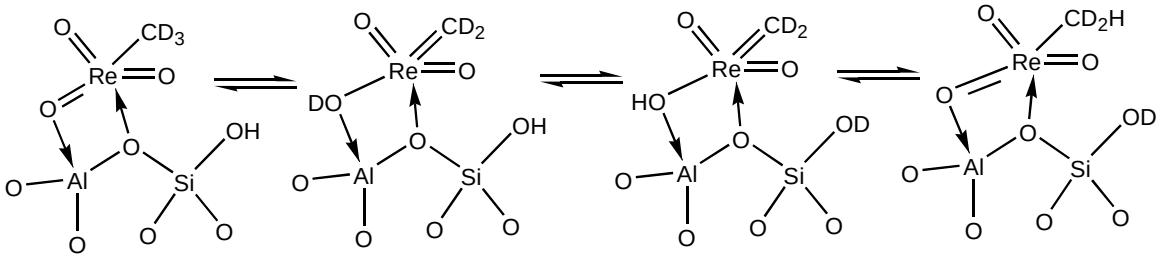

Scheme 1. Proposed mechanism of H/D exchange process for $MeReO_3$ supported on silica-alumina: (a) tautomerization to methylidene; H/D exchange with a neighboring silanol; tautomerization to methyl form.

DFT calculations elucidate how the silica-alumina support promotes tautomerization of $MeReO_3$. The energy difference between tautomers of $MeReO_3$ grafted onto the silica-alumina cube, Figure 6, is only 38 kJ/mol. The more favorable proton transfer relative to molecular $MeReO_3$ is a consequence of the strong binding of an oxo ligand to an Al site. This Lewis acid-base interaction leads to substantial

lengthening of the Re-O multiple bond, reducing the bond order and making this oxygen ligand a better proton acceptor. Investigation of the role of the methylene tautomer in olefin metathesis using isotope labeling studies must take facile H/D exchange with support protons into account. The exchange can be blocked by capping the surface hydroxyls with hexamethyldisilazane; this has the added benefit of suppressing olefin isomerization side-reactions catalyzed by silica-alumina.

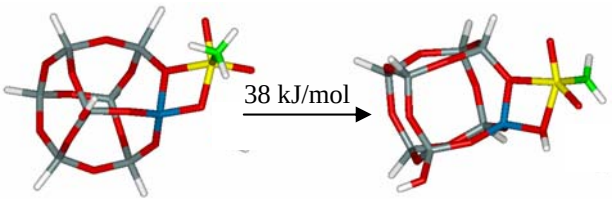

Figure 6. Energy-minimized structures of methyl and methylene tautomers for grafted $MeReO_3$ on a silica-alumina cube model.

Publications:

A. W. Moses, N. A. Ramsahye, B. F. Chmelka, J. Eckert, S. L. Scott, "Methyltrioxo-rhenium Activation by Chemisorption on Silica-Alumina", *J. Am. Chem. Soc.*, submitted for publication.

A. W. Moses, N. A. Ramsahye, S. K. Chattopadhyay, J. Eckert, S. L. Scott, "Evidence for Spontaneous Tautomerization of Methyltrioxorhenium Supported on Silica-alumina", manuscript in preparation.

Session B:

Clusters, Supramolecules and Biomolecules—Free and Confined In Pores and On Surfaces

Synthetically Modified Viral Capsids: Building Blocks for Nanoscale Materials

Matthew B. Francis
Department of Chemistry, University of California, Berkeley, CA 94720-1460, and Material Science Division, Lawrence Berkeley National Labs, Berkeley, CA 94720

The protein shells of viruses provide promising scaffolds for the construction of new materials. In addition to possessing nanoscale dimensions overall, the subunits that comprise the capsid shells can display attached components in a highly ordered fashion. To take advantage of these possibilities, orthogonal chemical strategies have been developed to functionalize the exterior and the interior surfaces of two different viruses. Polymer chains have been attached to the outer surface of bacteriophage MS2, and small molecule cargo has been installed inside. Similarly, hydrophobic groups have been installed on the exterior of the rod-like tobacco mosaic virus, and metal binding sites have been introduced in the hollow core. The physical properties and future applications of these materials will be presented.

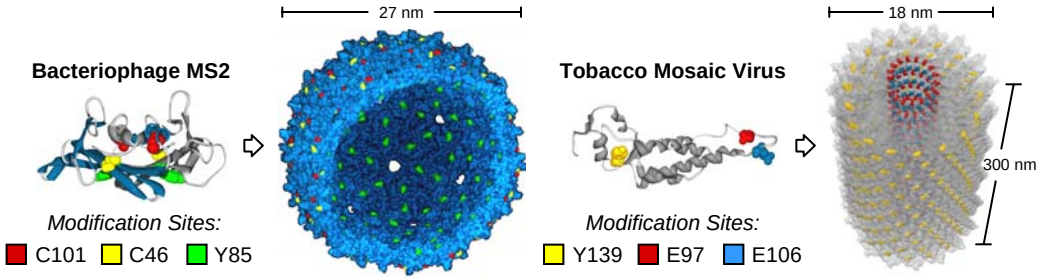

DE-FG02-87ER13790 & DE-FG02-04ER15513 **Bruce C. Gates**

The Role of Cations in Supported Metal Nanocluster Catalysts

Students: Bryan Enderle, Javier Guzman, Yalin Hao, Scott Kronewitter, Fen Li

Contact: Bruce C. Gates, Dept. of Chemical Engineering & Materials Science, University of California, Davis, CA 95616. Phone: (530) 756-4771; email: bcgates@ucdavis.edu

Goals

To prepare oxide- and zeolite-supported transition metal complexes and clusters; characterize by physical methods; determine their catalytic properties; and develop relationships between structure and catalytic activity. In particular, to focus on the role of cations in supported metal complexes and clusters and their influence on structure, reactivity, and catalytic properties.

Recent Progress

A review of our research area has been published in *Dalton Transactions*.[1] When metal complexes and clusters are bonded to oxide or zeolite supports, they may combine the technological advantages of solid catalysts (robustness for high-temperature operation, lack of corrosiveness, ease of separation from products) with the selectivity of soluble molecular catalysts. Supported mononuclear metal complexes are typically synthesized by the reaction of a mononuclear organometallic compound with oxygen atoms or OH groups of the support, giving structures shown by infrared, X-ray absorption, and NMR spectroscopies and density functional theory to be analogous to those of molecular species, but with the support playing the role of a multidentate ligand, bonding strongly to the metal and holding the groups apart from each other on the support surface. Some supported metal complexes have new and unexpected catalytic activities. Supported metal clusters are formed by adsorption or surface-mediated synthesis of metal carbonyl clusters, which under some conditions may be decarbonylated on the support with the metal frame remaining essentially intact. The decarbonylated clusters are bonded to the supports by metal–oxygen bonds similar to those characterizing supported metal complexes; even noble metals in clusters on supports at the metal–support interface are cationic, and the metal–oxygen distances are about 2.1–2.2 Å, matching the distances in mononuclear metal complexes with metal-oxygen bonds. Metal clusters are preferentially bonded at defect sites on oxide surfaces. The catalytic activities of supported metal clusters of only a few atoms are distinct from those of bulk metals; the supports act as ligands affecting the catalysis.

Metal Clusters in Zeolites: Zeolite NaY-supported $Ir_4(CO)_{12}$ was prepared by direct deposition onto the outside surface of the zeolite crystals and by reductive carbonylation of $Ir(CO)_2(acac)$ sorbed in its pores. These samples and the products of their decarbonylation and subsequent recarbonylation were characterized by infrared and extended X-ray absorption fine structure spectroscopies. The data show that the clusters in the zeolite pores were molecularly dispersed and could be reversibly decarbonylated and recarbonylated, whereas those on the outer surface outside the pores were aggregated under decarbonylation condition (300 °C in He) and could not be reversibly recarbonylated. The results demonstrate stabilization of the molecular clusters entrapped in the pores. The assembly of $Ir_4(CO)_{12}$ from $Ir(CO)_2(acac)$ precursors in the supercages of zeolite NaY was investigated by extended X-ray absorption fine structure and *in-situ* infrared (IR) spectroscopies. The data show that the conditions of pretreatment of the zeolite significantly affect the formation process of $Ir_4(CO)_{12}$. When the zeolite was initially largely dehydrated, so that the precursor molecules were well dispersed in the zeolite cages, dimeric intermediates in the formation of $Ir_4(CO)_{12}$ (approximated as $Ir_2(CO)_8$) were observed by both IR and EXAFS spectroscopies. In contrast, when the zeolite initially contained a substantial amount

of water, the resultant Ir_4 clusters were formed faster than those in dehydrated zeolite, and evidence of intermediates was not observed. The results show how synthesis in the confined spaces of the zeolite nanopores—in the absence of solvents—affords opportunities to control and elucidate the chemistry, different from those in solution.

Supported rhenium complexes: Rhenium carbonyls bonded to dealuminated Y zeolite (DAY) were synthesized from $HRe(CO)_5$ and characterized by infrared and extended X-ray absorption fine structure spectroscopies. In the zeolite calcined at 573 K, a mixture of rhenium carbonyls was formed, but in the zeolite calcined at 773 K, a nearly unique rhenium carbonyl was formed, represented as $Re(CO)_3\{O_{R4}^{2-}\}_2\{O_{R6}^{2-}\}$, with rhenium bonded to three surface oxygen atoms at a T5 site located at an aluminum center in the zeolite (the braces signify sites on the zeolite surface and the subscripts R4 and R6 refer to surface oxygen atoms at four-ring site and six-ring sites, respectively). The three surface oxygen atoms in the complex are not all equivalent, giving rise to a slightly distorted C_{3v} symmetry, consistent with the observed infrared spectra. Two Re–support oxygen distances were found by EXAFS spectroscopy, 2.09 and 2.47 Å. The Re–C and Re–carbonyl-oxygen distances were found to be 1.96 and 3.14 Å, respectively. The data show that rhenium carbonyls are good probes of three-fold surface sites of zeolites and oxides.

Supported gold catalysts: X-ray absorption near edge spectra and temperature-programmed oxidation and reduction data demonstrate that Au(I) and Au(0) are both present in working MgO-supported gold catalysts for CO oxidation. EXAFS data indicate gold clusters with essentially the same average diameter (about 30 Å) in each catalyst sample. Thus, the results provide no evidence of an effect of gold cluster size on the catalytic activity, but both the catalytic activity and the surface concentration of Au(I) were found to decrease with increasing CO partial pressure (as Au(0) was increasingly formed), showing that the catalytic sites incorporate Au(I) (Fig. 1).

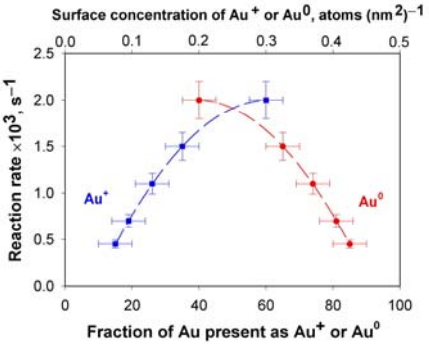

Figure 1. Correlation of the catalytic activity with the percentage and surface concentration of cationic and zerovalent gold (the concentrations of gold were calculated on the basis of the approximate surface area of MgO).

The structure, electronic state, and reactivity of MgO-supported gold cluster catalysts were investigated *in situ* during CO oxidation reaction with X-ray absorption spectroscopy (XAS) and with a once-through isothermal tubular packed-bed flow reactor. The data suggest that gold nanoparticles containing cationic gold(I) and zero valent gold are the stable species (being of about 30 Å in diameter) during CO oxidation reaction, regardless of the initial structure and oxidation state of the supported gold catalyst.

Mononuclear gold complexes supported on MgO powder were prepared by adsorption of $Au(CH_3)_2(C_5H_7O_2)$ and tested as catalysts for ethylene hydrogenation at atmospheric pressure and 353 K. The catalyst was characterized in the working state with extended X-ray absorption fine structure (EXAFS), X-ray absorption near edge structure (XANES), and infrared (IR) spectroscopies. EXAFS and XANES data demonstrate the presence of mononuclear Au(III) complexes as the predominant surface gold species during catalysis, with no evidence of metallic gold clusters, confirmed by the lack of Au–Au contributions in the EXAFS spectra and the presence of the characteristic features of Au(III) in the XANES spectra. The mononuclear gold complex is bonded to two oxygen atoms of the MgO surface at an Au–O distance of 2.16 Å. Ethyl and π-bonded ethylene on the mononuclear gold were identified by IR spectroscopy, with the former identified as a reactive intermediate and the latter apparently a spectator. Hydrogen on

the mononuclear gold is inferred to form by dissociative adsorption of H_2, as indicated by the order of the catalytic reaction in H_2 of 0.5. Gold catalysts supported on γ-Al_2O_3 (Au/γ-Al_2O_3) were prepared by deposition-precipitation of aqueous $HAuCl_4$ and, alternatively, by deposition of $Au(CH_3)_2(acac)$ from pentane solution. The samples were characterized by in-situ XANES and temperature-programmed reduction and by their performance as CO oxidation catalysts at room temperature. The Au was found to be present as Au(III) in both as-prepared catalysts, and the Au(III) was stable upon exposure to reducing gases at room temperature. Reduction of Au(III) occurred at elevated temperatures, and the rate and extent of reduction were found to depend strongly on the reducing conditions. Water vapor facilitated reduction, but only after the sample had been reduced to some extent by CO or H_2. Exposure of an as-prepared catalyst to a catalytically reacting mixture of CO + O_2 at 100 °C was effective in activating it, though to a lesser extent. The data indicate that zerovalent Au is necessary for catalytic activity, but there is no correlation between the activity and the extent of reduction, and both cationic Au and water or surface species derived from water may also play a role in the catalytic sites.

Publications citing support from the DOE grant, 2003–2005

1. "Structure and Reactivity of a Mononuclear Gold Complex Catalyst Supported on Magnesium Oxide," J. Guzman and B. C. Gates, *Angew. Chem. Int. Ed.*, **42**, 690 (2003).
2. "Oxidation States of Gold in MgO-Supported Complexes and Clusters: Characterization by X-ray Absorption Spectroscopy and Temperature Programmed Oxidation and Reduction," J. L. Guzman and B. C. Gates, *J. Phys. Chem. B*, **107**, 2242 (2003).
3. "Oxidation of Supported Rhodium Clusters by Support Hydroxyl Groups," G. N. Vayssilov, B. C. Gates, N. Rösch, *Angew. Chem. Int. Ed.*, **42**, 1391 (2003).
4. "Reaction of $Au(CH_3)_2(acac)$ on γ-Al_2O_3: Characterization of the Surface Organic, Organometallic, Metal Oxide, and Metallic Species," J. Guzman and B. C. Gates, *Langmuir*, **19**, 3897 (2003).
5. "Alkene Hydrogenation Catalyzed by Rhenium Carbonyls Bonded to Highly Dealuminated Y Zeolite: Spectroscopic Characterization of the Working Catalyst, " B. Enderle and B. C. Gates, *J. Mol. Catal. A Chem.*, **204**, 473 (2003).
6. "Supported molecular catalysts: metal complexes and clusters on oxides and zeolites," J. Guzman and B. C. Gates, *Dalton Trans.*, **2003**, 3303 [Dalton Perspective].
7. "Synthesis and Structural Characterization of Iridium Clusters Formed Inside and Outside the Pores of Zeolite NaY," F. Li and B. C. Gates, *J. Phys. Chem. B*, **107**, 11589 (2003).
8. "Metal Carbonyl Cluster Synthesis in Nanocages: Spectroscopic Evidence of Intermediates in the Formation of $Ir_4(CO)_{12}$ in Zeolite NaY," F. Li and B. C. Gates, *J. Phys. Chem. B*, **108**, 11259 (2004).
9. "A rhenium carbonyl bonded to highly dealuminated zeolite Y: structure determination by infrared and X-ray absorption spectroscopies," B. Enderle and B. C. Gates, *Phys. Chem. Chem. Phys.*, **6**, 2484 (2004).
10. "Catalysis by Supported Gold: Correlation Between Catalytic Activity for CO Oxidation and Oxidation States of Gold," J. Guzman and B. C. Gates, *J. Am. Chem. Soc.*, **126**, 2672 (2004).
11. "Formation of Gold Clusters on TiO_2 from Adsorbed $Au(CH_3)_2(C_5H_7O_2)$: Characterization by X-Ray Absorption Spectroscopy," J. Guzman, S. Kuba, J. C. Fierro-Gonzalez, and B. C. Gates, *Catal. Lett.*, **95**, 77 (2004).
12. "A Mononuclear Gold Complex Supported on MgO: Spectroscopic Characterization during Ethylene Hydrogenation Catalysis," J. Guzman and B. C. Gates, *J. Catal.*, **226**, 111 (2004).
13. "Activation of Au/γ-Al_2O_3 Catalysts for CO Oxidation: Characterization by X-ray Absorption Near Edge Structure and Temperature Programmed Reduction," C. K. Costello, J. Guzman, J. H. Yang, Y. M. Wang, M. C. Kung, B. C. Gates, and H. H. Kung, *J. Phys. Chem. B*, **108**, 12529 (2004).
14. "Effects of Adsorbates on Supported Platinum and Iridium Clusters: Characterization in Reactive Atmospheres and during Alkene Hydrogenation Catalysis by X-ray Absorption Spectroscopy," O. S. Alexeev, F. Li, M. D. Amiridis, and B. C. Gates, *J. Phys. Chem. B*, **109**, 2338 (2005).
15. "Synthesis and Reactivity of Dimethyl Gold Complexes Supported on MgO: Characterization by Infrared and X-Ray Absorption Spectroscopies," J. Guzman, B. G. Anderson, C. P. Vinod, K. Ramesh, J. W. Niemantsverdriet, and B. C. Gates, *Langmuir*, in press (2005) [web version available].

DE-FG02-03ER15462 **Mekki Bayachou**

Electron transfer, Oxygen Activation, and NO Biosynthesis: An Integrative Electrochemical, Biochemical, and Computational Approach

PI: Mekki Bayachou
Co-PIs: Gogonea, V. (Cleveland State Univ.) and Zhou, A. (Cleveland State Univ.)
Postdocs: Lee Chunyeon; Biswas, Pradip; Quirk, David
Students: Boutros, A. Jean; McCulloch, Melissa; Li, Ling; Dogaru, Daniela; Peiris, Pubudu; Shy. Jacinto; Jiansen Niu

Contact Information: Department of Chemistry SR397, Cleveland State University, Cleveland, OH 44115
Phone: 216-875-9716
Fax: 216-687-9298
m.bayachou@csuohio.edu

Goals:

The bio-catalytic transformations carried out by enzymes are of particular interest for the fundamental understanding of nature's ultimate control of chemical reactivity. Developing an understanding of the mechanisms of elemental steps of enzymatic catalysis is one of the main headlines of the overall research goals of this project. We are particularly interested in mechanistically "visualizing" the synergistic structural and kinetic control of elemental steps involved in the biocatalytic synthesis of nitric oxide (NO) by nitric oxide synthases (NOS). NOS enzymes belong to a family of complex flavo-heme enzymes which carry the five-electron oxidation of the substrate L-arginine using oxygen as a co-substrate to the product, NO, and L-citruline as a byproduct. The reaction takes place on an Fe-heme active center and proceeds in intricate steps with perfect coordination of a number of partners and superior kinetic and structural control of every step in the overall path. This represents a perfect platform for us to learn more how this complex catalysis is carried out at the atomic level. We are particularly interested in investigating the molecular mechanisms involved in the regulation and execution of electron transport and oxygen activation at various steps of the NOS catalysis. In this project we use an approach integrating direct electrochemistry, site-directed mutagenesis/molecular biology and computational chemistry to develop molecular-level understanding of the NOS biocatalysis, and particularly how the long-range structural control and tunable redox activity affect kinetics of critical steps of this catalysis.

Specific goals for the current funding period include thorough investigation of the first electron transfer event of the NOS catalytic cycle, and correlation of the heme pocket structure to direct electrochemical response. In addition, we set out to study closely the role of the tetrahydrobiopterin cofactor (H_4B) in the activation of the critical ferrous-dioxy intermediate. We therefore planned to address the spectro-electrochemical properties of H_4B on one hand, and redox properties of the ferrous-dioxy intermediate on the other. Other specific goals

include kinetic investigation of immobilized NOS oxygenase under turnover conditions, including accurate determination of NO generated in situ, and identification of a ferrous-nitrosyl intermediate involved in a dynamic feedback inhibition of the enzymatic function. On the computational front, and to better help our experimental endeavors, plans are set to develop an interface coupling the Car-Parrinello molecular dynamics code to the popular Gromacs molecular mechanics code. In the same front, the determination of crucial OPLS parameters of the P450 heme group of the NOS oxygenase as well as a zinc finger structural moiety is targeted. Finally, our previous experimental and computational effort identified possible critical residues of interest in the NOS cycle; we therefore set out to study experimentally the functional importance of these residues through site-directed mutagenesis.

DOE Interest:

Design of the next generation of catalysts integrating smart molecular features, found for instance in the function of enzymes, remains a challenge, in part because of our limited fundamental understanding of how elemental steps of complex enzymatic reactions are controlled. Therefore, developing a molecular-level understanding of the catalytic function of nature's best catalysts (i.e. enzymes), their dynamic structural flexibility, and long-range ultimate control of reactivity and selectivity, is a pre-requisite to integrate these important concepts in the challenge of molecular design of next generation of catalysts.

Research Plan:

The catalytic function of NOS enzymes embodies a unique case of ultimate molecular control exhibited by a "living catalyst" in very mild conditions. This case offers an ideal platform for us chemists to learn more from nature's optimal control of catalysis and chemical transformations.

To address the complex function of the biocatalytic synthesis of nitric oxide, we adopted a research plan that coordinates cross-disciplinary efforts among three research teams. In this unique setting, our synergistic efforts revolve around experimental measurements of tunable redox properties of various states of the oxygenase domain of NOS and critical intermediates in the catalytic cycle. Our direct electrochemical and spectro-electrochemical investigations are carried on both wild-type and mutants prepared by site-directed mutagenesis, and which are judiciously identified by molecular dynamics coupled to QM/MM computational calculations as candidates to probe our hypotheses on electron transport and oxygen activation. Our experimental observations and measurements also provide feed-information for more computational investigations, which in turn yields to insights on structural information vital to NOS catalysis, and that can be tested experimentally. The Bayachou lab at CSU conducts all direct electrochemical and spectro-electrochemical efforts, including enzyme immobilization, interface characterization, and *in situ* assays of activity. The Gogonea lab carries out computational investigations with close feedback with the Bayachou lab. The Zhou lab conducts all aspects of biochemical and molecular biology efforts, including NOS-oxygenase expression, purification, and characterization. Molecular biology efforts are guided by findings from direct electrochemical investigations in close interaction with the computational calculations. This system-approach that we adopted is powerful to meet the challenge of our chosen biocatalysis platform, the NOS catalysis, for exploration and development of a clear understanding of the modulated redox properties of NOS, the intricate molecular control of oxygen activation and other intermediates in the path of NO biosynthesis.

Recent Progress:

Significant progress has been achieved on all fronts and according to the objectives of the current period. Below, we briefly outline major results for each specific goal.

Thorough characterization of NOS oxygenases embedded in bilayered thin surfactant films on electrode surface: Understanding how the NOS oxygenases are embedded in our bilayered films on electrode surfaces is of particular interest. In this period, we used high resolution atomic force microscopy (AFM) to characterize the heme enzymes in our films. We find that all the NOS oxygenase enzymes are totally embedded in the relatively 1-micron thick film. There was no evidence for enzymes protruding from the film, nor was there evidence for enzyme aggregates on the surface. Topographically, the surface of the film appears very smooth and all NOS enzymes well embedded in the bilayered film.

Characterization of the first electron transfer of the catalytic cycle: We thoroughly characterized the first electron transfer to the iron heme of NOS oxygenases (iNOSoxy and nNOSoxy). Heterogeneous rates for electron transfer were determined for NOS oxygenases embedded in bilayered thin films on electrodes. We also continued investigations on how the redox properties of the heme catalytic center are modulated by the substrate and the cofactor. We also closely determined substrate and cofactor relative affinities to Fe^{III} and Fe^{II} redox states of the NOS oxygenase.

Correlation of structure of heme pocket to electrochemical response: We interrogated the role of a conserved residue in the heme pocket in the redox behavior of the heme center and particularly in relation to the first electron transfer. In initial spectro-electrochemical investigation, we showed that a proximal tryptophane residue (Tryp 409) is apparently crucial in modulating the redox behavior of NOS. In the current period we carried thorough electrochemical investigation of the W409F mutant and contrasted its behavior to wild type NOS oxygenase.

Relative Stability of the ferrous dioxy intermediate and effect of the tetrahydrobiopterin cofactor: We carried out comparative study of the oxygen activation gate, the ferrous dioxy intermediate, in the presence and absence of the H_4B cofactor. Although this intermediate is fast decaying and fast scans need to be utilized to track it, the presence of H4B cofactor seem to make it less stable and nearly undetectable.

NOS under turnover conditions; electrochemical measurement of NO generated in situ: In effort to understand better our electrochemically-driven NOS turnover in the thin films, we developed unique carbon fibers modified with a nano-structured catalyst and with enhanced NO detection capability. With this setup were able to measure in real-time NO generated on our NOS modified electrodes, on which NO synthesis is driven and monitored electrochemically. We also designed other fibers with enhanced detection of peroxynitrite, a signature of potential uncoupling of oxygen activation and NO synthesis. All of these endeavors are of particular importance in the study of NOS-modified electrode under turnover conditions.

Ferrous-nitrosyl form of NOS: we thoroughly characterized this intermediate involved in the dynamic feedback inhibition of NOS catalysis. A redox midpotential of ca. -850 mV/AgAgCl has been determined for this intermediate in the surfactant film. In addition the

preliminary results on the kinetic investigation of the catalytic reduction of the product, nitric oxide, by the NOS enzyme have been obtained.

An interface coupling the CPMD code to Gromacs MM code and OPLS parameters for critical parts of the functional NOS dimer: To better help the experimental effort, we decided to develop an interface between two well known computational codes: the QM code CPMD (Car-Parrinello molecular dynamics) and the MM code Gromacs (Groningen Machine for Chemical Simulations). During this development phase we aslo addressed some difficulties that QM/MM methods share, that is, the treatment of the electrostatic interactions between the QM and MM regions. We also developed OPLS (Optimized Potentials for Liquid Simulation) parameters for the P450 heme (heme ligated by cysteine) and a zinc finger moiety (Zn ligated by four cysteine residues) that bridges between tow NOS monomers. The OPLS parameters were developed using a genetic algorithm (GA) optimization program developed in our group. Molecular mechanics optimization using these parameters reproduces the quantum mechanical geometry and vibrational frequencies.

New mutants to interrogate a conserved residue about its potential role in electron transfer, and in assisting H_4B-mediated oxygen activation: an arginine residue, R381 in iNOSoxy, which is conserved among all NOS isoforms and throughout species, is suspected to play a crucial role in assisting the second electron transfer needed for oxygen activation within the NOS catalytic cycle. We set out to change the nature of this residue to interrogate its importance for oxygen activation and overall in enzyme turnover. In this regard, two site-directed mutants, R381K and R381A, are targeted and one of them (R381K) successfully expressed. Direct electrochemical characterization of redox behavior of this mutant is now planned, as well as its kinetic characterization under turnover conditions both in films (i.e. electrochemically driven) and in solution (chemically-driven).

Future Plans:

Future plans include thorough electrochemical and spectro-electrochemical characterization of the new mutants in order to compare and contrast their behavior to that of wild type, and determine the functional roles of the residues identified. We also will finalize the characterization of redox properties of the ferrous-dioxy intermediate and how these are modulated by identified residues in the heme pocket. In addition, extensive molecular dynamics simulations coupled to QM/MM calculations will now be facilitated on our newly developed interface, which will help identify more structural features of mechanistic importance in the NOS catalysis. These predictions will in turn be probed experimentally through site-directed mutagenesis and spectro-electrochemical investigations. In parallel, we will continue our electrochemical investigation on the catalytic reduction of the NOS reaction product, i.e. NO, by the NOS oxygenase itself in thin film. The kinetic investigation of this catalytic reaction, in combination with inhibition studies using potent NOS inhibitors, will help us quantify the degree of dynamic feedback deactivation of NOS oxygenase during catalytic turnover.

Publications

1. Bayachou, M.; Boutros, J. “Direct electron transfer to the oxygenase domain of neuronal nitric oxide synthase (NOS): Exploring unique redox properties of NOS enzymes”, *J. Am. Chem. Soc.*, **2004**, *126*, 12722-12723.

2. Perera, I.; Bayachou, M. “Eliminating absorbing interference using the H-point standard addition method: case of Griess assay in the presence of interferent heme enzymes such as NOS” *Anal. Bioanal. Chem*., **2004**, *379*, 1055-1061.
3. Imoos, C.E.; Chou, J.; Bayachou, M.; Farmer, P.J. “Electrocatalytic reductions of nitrite, nitric oxide, and nitrous oxide by thermophilic cytochrome P450CYP119 in film-modified electrodes and an analytical comparison of its catalytic activities with myoglobin” *J. Am. Chem. Soc*., **2004**, *126*, 4934-4942.
4. He, P.; Bayachou, M. “Layer-by-layer fabrication and characterization of DNA-wrapped single-walled carbon nanotubes”* *Langmuir*, **2005,** Accepted (to appear ASAP).*this is a development of another platform on which NOS and other enzymes of interest can be embedded and studied electrochemically.
5. Peiris, P; Peteu, S.; Bayachou, M. “Electrochemical sensors for peroxynitrite detection on NOS-modified electrodes” *Anal. Chem.* **2005**, submitted.
6. Bayachou, M. Peiris, P. “Carbon fiber modified with nanostructured catalyst for ultra-sensitive nitric oxide detection” *Anal. Chem.* **2005**, to be submitted after approval of a patent (now disclosed to CSU).
7. Gogonea V.; d “Potential energy surface for the reaction of imidazole with peroxynitrite: A density functional theory study” *Int. J. Quant. Chem.*, **2005** Accepted, in print.
8. Biswas, P. K.; Gogonea, V. “A renormalized electrostatic coupling Hamiltonain for hybrid quantum mechanical molecular mechanical calculations” *J. Chem. Phys.*, **2005**, submitted.
9. Gogonea, V.; Shy, J. “Derivation of force field parameters for molecular mechanics atom types used in computer simulations: A combined genetic algorithm – neural networks based methodology”, *J. Comp. Chem.*, **2005**, to be submitted
10. Gogonea, V.; Biswas, P. K.; Shy, J.; Wagner, M. “Molecular dynamics simulation of inducible nitric oxide synthase: The role of tetrahydrobiopterin cofactor in enzyme’s activity” *J. Phys. Chem. B*, **2005**, to be submitted.
11. Boutros, A. J.; **Bayachou, M.** “Turnover of nitric oxide synthase on NOS-modified electrodes: NO biosynthesis driven electrochemically” *Angewandte Chemie Int. Ed.* **2005**, in preparation.

DE-FG03-05ER15632 **John A. Shelnutt**

Growth of Metal and Semiconductor Nanostructures Using Localized Photocatalysts

Students:	Raid Haddad (UNM)
Postdocs:	Zhongchun Wang (UGA), Haorong Wang (UGA)
Collaborators:	Eric Nuttall (UNM), Frank van Swol (Sandia, UNM), Yujiang Song (SNL), Yingbing Jiang (UNM), Craig J. Medforth (SNL), Eulalia Pereira (U Porto)
Contact:	John A. Shelnutt, Advanced Materials Laboratory, 1001 University Blvd. SE, Albuquerque, NM 87106 Phone: (505) 272-7160; Email: jasheln@unm.edu Web page: http://jasheln.unm.edu

Goal

Our main objective is to investigate a new and novel light-driven approach to the controlled growth of metal and semiconductor nanostructures and nanomaterials. This bio-inspired photochemical process uses porphyrin photocatalysts to produce metal nucleation and growth centers at which aqueous metal ions are reduced at ambient temperatures. By pre-positioning the porphyrins at the nanoscale, the location and morphology of the metal nanostructures can be controlled. Self-assembly, chemical confinement, and molecular templating are some of the methods used for nanoscale positioning of the photocatalyst molecules. When exposed to visible light, the localized porphyrins reduce and deposit metal in their vicinity leading to the formation of the nanostructures. Our goals are to elucidate the processes involved in the photocatalytic growth of metal nanostructures, and in so doing discover the range of nanomaterials that can be made by these methods.

Recent Progress

Surfactant-Templated Platinum and Palladium Nanostructures: We have continued to study the photocatalytic method for controlling the growth of novel platinum metal nanostructures and nanomaterials templated on surfactant assemblies (especially liposomes) containing the photocatalyst. When the porphyrin photocatalyst is localized in micelles, we previously had obtained three-dimensional globular dendrites with diameters between 3-100 nm, and we showed that the size and uniformity of these nanodendrites could be controlled by altering the platinum-to-photocatalyst concentration ratio and/or the light exposure. Size control was realized by the Sn-porphyrin growing an initial population of platinum seed nanoparticles as growth centers. We also showed that 2-nm thick dendritic sheets of platinum could be grown on liposomal surfaces.

The control of Pt growth on liposomes using Sn-porphyrin photocatalysts (See Fig. 1) leads to a wide variety of useful Pt nanomaterials from large continuous dendritic Pt sheets covering aggregated liposomes (Fig. 1a), to individual 3-nm Pt particles (not shown) or small Pt dendritic sheets (Pt daisies) decorating the surface of the liposomes, to joined Pt daisies coating individual liposomes (Fig. 1b and Inset).

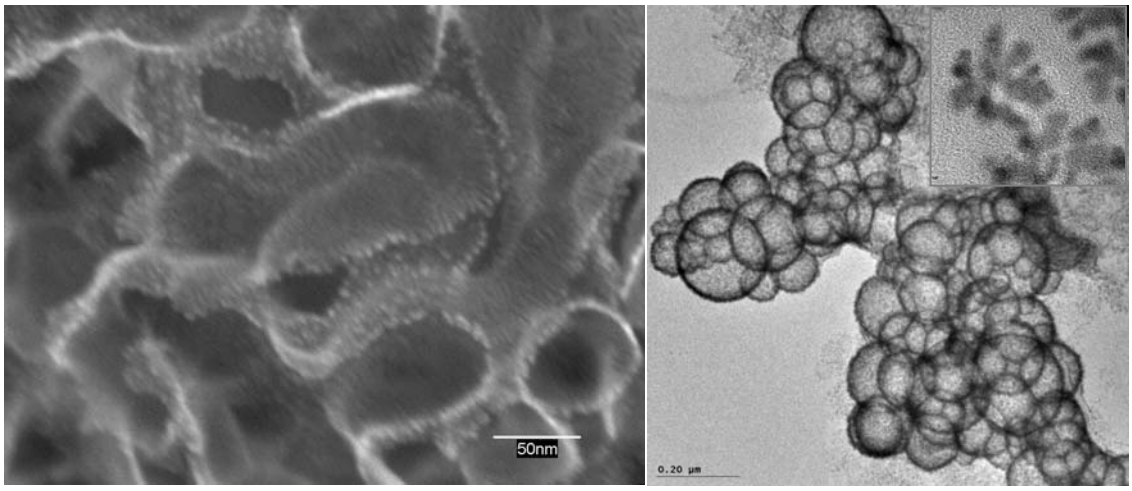

Figure 1. (a) Extended Pt dendritic sheet and (b) joined Pt "daisies" covering aggregated liposomes. Inset: Pt daisies linked together at tips of the arms of the dendrites.

We anticipate that these Pt nanomaterials may provide unique electrocatalytic properties as a consequence of their extended structure. Significantly, these self-supporting, high surface area formulations may have bulk Pt catalytic properties while retaining nanometer scale feature size. Surface areas measured by BET and CO-stripping methods are indistinguishable from commercial fuel-cell grade platinum black (Aldrich, ETEK), and activity in the oxygen reduction reaction is also equivalent.

Photocatalytic Porphyrin Nanostructures as Templates for Platinum and Gold: We recently discovered that porphyrins can form nanotubes and other nanostructure like fiber, planks, *etc*. composed entirely of mixtures of two porphyrins—one anionic and the other cationic. When one of these porphyrins is photocatalytic, the nanotubes and other nanostructures can serve as templates for the growth of metal which can deposit selective onto surfaces (Fig. 2).

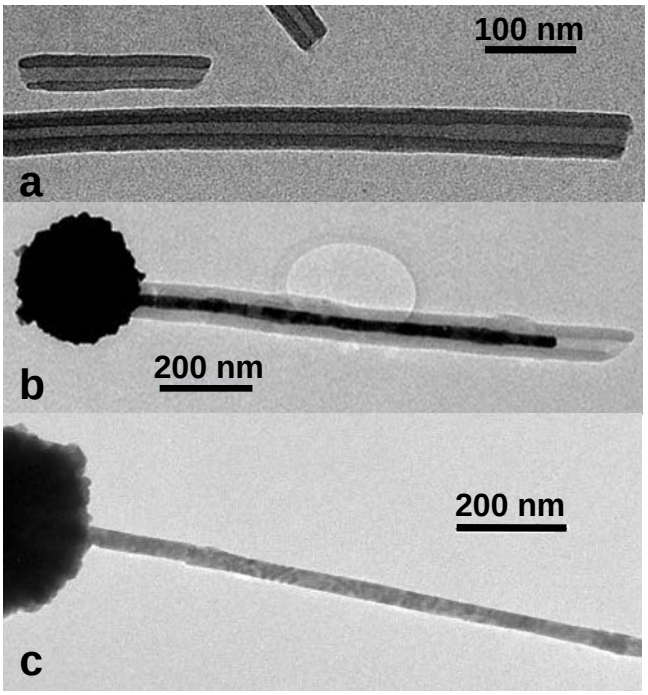

Figure 2. *TEM images of (a) the porphyrin nanotubes, (b) a gilded nanotube, and (c) a gold wire obtained after the porphyrin tube has been dissolved away, demonstrating the structural integrity of the free standing nanowires.*

DOE Interest

The research has lead to nanoengineered materials for applications in catalysis, electro-catalysis, and possibly nano-electronics and photonics. While composed of platinum, palladium, and gold deposited onto the templating nanostructures, the synthetic methods developed may also be useful for other metals and semiconductors. A fundamental understanding of the uses and limitations of photocatalysis as a

means of producing metal and semiconductor nanostructures and nanomaterials is emerging and is expected to lead to further new nanostructures and energy applications. We are in CRADA negotiations with an automotive manufacturer for developing the Pt nanomaterials as electrocatalysts and with InfraSUR LLC, a small business, for using photocatalytic metal reduction for environmental remediation.

Future Plans

We need to further explore the role of interaction between the surfactant, the reductant (ascorbic acid), and the metal surface in controlling the dendritic growth process. We will also investigate additional templating materials, develop the photocatalytic method for new metals and alloys (Pt, Pd, Ni, Fe, Rh), formulate new composite nanodevices by sequential addition of different metals, determine the minimum size of nanoparticles that can be made, and continue to determine the thermal and mechanical stability, porosity, and other materials properties.

For the porphyrin-nanostructure templates, we will make new metal-nanotube composite structures and investigate their photocatalytic, optical, and electronic properties, particularly their light-harvesting and electron-transport properties. The plasmonic properties of metal nanostructure grown inside and/or outside of the tubes may also be investigated.

Now that we have obtained control over the diameter of peptide nanotubes, we will study the potential synthesis and uses of porphyrin-modified tubes for growing metal nanostructures. We will also examine the photocatalytic reduction of other metals and semiconductors for waste treatment and nanotagging of proteins and membranes. Experimental techniques to be used are electron microscopy (TEM, SEM), AFM, confocal microscopy, XRD, UV-visible, fluorescence and Raman spectroscopy.

Publications (2003-2005)

- Song, Y.; Yang, Y.; Medforth, C. J.; Pereira, E.; Singh, A. K.; Xu, H.; Jiang, Y.; Brinker, C. J.; van Swol, F.; Shelnutt, J. A. "Controlled Synthesis of 2-D and 3-D Dendritic Platinum Nanostructures" *J. Am. Chem. Soc.* **2004**, *126*, 635-645.
- Song. Y.; Challa, S. R.; Haddad, R. E.; Medforth, C. J.; Qiu, Y.; Watt, R. K.; Peña, D. A.; Miller, J. E.; van Swol, F.; Shelnutt, J. A. "Synthesis of peptide-nanotube platinum-nanoparticle composites" *Chem. Commun.* **2004**, 1044-1045.
- Song. Y.; Pincus, J.; Sasaki, D.; Medforth, C. J.; Qiu, Y.; Shelnutt, J. A. "Photocatalytically Nanoengineered Platinum Foam-Like Materials Templated on Liposomes" *J. Am. Chem. Soc.* **2005** in preparation.
- Song, Y.; Haddad, R. E.; Jia, S.-L.; Hok, S.; Olmstead, M. M.; Nurco, D. J.; Schore, N. E.; Zhang, J.; Ma,; J.-G.; Smith, K. M.; Gazeau, S.; Pecaut, J.; Marchon, J.-C.; Medforth, C. J.; Shelnutt, J. A. "Energetics and Structural Consequences of Axial Ligand Coordination in Nonplanar Nickel Porphyrins" *J. Am. Chem. Soc.* **2005**, *127*, 1179-1192.
- Wang, Z.; Medforth, C. J.; Shelnutt, J. A. "Porphyrin Nanotubes by Ionic Self-Assembly" *J. Am. Chem. Soc*. **2004**, *126*, 15954-15955.
- Wang, Z.; Medforth, C. J.; Shelnutt, J. A. "Self-Metallation of Photocatalytic Porphyrin Nanotubes" *J. Am. Chem. Soc*. **2004**, *126*, 16720-16721.

DE-FG02-04ER15598 **James F. Haw (USC)**
DE-FG02-04ER15600 **Bruce C. Gates (UC Davis)**
DE-FG02-04ER15601 **Mark E. Davis (Caltech)**
DE-FG02-04ER15599 **John J. Rehr (U Washington)**

CATALYSIS SCIENCE INITIATIVE: **Supported Molecular Catalysts: Synthesis, In-Situ Characterization and Performance**
Period: 8/1/04 to 7/31/07

Additional PIs: Nigel Browning (UC Davis), Simon Bare (UOP LLC), John Low (UOP LLC), David Dixon (U Alabama), Juergen Eckert (LANL), Chi-Chang Kao (NSLS), Daniel Fischer (NIST), John Nicholas (Neurionpharma)
Post-docs: David Marcus (USC), Fernando Vila (U Washington),
Students: Justin Ehresmann (USC), Joe Abubakar (USC), Jeff Lee (USC), Yoni Blau (USC), Fen Li (UC Davis—former), Vinesh Bhirud (UC Davis—former), Rodrigo Lobo (UC Davis—current), Alper Uzun (UC Davis—current), Ryan Zeidan (Caltech)

University of Southern California
Department of Chemistry
Los Angeles, CA 90089
(213) 740-1022
jhaw@usc.edu

University of California, Davis
Department of Chemical
Engineering and Materials Science
One Shields Avenue, Davis, CA 95616
(530) 752-3953
bcgates@ucdavis.edu

California Institute of Technology
Department of Chemical Engineering
Pasadena, CA 91125
(626) 395-4251
mdavis@cheme.caltech.edu

University of Washington
Department of Physics
Seattle, WA 98195-1560
(206) 543-8593
jjr@phys.washington.edu

Goals:

The goals of this multi-investigator project are to investigate supported metal-complex and metal-cluster catalysts synthesized to have virtually molecular structures, including representations of the metal, the support, and the adsorbed species and with the samples in the catalytically functioning state. The project will bring together theory and experiment, including characterization by IR, EXAFS, XANES, NMR, and other spectroscopies, as well as high-resolution TEM. Much of the work is to be carried out with zeolites as catalyst supports, and this will link with work on zeolites themselves as catalysts. The project started on August 1, 2004. Research accomplished in the period of eight months since then is summarized in this report. Papers listed below have been submitted for publication, but it is too early in the project for any publications to have appeared.

DOE Interest:

Catalysts consisting of nearly uniform (molecular) structures on solid supports offer the advantages of solids (ease of separation from products, lack of corrosion) combined with the advantages of molecular catalysts in solution, including high selectivities. Supported molecular catalysts can be designed to offer

- robustness for operation at high temperatures
- sites in cages for control of the nanoenvironment and transport selectivity; and

- multicenter catalytic sites in cages and porous confines to facilitate subtle control of reaction chemistry, even for multistep reactions.

The latter catalysts mark a significant step toward the subtlety and selectivity of nature's catalysts, the enzymes.

Supported molecular catalysts have already found important industrial applications, exemplified by the metallocenes used for alkene polymerization. This class of catalyst—of interest because precisely synthesized samples can be so highly uniform and subject to such incisive characterization—also offers compelling opportunities for fundamental investigations that will propel the rapid advancement of catalysis science. These catalysts will stimulate collaborations between experimentalists and theorists; between synthesis, characterization, and performance experts; and between those whose roots are in molecular chemistry, surface chemistry, materials science, and biosciences. Our proposal is for a concerted attack on the science of supported molecular catalysts.

Research Plan:

The technological advantages of solid catalysts (robustness for operation at high temperatures, lack of corrosion, and ease of separation of products) can be combined with the advantages of soluble catalysts (e.g., selectivity) by synthesis of structurally discrete, nearly uniform catalysts on supports. Such supported molecular catalysts have already found important industrial applications (e.g., for alkene polymerization). They also open a door to unprecedented fundamental understanding. Because catalysts with precisely synthesized sites can be characterized incisively, the proposed research will propel the advancement of catalysis to a new level, stimulating the unification of the now disparate subfields of homogeneous, heterogeneous, and bio catalysis.

We will use molecular chemistry in the nano-scale cages of zeolites and on surfaces of tailored porous solids for precise synthesis of catalysts with discrete, uniform, well-defined sites, ranging from acids to metal complexes and nano-clusters, characterizing them–in the functioning state–with the following advanced experimental techniques (among others):

- X-ray absorption spectroscopy;
- NMR spectroscopy;
- IR spectroscopy;
- UV-visible spectroscopy;
- Neutron scattering and spectroscopy;
- EPR spectroscopy; and
- High-resolution TEM.

Fundamental theory will be used in concert with experimentation to interpret the results, provide bases for design of new catalysts, and improve methods of data analysis.

Recent Progress:

The most thoroughly investigated and best-understood supported catalysts are metal complexes such as $Rh(CO)_2$ and metal clusters such as Ir_4. One of our goals was to prepare supported rhodium complexes with ligands that are more reactive than CO and that could be catalytic reaction intermediates. We have preliminary data characterizing Rh complexes on zeolite USY (and on MgO) incorporating ethylene ligands; these can be hydrogenated to give ethane, and the sample appears to be a catalytic intermediate in alkene hydrogenation. The samples have been characterized by IR and EXAFS spectroscopies in the Gates group, with ^{13}C NMR experiments underway in the Haw laboratory.

Some of the best-defined clusters on supports are osmium clusters synthesized from osmium carbonyls such as $Os_3(CO)_{12}$. Oxidative fragmentation of these clusters adsorbed on MgO powder was investigated by X-ray absorption spectroscopy and scanning transmission electron microscopy (STEM)

(in a collaboration involving the Gates and Browning groups), Figure 1. Exposure of the clusters to air leads to their fragmentation, oxidation of the osmium, and formation of ensembles consisting of three Os atoms. X-ray absorption near edge spectra demonstrate the oxidative nature of the fragmentation process. Extended X-ray absorption fine structure (EXAFS) spectra indicate an average Os–Os distance of 3.33 Å, consistent with the formation of ensembles of three Os atoms on the support. STEM images confirm the presence of such tri-nuclear ensembles, and the diameters of the observed scattering centers (6.0 Å) match that indicated by the EXAFS results. The result is important in demonstrating that we can prepare nearly uniform supported metal clusters with our synthesis methods.

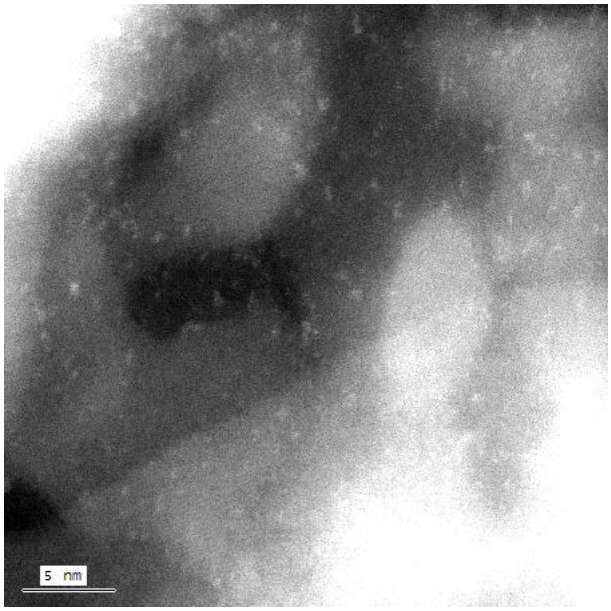

Figure 1. Z-Contrast image of sample formed from $Os_3(CO)_{12}$ supported on MgO after treatment in air at room temperature for 1 h.

We prepared a family of iridium clusters in zeolite NaY, including Ir_4 and Ir_6. Because recent theoretical work shows that such small noble metal clusters on hydroxylated supports are strongly stabilized by the presence of hydride ligands (formed by reverse spillover from support OH groups), we reasoned that it should be possible to detect the hydrogen on the clusters experimentally, even in the absence of H_2 gas in contact with the sample. Zeolite-supported iridium clusters were prepared by reductive carbonylation of $Ir(CO)_2(acac)$ sorbed in the zeolite pores to form $Ir_6(CO)_{16}$, which was decarbonylated by treatment in He. The Ir content of the samples was as high as 33.0 wt%. EXAFS spectra of the decarbonylated samples indicate that the clusters are well approximated as octahedral Ir_6 in the zeolite cages. The high loadings of clusters in the zeolite allowed characterization of the hydride ligands formed by ^1H NMR spectroscopy and inelastic neutron scattering spectroscopy (Figs 2, 3). These ligands were found to exist on the clusters even in the absence of H_2 in the gas phase, presumably equilibrated with OH groups on the zeolite. The data suggest the presence of both terminal and bridging hydride ligands on the clusters. The H/Ir atomic ratio is estimated to be approximately 0.01 on the basis of the ^1H NMR data and thermogravimetric analysis of the zeolite. This part of the research was a collaboration involving the Gates and Eckert groups.

We are interested in supported rhenium clusters, in part because this group 7 metal, being more oxophilic than group 8 metals, tends to form cationic species on supports. To form supported tri-rhenium raft-like structures on γ-Al_2O_3, we used the precursor $H_3Re_3(CO)_{12}$ having a triangular framework of Re atoms. Motivated as well by a report by Bare et al. at UOP of catalytic properties of highly dispersed supported rhenium for hydrocarbon conversion, we are planning to investigate these materials as catalysts

for hydrocarbon conversion reactions (hydrogenolysis, hydrogenation, isomerization, and metathesis) under various reaction conditions and after various treatments; this work is to be done at UOP.

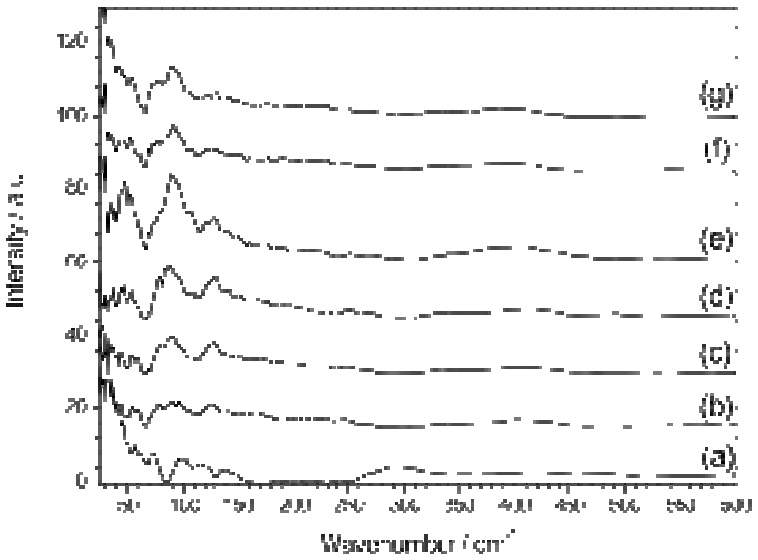

Figure 2. Incoherent inelastic neutron scattering spectra (IINS) (< 500 cm^{-1}) of the blank and supported cluster samples: (a) zeolite NaY; (b) zeolite NaY incorporating clusters approximated as Ir_6; (c) latter sample after vacuum treatment; (d) after treatment in H_2 at 25 °C; (e) after treatment in H_2 at 200 °C; (f) after replacement of H_2 with D_2 at 200 °C; (g) after replacement of D_2 with H_2 at 25 °C.

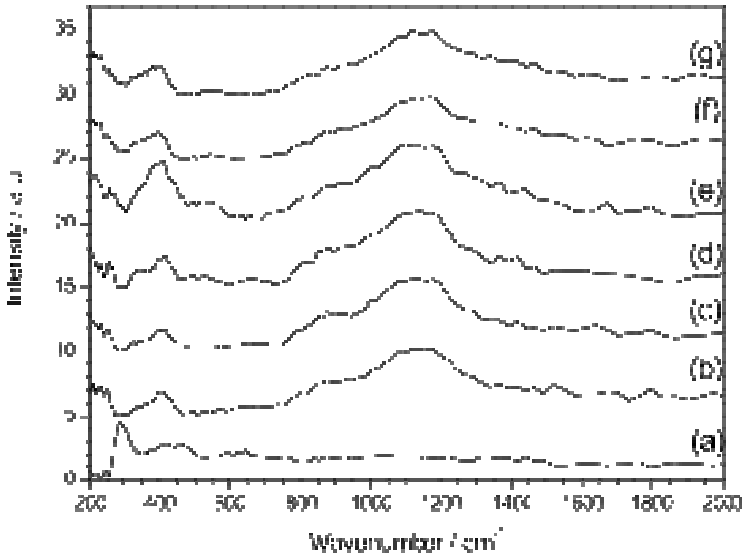

Figure 3. IINS spectra (400–2000 cm^{-1}): (a) zeolite NaY; (b) zeolite NaY incorporating clusters approximated as Ir_6; (c) latter sample after vacuum treatment; (d) after treatment in H_2 at 25 °C; (e) after treatment in H_2 at 200 °C; (f) after replacement of H_2 with D_2 at 200 °C; (g) after replacement of D_2 with H_2 at 25 °C.

X-ray absorption spectroscopy of the samples has already been done by the Gates group. The results of the EXAFS data analysis of the as-prepared sample and the sample treated at 673 K under H_2 flow are consistent with the presence of the intact precursor on the support. When this sample was decarbonylated in H_2 at 673 K, the resulting sample was found to be characterized by EXAFS parameters that are consistent with IR results in indicating virtually complete decarbonylation. The Re–Re coordination number of 2.2 is consistent, within the typical experimental uncertainty in such EXAFS data, with the formation of trinuclear Re rafts.

To provide insight into the electronic state of the Re in these samples, we measured XANES at the Re L_{III} edge. The intensity of the white line and the observed edge energy shift are used as indicators of the electronic state of Re. Comparisons of the results characterizing the supported rhenium samples with the XANES signatures of various standards were made. The reference compounds with Re in various oxidation states were Re_2O_7, ReO_3, $ReO_2 \cdot 2H_2O$ and Re metal for the oxidation states +7, +6, +4 and 0, respectively. The data indicate the increase of the Re L_{III} edge energy with the increase in the oxidation state of the reference. However, the monochromator step size used was 1 eV, leading to a relatively large error in edge position determination. The observed Re L_{III} edge energy shift representing the sample decarbonylated at 673 K (+2 eV) is indicative of the cationic character of the Re. A more certain assignment of oxidation state of Re will be possible with higher energy resolution and smaller monochromator steps. Furthermore, the white line intensity characterizing the decarbonylated sample is comparable to that observed for references with Re in the +4 and +6 oxidation state. Thus, on the basis of the comparison of observed XANES signature with those of references, the oxidation state of the Re is tentatively inferred to be in the range of +4 to +6. Hence, the decarbonylated samples, modeled as tri-rhenium rafts, show the Re atoms to be electron deficient and cationic in nature. The structural geometry of Re surroundings and the ligands present on it greatly influence the whiteline features, making it difficult to assign particular oxidation state for the Re. These experimental results will be compared with theoretical calculations at density functional level by the Dixon group and FEFF calculation of the XANES features by the Rehr group.

In earlier work, the Rehr group has shown the benefit of using *ab-initio* fully self-consistent XANES simulations using the software FEFF8 to elucidate the effect of cluster size and geometry on the Pt L-edge XANES of small Pt clusters. We now have compared the results of Re L-edge FEFF8 calculations with experimental results for supported rhenium catalysts. Calculations were carried out for various sizes and geometries of γ-alumina-supported rhenium clusters. The FEFF8 simulations were carried out both for rhenium clusters adsorbed on energy-minimized structures of the (110)-terminated alumina surface and bulk terminated surfaces.

The simulations show a strong dependence of the Re L_3-edge white line on the rhenium cluster size for naked clusters. The white line intensity converges for clusters of more than 39 atoms and agrees well with experimental results characterizing rhenium metal. The emergence of a resonance 10 eV above the white line for rhenium clusters containing more than 13 atoms is reproduced in the simulations. The results provided a basis for evaluating the cationic behavior of rhenium in small supported clusters on the basis of changes in the local density of states of the rhenium and the associated charge transfer. Figure 4 shows the theoretical Re L_3-edge XANES of rhenium clusters of varying sizes on bulk-terminated γ-alumina. The large white line variation observed in naked clusters is clearly suppressed. This work shows that a better understanding of the electronic and conformational structures of supported metal clusters can be gained from combining theoretical calculations of both the spectra and electronic structure with experiment.

A computational effort has been initiated in support of the experimental work. A set of Re_xO_y compounds with different substituents has been studied at the density functional theory level, including $ReO_2(OH)_2(OSiH_3)$, ReO_3OReO_3,$ReO_3OSi(OH)_3$, $ReO_2(OH)(OSiH_3)_2$, $ReO_2(OH)_2OReO_2(OH)_2$, and $ReO_2(OH)OReO_2(OH)$. An example of one of these structures is shown here. These compounds serve as models of rhenium oxide clusters by themselves and with silica surfaces. We have calculated the structures, vibrational spectra, Bronsted acidity and basicity, and Lewis acidity (based on the fluoride affinity scale developed by Dixon and Christe) of these structures. The calculations were done with polarized double zeta basis sets and the Stuttgart effective core potentials at the local and gradient corrected levels. Examples of specific results include: for ReO_3OH, the acidity ($ReO_3OH \rightarrow ReO_4^-$) of 295 kcal/mol, which shows that ReO_3OH is a strong acid and substantially more acidic than H_2SO_4 in the gas phase, the basicity ($ReO_3OH \rightarrow ReO_3(H_2O)^+$) of 153 kcal/mol—which shows that ReO_3OH is a very weak base and is less basic than H_2O in the gas phase, and the high Lewis acidity (fluoride affinity) of 113 kcal/mol is comparable to that of AlF_3 or SbF_4Cl, and the basicity of ReO_3OReO_3 of 200 kcal/mol is comparable to that of NH_3.

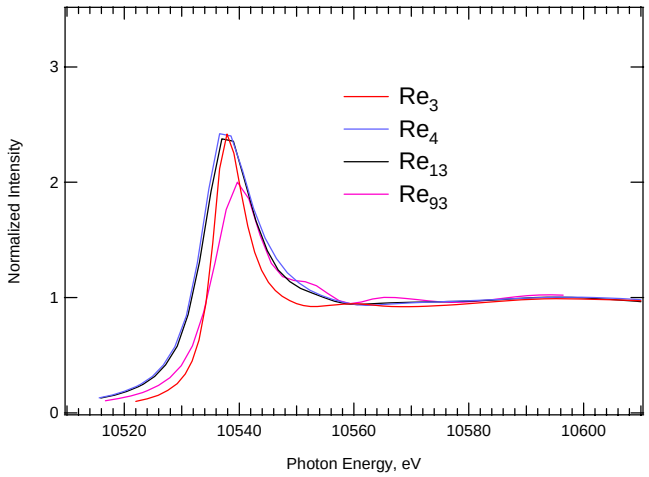

Figure 4. Theoretical Re L_3-edge XANES of Re clusters supported on a bulk terminated γ-alumina surface.

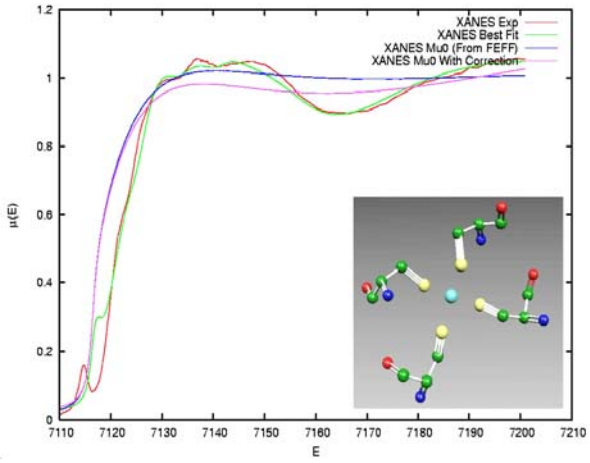

Figure 5. Illustration of the use of Bayesian analysis to fit data representing a single metal atom complex of oxidized pyrococcus furious rubredoxin.

The Rehr group has developed methods, based on the work of Krappe and Rossner, for fitting XANES data such as those shown in Figure 5 for a biological molecule. Beginning with structural models, such as might be determined with molecular dynamics modeling or EXAFS data/fitting, we restrain parameters using the uncertainties determined by the aforementioned techniques and Bayesian analysis methods. The advantage of using Bayesian restraints is that only parameters that are truly relevant to the fit will be varied. Figure 5 illustrates the use of the procedure to fit data representing a single-metal-atom complex comparable to supported metal complex catalysts.

Publications

1. Li, F.; Yu, P.; Hartl, M.; Daemen, L. L.; Eckert, J.; Gates, B. C. "Supported Iridium Clusters with Hydride Ligands: Characterization by EXAFS, NMR, and Inelastic Neutron scattering Vibrational Spectroscopies," *J. Phys. Chem. B*, submitted.
2. Bhirud, V. A.; Iddir, H.; Browning, N. D.; Gates, B. C. "Intact and Fragmented Triosmium Clusters on MgO: Characterization by X-Ray Absorption Spectroscopy and High Resolution Transmission Electron Microscopy," *J. Phys. Chem. B*, submitted.
3. Vila, F.; Kas, J.; Rehr, J. J.; Low, J. J.; Bare, S. R. "Towards an Understanding of the Re L_3-edge of XANES of Re/γ-Al_2O_3," paper to be presented at North American Catalysis Society meeting, Philadelphia, May 2005.

Nanocatalysts: Synthesis, Properties, and Mechanisms

Co-PI: Sheng Dai
Collaborators: David. R. Mullins, Edward W. Hagaman, Stephen J. Pennycook, Viviane Schwartz, Sergey Rashkeev
Postdocs: Wenfu Yan, Haoguo Zhu, Bong-Kyu Chang, Shannon Mahurin, Andrew Lupini

Chemical Sciences Division , Oak Ridge National Laboratory, Oak Ridge, TN 37831-6201
overburysh@ornl.gov

Goal

Explore and exploit novel synthetic techniques to prepare nanostructured catalysts with high selectivity and activity. This work focuses on the use of functionalization as a possible means to study and control particle size and metal-support interactions.

Recent Progress

Silica is an important support because various nanostructured morphologies can be synthesized. Periodic mesoporous silicas are potential candidates for templates to synthesize supported nanocrystals with controlled size and shape. This is of exceeding importance for Au catalysts which have been shown to very sensitive to Au particle size and/or structure. Although the deposition-precipitation (DP) method can be used to prepare gold nanoparticles on titanium oxide substrates, it is difficult to deposit gold nanoparticles (<30 Å) on silica materials with this methodology. In the DP method, the isoelectric point (IEP) of the support matrixes plays a key role in the successful incorporation and dispersion of nanoparticles on porous oxide supports. However, the IEP of silica materials is too low (~2) for effective deposition of $Au(OH)_3$. We have now learned how to prepare Au catalysts on any form of silica using co-synthesis methods. The essence of our sol-gel co-synthesis method is to combine simultaneously template synthesis of the silica with the introduction of metal ions *via* bi-functional silane ligands. Various template molecules may be used leading to different structural morphologies. Au attachment is mediated by interaction with the bi-functional ligand during sol-gel condensation. The gold precursors can be chemically complexed within the pores of functionalized mesoporous silica materials and the growth of gold nanoparticles can be subsequently achieved by mild chemical reductions. The drawback of this approach is that the functional groups could interfere with catalytic reactions by capping active sites. We have found that in spite of achieving the desired Au particle size and loading, the mesoporous silica based catalysts were generally quite inactive.

Another strategy to overcome the low IEP of silica-based materials is to introduce a high-IEP oxide component into silica materials via surface sol-gel process (SSP) modification Fig 1. The essence of this methodology involves the introduction of a high-IEP oxide component on mesoporous silica surfaces to decrease the negative charges of silica surfaces. The SSP was originally developed by Kunitake and co-workers, and enables the molecular-scale control of film thickness over a large 2D substrate area. The SSP technique generally consists of two half reactions: (a) non-aqueous

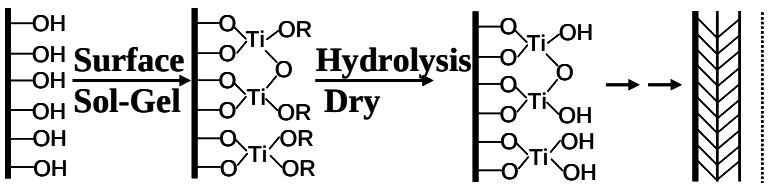

Fig. 1 Scheme illustrating the surface sol-gel process

condensation of metal-alkoxide precursor molecules with surface hydroxyl groups and (b) aqueous hydrolysis of the adsorbed metal-alkoxide species to regenerate surface hydroxyls. The iteration of the above sequential condensation and hydrolysis reactions allows the layer-by-layer coating of a selected metal oxide on a hydroxyl-terminated surface.

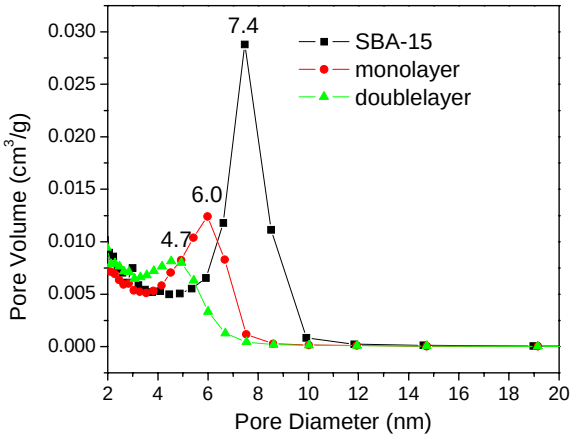

Fig. 2. BJH pore size distribution for TiO_2 funtionalized silica SBA-15

In principle, single or multilayer supports, of different types of modifiers and deposited in any order, can be prepared on any silica, and used as a support. The resulting functionalized silica supports allow a systematic investigation of key support effects imposed by interfacial layer, including compositions, acidities, redox properties, and thickness. Using this approach, we have synthesized a variety of layered silica supports functionalized with TiO_2 and Al_2O_3. Amorphous non-porous silica (Cabosil) and mesoporous SBA-15 silica have been used as base supports. ^{29}Si NMR confirms that both the titania and alumina react at surface silanols, indicated by a marked decrease of the Q3 signal and a corresponding increase in the Q4 peak. X-ray absorption spectroscopy at the Ti K edge indicates that the Ti exists in an environment of lowered oxygen coordination compared to bulk oxide, supporting the conclusion that the Ti is present as a single layer rather than condensed form of oxide. The monolayer deposition on mesoporous silica was most clearly demonstrated by the BET gas adsorption which shows the mean pore size distribution that stepwise decreases with single and double layer depositions. (Fig 2). Chemical analysis of the titania-functionalized silica by ICP indicates that a single layer covers only a fraction of the silica surface and therefore must be patchy, but second layer deposition results in roughly three-fold increase suggesting saturation of all titanols resulting from the first layer deposition. Single-layer alumina functionalization results in slightly more than monolayer coverage, an observation which can be explained by dimeric and tetrameric forms known to exist in the Al alkoxide precursor

Au was deposited onto the functionalized supports using DP under identical conditions at pH 10 . We find that single TiO_2 monolayer functionalization can render the resulting Au catalyst highly active for CO oxidation (Fig 3). High activities were achieved by starting with either the non-porous or the mesoporous silica. In the absence of functionalization, the Au/SBA-15 support exhibited no detectable activity. Using Cabosil functionalized with a single monolayer of alumina as a Au support yielded a catalyst with very poor, unstable activity. XRD suggests that the single layer alumina derived Au catalysts deactivates due to facile Au particle growth. If a double layer of alumina is used, the catalyst activity and stability is considerably improved, but is still inferior to that from the single titania overlayer. Deposition of alumina onto a monolayer of titania resulted in possibly the most active and stable catalyst. EXAFS demonstrates that the Au particles of this catalyst are quite stable to sintering showing an increase in mean Au-Au coordination number from 3 to about 8.5 after calcining to 500 C. XANES was conducted to examine

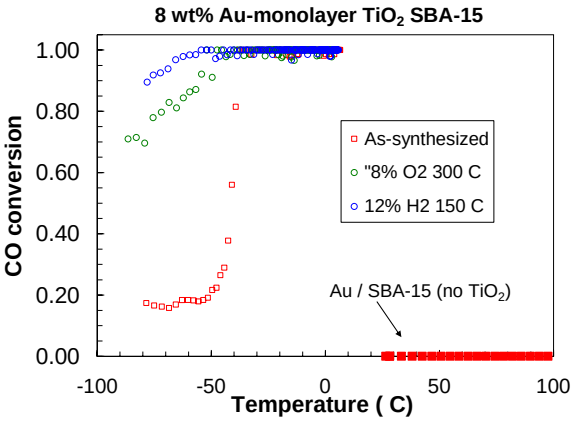

Fig. 3 Comparison of activity for CO oxidation

the oxidation state of the Au particles of the active catalysts. Similar to previous results on bulk titania crystals, the supported Au particles exist in an oxidic state after D-P and rapidly and irreversibly reduce to metallic Au following mild reduction in hydrogen. This behavior was universally true of Au on all the TiO_2 and Al_2O_3 layered supports. The implications of the sensitivity to underlayers and layer thickness is currently under study.

DOE interest

New catalysts are needed to achieve incremental or revolutionary improvements in technologies related to emission control, fuel cells and hydrogen utilization. This work provides a research basis for preparing, testing and understanding catalysts with potential application in these technologies.

Future Plans

The controlled synthesis of interfacial layers will be extended to manipulate nanoscopic architectures of catalytic reaction centers. Activity and stability of layered catalysts vary widely depending upon the silica functionalization. Work is in progress to determine if the variation in activity is described primarily by growth in Au particle size or if other factors also play a role. The adsorption of reactants and products on the functionalized catalysts will be studied by FTIR and pulsed reaction to determine how if it is influenced by support variation.

Publications

- Franceschetti, A., Pennycook, S. J. and Pantelides, S. T.,"Oxygen chemisorption on Au nanoparticles", Chem. Phys. Lett., 374, 471 (2003).
- Hagaman, E. W., Zhu, H., Overbury, S. H. and Dai, S.,"13C NMR Characterization of the organic constituents in ligand-modified hexagonal mesoporous silicas-media for the synthesis of small, uniform-size gold nanoparticles", Langmuir, 20, 9577 (2004).
- Lee, B., Zhu, H. G., Zhang, Z. T., Overbury, S. H. and Dai, S.,"Preparation of bicontinuous mesoporous silica and organosilica materials containing gold nanoparticles by co-synthesis method", Microporous and Mesoporous Materials, 70, 71 (2004).
- Overbury, S. H., Ortiz-Soto, L., Zhu, H. G., Lee, B., Amiridis, M. D. and Dai, S.,"Comparison of Au catalysts supported on mesoporous titania and silica: investigation of Au particle size effects and metal-support interactions", Catal. Lett., 95, 99 (2004).
- Schwartz, V., Mullins, D. R., Yan, W., Chen, B., Dai, S. and Overbury, S. H.,"X-ray absorption fine structure study of Au supported on TiO_2", J. Phys. Chem. B, 108, 15782 (2004).
- Yan, W., Chen, B., Mahurin, S., Hagaman, E. W., Dai, S. and Overbury, S. H.,"Surface sol-gel modification of mesoporous silicas with TiO_2 for the assembly of ultrasmall Au particles", J. Phys. Chem. B, 108, 2793 (2004).
- Yan, W. F., Chen, B., Mahurin, S. M., Dai, S. and Overbury, S. H.,"Brookite-supported highly stable gold catalytic system for CO oxidation", Chem. Commun., 1918 (2004).
- Zhu, H. G., Lee, B., Dai, S. and Overbury, S. H.,"Coassembly synthesis of ordered mesoporous silica materials containing Au nanoparticles", Langmuir, 19, 3974 (2003).
- Zhu, H., Pan, Z., Chen, B., Lee, B., Mahurin, S. M., Overbury, S. H. and Dai, S.,"Synthesis of ordered mixed titania and silica mesostructured monoliths for gold catalysts", J. Phys. Chem. B, *108*, 20044, (2004).
- Yan, W., Chen, B., Mahurin, S. M., Schwartz, V., Mullins, D. R., Lupini, A., Pennycook, S. J., Dai, S., et al.,"Preparation and comparison of supported gold nanocatalysts on anatase, brookite, rutile, and P25 polymorphs of TiO2 for catalytic oxidation of CO", submitted to J. Phys Chem (2005).
- Yan, W., Overbury, S. H., and Dai, S. “Nonhydrolytic layer-by-layer surface sol-gel modification of powdered mesoporous silica materials with TiO_2,” Chem. Mater. In press.
- Dai, S. and Barnes, C. E. “Mesoporous Materials,” in *Encyclopedia of Supramolecular Chemistry*, Marcel Dekker, p108-117, **2004**.

DE-FG03-02ER15345 **Daniel E. Resasco**

Controlling Structural Characteristics of Single-Walled Carbon Nanotubes (SWNT) by Tailoring Catalyst Composition and Synthesis Conditions

Students: L. Balzano, Jose E. Herrera, Liang Zhang
Collaborators: R. B. Weisman (Rice), P. Balbuena (TAMU), Ming Zheng (Dupont)
Contact: D. Resasco, 100 E. Boyd St, Norman OK 73019;
phone: (405) 325-4370; Email: resasco@ou.edu web page: www.ou.edu/engineering/nanotube

Goal

Advance the knowledge of the mechanisms responsible for the formation of single-walled carbon nanotubes to get control over their structural parameters (diameter and chirality). Through a detailed knowledge of the growth mechanism it will be possible to produce SWNT with tailored properties that are directly related to the structural parameters.

Recent Progress

Single-walled carbon nanotubes (SWNT) have shown promising potential in many areas that range from composites to advanced electronic materials and biomedical applications. Responsible for their exceptional properties is their unique structure, which is fully described by two integers, *n and m*, that identify the chiral vector and determine the nanotube diameter and helicity. We have developed a synthesis method (CoMoCAT) based on the controlled reaction of carbon monoxide (CO) on a Co-Mo/SiO_2 catalyst,[1] under conditions that result in unprecedented selectivity towards SWNT, as opposed to other less desired forms of carbon, such as graphite nanofibers. Because the electronic and optical properties of single-walled carbon nanotubes depend sensitively on tube structure, a major goal in nanotube production is to control the distribution of nanotube diameters and chiralities in the product. The metal (cobalt) cluster dimension is a key factor in the selectivity towards SWNT and it can also determine (n, m) distribution. The cluster growth is hindered by the interaction with the substrate and it is therefore possible to control the growth rate.

A) Controlling diameter and chirality of SWNT

The nanotubes produced by our CoMoCAT process exhibit a uniquely narrow distribution of diameters, which can be varied by adjusting the process parameters.

A.1. <u>Changing (n,m) structure by varying synthesis temperature</u>: It is well known that the quasi-one-dimensionality of SWNT gives origin to sharp van Hove singularities in the density of electronic states. As a result, the optical properties of SWNT are dominated by transitions between van Hove singularities on opposite sides of the Fermi level. The absorption spectra for the different nanotubes extracted from the CoMoCAT750, CoMoCAT850 and CoMoCAT950 by suspending them in NaDDBS surfactant show only a few sharp absorption peaks with a low background were obtained in the entire Vis-NIR spectrum, in good agreement with previous PL results that evidenced the presence of few nanotube types, with similar diameter and chirality. With such a small number of nanotube types present in the sample, a detailed analysis and

(n,m) assignment of the SWNT present in the sample is possible. Within the semiconducting nanotubes in the sample, the (6,5) type is the major constituent of CoMoCAT750 sample, while (7,6) dominates in CoMoCAT850 and (8,7) in CoMoCAT950. This trend is in agreement with Raman results and previously reported TEM results that indicate that higher synthesis temperatures lead to SWNT of larger diameter. What is now more remarkable is that we can precisely identify the (n,m) types that dominate the nanotube population on the different samples.

A.2. <u>Changing (n,m) structure by varying catalyst composition</u>: One might argue that the (n,m) structures that are produced with high selectivity in our Co-Mo catalysts are simply the most stable structures at each temperature. However, we have recently shown that not only the synthesis temperature but also the composition of the catalyst determine the type of SWNT that is produced. Therefore, one of the goals of the current proposal will be to determine the influence of catalytic (kinetic) and structure stability (thermodynamic) effects in determining the (n,m) structure. By using the same Co-Mo loading and method of preparation, but varying the support from SiO_2 to MgO we observed a dramatic difference in the type of SWNT obtained under identical reaction conditions. While the Co-Mo/SiO_2 produced mostly (6,5) the Co-Mo/MgO produced greater amounts of (7,5), (7,6), and (8,4) nanotubes. Clearly, the interaction of Co and Mo with the support generates a Co-Mo species on the surface that reacts differently to the CO.

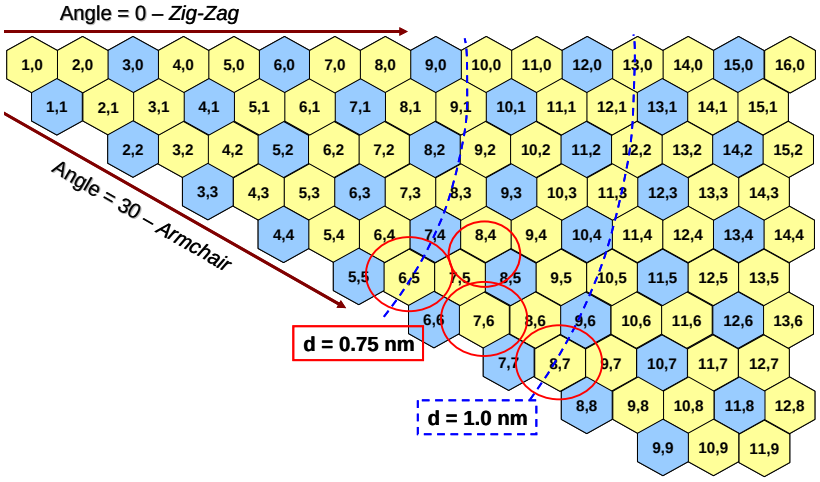

Figure 1. Map of possible nanotubes. Diameter increases radially outward and chiral angle increases from top down, from zig-zag to armchair. Red circles indicate those (n,m) that have been observed under different conditions, i.e. growth temperature or catalyst support.

As a result, the decomposition process that leads to the formation of Co clusters may occur at different rate and may go through different sizes and crystal structures. This is an important result because it demonstrates that the (n,m) structures produced over solid catalysts are a strong function of the catalyst, not only the reaction conditions. Our recent simulations yielded insights into the morphologies of Co clusters deposited on different substrates; the linkage to specific chiralities may also be investigated by these methods as discussed in a later section.

We believe that it is possible to have control of the (n,m) nanotubes that are produced, while keeping high selectivity. One important aspect to take into account is that all of the (n,m) structures produced on these Co-Mo catalysts have a chiral angle

close to 30^{o}, "armchair" configuration and far from the "zig-zag" type (see nanotubes indicated with red circles in Fig. 1). Our modeling studies give support to the idea that the structures near the "armchair" type could be favored during synthesis, while still in contact with the surface of the cluster. In a recent collaboration with our group, Pimenta, Jorio et al., who are Raman specialists and use a combination of 34 different laser to essentially cover all the resonance, have evaluated our CoMoCAT750 material. In addition to the semiconducting (6,5) and (7,5), the sample contains small amounts of metallic (7,4), which, as shown in Fig. 1 has the same diameter as (6,5). In this particular sample, the ratio of semiconducting/metallic was found to be 10/1. That is, for a specific diameter (in this case 0.75 nm) the distribution drops very quickly as the chiral angle increases. The intensity drops quickly from both a given diameter AND a given chiral angle. This trend opens an interesting possibility. For example, if we are able to generate conditions in which nanotubes with the diameter that corresponds exactly to an armchair nanotube, e.g. (6,6), then the sample that we will obtain will have a ratios of metallic/semiconducting much greater than one.

B) Controlling length of SWNT

For many applications in nanotechnolgy, it may be important to have a narrow distribution of length and it is not known at this moment what controls the length. Our hypothesis is that in order to continue to grow, the nanotube-metal interface cannot be perturbed too much. As a result, if the free displacement of the growing tube is hindered by the pore structure of by its "sticky" interaction with other bundles that may not be growing at the same rate, the growth will be hindered and eventually stopped. The image (a) in the figure below illustrates the "sticky" interaction via Van der Waals forces between adjacent SWNT bundles. The image (b) shows SWNT grown on CoMoCAT catalysts deposited on quartz and exposed to CO. The image clearly shows that when the nanotubes encounter another bundle, or the surface, they stop growing.

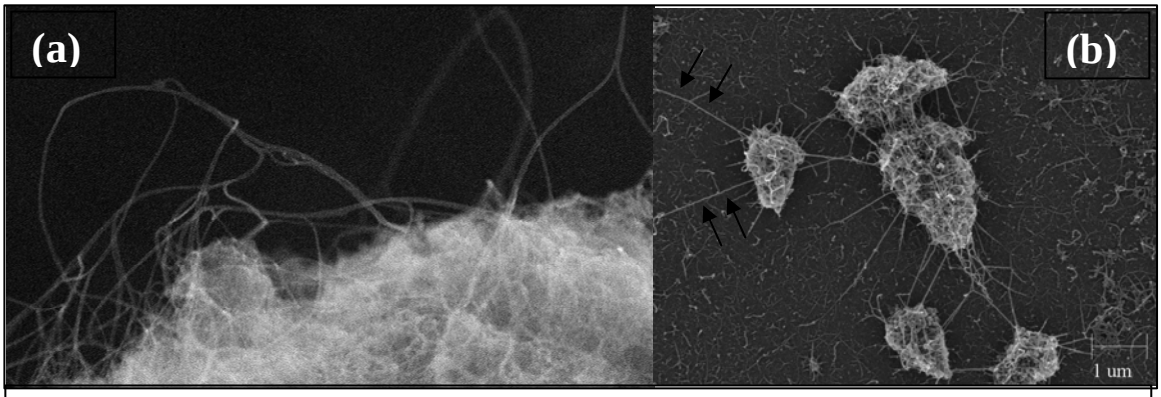

Figure 2. SEM images of SWNT grown on Co-Mo catalysts. (a) illustrates the joining of bundles during their growth; (b) illustrates that when the nanotubes have not joined other bundles, they can be long (arrows), but when they get in contact with other bundles, such as those in another particle, the growth stops.

Recent publications (2004)

- D. E. Resasco, L. Balzano, J. E. Herrera, O. Matarredona, and L. Zheng, American Institute of Physics Conf. Proc. 723, pp. 27 (2004).
- J. E. Herrera and D. E. Resasco, Journal of Catalysis 221, (2004) 354
- D. E. Resasco, J. E. Herrera, and L. Balzano, J. Nanosci. Nanotech. 4, 398 (2004)
- Daniel E. Resasco and Jose E. Herrera, "Structural Characterization of Single-Walled Carbon Nanotubes" in Encyclopedia of Nanoscience and Nanotechnology, (2004) American Scientific Publishers (H. S. Nalwa Ed.), Vol. 10, pp 125-147.

Session C:

Surfaces and Interfaces under Reaction

Environmental Catalysis at the Interface of Metals and Metal Oxides

William F. Schneider, Departments of Chemical and Biomolecular Engineering and Chemistry and Biochemistry, University of Notre Dame, Notre Dame, IN, 46556
wschneider@nd.edu

Innovation in environmental catalysis—that is, catalysis related to sustainable production and consumption of energy and materials—is one of the most pressing societal needs of the day. Many of the most widely used environmental catalysts, such as those used in automotive emissions control, are complicated mixtures of metals and metal oxides. While these work very well in some regimes, our ability to reduce cost or design performance in a rational fashion is limited by the lack of firm understanding of how these components interact at the nanoscale. Progress against these problems will require the joint efforts of experiment, simulation, and theory. In this talk, the results of first-principles simulation and theoretical considerations to contrast the reactivity of metals and metal oxides in the context of NO_x aftertreatment will be discussed, and thoughts on future opportunities in nanoscale metal/metal oxide environmental catalysis offered.

DE-FG02-04ER15587

J. Mike White (U. Texas at Austin)
C. Buddie Mullins (U. Texas at Austin)

The Surface Chemistry of Size-Controlled Oxide-Supported Ir Nanoclusters

Dept. of Chemistry and Biochemistry
University of Texas at Austin
Austin, TX 78712
jmwhite@mail.utexas.edu
jm.white@pnl.gov

Dept. of Chemical Engineering
University of Texas at Austin
Austin, TX 78712
mullins@che.utexas.edu

Goals

Surface science studies have shown that single-crystalline, macroscopic iridium can readily activate C-H bond cleavage in alkanes at low temperatures. Additionally, studies of nanoclusters of metals have shown that such samples can behave differently catalytically than macroscopic sized samples of the same metal. Here, we are studying nanoclusters of iridium as a function of cluster size to explore how differently they might behave compared to bulk iridium. In particular we wish to explore their effectiveness at activating methane and halogenated methanes.

DOE Interest

Natural gas is an under-utilized resource in part due to the difficulty in breaking the C-H bond in methane under favorable catalytic conditions. Additionally, halogenated hydrocarbons are large components of waste streams in some chemical processes and catalytic conversion is an attractive option. Size-selected iridium clusters hold some promise for activating both methane and halogenated methanes under conditions more favorable for chemicals and fuels production. Additionally, our studies will yield more general insights into the catalytic properties of supported metals as a function of nanocluster size.

Research Plan

We are exploring three methods of preparing/depositing size-selected Ir nanoclusters on metal oxide wafers: (1) preparation employing surfactant-stabilized, size-selected nanoclusters, (2) deposition by magnetron sputtering of an Ir target coupled with quadrupole mass separation, and (3) preparation by vapor deposition from an iridium filament.

The first method is our preferred method of sample preparation and here we depend on the synthetic skills of our UT-Austin colleague, Prof. Brian Korgel, who is a collaborator. The Ir particles typically will have been stabilized in solution with adsorbed surfactants and can be prepared with size distributions with standard deviations of 5 to 10%. There are several plausible deposition methods. The simplest is to dip-coat but Langmuir-Blodgett and spin coating procedures may be useful. After installing the coated substrate in the molecular beam machine, the surfactant must be removed without

agglomerating the metal. Our plan of attack will involve processing a single layer of the surfactant-stabilized moieties at cryogenic temperatures using some combination of electron-induced chemistry and oxygen atoms generated in a plasma source. Atomic oxygen is expected to combust (or partially combust) the surfactant molecules leading to CO_2, H_2O and, plausibly, partially oxidized species such as methanol, that will desorb and be pumped away. Such methods have been successfully employed previously with supported gold clusters.

Once prepared, physical characterization of Ir nanoclusters lies at the heart of our research, and will be vigorously pursued using our Variable Temperature-STM machine. For selected samples, we will, in addition, make use of facilities available on a scheduled basis in the Texas Materials Institute including, Transmission Electron Microscopy (JEOL 2010F TEM) featuring a Field Emission Gun (FEG) and Ultrahigh-Resolution Observation System) and, as needed, Secondary Ion Mass Spectrometry, Monochromatic X-ray Photoelectron Spectroscopy and Atomic and Interfacial Force Microscopy.

After controlled deposition of Ir nanoclusters at cryogenic temperatures onto bare or ice-covered oxide, STM images will be gathered as a function of time, temperature, and exposure to adsorbates of interest. While this is a very labor intensive, demanding and time-consuming process, the potential reward is worth the effort, particularly when coupled with the molecular beam measurements of the chemical properties (described below). In this context, the STM measurements must be extensive enough to deliver adequate statistics that characterize the distributions of particles for samples selected for transfer to the beam scattering instrument; gathering ensemble averages for key particle dimensions and topology is necessary for adequate interpretation of the beam scattering data.

Once protocols are established for preparing planar samples with reproducible Ir nanocluster distributions in the STM machine, key samples will be studied in the beam machine where we will characterize the chemistry of the supported iridium clusters employing reactive scattering methods, temperature programmed desorption (TPD), *in situ* ambient pressure steady state reactivity measurements, as well as other standard surface science instrumentation. We will begin our studies of the reactive chemistry by studying low-molecular-weight alkanes (methane and ethane) and chlorinated methanes. The number of measurements required for chemical characterization on a given sample is much larger than in the STM work so very careful selections must be made.

Alkanes: Based on experimental measurements acquired at UT-Austin and elsewhere regarding a comparison of Ir(110) versus Ir(111), there is a strong structural sensitivity in the reactivity of alkanes over iridium. For both ethane and propane the reaction is very facile on Ir(110) but immeasurable on Ir(111) in UHV, whereas for methane the initial reactivity on the (110) surface is approximately ten times higher (at the same temperature) than on Ir(111). We will begin our investigations by studying the reactions of methane and ethane on metal oxide supported Ir nanoclusters as a function of particle size and substrate temperature. While we expect ethane to be quite reactive for all Ir nanocluster sizes, this is not expected for methane. We will search for cluster sizes that activate methane at lower temperatures than on the (110) single crystal surface. Since the number of not-fully-coordinated sites on the Ir(110) surface is much higher than on the Ir(111) surface there is some hope that small Ir particles will be more reactive

toward methane than Ir(110) as they potentially have an even larger concentration of such sites.

Since it is important to connect STM and UHV reactive scattering results with each other and with higher pressure steady-state catalytic and transient kinetics, we will also study reactions of methane on our prepared surfaces in an *in situ* ambient. At steady-state we can flow methane into the cell with other reactants (e.g., D_2, H_2, etc) and probe for reaction products. We can also expose the prepared samples to methane at ambient pressure for a fixed amount of time and then measure the amount of dissociation via Auger spectroscopy or by titration with oxygen.

Chlorinated methanes: We will also study the reactions of chlorinated methanes with our Ir nanocluster decorated metal oxide surfaces and contrast these results to comparable data from Ir single crystal investigations we have previously obtained. We will begin these experiments by studying the reaction of CCl_4 with both bare and pre-covered supported iridium clusters since we have substantial experience with such reactions on the (110) and (111) surfaces. In particular, the reaction of chlorinated methanes with hydrogen precovered Ir nanoclusters will be pursued with the objective of converting the chlorinated methane in to a less chlorinated molecule and perhaps per-hydrido methane. We have evidence that this reaction can be driven at temperatures below 300 K on Ir(110), but not on Ir(111), employing CCl_4 and $HCCl_3$, again indicating structural sensitivity. Nanocluster size will be varied to test whether the less reactive partially chlorinated methanes (i.e., H_2CCl_2, and H_3CCl) can be activated and to test whether the selectivity of the conversion of CCl_4 and $HCCl_3$ to methane and/or other environmentally benign products can be facilitated.

Recent Progress

Thus far we have been studying sample fabrication by two methods: (i) deposition of size-selected, surfactant-covered iridium nanoclusters on a TiO_2 wafer by simply placing a droplet of the solution "carrying" the clusters on the titania, and (ii) vapor deposition of iridium clusters onto a TiO_2 wafer from a hot iridium filament. Regarding the first method, we have thus far not been highly successful at removing the surfactant ligands from the deposited iridium clusters. After deposition of the surfactant covered iridium clusters we observe with Auger spectroscopy that the amount of carbon on the surface is quite large and upon removal of this carbon we are unable to identify any iridium on the sample. We are continuing to study this issue. Simultaneous with these studies we have been constructing and testing an iridium evaporator for sample synthesis. Iridium requires very high temperatures for evaporation and thus, the successful design of this device has proven to be quite demanding. We have successfully deposited iridium on to the TiO2 surface but this has been accompanied by the co-deposition of carbon and other contaminants (including Cl). We are currently working at reducing the contamination and also strategies for cleaning the sample after deposition. After successful sample synthesis we plan to study methane and chloromethane chemistry on the Ir clusters as well as beginning the physical characterization by STM.

Publications 2003-2004 J. M. White

J.W.Lee, A. Carroll, A. Patenaude, S. Kim, and J.M. White, "$KHCO_3$ Mineralization Self-assembled on Aminopropyl Organosilica," *Langmuir,* **20**(1), (2004) 273-275.

J. Qi, C. Mao, J.M. White, and A. Belcher, "Optical anisotropy in individual CdS quantum dot ensemble," *Physcial Review B.,* **68**, (2003) 125319-1-6.

S.Y. Lee, B. Luo, Y.-M. Sun, J.M. White, and Kim Y., "Thermal Decomposition of Dimethylaluminum isopropoxide on Si (100)," *Applied Surface Science.,* **222**,(2004) 234-242.

White, J.M., Szanyi, J., and Henderson, M.A., "The Photo-Driven Hydrophilicity of Titania: A Model Study Using TiO_2(110) and Adsorbed Trimethyl Acetate," *J. Phys. Chem. B.,* **107** (2003) 9029-9033.

Henderson, M., White, J., Uetsuka, H., Onishi, H., "Photochemical Charge Transfer and Trapping at the Interface Between an Organic Adlayer and an Oxide Semiconductor," *J. Am. Chem. Soc.,* **125** (2003) 14974-14975.

Luo, B., Lee, Y.S., and White, J.M., "Adsorption, desorption and reaction of a gallium nitride precursor, $(H_2GaNHNMe_2)_2$ on HfO_2," *Chemistry of Materials,* **16** (2004) 629-638.

Ni, J., Lee, S.W., White, J.M., and Belcher, A., "Molecular Orientation of ZnS Nanocrystal-Modified M13 Virus on Silicon Substrate," *J. Polymer Sci. B: Polymer Physics,* **42**, (2004) 629-635.

W. Zhao, W. Wei, and J. M. White, "Thermal desorption of Tris (8-hydroxyquinoline) aluminum (III) (Alq_3) on Cu (111)" *Chemistry of Materials,* **15**,(2003) 4819-4822.

W. Zhao, W. Wei and J. M. White, "Two-photon photoemission spectroscopy: Naphthalene on Cu (111)," *Surface Science,* **547** (2003) 374-384.

Q. Wang, J. G. Ekerdt, D. Gay, Y-M. Sun, J. M. White, "Low temperature CVD and scaling limit of ultrathin Ru films," *Applied Physics Letters,* **84** (2004) 1380-1382.

W. Zhao, W. Wei, J. Lozano, J.M. White, " Interfacial Electronic Structures of Tris(8-hydroxyquinoline) aluminum (III) (Alq_3) on Cu (111)," *Chemistry of Materials,* **16** (2004) 750-756.

J.M. White, J. Szanyi, M. Henderson, "Thermal chemistry of trimethyl acetic acid on TiO_2(110)" *J. Phys. Chem. B,* **108** (2004) 3592-3602.

W. X Huang and J.M.White, "Growth and Orientation of Naphthalene Films on Ag(111)" *J. Phys. Chem. B,* **108** (2004) 5060-5065.

W. Zhao, I. Lee, S.K. Kim, J.M. White, "Photodissociation at 193nm of tert-butyl nitrite on Ag(111)," *J. Phys. Chem. B,* **108(38),** (2004), 14276-14281.

Sun, Y.-M.; Eklund, J.; Wang, Q.; Gay, D.; White, J.M. "Electron beam induced carbon deposition and etching," *Materials Research Society Symposium Proceedings,* **750**, (2003), 481-486.

Engbrecht, E.R.; Cilino, C.J.; Junker, K.H.; Sun, Y.-M.; White, J.M.; Ekerdt, J.G. "Characterization of boron carbonitride films deposited by low temperature chemical

vapor deposition," *Materials Research Society Symposium Proceedings*, **766**, (2003) 351-356.

S. Wang, Y.-M Sun, Q. Wang and J. M. White, "Electron beam induced initial growth of platinum films using $Pt(PF_3)_4$," *J. Vac. Sci. Technol. B.* **22**(4), (2004), 1803-1806.

W. Zhao, T. Cao, J. M. White, "On the origin of green emission in polyfluorene polymers: The roles of thermal oxidation degradation and cross- linking," *Advanced Functional Materials* **14**(8), (2004) 783-790.

W. X. Huang, J. M. White, " Fluorine substitution effect on the reaction pathway if CH_3CH_2(a) and CF_3CH_2(a) on Ag(111)," *J. Phys. Chem. B,* **108**(23), (2004), 7911-7916.

Jooho Kim, Z. Dohnálek, J.M. White, Bruce D. Kay, " Reactive Growth of Nanoscale MgO films by Mg Atom Deposition onto O_2 Multilayers" *J. Phys. Chem. B,* **108**(31), (2004) 11666-11671.

W. Wei, W.X. Huang, J.M. White, "Adsorption of Styrene on Ag(111)," *Surface Sci.* **572** (2004) 401-408.

Mingji Wang, Kenneth M. Liechti, J. M. White, and Robb M. Winter, "Nanoindentation of Polymeric Thin Fims with an Interfacial Force Microscope," *Journal of the Mechanics and Physics of Solids,* **52**(10), (2004), 2329-2354.

W.X. Huang, J. M. White, " A Spectroscopic Investigation of Carbon-Carbon Bond formation by Methylene insertion on a Ag(111) Surface: Mechanism and Kinetics," *J. Am. Chem. Soc.*, **126**(44), (2004), 401-408.

X.-M. Yan, M. D.Robbins, J. M .White, "Thermal properties of t-butyl nitrite (TBN) on Cu(111)," *J. Phys. Chem. B,* **108**(49), (2004), 18925-18931.

M. Wang, K. M. Liechti, V. Srinivasan, J. M. White, P. J. Rossky, M. T. Stone, "A Hybrid Continuum-Molecular Analysis of IFM Experiments on a Self-Assembled Monolayer," *J. Applied Mechanics* (in press).

J. M. White, Michael A. Henderson, Hiroshi Uetseka, Hiroshi Onishi, "Photoinduced redox reaction of carboxylates on TiO_2(110)," Proceedings of SPIE, Vol. **5513** (2004) 157-164, Gregory V. Hartland and X.-Y. Zhu, eds.

W. Wei and J. M. White, "Two-photon photoemission spectroscopy: atomic oxygen on Cu(111) and styrene on oxygen covered Cu(111)," Proceedings of SPIE, Vol. **5513** (2004) 66-75, Gregory V. Hartland and X.-Y. Zhu, eds.

S. Wang, Y.-M. Sun, J. M. White, A. Stivers, and T. Liang, "Electron beam-assisted etching of CrO_x films by Cl_2," *JVST B* **23**, (2005), 206-209.

S. Wang, Y.-M. Sun, and J. M. White, "Electron induced deposition and *in-situ* etching ofCrO_xCl_yfilms," *Appl. Surf. Sci.* (in press).

Y.-M. Sun, S. Wang, J. M. White, "Electron Assisted Chemical Etching of Oxidized Chromium," *Appl. Surf. Sci.* (in press).

W. Wei, W. Zhao and J. M. White, "Directly probing the hybrid bonding of styrene on Cu(111)," *JACS* (Communication) **126**(50), (2004), 16340-16341.

Y.-M. Sun, E. R. Engbrecht, T. Bolom, C. Cilino, J. H. Sim, J. M. White, J. G. Ekerdt, and K. Pfeifer, "Ultra thin tungsten nitride film growth on dielectric surfaces," *Thin Solid Films,* **458**, (2004), 251-256.

Publications 2003-2004 C. B. Mullins

P. L. Tanaka, D. D. Riemer, S. Chang, G. Yarwood, E. C. McDonald-Buller, E. C. Apel, J. J. Orlando, P. J. Silva, J. L. Jimenez, M. R. Canagaratna, J. D. Neece, C. B. Mullins, and D. T. Allen "Direct Evidence for Chlorine-Enhanced Urban Ozone Formation in Houston, TX," *Atmos. Environ.* **37**, 1393-1400 (2003).

P. L. Tanaka, E. C. McDonald-Buller, S. Chang, G. Yarwood, Y. Kimura, J. D. Neece, C. B. Mullins, and D. T. Allen, "Development of a chlorine mechanism for use in the Carbon Bond IV chemistry model," *J. Geophys. Res.* **108(D4)**, 4145-4157, doi:10.1029/2002JD002432, (2003).

P. L. Tanaka, D. T. Allen, and C. B. Mullins "An Environmental Chamber Investigation of Chlorine-Enhanced Ozone Formation in Houston, TX," *J. Geophys. Res.* **108(D18)** 4576-4586, doi:10.1029/2002JD003314, (2003).

C. T. Reeves, R. J. Meyer, and C. B. Mullins, "Dissociative adsorption and hydrodechlorination of CCl_4 on Ir(110)," *J. Mol. Catal. A: Chem.* **202**,135-146 (2003).

T. S. Kim, J. D. Stiehl, C. T. Reeves, R. J. Meyer, and C. B. Mullins, "Cryogenic CO oxidation on TiO_2 supported gold nanoclusters pre-covered with atomic oxygen," *J. Am. Chem. Soc.* **125**, 2018-2019 (2003).

D. J. Safarik, R. J. Meyer, and C. B. Mullins, "Thickness dependent crystallization kinetics of sub-micron amorphous solid water films," *J. Chem. Phys.* **118**, 4660-4671 (2003).

Invited Book Chapter: S. M. McClure, M. I. Reichman, D. C. Seets, P. D. Nolan, G. O. Sitz, and C. B. Mullins, "Dynamics of precursors in activated dissociative chemisorption systems," (Feb. 2003).

D. J. Safarik and C. B. Mullins, "A new methodology and model for characterization of nucleation and growth kinetics in solids," *J. Chem. Phys.* **119**, 12510-12524 (2003).

J. D. Stiehl, T. S. Kim, S. M. McClure, and C. B. Mullins, "Evidence for molecularly chemisorbed oxygen on TiO_2 supported gold nanoclusters and Au(111)," *J. Am. Chem. Soc.* **126**, 1606-1607 (2004).

D. J. Safarik and C. B. Mullins, "The nucleation rate of crystalline ice in amorphous solid water," *J. Chem. Phys.* **121**, 6003-6010 (2004).

J. D. Stiehl, T. S. Kim, C. T. Reeves, R. J. Meyer, and C. B. Mullins, "Reactive scattering of CO from an oxygen atom covered Au/TiO_2 model catalyst," *J. Phys. Chem. B* **108**, 7917-7926 (2004).

S. M. McClure, T. S. Kim, J. D. Stiehl, P. L. Tanaka, and C. B. Mullins, "Adsorption and reaction of nitric oxide with atomic oxygen covered Au(111)," *J. Phys. Chem. B* **108**, 17952-17958 (2004).

J. D. Stiehl, T. S. Kim, S. M. McClure, and C. B. Mullins, "Reaction of CO with molecularly chemisorbed oxygen on TiO_2-supported gold nanoclusters," *J. Am. Chem. Soc.* **126**, 13574-13575 (2004)

DE-AC02-98CH10086

Jan Hrbek (BNL), James T. Muckerman (BNL), and
Michael G. White (BNL, SUNY Stony Brook)

Catalysis on the Nanoscale: Preparation, Characterization and Reactivity of Metal-Based Nanostructures

Additional PIs: Jose Rodriguez (BNL)
Post-Docs: Tanhong Cai, Ping Liu, Denis Potapenko, Xianqin Wang
Graduate students (SUNY Stony Brook): James Lightstone, Melissa Patterson, Jillian Horn

Chemistry Department
Brookhaven National Laboratory
Upton, NY 11973
hrbek@bnl.gov, muckerma@bnl.gov

Department of Chemistry
SUNY Stony Brook
Stony Brook, NY 11794
mgwhite@notes.cc.sunysb.edu, mgwhite@bnl.gov

Goals

The purpose of this project is to explore and manipulate the size, morphology and chemical environment of metal and metal compound nanoparticles with the goal of optimizing their reactivity with respect to elementary reactions that are of widespread interest in heterogeneous catalysis. Theoretical and experimental studies of extended surfaces and nanoparticles supported on metallic and metal oxide surfaces are used to investigate the role of size, structure (electronic and atomic), chemical composition and substrate interactions on catalytic activity. This effort emphasizes the use of unique photon facilities available at the National Synchrotron Light Source for characterizing the structure, composition and reactivity of catalytic surfaces.

Approach

We propose to modify the catalytic activity of metal-based catalysts through manipulation of the local electronic structure of the metal active site. For example, it is well known that the active sites on metal single crystals are often associated with defects or step edges, where the metal atoms have lower coordination number and experience a different local electronic environment. Reducing the active catalyst material to nanometer sized particles achieves modification of surface activity through the generation of many coordinatively unsaturated edge sites, as well as introducing particle-support interactions which can strongly influence the electronic structure of the metal particle. For nanoparticles of a few nanometers in size, further modification of the electronic structure results from quantum confinement, where the particles act more like molecular clusters than bulk metals. Our approach here is to not only use particle size and support environment to modify reactivity, but also to modify the local electronic environment of the active metal by incorporation into a molecular compound or alloy (*e.g.*, carbide, nitride or sulfide), or doping into an oxide of a different metal. Compared to their bulk form, nanostructured forms of these transition metal alloys or compounds (TMX) may exhibit novel catalytic behavior as a result of unusual surface structures and/or substrate interactions.

Recent Progress

Formation of supported TMX nanoparticles by reactive deposition: The preparation of nanoclusters with narrow and tunable size distributions is crucial for developing a fundamental understanding of structure-reactivity correlations. In this work we are using reconstructed metal surfaces that display the strain-relieved patterns which act as templates for metal cluster nucleation. Specifically we are using the $(22 \times \sqrt{3})$-Au(111) reconstructed surface which exhibits a herringbone pattern resulting from strain-induced dislocations of the surface atoms. The alternating regions of fcc and hcp packing lead to "elbow" surface structures which have been found to act as nucleation sites for self-limited growth of metal nanoparticles. The Au surface is also relatively inert, so that reaction studies can be performed on the nanoclusters without contributions from the Au substrate.

By modifying gold surface with chemisorbed or physisorbed layers of reactants we can also control both the composition and morphology of the growing nanoparticles. The first example was a preparation of RuS_2 islands by deposition of Ru carbonyl on sulfur saturated Au surface at elevated temperatures. More recently, we

have demonstrated a new approach for generating nanoparticles of transition metal compounds (TMX), e.g., carbides, oxides, and sulfides. This approach is called *Reactive Layer Assisted Deposition* (RLAD) and involves the deposition of a metal vapor onto a single or multilayer of a reactive compound such as ethylene, ammonia, water or hydrogen sulfide. The "hot" metal atoms react on contact with the cold molecular film to form metal compounds that nucleate as small nanoclusters on the Au(111) surface. The main advantages of RLAD over alternative methods are (1) the entire process can be performed at low temperature which strongly influences nucleation and growth; (2) the resulting TMX particles have nearly bulk-like compositions. The RLAD method was first demonstrated for the production of MoC_x (x~1) nanoparticles on Au(111) which were found by STM to have a narrow size distribution with an average diameter of 1.6 nm. The latter nucleated as "twins" on either side of the Au(111) "elbow" sites in the fcc stacking troughs. Auger and XPS showed that the electronic structure and composition of the MoC_x particles is similar to single crystal $Mo_2C(0001)$ surface.

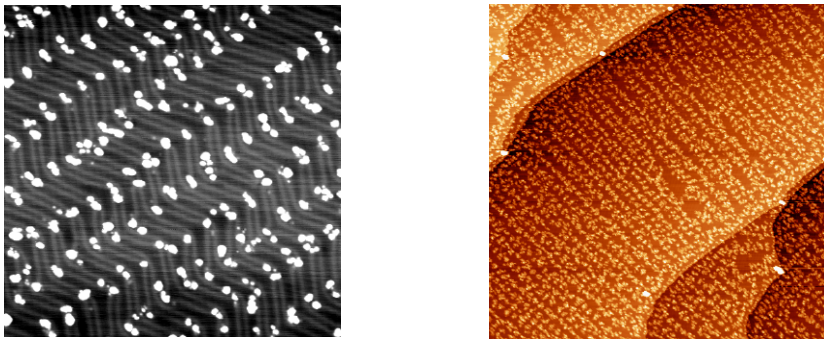

Fig. 1: Left panel: STM images of MoC_x nanoparticles with approximately 0.1 ML Mo deposited by RLAD. Image size: 100 × 100 nm. Right panel: STM images of TiO_2 nanoparticles surface prepared by depositing 0.1ML Ti on a 30 ML thick H_2O layer on Au(111) at 90 K. The size of the TiO_2 particles is ~1 nm. Image size 400 nm x 400 nm.

The RLAD method was also used to form nanocrystallites of TiO_2 by depositing Ti atoms on molecular films of H_2O (or NO_2) on a Au(111) substrate at 90 K. The reaction processes, structures and electronic properties of the TiO_2 particles were studied by XPS and STM. Pure TiO_2 particles with sizes of ~1nm were obtained at 300 K by using H_2O as the reactive layer. When NO_2 was used as the reactive layer, NO_3 radical is formed on the surface of TiO_2 particles at temperature bellow 500 K. Further annealing the sample induces the desorption of all N-containing species and leaving behind pure TiO_2 rutile and anatase particles with size ~5 nm, along with flat shape and various facets. Scanning tunneling spectroscopy (STS) displays different electronic structures for different sizes of the TiO_2 particles.

The structural and electronic properties of nanostructured $Ce_{1-x-y}Zr_xTb_yO_2$ ternary oxides: Ceria-based ternary oxides are widely used in many areas of chemistry, physics and materials science. Synchrotron-based time-resolved X-ray diffraction (TR-XRD), X-ray absorption near edge spectroscopy (XANES), Raman spectroscopy (RS), and density-functional (DF) calculations were used to study the structural and electronic properties of Ce-Zr-Tb oxide nanoparticles. The nanoparticles were synthesized following a novel microemulsion method and had sizes in the range of 4 to 7 nm. The $Ce_{1-x-y}Zr_xTb_yO_2$ ternary systems exhibit a complex behavior that *cannot* be predicted as a simple extrapolation of the properties of $Ce_{1-x}Zr_xO_2$, $Ce_{1-x}Tb_xO_2$ or the individual oxides (CeO_2, ZrO_2 and TbO_2). The doping of ceria with Zr and Tb induces a decrease in the unit cell, but there are large positive deviations with respect to the cell parameters predicted by Vegard's rule for ideal solid solutions. The presence of Zr and Tb generates strain in the ceria lattice through the creation of crystal imperfections and O vacancies. The O K-edge and Tb L_{III}-edge XANES spectra for the $Ce_{1-x-y}Zr_xTb_yO_2$ nanoparticles point to the existence of distinctive electronic properties. In $Ce_{1-x-y}Zr_xTb_yO_2$ there is an unexpected high concentration of Tb^{3+}, which is not seen in TbO_2 or $Ce_{1-x}Tb_xO_2$ and enhances the chemical reactivity of the ternary oxide. Tb↔O↔Zr interactions produce a stabilization of the Tb(4f,5d) states that is responsible for the high concentration of Tb^{3+} cations. The behavior of $Ce_{1-x-y}Zr_xTb_yO_2$ illustrates how important can be metal↔oxygen↔metal interactions for determining the structural, electronic and chemical properties of a ternary oxide.

***In situ* Time-resolved characterization of CuO-CeO_2 catalysts during the water gas shift reaction:** A big challenge within the world demand for energy is the need to protect our environment by increasing energy efficiency and through the development of "clean" energy sources. Hydrogen is a potential answer to satisfying many of our energy needs while reducing (and eventually eliminating) carbon dioxide and other greenhouse gas emissions. The water–gas shift (WGS) reaction ($CO + H_2O = CO_2 + H_2$) is used in industrial hydrogen production as well as in fuel processing for fuel cell applications. In this work, synchrotron-based *in situ* time-resolved X-ray diffraction (TR-XRD) and time-resolved X-ray absorption fine structure (TR-XAFS) were employed to study the WGS reaction over CuO-CeO_2 nanoparticles. Figure 2 (left panel) indicates that copper in the samples underwent an oxidation state change from CuO to metallic Cu during the WGS reaction when the temperature increased from 200 to 300°C. Figure 2 (right panel) also shows the relative hydrogen concentrations in the products at different temperatures as a function of time for nanoparticles consisting of 5%CuO/CeO_2 and $Cu_{0.2}Ce_{0.8}O_2$, as well as the reference compound, bulk CuO. The data were obtained while TR-XRD patterns were collected at the same time. By comparison of the TR-XRD data and the hydrogen production date for the 5% CuO/CeO_2 sample (see Figure 2), it is clear that the activity of the catalysts was closely related to the formation of the metallic Cu. No activity was observed for all the samples when there was not a metallic Cu phase at low temperature (200ºC). However, the high activity could not be obtained only on metallic copper as indicated from the CuO result in Figure 2. The ceria support played a role in the WGS reaction. The lower activity at 500°C than at 400°C for 5% CuO/CeO_2 is possibly due to the sintering of the ceria nanoparticles as indicated in Figure 3.

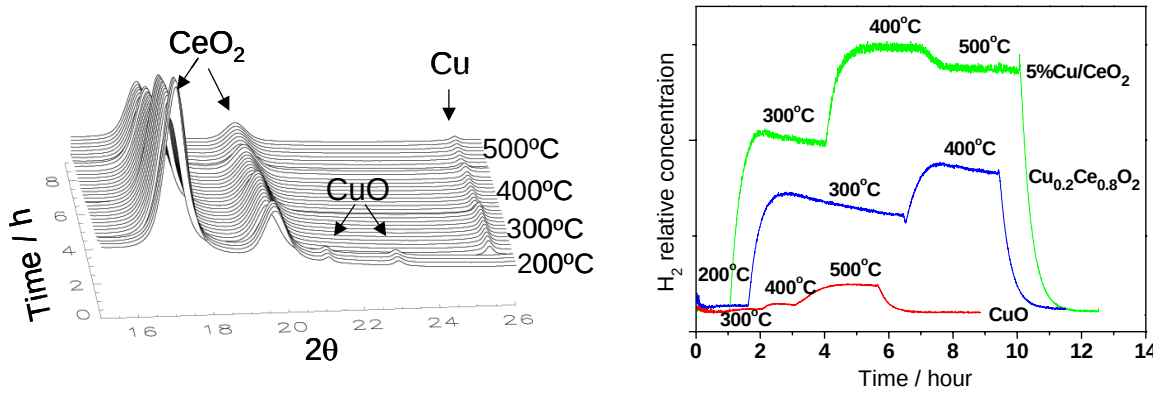

Figure 2. Left panel: TR-XRD patterns for 5%CuO/CeO_2 during the WGS reaction.(λ=0.921Å). Right panel: Relative H_2 concentrations in the products.

Gas-phase TMX clusters: formation, reactivity and size-selected deposition: We have recently constructed a new apparatus for the preparation metal containing clusters (≤ 200 atoms; ≤ 2nm), which can be mass-selected for size-dependent reactivity studies in the gas-phase and deposited on surfaces. Initial experiments have been focused on generating clusters of early transition metal compounds (carbides, nitrides, oxides, sulfides), which are known in their bulk form to be active catalysts for a wide range of heterogeneous reactions, such as hydrodesulfurization, and hydrocarbon isomerization and dehydrogenation. Using a magnetron sputtering source, we demonstrated the ability to form a wide range of bare metal, metal carbide and metal sulfide cluster ions of Ti, V, Zr, Nb and Mo. Currently, we are using gas-phase association and reaction in a hexapole scattering cell to explore the strcuture and reactions of mass-selected clusters. In the case of the titanium carbide MetCar, Ti_8C_{12}, we have investigated gas-phase reactions with a wide array of sulfiur compounds (H_2S, CH_3SH, C_4H_4S, SO_2, SCO, CS_2). This study was motivated by recent theoretical calculations by Liu, Muckerman and Rodriguez that showed that the Ti_8C_{12} cluster exhbited catalytic activity in the hydrdesulfurization reaction of thiophene (C_4H_4S). Our experiments show that in addition to simple association of up to eight weakly bound molecules (one per metal atom), all of the sulfur compounds examined (except for H_2S) also showed evidence of dissociative adsorption in which the fragments of the sulfur molecule were found attached to the intact MetCar cluster. Of particular interest is the observation that thiophene decomposition on Ti_8C_{12} only occurs after the adsorption of 3-4 molecules, suggesting the "activation" of the MetCar cluster before it can induce dissociation of the next adsorbed thiophene (see Figure 3). These trends have been reproduced in the theoretical DFT calculations currently in progress by Liu, Muckerman and Rodriguez.

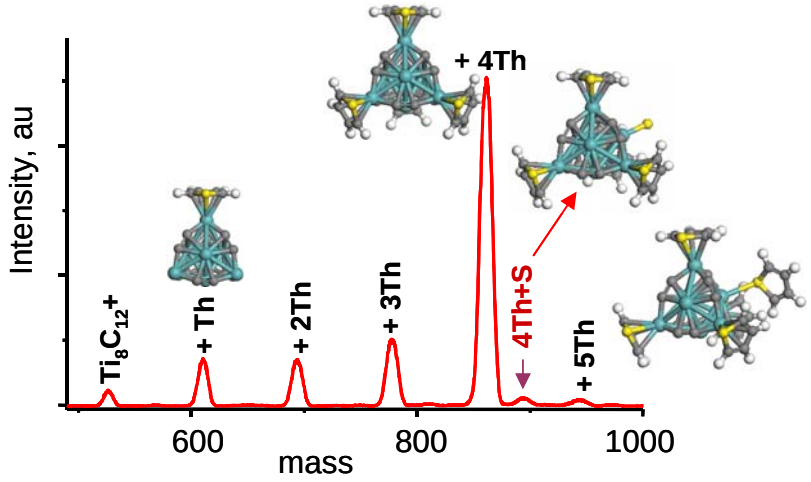

Figure 3: Mass spectra of the products resulting from the reaction of thiophene with the $Ti_8C_{12}^+$ MetCar cation. Also shown are optimized theoretical structures for the $Ti_8C_{12}^+ \bullet (C_4H_4S)_n$ adducts and reaction products.

Screening of metal carbide surfaces and metcars as HDS catalysts: We have examined the interaction of the metal carbide systems (M_2C, MC bulk surfaces as well as the M_8C_{12} metcars where M = Ti, V and Mo) with thiophene (C_4H_4S) and S. In these calculations, the adsorbates and the metcars were allowed to relax in all degrees of freedom. The top three layers of the surfaces were relaxed along with the adsorbates while the bottom layer was held fixed at the calculated bulk lattice positions. In all cases, the M_2C surfaces bound both thiophene and S strongly, but the MC surfaces bound both thiophene and S quite weakly. The corresponding metcars were found to bind both thiophene and S moderately. These results suggested that the M_2C surfaces would not be good HDS catalysts despite the fact that they could dissociate thiophene because they bound the S product too strongly. The MC surfaces would not be good catalysts because they are not active enough to dissociate thiophene even though the product S could easily be removed. The metcars, with their intermediate activity towards both reactant and product, are more promising candidates for an HDS catalyst.

The Ti_8C_{12} metcar: A new model catalyst for hydrodesulfurization: Elementary reaction steps and barriers for thiophene hydrodesulfurization (HDS) on a Ti_8C_{12} nanoparticle were investigated using density functional theory. It was found that despite of its high carbon concentration, Ti_8C_{12} displays a superior catalytic potential for hydrodesulfurization. Figure 4 shows different steps for the HDS of thiophene (C_4H_4S) on the metcar. They involve the dissociative adsorption of H_2, the adsorption of C_4H_4S, the cleavage of C-S bonds, the hydrogenation and desorption of C_4H_4 fragments, and the removal of S adatoms as gaseous H_2S. The calculated energy changes are shown in Figure 2. Compared to the industrial catalysts, the hydrogen dissociation and C-S bond cleavage on Ti_8C_{12} are more facile, and the removal of sulfur is energetically comparable. Our results also show that the catalytic activity of Ti_8C_{12} can be associated with its unique structure that is quite different from that of bulk metal carbides.

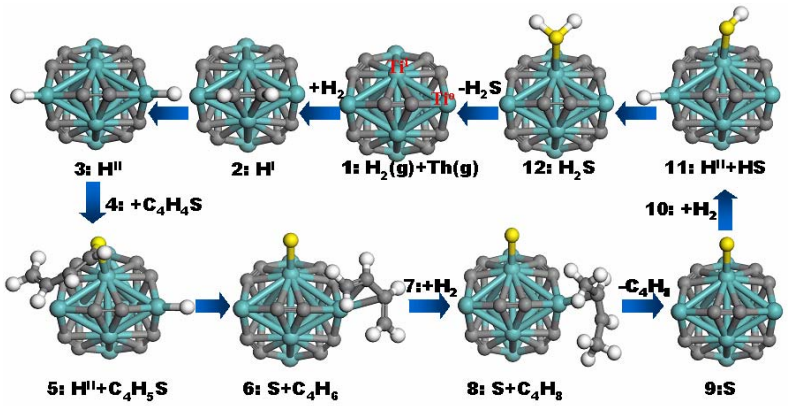

Figure 4: Catalytic hydrodesulfurization of thiophene on the Ti_8C_{12} Met-Car.

Publications 2003-2005

"Gas-Phase Production of Molybdenum Carbide, Nitride and Sulfide Clusters and Nanocrystallites", J. M. Lightstone, H. Mann, M. Wu, P. M. Johnson, and M. G. White, *J Phys. Chem*., B107, 10359-10366 (2003).

"Ru Nanoclusters Prepared by $Ru_3(CO)_{12}$ Deposition on Au(111)", Cai, T.; Song, Z.; Chang, Z.; Liu, G.; Rodriguez, J. A.; Hrbek, J., *Surf. Sci*. 538, 76-88 (2003).

"The Deposition of Mo Nanoparticles on Au(111) from a $Mo(CO)_6$ Precursor: Effects of CO on Mo-Au Intermixing", Liu, P.; Rodriguez, J. A.; Muckerman, J. T.; Hrbek, J., *Surf. Sci*., 530, L313-L321 (2003).

"Interaction of CO, O and S with Metal Nanoparticles on Au(111): A Theoretical Study", Liu, P.; Rodriguez, J. A.; Muckerman, J. T.; Hrbek, J., *Phys. Rev.* B, 67, 155416 (2003).

"Chemical Reactivity of Metcar Ti_8C_{12}, Nanocrystal $Ti_{14}C_{13}$ and A Bulk TiC(001) Surface: A Density Functional Study", Liu, P.; Rodriguez, J. A.; Hou, H.; Muckerman, J. T., *J. Chem. Phys*., 118, 7737-7740 (2003).

"Interaction of Sulfur Dioxide with Titanium-Carbide Nanoparticles and Surfaces: A Density Functional Study", Liu, P.; Rodriguez, J. A., *J. Chem. Phys.*, 119, 10895-10903 (2003).

"SnO_2 Nanoribbons as NO_2 Sensors: Insights from First-principles Calculation", Maiti, A.; Rodriguez, J. A.; Law, M.; Kung, P.; McKinney, J. R.; Yang, P., *Nanoletters*, 3, 1025-1028 (2003).

"Properties of CeO_2 and $Ce_{1-x}Zr_xO_2$ Nanoparticles: XANES, Density Functional, and Time-Resolved XRD Studies", Rodriguez, J. A.; Hanson, J. C.; Kim, J.-Y.; Liu, G.; Iglesias-Juez, A.; Fernandez-Garcia, M., J., *Phys. Chem*. B 107, 3535-3543 (2003).

"Activation of Au Nanoparticles on Oxide Surfaces: Reaction of SO_2 with Au/MgO(100)", Rodriguez, J. A.; Perez, M.; Jirsak, T.; Evans, J.; Hrbek, J.; Gonzalez, L., *Chem. Phys. Lett*., 378, 526-532 (2003).

"The Behavior of Mixed-Metal Oxides: Structural and Electronic Properties of $Ce_{1-x}Ca_xO_2$ and $Ce_{1-x}Ca_xO_{2-x}$", Rodriguez, J. A.; Wang, X.; Hanson, J. C.; Liu, G.; Iglesias-Juez, A.; Fernandez-Garcia, M. J., *Chem. Phys*., 119, 5659-5669 (2003).

"A Novel Growth Mode of Mo on Au(111) from a $Mo(CO)_6$ Precursor: An STM Study", Song, Z.; Cai, T.; Rodriguez, J. A.; Hrbek, J.; Chan, A. S. Y.; Friend, C. M., *J. Phys. Chem*. B, 107, 1036-1043 (2003).

"Molecular Level Study of the Formation and the Spread of MoO_3 on Au(111) by STM and XPS", Song, Z.; Cai, T.; Chang, Z.; Liu, G.; Rodriguez, J. A., *J. Am. Chem. Soc*., 125, 8059-8066 (2003).

"Kinetic Characterization of PtRu Fuel Cell Anode Catalysts Made by Spontaneous Pt Deposition on Ru Nanoparticles", Wang, J. X.; Brankovic, S. R.; Zhu, Y.; Hanson, J. C.; Adzic, R. R., *J. Electrochem. Soc.*, 150, A1108-A1117 (2003).

"A Computational Study of the Geometry and Properties of the Metcars Ti_8C_{12} and Mo_8C_{12} ", Hou, H.; Muckerman, J. T.; Liu, P.; Rodriguez, J. A., *J. Phys. Chem*. A 107, 9344-9356 (2003).

"Sono Synthesis and Characterization of Nanophase Molybdenum-Based Materials for Catalytic Hydrodesulfurization", Mahajan, D.; Marshall, C. L.; Castagnola, N.; Hanson, J. C., *Appl. Catal.* A, 258, 83-91 (2004).

"Uexpected chemical activity in metal compound nanoparticles: electronic and steric effects in M_8C_{12} (M=Ti,V,Mo) metcars", P. Liu, J. A. Rodriguez and J. T. Muckerman, *J. Chem. Phys.* 121,10321-10324 (2004).

"The Ti_8C_{12} metcar: A new model catalyst for hydrodesulfurization", P. Liu, J. A. Rodriguez and J. T. Muckerman *J. Phys. Chem. B* 108,18796-18798 (2004).

"Desulfurization of SO_2 and thiophene on surfaces and nanoparticles of molybdenum carbide: unexpected ligand and steric effects", P. Liu, J. A. Rodriguez and J. T. Muckerman, *J. Phys. Chem. B* 108, 15662-15670 (2004).

"Why is Re-Re bond formation/cleavage in $[Re(bpy)(CO)_3]_2$ different from that in $[Re(CO)_5]_2$? Experimental

and theoretical studies on the dimmers and fragments", E. Fujita and J. T. Muckerman, *Inorg. Chem*. 43, 7636-7647 (2004).

"Preparation and Structural Characterization of RuS_2 Nano-Islands on Au(111)", T. Cai, Z. Song, J. A. Rodriguez and J. Hrbek, *J. Am. Chem. Soc.* 126**,** 8886-8887 (2004).

"Nanostructured Oxides in Chemistry: Characterization and Properties", M. Fernandez-Garcia, A. Martinez-Arias, J. C. Hanson and J. A. Rodriguez, *Chem. Rev.* 104**,** 4063-4104 (2004).

"The Chemical Activity of Metal Compound Nanoparticles: Importance of Electronic and Steric Effects in M_8C_{12} (M=Ti, V, Mo) Metcars", P. Liu, J. A. Rodriguez and J. T. Muckerman, *J. Chem. Phys.* 121**,** 10321-10324 (2004).

"Structure and Reactivity of Ru Nanoparticles Supported on Modified Graphite Surfaces: A Study of the Model Catalysts for Ammonia Synthesis", Z. Song, T. Cai, J. C. Hanson, J. A. Rodriguez and J. Hrbek, *J. Am. Chem. Soc.* 126**,** 8576-8584 (2004).

"The Behavior of Mixed-Metal Oxides: Physical and Chemical Properties of Bulk $Ce_{1-x}Tb_xO_2$ and Nanoparticles of $Ce_{1-x}Tb_xO_y$ ", X. Wang, J. C. Hanson, G. Liu, J. A. Rodriguez, A. Isglesias-Juez and M. Fernandez-Garcia, *J. Chem. Phys.* 121**,** 5434-5444 (2004).

"Nanostructured Oxides in Chemistry: Characterization and Properties", Fernandez-Garcia, M.; Martinez-Arias, A.; Hanson, J. C.; Rodriguez, *J. A., Chem. Rev*. 104, 4063-4104 (2004).

"Structure and Reactivity of Ru Nanoparticles Supported on Modified Graphite Surfaces: A Study of the Model Catalysts for Ammonia Synthesis", Song, Z.; Cai, T.; Hanson, J. C.; Rodriguez, J. A.; Hrbek, J., *J. Am. Chem. Soc.* 126, 8576-8584 (2004).

"The Ti_8C_{12} Nanoparticle: A New Catalyst for Hydrodesulfurization", P. Liu, J. A. Rodriguez and J. T. Muckerman, *J. Phys. Chem. B* (Communication) 108, 18796-18798 (2004).

"Gold Nanoparticles on Titania: Activation and Behavior", Rodriguez, J. A., in *Dekker Encyclopedia of Nanoscience,* ed.; 'Ed.'^'Eds.' Dekker Publishing: New York, NY, 2004. Pages 1297-1304 (submitted).

"Physical and Chemical Properties of Novel Tb-Doped Cerium Oxide Nanoparticles", Wang, X.; Hanson, J. C.; Liu, G.; Rodriguez, J. A., *J. Chem. Phys*. 121, 5434-5444 (2004).

"XANES Characterization of Extremely Nanosized Metal Carbonyl Subspecies (Me=Cr,Mn,Fe and Co) Confined onto the Mesopores of MCM-41 Materials", J. M. Ramallo-Lopez, E. J. Lede, F. G. Requejo, J. A. Rodriguez, J.-Y. Kim and R. Rosas-Salas, *J. Phys. Chem. B,* 108, 20005-20010 (2004).

"Reactivity Studies with Gold-Supported Molybdenum Nanoparticles", D. V. Potapenko, J. M. Horn, R. J. Beuhler, Z. Song and M. G. White, *Surf. Sci.* 574, 244-258 (2005).

"The Characterization of Molybdenum Carbide Nanoparticles Formed on Au(111) using Reactive-Layer Assisted Deposition", J. M. Horn, Z. Song, D. V. Potapenko, J. Hrbek and M. G. White, *J. Phys. Chem. B* (Communication) 109**,** 44-47 (2005).

"Physical and Chemical Properties of $Ce_{1-x}Zr_xO_2$ Nanoparticles and $Ce_{1-x}Zr_xO_2$(111) Surfaces: Synchrotron-based Studies", J. A. Rodriguez, X. Wang, G. Liu, J. Hanson, J. Hrbek, C. H. F. Peden, A. Iglesias-Juez and M. Fernandez-Garcia, *J. Molec. Catalysis A* 228, 11-19 (2005).

"First-Principles Study of Ti-Catalyzed Hydrogen Chemisorption on an Al Surface: A Critical First Step for Reversible Hydrogen Storage in $NaAlH_4$", S. Chaudhuri and J. T. Muckerman, *J. Phys. Chem. B* (Communication), in press.

DE-FG03-03ER15463 **Tony Heinz, Stephen O'Brien (Columbia U.)**
DE-FG03-03ER15464 **Ludwig Bartels (UC Riverside)**
DE-FG03-03ER15465 **Talat Rahman (Kansas State U.)**

CATALYIS SCIENCE INITIATIVE: Controlling Structural, Electronic and Energy Flow Dynamics of Catalytic Processes through Tailored Nanostructures

Graduate students: T. Andelman (Columbia), S. Hong (KSU), T. Jiao (UCR), I. Mandelbaum (Columbia), F. Mehmood (KSU), R. Perry (UCR), D. Quinn (Columbia), B. White (Columbia), C.-K. Wu (Columbia), M. Yin (Columbia)
Post-docs: D. Vempaire (UCR), L. Huang (Columbia), B. V. Rao (UCR), E. Shevchenko (Columbia), S. Stolbov (KSU), A. Thoss (UCR)
Collaborators: T. Ala Nissilla (Helsinki), L. E. Brus (Columbia), K. P. Bohnen (Karlsruhe), C. Burda (Case Western), G. Ertl (FHI Berlin), P. Feibelman (Sandia), R. Friesner (Columbia), H.-J. Freund (FHI Berlin), R. Heid (Karlsruhe), C. Henry (Marseille), J. Hone (Columbia), J. Koberstein, C. Murray (IBM Watson Research Center), G. Neumark (Columbia), M. Steigerwald (Columbia), N. Turro (Columbia), O. Trushin (Yaroslav), Y. Zhu (BNL)

Center for Integrated Science and Engineering
Columbia University
530 West 120th St.
New York, NY 10027
tony.heinz@columbia.edu

Department of Chemistry
Pierce Hall
University of California
Riverside, CA 92521
ludwig.bartels@UCR.edu

Department of Physics
Kansas State University
Manhattan, KS 66506
rahman@phys.ksu.edu

Goals:

The overall goal of the project is to pursue the understanding and development of new catalysts that produce specific surface reactions by controlling reaction pathways through modification of the electronic states, steric constraints, and energy flow dynamics using nanostructured materials. Three research themes are being followed to support this challenging long-term goal: (1) The synthesis of highly controlled nanostructured materials that will serve as model catalysts; (2) experimental investigations of controlled diffusion and non-equilibrium processes on surfaces and nanostructures; and (3) theoretical investigations to understand the electronic properties, dynamics, and reactivity of the corresponding systems. Principal emphasis in the synthetic area is placed on self assembly techniques on the generation of multi-component systems with enhanced functionality. Within the experimental surface-science component, research involves the traditional tools of surface science, but also places special emphasis on scanning tunneling microscopy to understand the nature of behavior on heterogeneous surfaces and laser sources to induce and probe nonequilibrium processes. The theoretical component involves extensive numerical techniques to address realistic materials and processes.

DOE Interest:

Catalytic reactions are of central importance for a broad range of industrial and environmental processes ranging from catalytic oxidation of CO in exhaust systems to catalytic hydro-desulfurization of gasoline. The improved understanding of catalytic processes on the atomic scale afforded by application of methods that can follow molecular dynamics at high excitation levels combined with the design of optimized nanostructured catalysts should lead to advances in catalytic yield and selectivity, with the potential for impact on a diverse and significant set of chemical processes.

Recent Progress:

Nanostructured Materials for Catalysis Science

At Columbia the O'Brien group has pursued research into the synthesis of new nanostructured materials and assemblies. The work has examined several systems, include copper oxide (Cu_2O) nanoparticles, model nanoparticle superlattices comprised of two distinct materials, and improved catalytic growth of carbon nanotubes

by chemical vapor deposition. The latter example is one where nanoscale catalysts are already being extensively used to optimize the selectivity of catalytic growth. We report briefly on these advances.

Copper (I) oxide (Cu_2O) is a metal-oxide semiconductor with promising applications in solar energy conversion and catalysis. To understand the $Cu/Cu_2O/CuO$ system at the nanoscale, we have developed a method for preparing highly uniform monodisperse nanocrystals of Cu_2O. The procedure also serves to demonstrate our development of a generalized method for the synthesis of transition metal oxide nanocrystals. Cu nanocrystals are initially formed and subsequently oxidized to form highly crystalline Cu_2O. The volume change during phase transformation can induce crystal twinning. Absorption in the visible region of the spectrum gave evidence for the presence of a thin, epitaxial layer of CuO, which is blue shifted, and appears to increase in energy as a function of decreasing particle size. XPS confirmed the thin layer of CuO, calculated to have a thickness of ~ 5 Å. We note that the copper (I) oxide phase (favorable for catalysis) is surprisingly well-stabilized at this length scale. In addition, to the oxide particles, progress has been made in the synthesis of highly monodisperse Pd and Pt nanoparticles with diameters in the nanometer range. In conjunction with Nick Turro (Columbia), a catalysis reactor and GC-MS system has been developed for initial screening of catalytic CO oxidation in these materials.

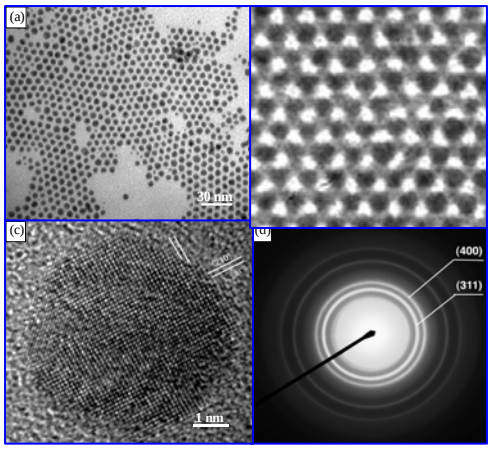

Fig. 1. (a) TEM micrograph of self-assembled 6-nm diameter Cu_2O nanocrystals; (b) TEM image showing a larger area view of a close-packed superlattice of 6-nm Cu_2O nanocrystals. (c) High resolution image showing the single crystal and high crystallinity; (d) Selected area electron diffraction pattern of Cu_2O nanocrystals.

As an exploratory aspect of this program, we wish to examine the possibility of catalytic reactions that utilize two distinct and controlled material sub-systems. This capability could be of particular importance for problems such as photo-catalysis, where one subsystem could be optimized to capture the excitation of solar radiation, while another material to which this non-equilibrium excitation is transferred would be optimized for catalytic activity. This long-term goal is being supported by work in the O'Brien group in which the recent progress in synthesis of different types of nanoparticles with controllable size and shape is opening up the possibility of using nanoparticles as "building blocks" for the construction of two and three-dimensionally ordered arrays. Ideally such structures will form will ordered crystals of different nanoparticles, yielding materials with homogeneous long-range order and highly controlled properties. In collaboration with Chris Murray (IBM) and the Columbia MRSEC program, the O'Brien group has succeeded in preparing a wide range of metal/semiconductor and metal-oxide/semiconductor bimodal superlattice structures with highly defined structures and remarkable long-range order. These will serve as model systems for exploring energy transfer and potential catalytic reactions.

Single-wall carbon nanotubes (SWNTs) constitute a further class of materials being investigated at Columbia as part of the Catalysis Science Initiative. In this effort, O'Brien and collaborators are concerned with catalytic growth by chemical vapor deposition (CVD) and Heinz and collaborators are involved in detailed characterization of the resulting SWNTs and their properties. The interest in this material system is two fold. One motivation concerns the optimization of the metallic catalysts used in the CVD growth of this model nanosystem. Because of the dramatically different properties of SWNTs depending on their precise structure (diameter and chiral angle), there is enormous interest in improved control of the catalytic growth and selectivity. In addition, the potential integration of SWNTs into electronic devices and other applications requires reliable high-yield catalytic growth methods. A second motivation concerns the potential of SWNTs in catalysts for other reactions. We are particularly interested, in conjunction with the discussion above, in examining their potential for carrying excitation from one nanostructure to the other, given the remarkable electrical and optical properties associated with their highly 1-dimensional structure.

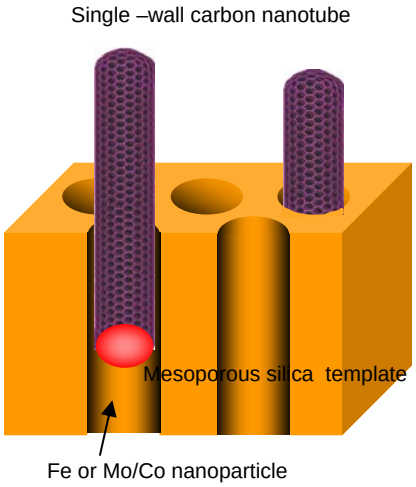

Fig. 2. Templated growth of single-wall carbon nanotubes

To further these research aims, O'Brien has developed techniques based on CVD growth of SWNTs using templated metal catalyst particles. In this approach (Fig. 2), highly porous materials, such as porous silicon, mesoporous silica, anodic aluminum oxide film (AAO) in the pore range of a few to several hundred nanometers), have shown excellent performances in CVD synthesis of aligned multi-wall carbon nanotubes. For these templates, however, there are few successful cases in growing highly aligned SWNTs either because the pore is not uniform or because the pore size is too large compared with that of SWNTs. Recently, we used highly stable mesoporous silica thin films (SBA series) with uniform mesopore sizes of 2-6 nm (matching the SWNT size range) and preferentially oriented pore direction as a template to successfully control the oriented growth of SWNTs. Catalyst precursors for Fe, Mo and Co (e.g., $FeCl_3$) are incorporated into the mesostructure during a sol-gel process. Following calcination, nanometer-sized metal oxide (e.g. Fe_2O_3) particles are produced within mesoporous channels with the particle size limited by the channel dimension, which, in turn, controls the size of carbon nanotubes grown by CVD. We wish to understand the mechanism of growth of carbon nanotubes from the catalyst nanoparticles to improve growth selectivity.

With respect to characterization of the resulting SWNTs, Heinz and Columbia collaborators Louis Brus and Jim Hone have developed a novel optical analysis technique based on Rayleigh or elastic light scattering. The method has sensitivity to individual SWNTs and yields high-quality optical spectra of both metallic and semiconducting nanotubes with rapid data collection rates. On-going research should allow a complete structural [(n,m) indices] analysis of individual tubes to be obtained from the optical data. This capability will provide not only a method to determine the degree of selectivity in the catalytic growth, but to examine individual nanotubes and correlate their structure with the local growth conditions, thereby providing a means to understanding methods of enhanced catalytic selectivity in nanotube growth.

In related investigations of SWNTs, Heinz and Columbia collaborators Louis Brus, Nick Turro, and Rich Friesner have applied optical techniques to investigate prototypical surface chemistry on the sidewalls of SWNTs. It was demonstrated using temperature-programmed desorption for SWNTs in solution phase that adsorbed molecule oxygen would desorb at temperatures near 100C, suggesting binding energies of ~ 1 eV. The optical monitoring via fluorescence efficiency permitted the relative behavior of SWNTs of different chiral structure to be examined. The role of protonation of the adsorbed oxygen in influencing the photo-physical properties of the SWNTs was also explored. It was found that only a few protonated adsorbed oxygen molecules could led to a significant quenching of fluorescence in these structures. Other investigations have sought to examine the possibility of retaining or transporting photo-generated excitation in SWNTs. This research has been motivated by many recent studies demonstrating the possibility of both photo- and electroluminescence of SWNTs. In work carried out by Heinz and collaborators at Columbia, the rate of radiative and non-radiative decay channels for photoexcited SWNTs was investigated using ultrafast pulsed lasers. A new non-radiative decay channel associated with Auger recombination (or exciton-exciton annihilation) was identified.

Probing and Controlling Surface Dynamics, Order, and Diffusional Processes on the Atomic Scale

In joint work between the Heinz group at Columbia and the Bartels group at UC Riverside, the influence of high levels of electronic excitation in metal substrates on surface processes was examined. These studies are motivated by a need to understand the fundamentals of adsorbate/substrate energy transfer to evaluate the possible role of non-equilibrium catalytic processes. They are also motivated by a desire to combine pulsed laser techniques with scanning tunneling microscopy (STM) to reach both the ultrafast time scale and the atomic length scale. In addition to the general interest and importance of this possibility, it has implications for catalysis science, where one wishes to have understanding on the atomic scale, but is often precluded from applying optimized local probing techniques like STM because the rates of motion under realistic catalytic conditions are far too high. In

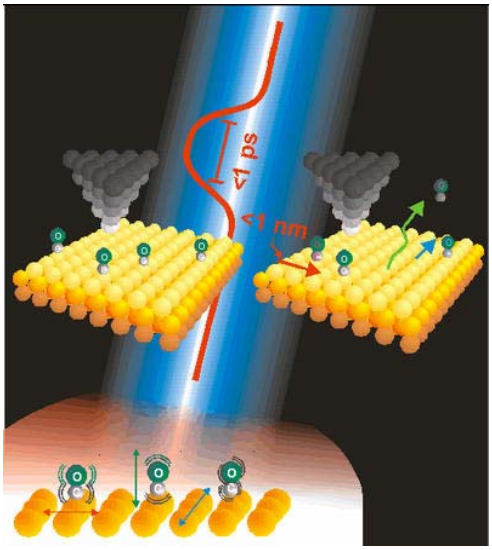

Fig. 3. Schematic representation of investigation of surface diffu and desorption of CO/Cu(110) using femtosecond laser excitation

this context, ultrafast lasers can allow one to reach high rates and excitation densities for exceedingly short periods of time over which only small displacements are expected even when atomic and molecular motion is very rapid.

This investigation revealed that the high density of electronic excitation produced in the substrate could couple to adsorbate motion, producing ultrafast response and distinctive branching ratios through this non-adiabatic coupling. In particular, the relative propensity for diffusion and desorption was dramatically different from any conventional thermal regime. So to was the degree of in-plane anisotropy in the diffusion rate: Under thermal conditions, a strong preference for diffusion along the atomic rows of the Cu(110), while for the high-excitation regime only a weak anisotropy was observed by the direct STM measurements. These investigations have led to an increased understanding of then nature of non-adiabatic energy transfer between metals and model adsorbates. From the experimental standpoint, the measurement technique can be viewed as having pushed the STM into probing much faster processes. Although the STM analyses were performed only before and after laser excitation, they monitored molecular motion occurring on the time scale of picoseconds.

In preparation for similar measurements on Cu(111), the Bartels group has characterized the diffusive behavior of CO on extended terraces of Cu(111). The (111) surface of fcc metals are more relevant than their (110) surface, as they constitute the thermodynamic equilibrium surface and are exhibited predominantly by realistic metal particles. Of particular interest for the upcoming measurements are the interactions between adsorbates. For this reason, we investigated the diffusion of CO molecules in the vicinity of other CO molecules in detail. We found a significant acceleration of adsorbate diffusivity with increasing local coverage until a regime is reached, in which the adsorbates block the diffusion of their neighbors for steric reasons. By development of a novel way of evaluating diffusion data obtained at low coverages, we could successfully model the acceleration of diffusion.

The behavior of sulfur-containing compounds on metal catalyst particles is important for the hydrodesulfurization of gasoline. We investigated the diffusion behavior of thiophenol on Cu(111) in preparation of measurements utilizing substrate heating by femtosecond laser irradiation. We find that thiophenol molecules aggregate to oligomers up to the heptamers but do not form extended islands. A careful study of the behavior of benzenethiol during equilibrium substrate heating revealed much of the energetics of the underlying process. Currently modeling of the system in collaboration with the Rahman group is under way.

The Bartels group has also completed the investigation of halogen-substitution of benzenethiol on the formation of island upon adsorption onto a Cu(111) surface from the gas phase. We found a strong impact of substitution on

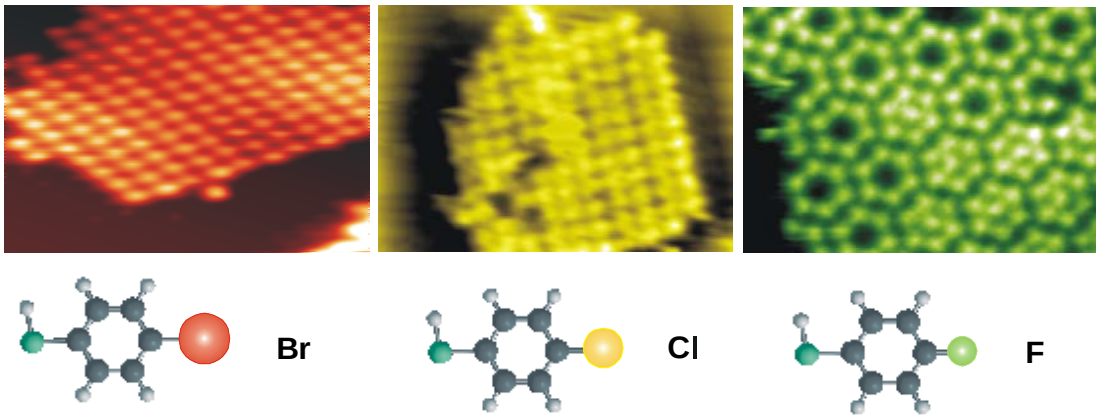

Fig. 4. Ordered patterns of bromo-thiophenol (TP), chloro-TP, fluoro-TP. The plot correlates the difference of electronegativity between the *m*-/*p*- substituent (solid) with the complexity of the film unit cell (open).

the resultant surface patterns. For para-substitution, we found the molecular quadrupole moment to determine the film pattern. Asymmetrically substituted species become chiral once they adsorb flat on a surface. The enantiomers separate on the surface and form locally enantiopure surface patterns.

Utilizing the knowledge we gained about thiophenol diffusion, the Bartels group set out to validate it by encoding specific surface behavior, namely unidirectional diffusion on the isotropic Cu(111) surface, into a molecule. In conjunction with theoretical modeling in the Rahman group, we identified 9,10-dithioanthracene as a species, whose surface diffusion is restricted to one direction due to guidance of its diffusive motion by the interplay of the substrate interaction of the aromatic moiety and the two sulfur substrate linkers. To prevent disulfide-polymerization during deposition, we synthesize 9,10-diacethylthioanthracene, which becomes un-protected by post-deposition annealing. We observed several thousand diffusion events of dithioanthracene and found exclusive diffusion along the substrate high-symmetry direction (i.e. [1$\underline{1}$0]), but no molecular rotation or transversal diffusion. Theoretical modeling by the group of co-PI Rahman KSU group shows that dithioanthracene moves in a way that can be viewed as walking across the surface, always leaving one sulfur substrate linker stationary to guide its motion.

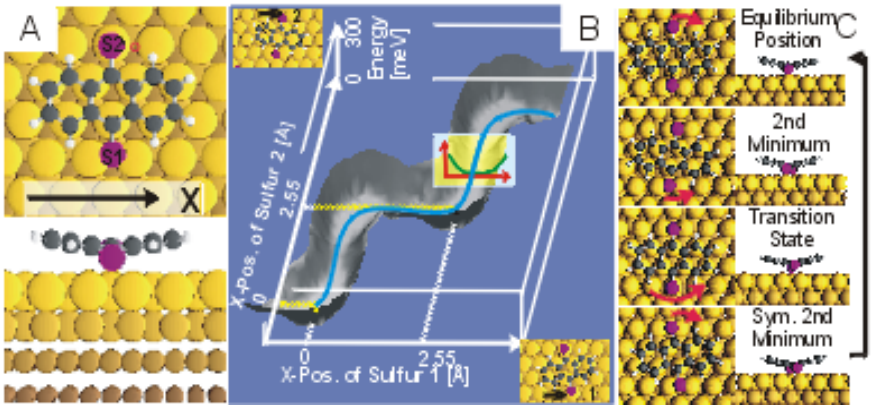

Fig. 5. A) 9,10-dithioanthracene adsorption orientation, B) diffusion potential trough as calculated in collaboration with the Rahman group and C) molecular configuration during diffusion.

In order to further the link the detailed surface science studies being undertaken by the Bartels and Heinz groups with the development of nanostructures being prepared by wet chemistry by the O'Brien group and others, the Bartels group is developing a technique that allows deposition of species directly from the solution phase onto a surface held under UHV conditions. This will ultimately enable us to study the impact of a range of well-characterized nanostructured materials in catalytic in a highly controlled environment with advanced analysis capabilities. Initial tests of the deposition method have used substituted thiophenols as test solutes and cyclohexane as a solvent show that we can deposit clean adsorbate coverages by microsecond pulsed-valve deposition. Currently, we start experiments with toluene as a solvent because we found that the solubility of species of interest (oxide nanoparticles, large molecules, etc.) in cyclopean is too low to permit convenient deposition.

Ab-Initio Theoretical Studies

Ab-initio electronic structure calculations play a critical role in providing underlying physical understanding of the experimental program. This component of the program is being carried out by the Rahman group at Kansas State University. Rahman's group has the specific goal of obtaining theoretical insights into the structural, dynamical, thermodynamical, and kinetic factors that foster enhancement of rates of chemical reactions of prime technological importance. Of particular interest is the nature of the binding of the reactants to the substrate, and the energetics and dynamics of various competing processes including diffusion of the adsorbates on inhomogeneous (stepped, kinked, facetted nanoparticles, with co-adsorbates, etc.) surfaces. Through accurate theoretical calculations and computer simulations, Rahman's group is thus responsible for identifying microscopic processes which control the reactivity of surfaces, supported nanoparticles, and their interfaces. In developing the

framework for these investigations, Rahman's group is engaged in collaborative work with experimental groups of Bartels at University of California-Riverside, and Heinz and O'Brien, at Columbia University.

In the quest for new ways to enhance and control reaction rates, it should be mentioned that defects like steps have already been shown to facilitate certain reactions like molecular dissociations. Alkali addition has also been found to give rise to enhanced reaction rates. More recently, nanoparticles of metals such as Au and Pd and of oxides have been found to be highly reactive. These important results, however, have been achieved through trial and error and lack a systematic and robust foundation with good predictive power which is essential for practical applications. Rahman's activity under the present grant is already engaged in developing a framework for systematic understanding of factors, like the ones mentioned above, that enhance catalytic activity at nanostructured surfaces. This is done through the application of a combination of techniques including *ab-initio* electronic structure calculations based on density functional theory and a novel approach to kinetic Monte Carlo simulations. Specific recent theoretical advances as part of the Catalysis Science Initiative include the following.

In efforts to understand and predict factors that may enhance and/or channel the diffusion and reactivity of molecules on metal surfaces, we have carried out *ab-initio* electronic structure calculations of the dynamics of CO and O_2 on Cu(111) and Pd(111) in the presence of alkali co-adsorbates. A large softening in the vibrational frequencies of these molecules is found as they approach the metal surface and even before adsorption, as a result of the sea of low lying collective excitations induced by the alkali atoms. Since the effect is localized above the surface, STM measurements are ideally suited to confirm our predictions. Related calculations of the diffusion of CO on Cu(111) were performed in connection with the experiments of Bartels and Heinz groups who are also planning to observe the effect of alkali adsorption on the system.

In a collaborative work with Bartels group (see above), the Rahman group investigated the adsorption characteristics of benzenethiol molecules on Cu(111). Our results were helpful in the analysis of the STM data and provide good rationale for manner in which the S atoms anchor on Cu(111) and the nature of the adsorbate-substrate interaction. We are intrigued by the aggregation of the benzenethiols into heptamers,. We are working with Bartels group to provide a theoretical basis for this observation. We are also investigating the diffusion energetics for these molecules on Cu(111).

To support the experiments of Bartels group concerning the guided diffusion of 9,10-dithioanthracene (DTA), the Rahman mapped out the potential energy surface that the molecule sees on Cu(111) using electronic structure calculations based on density functional theory (Fig. 5). As predicted by theory, DTA was found to diffuse exclusively along one direction by means of a biomimetic guidance scheme.

As a step towards understanding the relative role of steps and elemental metal in a specific chemical reaction, we have calculated adsorption energies (E_{ad}), diffusion barriers and the first dissociation barriers (E_1) for NH_3 on the Ni(111), Pd(111), Ni(211) and Pd(211). The top sites are found to be preferred for NH_3 adsorption on Ni(111) and Pd(111) and the diffusion barrier is substantially higher for Pd(111) than for Ni(111). We also find that during the first dissociation step (NH_3 => NH_2 +H) on Ni(111), NH_2 moves from the top site to the nearest hollow site, while on Ni(211) it moves from the initial top site at the step edge to the bridge site on the same step chain. H is found to occupy the hollow sites for both surfaces. For the reaction on Ni(111), the adsorption energy is found to be lower that the dissociation energy by 0.23 eV, while at the step of Ni(211), E_1 and E_{ad} are almost equal to each other. This suggests that the molecule will rather desorb on Ni(111) than dissociate, whereas at the step the dissociation is favorable.

RuO_2 surfaces have recently been proposed to be highly reactive for CO oxidation, but not for NO. To understand the rationale for the difference the Rahman group has carried out a systematic analysis of CO and NO on RuO_2(110) to find that density functional theory calculations can indeed relate the difference in behavior to the nature of the bonding between the two molecules and the surface.

Publications 2004-05:

1. L. Bartels, F. Wang, D. Moeller, E. Knoesel, T. F. Heinz, "Real-Space Observation of Molecular Movement Induced by Femtosecond Laser Pulses," Science **305**, 648 (2004).
2. K. L.Wong, X. Lin, K.-Y. Kwon, G. Pawin, B. V. Rao, A. Liu A., L. Bartels, S. Stolbov, T. S. Rahman, "Halogen-Substituted Thiophenol Molecules on Cu(111)," Langmuir **20**, 10928 (2004).
3. M. Yin, Y. Gu, I. L. Kuskovsky, T. Andelman, Y. Zhu, G. F. Neumark, and S. O'Brien, "Zinc Oxide Quantum Rods," J. Am. Chem. Soc. 126, 6206 (2004).
4. J. I. Dadap and T. F. Heinz, "Second-Harmonic Spectroscopy," in Encyclopedia of Modern Optics, ed. by B. D. Guenther (Elsevier, Amsterdam, 2004).
5. M.Y. Sfeir, F. Wang, L. M. Huang, C.C. Chuang, J. Hone, S.P. O'Brien , T. F. Heinz, and L. E. Brus, "Probing Electronic Transitions in Individual Carbon Nanotubes by Rayleigh Scattering," Science **306,** 1540 (2004).
6. K. Wong, K.-Y. Kwon, B. V. Rao, A. Liu, and L. Bartels, "The Effect of Halo-Substitution on the Geometry of Arenethiol Films on Cu(111)," J. Am. Chem. Soc. **126**, 7762 (2004).
7. E. Knoesel, M. Bonn, J. Shan, F. Wang, and T. F. Heinz, "Conductivity of Solvated Electrons in Hexane Investigated with Terahertz Time-Domain Spectroscopy," J. Chem. Phys. **121,** 394 (2004).
8. G. Dukovic, B. E. White, Z. Zhou, F. Wang, S. Jockusch, M.L. Steigerwald, T. F. Heinz, R. A. Friesner, N.J. Turro, and L.E. Brus, "Reversible Surface Oxidation and Efficient Luminescence Quenching in Semiconductor Single-Wall Carbon Nanotubes," J. Am. Chem. Soc. **126,** 15269 (2004).
9. F. Wang, G. Dukovic, E. Knoesel, L.E. Brus, and T.F. Heinz, "Observation of Rapid Auger Recombination in Optically Excited Semiconducting Carbon Nanotubes," Phys. Rev. B**70**, 241403 (2004).
10. B. V. Rao, K.-Y. Kwon, A. Liu, and L. Bartels, "Measurement of a Linear Free Energy Relationship One Molecule at a Time," Proc. Nat. Acad. Sci. **101**, 17920 (2004).
11. S. Stolbov, F. Mehmood, T. S. Rahman, I. Makkonen, P. Salo, and M. Alatalo, "Site Selectivity in Chemisorption of C on Pd(211)," Phys. Rev. B**70**, 155410 (2004).
12. D. P. Quinn and T. F. Heinz, "Use of Electronic Friction to Model Isotope Effect in Laser-Induced Desorption of O_2/Pd(111)," J. Chem. Phys. (submitted).
13. Femtosecond Laser-Induced Desorption of O2/Pd(111)
14. S. Stolbov, and T. S. Rahman, "First-Principles Study of the Origin of Alkali Promotion of Reactivity of Metal Surfaces," Phys. Rev. Lett. (submitted) (Cond-mat/0407404).
15. S. Stolbov and T. S. Rahman, "First Principles Study of the Adsorption, Diffusion and Dissociation of NH_3 on Ni and Pd Surfaces," J. Am. Chem. Soc. (submitted).
16. K-Y. Kwon, K. L. Wong, G. Pawin, L. Bartels, S. Stolbov, and T. Rahman, "A Single-Molecule Shuttle: Walking Molecules Can Stay the Course," Nature (submitted).

DE-FG02-01ER15183 **Gary L. Haller**

Nanopore Radius Of Curvature Effect On Catalysis And Catalytic Particle Formation

Postdocs: Sangyun Lim
Students: Yanhui Yang, Chuan Wang, Guoan Du, Yuan Chen
Collaborators: Lisa Pfefferle, Dragos Ciuparu

Department of Chemical Engineering, Yale University, New Haven, CT 06520-8286
gary.haller@yale.edu

Goal

To investigate the radius of curvature effect of nanopore materials [Single Wall Nanotubes of carbon (SWNT) and mesoporous molecular sieves (MCM-41)] on adsorption and catalysis.

Recent Progress

Multivariate Correlation and Synthesis Prediction of Co-MCM-41: The synthesis process for MCM-41 materials comprise many process variables, several of which interact. For example, the main independent variable of interest is the pore diameter that is varied by changing the chain length of the templating surfactant, but this also affects the degree of structural order (and in some cases the degree of incorporation of first-row transition metals). By using the designed experiment, statistical approach to synthesis, quantitative synthesis models have been developed. The model for V-MCM-41 had been described previously and we have now implemented a designed experiment for Co-MCM-41 that allows the synthesis of Co-MCM-41 with varying pore size but constant composition and a good degree of structural order [3].

Radius of Curvature Effects on the Air Oxidation of Methanol on V-MCM-41: We have used the designed experimental model (previously reported) to synthesize V-MVM-41 with varying pore size but constant composition and a high degree of structural order. We have also developed this synthesis based on a very pure silica source, Cab-O-Sil, to eliminate the acid sites (which produce the undesirable byproduct dimethyl ether). These two improvements have allowed us to reproduce the radius of curvature effect on low loading (<0.5 wt%) V-MCM-41 and to also demonstrate a radius of curvature effect on selectivity where the selectivity to formaldehyde approaches 100 % on the optimum pore size, see Figure 1.

Radius of Curvature Effect on Reduction Stability of Co-MCM-41and Ni-MCM-41: In an investigation of Co-MCM-41 reported previously, we observed that Co in MCM-41 was unusually stable with regard to reduction at 773K by hydrogen and that reducibility varies with pore size. This is perhaps the most dramatic effect of radius of curvature so far observed. It is of interest to compare Ni-MCM-41 to Co-MCM-41 both with regard to reducibility and as a catalyst for the synthesis of SWNT. Ni turns out to be much easier to reduce (see Figure 2) and there is little effect of the pore size on the reducibility. When the distribution of SWNT

synthesized on reduced Co-MCM-41 and Ni-MCM-41, the distribution of diameters of SWNT is more narrow for Co than Ni, even when they are compared under different conditions for optimized selectivity for both Co and Ni.

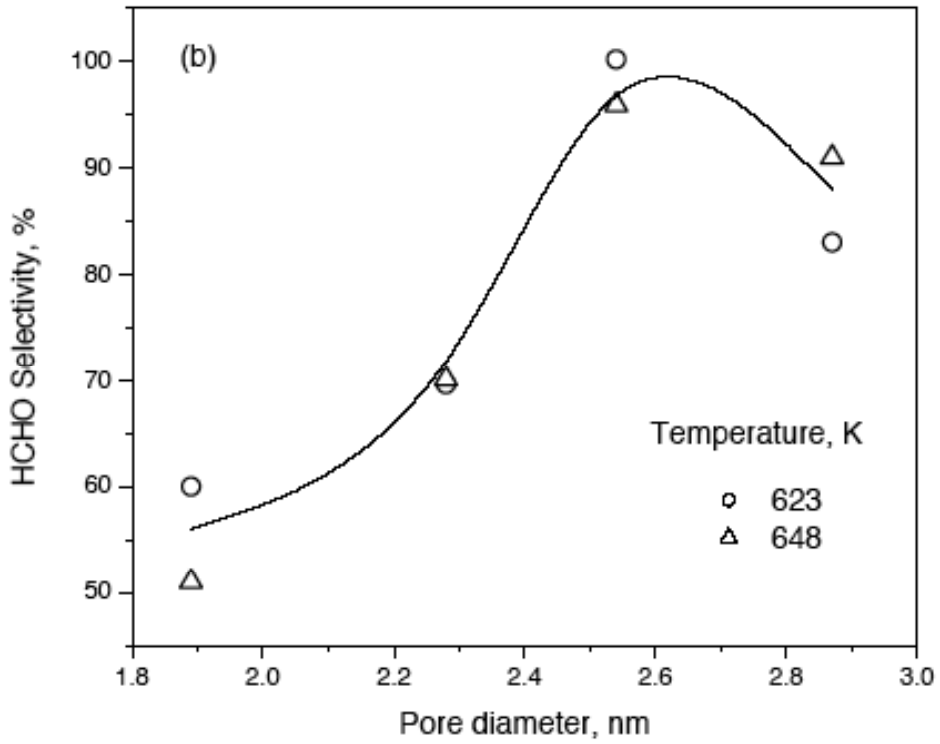

Figure 1

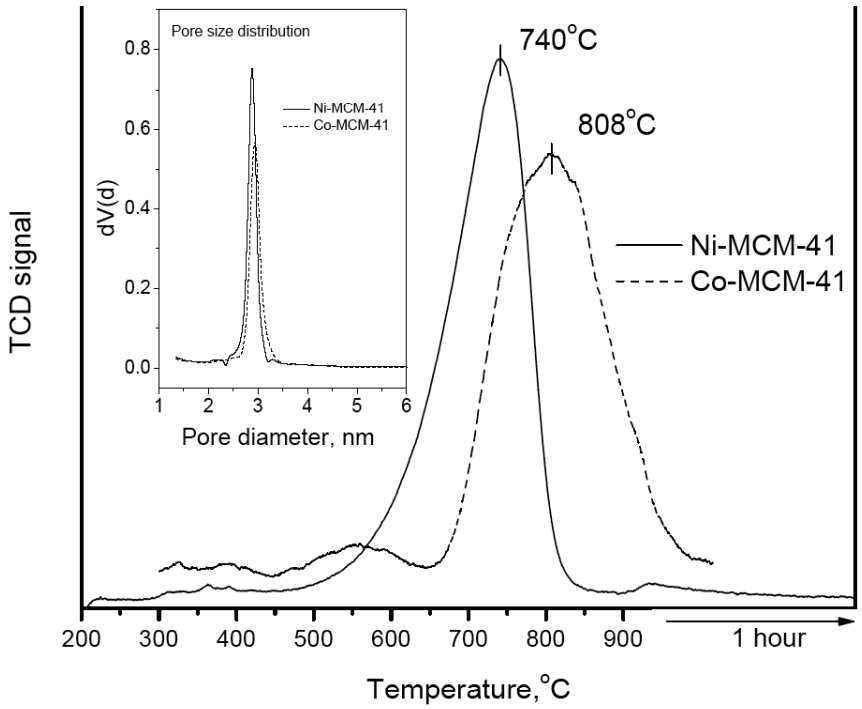

Figure 2

Radius of Curvature Effect on Co-MCM-41 Derived Catalysts for Synthesis of SWNT: Properties of SWNT depend on the tube diameter providing an incentive to find a catalyst that selectively produces a given size. Co-MCM-41 is a precursor to such a catalyst, produced by pre-reduction of Co-MCM-41to form a narrow distribution of Co clusters, and provides good selectivity and the flexibility to vary the SWNT average diameter with a distribution of about ±0.05 nm by catalyst design. We have refined the conditions for improving the yield and narrowness of the diameter distribution [4,5]. Catalyst pre-treatment and CO disproportionation (to form SWNT) reaction conditions were observed to strongly affect the diameter uniformity of SWNT grown on Co-MCM-41 catalysts. The pre-reduction and CO disproportionation reaction temperatures were varied systematically while the carbon loading and the SWNT diameter uniformity were monitored by TGA, Raman spectroscopy and TEM. The state of the catalyst during prereduction and the size of the cobalt clusters formed during the SWNT growth process were monitored by in-situ XANES during the pre-reduction of the Co-MCM-41, and ex-situ EXAFS of catalyst samples was performed after carbon deposition. These experiments allow establishing correlations between the SWNT quality and the state of the catalyst. Control of the cobalt cluster size in Co-MCM-41 is critical to the SWNT diameter control. The size of the cobalt cluster changes with the pre-reduction and SWNT synthesis temperatures, as well as with pore size of the Co-MCM-41. Uniform diameter SWNT can be grown in Co-MCM-41 by controlling pre-reduction and reaction temperatures. The influence of the CO pressure and of the duration of catalyst exposure to CO were systematically investigated with respect to the carbon yield, selectivity and diameter uniformity of the SWNT produced by CO disproportionation over Co-MCM-41 catalysts. The SWNT were characterized by Raman and NIR spectroscopy, while the

state of the catalyst and the size of the metallic cobalt clusters were investigated by X-ray absorption spectroscopy. The experimental results suggest that both the selectivity to SWNT and the uniformity of their diameters are controlled by the relative rates of the following competing processes: cobalt reduction, nucleation of cobalt into clusters and SWNT growth. It was found that reaction at low CO pressures leads to wider distribution of diameters and lower SWNT selectivity. The duration of catalyst exposure to CO was found to strongly affect the SWNT selectivity at the early stages of SWNT growth, while it has a minor effect on the SWNT diameter uniformity.

DOE Interest

Metal substituted MCM-41 can be used to prepare highly dispersed and stable supported first-row transition metals, e.g., Co, which are good catalysts for both traditional energy related reactions, e.g., Fischer-Tropsch synthesis, and emerging catalytic applications, e.g., synthesis of single walled nanotubes of carbon of narrow diameter distribution.

Future Plans

Our proposed research is a continuation of the investigation of radius of curvature effects on catalyst preparation, adsorption, and catalytic activity and selectivity. Preliminary experiments suggest that high dispersions of Co result because of metal cluster anchoring on unreduced Co ions. Our goals are to: a) to demonstrate the ion anchoring hypothesis, b) to improve the anchoring of Co using other ions, e.g., Ti^{4+}, Zr^{4+}, in MCM-41, c) to extend this anchoring to Ni to make high dispersions of Ni with a narrow size distribution, and d) to investigate activity of high dispersion Co and Ni for methanation of CO and CO_2.

Publications (2004-5)

1. Lim, Sangyun; Ciuparu, Dragos; Chen, Yuan; Pfefferle, Lisa; Haller, Gary L.. **Effect of Co-MCM-41 Conversion to Cobalt Silicate for Catalytic Growth of Single Wall Carbon Nanotubes.** Journal of Physical Chemistry B (2004), 108(52), 20095-20101.
2. Ciuparu, Dragos; Chen, Yuan; Lim, Sangyun; Yang, Yanhui; Haller, Gary L.; Pfefferle, Lisa. **Mechanism of Cobalt Cluster Size Control in Co-MCM-41 during Single-Wall Carbon Nanotubes Synthesis by CO Disproportionation.** Journal of Physical Chemistry B (2004), 108(40), 15565-15571.
3. Yang, Yanhui; Lim, Sangyun; Wang, Chuan; Du, Guoan; Haller, Gary L.. **Statistical analysis of synthesis of Co-MCM-41 catalysts for production of aligned single walled carbon nanotubes (SWNT).** Microporous and Mesoporous Materials (2004), 74(1-3), 133-141.
4. Chen, Yuan; Ciuparu, Dragos; Lim, Sangyun; Yang, Yanhui; Haller, Gary L.; Pfefferle, Lisa. **Synthesis of uniform diameter single wall carbon nanotubes in Co-MCM-41: effects of CO pressure and reaction time.** Journal of Catalysis (2004), 226(2), 351-362.
5. Chen, Yuan; Ciuparu, Dragos; Lim, Sangyun; Yang, Yanhui; Haller, Gary L.; Pfefferle, Lisa. **Synthesis of uniform diameter single-wall carbon nanotubes in Co-MCM-41: effects of the catalyst prereduction and nanotube growth**

temperatures. Journal of Catalysis (2004), 225(2), 453-465.
6. Ciuparu, Dragos; Chen, Yuan; Lim, Sangyun; Haller, Gary L.; Pfefferle, Lisa. **Uniform-Diameter Single-Walled Carbon Nanotubes Catalytically Grown in Cobalt-Incorporated MCM-41.** Journal of Physical Chemistry B (2004), 108(2), 503-507.
7. Amama, Placidus B.; Lim, Sangyun; Ciuparu, Dragos; Yang, Yanhui; Pfefferle, Lisa; Haller, Gary L.. **Synthesis, Characterization, and Stability of Fe-MCM-41 for Production of Carbon Nanotubes by Acetylene Pyrolysis.** Journal of Physical Chemistry B (2005), 109(7), 2645-2656.
8. Haider, Peter; Chen, Yuan; Lim, Sangyun; Haller, Gary L.; Pfefferle, Lisa; Ciuparu, Dragos. **Application of the Generalized 2D Correlation Analysis to Dynamic Near-Edge X-ray Absorption Spectroscopy Data.** Journal of the American Chemical Society (2005), 127(6), 1906-1912.
9. Lim, Sangyun; Ciuparu, Dragos; Chen, Yuan; Yang, Yanhui; Pfefferle, Lisa; Haller, Gary L.. **Pore Curvature Effect on the Stability of Co-MCM-41 and the Formation of Size-Controllable Subnanometer Co Clusters.** Journal of Physical Chemistry B (2005), 109(6), 2285-2294.

DE-AC03-76SF00098 **Gabor A. Somorjai**

Nanoscience and Nanoparticles for 100% Selective Catalytic Reactions

2-D nanostructured catalysts: G.A. Somorjai
3-D nanostructured catalysts: G.A. Somorjai, J.W. Ager III, H. Frei, M. Salmeron, T.D. Tilley

Chemical Sciences Division and Physical Biosciences Division,
Lawrence Berkeley National Laboratory, Berkeley, CA 94720
GASomorjai@lbl.gov

Goal:

The program focuses on the combined synthesis, characterization and reactivity of two and three-dimensional high surface area nanoparticle systems to achieve 100% selective catalytic reactions. The goal of the project is to explore the molecular and nanoscale variables, structure, composition and dynamic properties of catalysts in multipath surface catalyzed reactions. The three main areas of emphasis in this program are:

- to fabricate 2- and 3-dimensional catalyst systems with complete control of catalyst nanoparticle location, structure, thermal and chemical stability;
- to characterize these nanoscale systems by a combination of techniques that identifies their size, location, structure and composition during and after fabrication and under reaction conditions;
- to carry out multipath chemical reactions and correlate reaction selectivity with physical-chemical variables of nanoparticle catalyst fabrication with *in-situ* probes of the catalyst surface, whenever possible.

DOE Interest

The development of heterogeneous catalysts with 100% selectivity is a high priority goal for energy-efficient and environmentally friendly chemicals manufacturing. If this can be accomplished, there will be major gains in energy efficiency as undesirable byproducts that become waste are eliminated (green chemistry). This is one of the important missions of the DOE Basic Energy Sciences. Since we focus on the reforming reaction over platinum through studies of n-hexane and h-heptane conversion to high octane branched isomers and aromatic molecules, a higher concentration of naphtha can be converted to fuels. Similarly our studies of carbon monoxide hydrogenation over rhodium addresses the science of synthetic gas conversion to chemicals and fuels through the formation of oxygenates such as methanol and ethanol, etc. This is also part of the energy mission of Basic Energy Sciences of the Department of Energy.

Research Plan:

Selectivity, that is to produce one molecule out of many other thermodynamically feasible product molecules, is much less understood than activity in catalyst-based reactions. Small differences in potential energy barriers for elementary reaction steps control which reaction channel is more likely to yield the desired product molecule (selectivity) instead of the overall activation energy for the reaction that controls turnover rates (activity). Decades of R&D have produced industrial catalysts that possess nanosize features which contribute in a fundamental way to their function (activity and selectivity). For porous materials (e.g., those

based on zeolites) the pore size can exclude molecules with diameters larger than the pore to approach the active site inside the pore while smaller molecules can enter and react. For metal catalyst particles the presence of three-fold sites can facilitate organic rearrangements that produce aromatic molecules. Oxide-metal interface sites are implicated in changing both activity and selectivity of multipath reactions such as carbon monoxide hydrogenation. In general, little is known concerning possible correlations between catalyst selectivity and the size and shape of the metal catalyst particles and their location and bonding on the oxide support.

To achieve 100% selectivity catalyst materials science will have to undergo major developments in order to achieve atomic level control of parameters such as type of surface active sites, promoters, geometry and distance between active sites. In this project we are using nanotechnology approaches to study the nanoscience of catalyst selectivity and to design and synthesize new catalyst systems based on this knowledge.

Our approach is to fabricate metal nanoparticles of platinum and rhodium of equal size in the 1-10 nm range and disperse them on high surface area mesoporous oxide supports and on oxide films. Both the metal nanoparticles and the oxide supports are synthesized in our laboratories. The catalyst is characterized by a combination of techniques at each phase of preparation. These include X-ray diffraction, electron microscopy, light scattering, static and time-resolved Raman and FTIR spectroscopies, scanning probe techniques, high pressure photoelectron spectroscopy, physical adsorption and chemisorption. We then carry out catalytic reactions to evaluate selectivity and activity. We use ethylene hydrogenation, a surface structure insensitive reaction to independently determine the surface area of the exposed metal. Ethane hydrogenolysis is used to explore the particle size dependence of the turnover rate. Cyclohexene hydrogenation and dehydrogenation are employed to explore selectivity for a relatively simple reaction as a function of metal particle size, particle shape and the type of the oxide support. Selectivities in multipath reactions are explored for n-hexane conversion in the presence of excess hydrogen (reforming) for platinum and for carbon monoxide hydrogenation for rhodium as a function of metal particle size, shape, surface structure and oxide support.

Recent Progress

a) Synthesis. Progress in the synthesis of metal monodispersed nanoparticles in the 1-10 nm range and in developing procedures for encapsulating them in mesoporous oxides (silica, alumina) to form a nanoenginered catalyst is described. Two main synthesis routes for embedding Pt nanoparticles into mesoporous SBA-15 were explored. In the nanoparticle encapsulation (NE) method, monodispersed platinum nanoparticles in the size range of 1.7-7.1 nm are produced by reducing $H_2PtCl_6 \cdot xH_2O$ in solution followed by growth of SBA-15 around the particles using the standard production method developed by the Stucky group. In the capillary inclusion (CI) method previously prepared platinum nanoparticles were embedded into the channel system of mesoporous SBA-15 silica using low power sonication in a water/ethanol mixture. Extensive characterization studies have shown that the size of the nanoparticles and the structure of the SBA-15 are unaffected by the sonication, and that they are homogeneously dispersed inside the channels of SBA-15 and are not aggregated nor block the openings of the pores. For either synthesis method, the stabilizing polymer (poly(vinylpyrrolidone), PVP) that is bound to the nanoparticle surface must be removed for the catalyst to function. This must be done after the particles have been embedded within the mesoporous silica matrix and without destroying the monodispersity of the nanoparticles. Our most successful chemical approach has been to exchange the PVP with a organic molecule (hexadecanethiol) that is more weakly bound

to the Pt surface We have begun to explore removal of the polymer coating at lower temperatures using stronger oxidants, such as ozone (O_3), nitrogen dioxide (NO_2), hydrogen peroxide (H_2O_2) and organic peroxides (R-O-O-R).

Rhodium nanoparticles in the size range of 1.5 to 13.7 nm were synthesized by two different routes: (1) water-in-oil reverse micelles and (2) the reduction of $RhCl_3$ in ethylene glycol in the presence of a surface stabilizing polymer, polyvinylpyrrolidone (PVP). In the former method, the size of the micelle was 3 to 20 nm and could be controlled by changing the water to surfactant ratio was changed. The resulting rhodium nanoparticles exhibited a Gaussian size distribution (σ = 0.35 nm), with average diameters of 1.5, 2.2, and 2.9 nm. Larger particles could be made by the latter method. Rh nanoparticles were incorporated onto SBA-15 using the CI method discussed above. Chemisorption data were consistent with the metal particle sizes measured by TEM.

To make 2-D catalysts, we used Pt nanoparticles made by the method described above and using the Langmuir-Blodgett technique obtained self-assembled monolayers of these materials at variable packing, depending on the surface pressure employed. Present work is concentrating on removing the polymer coating from the nanoparticles without causing relocation or agglomeration of the particles. The synthetic method is under intense investigation to produce nanoparticles that covalently bound to the oxide supports as to prevent their mobility and aggregation during subsequent processing steps.

b) Characterization. Time-resolved FT-IR is used to directly compare the kinetic behavior of reaction intermediates with the rise of the final products. We use a reactor design in which a continuous gas flow of one reactant merges with a short (> 300 microsec) pulse of a second reactant in close proximity to the catalyst. To explore the feasibility of detecting and temporally resolving the infrared bands of surface intermediates upon ethylene hydrogenation under reaction conditions, we employed an industrial alumina-supported Pt catalyst (473 K, 1 atm, 9 L min^{-1} continuous H_2-N_2 flow). We observed two transient intermediates; one is ethylidyne (CH_3CPt_3), with bands at 1339 and 2880 cm^{-1} decaying with a time constant of 300 msec (473 K). A transient absorption at 1200 cm^{-1} with accompanying peaks at 2875 and 2860 cm^{-1} and a lifetime shorter than 100 msec was assigned, with the aid of isotopically labeled reactants C_2D_4 and D_2, to a surface ethyl species. The kinetic relationship between the surface C_2H_5Pt decay and the rise of gas phase C_2H_6 was elucidated by a comprehensive study of the temperature, H_2 concentration, and flow rate dependence of the temporal behavior at 25 msec resolution. Comparison of experiments between 473 and 323 K revealed an increase of the initial C_2H_5Pt yield by a factor of 6 with decreasing catalyst temperature, indicating a large increase of the fraction of surface ethyl species that survive on the millisecond time scale prior to hydrogenation to ethane. Over the same range of decreasing temperature, the ethane bands exhibit an increasingly pronounced rise at the expense of the initial (prompt) ethyl buildup. At the lowest temperature (323 K), the growth rate of C_2H_6 coincides with the decay rate of the C_2H_5Pt surface intermediate. To our knowledge, this constitutes the first demonstration of the kinetic relevancy of a surface intermediate of a heterogeneous catalytic reaction by directly linking its temporal behavior to the rise of the product. Consistent with the known spectator role of ethylidyne, none is detected in the first 25 msec spectrum at 323 K. The CH_3CPt_3 species grows in on the hundreds of millisecond time scale. Using Pt-loaded SBA-15 catalyst, the same temporal behavior of ethyl to ethane interconversion was observed, confirming that reactant adsorption or product release from the channels of the mesoporous support are not rate limiting.

In Pt-loaded SBA-15, UV-Raman spectroscopy was found to be sensitive to changes in support and metal particle surface structure while diffuse reflectance absorption FTIR was found to be sensitive to adsorbates and to the silica surface structure. We found that the standard techniques of pellet pressing used to prepare transmission FTIR samples (pressures in the range of 3 – 7 tons cm^{-2}) leads to collapse of the mesoporous structure in Pt/SBA-15. This effect also allowed definitive assignment of Raman and IR vibrational modes that are specifically associated with the mesoporous structure. *In-situ* FTIR was used during processing steps designed to activate the metal surface in Pt/SBA-15: alternating oxidizing (O_2 at 450 C) and reducing conditions (H_2/Ar 450 C). A peak at 908 cm^{-1} (two-membered surface siloxane groups) appears under oxidation conditions at the same time as peaks corresponding to free surface silanol groups on the support surface decrease. This surface reconstruction process is reversible; under reducing conditions the Si-OH intensity is restored and the strained siloxane peak disappears. This process does not occur at this temperature in SBA-15 without Pt. UV-Raman spectroscopy was used to examine metal-oxide modes in Pt- and Rh-loaded SBA-15. A PtO_x mode (530-580 cm^{-1}) was observed for loadings in the 2 – 7% range on SBA-15 and a RhO mode at 540 cm^{-1} was observed at 0.6% metal loading. The PtO_x peak disappears upon exposure of the catalyst to H_2 at 450 C, suggesting that the metal oxide is a very thin surface layer. It is possible that the observation of these modes is aided by resonance effects associated with the deep UV (244 nm) excitation source used. Initial *in-situ* FTIR reaction kinetics studies were performed using the conversion of ethylene to acetaldehyde at 50 C on 5% Pt/SBA-15. Formation of acetaldehyde is observed; this reaction does not occur at this temperature for dispersed Pt on amorphous SiO_2. An ethylidyne intermediate is observed, as well.

A unique High Pressure Photoelectron Spectroscopy (HPPES) endstation at the ALS was used to study the surface and near-surface region of a Cu catalyst and the adjacent gas-phase reactants and products under reaction conditions. The results show the existence of a linear correlation between catalytic activity and the presence of a sub-surface oxygen species. This can only be observed *in situ* because removal of the gas phase oxygen causes the disappearance of the sub-surface species. The concentration profile of the sub-surface oxygen within the first few nanometers below the surface was determined using photon energy-dependent depth-profiling. The experiments show that the pure metal is not active for methanol oxidation, and that a certain amount of oxygen has to be present in the sub-surface region to activate the catalytic reaction. Oxide formation was found to be detrimental to formaldehyde production. These results demonstrate that for an understanding of heterogeneous catalysts a characterization of the surface alone may not be sufficient, and that sub-surface characterization is essential. The nature of the adsorption sites of CO and NO on a Rh(111) surface was determined *in situ*, under gas mixtures of the reactants in the Pascal (1 Torr = 133 P) pressure range. Near room temperature NO readily displaces CO from threefold hollow sites when the NO partial pressure is below 30%. CO is displaced from top sites only at higher NO pressures. The kinetics of CO/NO exchange at top sites is very slow at room temperature (hours) and requires heating for complete exchange. The results confirm and extend previous studies using FTIR and STM.

c) Reaction studies. The hydrogenation/dehydrogenation of cyclohexene has been studied as a function of Pt particle size (1.7-7.1 nm) with the nanoparticle encapsulation (NE) samples at ambient pressure from 298–673 K. Thermodynamically, cyclohexane formation is exothermic and favored at low temperatures, while cyclohexene dehydrogenation to benzene is favored at high temperatures. Kinetic measurements demonstrate that cyclohexene conversion selectivity is not controlled by thermodynamics. Benzene production occurs at lower temperatures on more

highly dispersed samples and a decrease in the apparent activation energy for benzene formation occurs with increasing metal dispersion. Apparent activation energies for cyclohexane formation are ~ 8 kcal mol^{-1}, while the apparent activation energy for benzene formation is catalyst dependent and ranges from 12-20 kcal mol^{-1}. Over an appropriate temperature window, these differences in activation energy are manifested in significant changes in selectivity. All catalysts demonstrate a "bend-over" in activity for both reaction pathways as the temperature is increased; this is attributed to unfavorable cyclohexene adsorption thermodynamics. This is the first study demonstrating that particle size selectivity in hydrocarbon conversion.

Several catalytic reactions were studied using Rh/SBA-15 materials. Ethylene hydrogenation was chosen as a structure insensitive reaction. The turnover frequency is unchanged by the metal particle size or shape. The kinetic data were in agreement with values obtained for Rh single crystals and Rh foil, and confirmed the structure-insensitive nature of the reaction. Ethane hydrogenolysis was chosen as a structure sensitive reaction. The reaction leads to a single product, with the rate of formation being dependent on particle size, shape, and exposed facet. The reaction data for ethane hydrogenolysis revealed that TOFs varied non-linearly across an order of magnitude versus particle size in this small size regime, which indicates a size effect on reaction activity.

Publications (2003-2005)

Grunes, J., Zhu J., and Somorjai G. A., "Focus Article: Catalysis and Nanoscience," Chem. Commun. 2257 (2003). LBNL-52668

Hess, C., Hoefelmeyer, J. D., Tilley, T. D., "Spectroscopic Characterization of Highly Dispersed Vanadia Supported on SBA-15 Silica," J. Phys. Chem. B, submitted, LBNL-54467.

Ko, M. K. and Frei, H., "Millisecond FT-IR Spectroscopy of Surface Intermediates of C_2H_4 Hydrogenation over Pt/Al_2O_3 Catalyst under Reaction Conditions," J. Phys. Chem. B 108, 1805 (2004).

Konya, Z., Zhu, J., Szegedi, A., Kiricsi I., Alivisatos, A. P., and Somorjai, G. A., "Synthesis and Characterization of Hyperbranched Mesoporous Silica SBA-15," Chem. Commun. 314 (2003). LBNL-51646

Konya, Z., Puntes, V. F., Kiricsi, I., Zhu, J., Ager III, J. W., Ko, M. K., Frei, H., Alivisatos A. P., and Somorjai, G. A., "Synthetic Insertion of Gold Nanoparticles into Mesoporous Silica," Chem. Mat. 15, 1242 (2003). LBNL-51329.

Liu, H. and Mun, B. S., Thornton, G., Isaacs, S. R., Shon, Y.S., Ogletree, D.F., and Salmeron, M. "The Electronic Structure of ensembles of Gold nanoparticles: size and proximity effects." Submitted to Phys. Rev. B

Liu, H., Guo J., Thornton, G., Yin, Y., Augustsson, A., Dong, C., Alivisatos, A. P., Ogletree, D. F., Salmeron, M. "Resonant Inelastic X-ray Scattering in Ligand-Stabilized Cobalt Nanoparticles: Size-Dependent Low-Energy Excitations". In preparation.

Niesz, K., P. Yang, Somorjai, G. A., "Sol-gel Synthesis of Highly-Ordered Mesoporous Alumina," Chem. Mater., Manuscript submitted.

Requejo, F. G, , Hebenstreit, E. L. D., Ogletree, D. F., and Salmeron, M., "Bridging the pressure gap: in situ XPS study of site competition of CO and NO on Rh(111) in equilibrium with the gas phase" Journal of Catalysis 226, 83-87 (2004). LBNL-54248

Rioux, R. M., H. Song, B. Hsu, P. Yang, and G. A. Somorjai, Manuscript in Preparation.

Rioux, R. M., Song, H., Hoefelmeyer, J. D., Yang, P., and Somorjai, G. A., "High-Surface-Area Catalyst Design: Synthesis, Characterization, and Reaction Studies of Platinum Nanoparticles in Mesoporous SBA-15 Silica," J. Phys. Chem. B. ASAP Article (2004)

Rose, M. K., Borg, A., Dunphy, J. C., Mitsui, T., Ogletree, D. F., and Salmeron, M., "Chemisorption and dissociation of O_2 on Pd(111) studied by STM," Surf. Sci. 547, 162 (2003). LBNL-53563

Rose, M., Mitsui, T., Dunphy, J., Borg, A., and Salmeron, M., "Ordered Structures of CO on Pd(111) Studied by STM," Surf. Sci., 512, 259 (2002) LBNL-49381

Song, H., Rioux, R. M., Komor, R., Hoefelmeyer, J. D., Yang, P., Somorjai, G. A., "Catalysis Design: Synthesis, Characterization and Reaction Studies of Pt Nanoparticles Encapsulated in Mesoporous SBA-15 Silica." Manuscript in Preparation.

Wasylenko, W and Frei, H., "Millisecond FT-IR Monitoring of Propylene Hydrogenation of Pt/Al_2O_3 Catalyst." Manuscript in preparation.

Wasylenko, W. and Frei, H., "Direct Observation of Ethyl-to-Ethane Conversion upon C_2H_4 Hydrogenation over Alumina-Supported Pt by Time-Resolved FT-IR Spectroscopy." Manuscript submitted.

Yeom, Y. H., and Frei, H., "Time-Resolved Step-Scan and Rapid-Scan Fourier-Transform Infrared Spectroscopy," In-Situ Spectroscopy of Catalysts; Weckhuysen, B.M., Ed.; American Scientific Publishers, 2004. p.32.

Yin, Y., Rioux, R. M., Erdonmez, C. K., Hughes, S., Somorjai, G. A. and Alivisatos, A. P., "Formation of hollow nanocrystals through the nanoscale Kirkendall Effect" Science, 304, 711 (2004).

Zhu, J., Konya, Z., Puntes, V. F., Kiricsi, I., Miao, C. X., Ager III, J. W., Alivisatos, A. P., and Somorjai, G. A., "Encapsulation of Metal (Au, Ag, Pt) Nanoparticles into the Mesoporous SBA-15 Structure," Langmuir 19, 4396 (2003). LBNL-51370

DE-FG02-03ER46043 **David S. Sholl (Carnegie Mellon University)**
DE-FG02-03ER46043 **Andrew J. Gellman (Carnegie Mellon University)**
DE-FG02-03ER15474 **Wilfred T. Tysoe (University of Wisconsin, Milwaukee)**
DE-FG02-03ER15472 **Francisco Zaera (University of California, Riverside)**

CATALYSIS SCIENCE INITIATIVE:
Molecular Level Design of Chiral Heterogeneous Catalysts

Dept. Chemical Engineering
Carnegie Mellon University
Pittsburgh, PA 15213
Email: sholl@andrew.cmu.edu
ag4b@andrew.cmu.edu

Department of Chemistry
University of Wisconsin
3210 N. Cramer Street
Milwaukee, WI 53211 USA
Email: wtt@uwm.edu

Department of Chemistry
University of California
Riverside, CA 92521
Email: zaera@ucr.edu

Goals:

The main goal of this project is to determine the mechanisms by which enantioselectivity can be bestowed on heterogeneous catalysts. Specifically, chirality is to be imparted to achiral surfaces either by exposing chiral planes or by using chiral modifiers.

DOE Interest:

Enantioselectivity is critical in the production of numerous fine chemicals for bioactive applications such as pharmaceuticals. Chiral heterogeneous catalysis has a number of attractive features to offer for its use in fine chemical synthesis, but has so far not be incorporated in any commercial process. This is mostly due to the difficulty in designing such processes without an understanding of the parameters that control chirality and enantioselectivity on surfaces. The basic knowledge generated from the studies being carried out by our research team is expected to advance the development of heterogeneous chiral catalysis, and in more general terms, selectivity in catalysis.

Research Plan:

The hypothesis underpinning our collaborative research effort is that there are three possible origins to chirality and enantioselectivity on catalytic metal surfaces:

- chirality arising from adsorbates that form long-range chiral ensembles on the surface,
- chirality arising from 1:1 interactions between the reactant and individual adsorbed chiral molecules, and
- natural chirality arising from the atomic structure of the metal surface,

Our collaborative program is aimed to understand the relative importance of each of these three mechanisms in enantiospecific adsorption and catalytic reactions.

Recent Progress:

In terms of the formation of chiral superstructures on the surface upon adsorption of chiral modifiers, we have shown that such a mechanism is indeed operative upon adsorption of either (R)- or (S)-2-butoxide on Pd(111) and Pt(111) surfaces. The enantioselectivity of those systems has been tested by using (R)- or (S)-propylene oxide as probes, by both quantifying their

thermal desorption spectra and identifying the adsorbed species with infrared-absorption spectroscopy. Enantioselective adsorption of the propylene oxides is observed over a narrow range of 2-butoxide coverages near $\theta_{2\text{-ButO}} \sim 1/2$ monolayer, where it shows a preference for the homochiral surfaces, that is, for surfaces covered with butoxide moieties of the same chirality as the propylene oxide probe. This preference can reach an enhancement ratio (ER) of about two on the Pd(111) surface, but only an excess of ~ 35% on the platinum substrate. An example of the data obtained from these studies is provided in Figure 1.

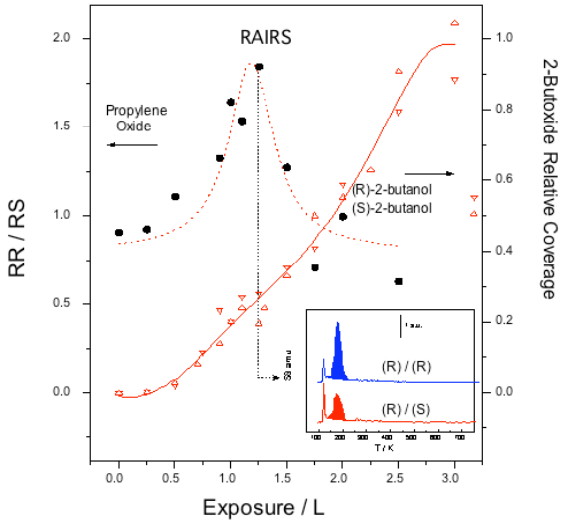

Figure 1. Plot of the relative coverages of (S)-2-and (R)-2-butoxides as a function of exposure on Pd(111) (right axis), along with a plot of the ratio of the coverage of (R)-propylene oxide adsorbed on (R)-2-butoxide-covered Pd(111) (RR) to the saturation coverage of (R)-propylene oxide adsorbed on (S)-2-butoxide (RR/RS) (left axis), as a function of 2-butanol exposure. Shown in the inset are typical desorption spectra of propylene oxide from 2-butoxide-covered Pd(111). This figure highlights the enantioselectivity for the adsorption of (R)-propylene oxide on chiral sites made by supra-molecular structures created upon adsorption of (R)-2-butoxide.

The effect of the formation of these chiral ensembles on the enantioselectivity of model heterogeneous catalysts was also studied theoretically in the framework of a cooperative sequential adsorption model. Analytical solutions were obtained for random adsorption onto a chirally-templated surface which indicate that the surface exhibits a maximum enantioselectivity of ~2.5, in agreement with the results from enantioselective chemisorption experiments cited above. A simple model that assumes that a single ensemble of chiral templating molecules on the surface can act to form enantioselective pockets for the adsorption of a chiral probe molecule indicates that the enantioselectivity can vary from unity only over a relatively narrow coverage range. It is proposed that, in addition to possessing a chiral center and being bonded to the surface, the templating molecule needs to be anchored by at least one second point to prevent it from rotating and permitting the asymmetry due to the chiral center to be averaged out.

The hypothesis of the need for two anchoring points for the templating molecule to increase enantioselectivity was tested next by systematically studying the adsorption of a series of organic acids and aminoacids on Pd(111). The results are summarized in Figure 2. In all cases, the maximum value of enantioselectivity is measured at about 50% of the saturation coverage, as with the alcohol. In addition, our data suggest that, at least in the case of alanine, the variation in enantioselectivity with coverage, which shows a similar variation to that found for 2-aminobutyric acid, may be due to a template structural change as the coverage increases. Thus, at low coverages alanine adsorbs in a η^3 configuration prone to the formation of an enantioselective template. At higher coverages, on the other hand, the structure evolves into a η^2 species, which does not form a chiral template because of the free rotation of the unanchored 2-butyl group. Also to note from the data in Figure 2 is the fact that no enantioselective adsorption

enhancement was seen with 2-methylbutanoic acid, valine, or leucine. Interestingly, a small (~25%) but discernible effect was seen with 2-methylbutanoic acid on Pt(111). The reasons for this discrepancy are still under investigation.

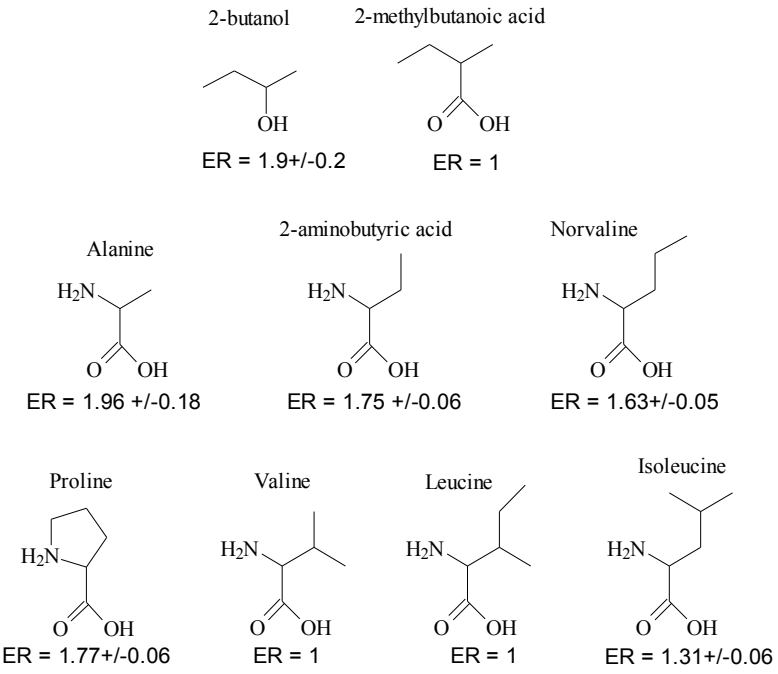

Figure 2. List of aminoacids used as templates and maximum enantioselectivities measured when using propylene oxide as a probe.

The experimental work was complemented with Density Functional Theory (DFT) calculations. Early experimental studies on the adsorption of glycine and alanine on Cu(110) and Cu(100) showed that both molecules form highly structured adlayers, but the determination of the specific molecular structures of those adlayers from experimental data has been controversial. For glycine/Cu(110), the existence of two distinct adlayer domains, one heterochiral and one homochiral, was proposed based on STM images. but this conclusion was later called into question by X-ray photoelectron diffraction (XPD) data. Our DFT calculations show unequivocally that the heterochiral adlayer is the only structure that appears on Cu(110), and that the multiple domains observed with STM can be understood as rotationally equivalent domains of this single adlayer. In contrast, calculations for glycine on Cu(100) show that two structurally distinct adlayers appear with essentially equal energies. Both of these structures are consistent with the XPD data. The results from our work on glycine adsorption are summarized schematically in Figure 3. Similar calculations for alanine adlayers on Cu(110) and Cu(100) have shown that the binding footprint of glycine on Cu surfaces provides an excellent starting point for describing the binding of alanine and other amino acids.

In terms of the mechanism for imparting chirality on surfaces based on a 1:1 modifier:reactant interaction, our studies have focused on the most widely studied example in chiral heterogeneous catalysis, that based on the templating of Pt with cinchonidine. Infrared spectroscopy has been used to characterize the adsorption of cinchonidine and other related modifiers in situ on Pt

surfaces. In general, it was determined that the chiral properties of the catalyst are defined by the nature of the adsorption of the chiral modifier, and that those in turn are influenced by the details of the cinchona/Pt system, by parameters such as the concentration of the modifier in solution, the type of solvent used, and the nature of the gasses dissolved in the liquid phase.

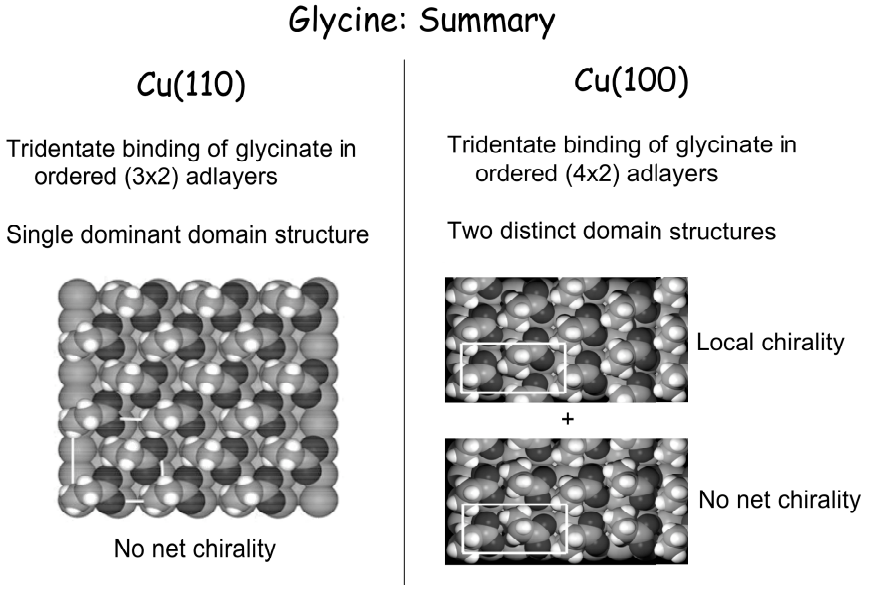

Figure 3. Summary of DFT calculations on the adsorbed structures formed by glycine on copper surfaces. On Cu(110) one single domain structure is formed, and no net chirality is observed. On Cu(100), by contrast, two distinct domains can be produced, and local chirality is possible. These results have helped resolved previous controversies regarding STM and XRD experiments, and can be used to test the viability of supramolecular structures.

Vibrational assignments for the cinchonidine were first made using a combination of experimental spectroscopic measurements and ab initio computational methods. Several bands in both the IR and Raman spectra were identified as useful in providing information regarding the mode of adsorption of cinchonidine on metal surfaces. It was then determined that the adsorption of the cinchona chiral template on Pt is very sensitive to the concentration in solution: while at low land intermediate concentrations the cinchonidine is bonded with the quinoline ring parallel to the surface, at high concentrations the ring is tilted away from the surface. The optimum enantioselectivity occurs under conditions that are consistent with a template adsorption geometry having the quinoline ring parallel to the surface.

The influence of different dissolved gases on the adsorption of cinchonidine from CCl_4 solutions onto polycrystalline platinum surfaces was characterized next. It was observed that most of the gases studied, which included Ar, N_2, O_2, air, and CO_2, neither enhance the adsorption of cinchonidine nor damage the cinchonidine adlayers once they have formed on the surface. On the other hand, H_2 was seen to play a unique role, initially facilitating the uptake of cinchonidine, but later removing some of the resulting adsorbed cinchonidine from the platinum surface. The solvent was also determined to have a strong influence on the adsorption of the chiral modifier on the surface of the catalysts. In particular, the polarity of the solvent was found to influence the kinetics of cinchonidine desorption into solution in a manner that correlates well with its influence on the enantioselectivity of the templated catalyst. It appears that cinchonidine adsorbs irreversibly on platinum from non-polar solutions such as cyclohexane, but can be easily removed by more polar solvents such as dichloromethane. The evolution of the cinchona adsorbed overlayer upon flushing with different solvents is illustrated in Figure 4. The behavior

observed in our studies correlates well both with the solubility of cinchonidine and with the performance of the cinchona/platinum catalyst as a function of the nature of the solvent.

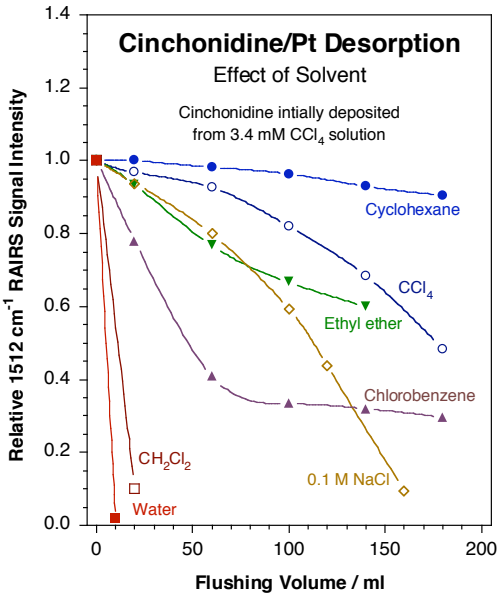

Figure 4. Desorption of cinchonidine adsorbed on a platinum surface as a function of rinsing volume for different solvents. In these experiments the cinchonidine was first adsorbed from a carbon tetrachloride saturated solution onto a polished polycrystalline platinum disk, and then flushed with sequential 20 ml aliquotes of the stated solvents. The remaining coverage of the adsorbate was determined in-situ by following the infrared absorption signal at 1512 cm^{-1}, which corresponds to an in-plane deformation of the quinoline ring. It is clearly seen here that the reversibility of the desorption is severely affected by the nature of the solvent, going from fast desorption in water and dichloromethane, to virtually irreversible adsorption in cyclohexane and other alkanes. This trend correlates well with the ability of cinchonidine to impart chirality to platinum catalysts for enantioselective hydrogenation.

More recent work has been directed at probing the parameters that control the adsorption geometry of the cinchona modifiers, and with that their efficiency in imparting enantioselectivity to catalytic processes. A comparative study was carried out using cinchonine, cinchonidine, quinine, quinidine, and the dihydro analogs of those four molecules. Significant differences were observed not only in their adsorption properties on the platinum surface, but also in their solubility in a number of solvents. Those differences were deemed due to intrinsic molecular properties associated with their structure. Both experimental NMR and theoretical DFT data suggest that the most stable configuration of each molecule may be determined by the steric effects exerted by the groups (vinyl, methoxy) bonded to the outside molecular frame, and that those may be different in each case. This behavior may account for the differences in catalytic enantioselectivity obtained with cinchonine vs. cinchonidine.

Finally, naturally chiral surfaces have been prepared by exposing high Miller index planes of fcc metals such as copper. Electron diffraction experiments have shown that these are indeed chiral, and desorption studies have indicated that their enantioselectivity originates with kinks on the surfaces. Our most recent work in this direction has extended the past research to studies of reactivity on these surfaces. Using chiral 2-bromobutane, it was possible to create chiral 2-butyl groups on naturally chiral Cu surfaces, and to show that the kinetics of their β-hydride elimination is enantioselective. The next step will be to investigate the possibility of imprinting chirality on achiral surfaces by using chiral adsorbate agents. The aminoacids being studied in connection with supramolecular structuring are ideal candidates for this work, and will be tested on several surfaces and under different conditions.

Publications:

1. J. D. Horvath and A. J. Gellman, Desorption of Chiral Compounds from Chiral Cu(643) and Achiral Cu(111) Surfaces, J. Am. Chem. Soc. 124 (2002) 2384.
2. D. Stacchiola, L. Burkholder and W.T. Tysoe, Enantioselective Chemisorption on a Chirally Patterned Surface in Ultrahigh Vacuum: Adsorption of Propylene Oxide on 2-Butoxy-Covered Pd(111), J. Am. Chem. Soc. 124 (2002) 8984.
3. J. D. Horvath and A. J. Gellman, Naturally Chiral Surfaces, Top. Catal 25 (2003) 9.
4. R. M. Hazen and D. S. Sholl, Chiral Selection on Inorganic Crystalline Surfaces, Nature Mat. 2 (2003) 367.
5. F. Roma, D. Stacchiola, G. Zgrablich and W. T. Tysoe, Theoretical Analysis of the Coverage Dependence of Enantioselective Chemisorption on a Chirally Patterned Surface, J. Chem. Phys. 118 (2003) 6030.
6. W. Chu, R. J. LeBlanc, C. T. Williams, J. Kubota and F. Zaera, Vibrational Band Assignments for the Chiral Modifier Cinchonidine: Implications for Surface Studies, J. Phys Chem. B 107 (2003) 14365.
7. J. D. Horvath, A. Koritnik, P. Kamakoti, D. S. Sholl and A. J. Gellman, Enantioselective Separation on a Naturally Chiral Surface, J. Am. Chem. Soc. 126 (2004) 14988.
8. P. Kamakoti, J. Horvath, A. J. Gellman and D. S. Sholl, Titration of Chiral Kink Sites on Cu(643) using Iodine Adsorption, Surf. Sci. 563 (2004) 206.
9. R. B. Rankin and D. S. Sholl, Assessment of Heterochiral and Homochiral Glycine Adlayers on Cu(110) Using Density Functional Theory, Surf. Sci. 548 (2004) 301.
10. D. Stacchiola, L. Burkholder and W. T. Tysoe, Enantioselective Chemisorption on a Chirally Modified Surface in Ultrahigh Vacuum: Adsorption of Propylene Oxide on 2-butoxide-Covered Pd(111), J. Mol. Catal. A 216 (2004) 215.
11. F. Romá, D. Stacchiola, W. T. Tysoe and G. Zgrablich, Lattice-Gas Modeling of Enantioselective Adsorption by Template Chiral Substrates, Phys. A. 338 (2004) 493.
12. Z. Ma, I. Lee, J. Kubota and F. Zaera, In-Situ Characterization of the Adsorption of Cinchona Chiral Modifiers on Platinum Surfaces, J. Mol. Catal. A: Chem. 216 (2004) 199.
13. Z. Ma and F. Zaera, In-Situ Reflection-Absorption Infrared Spectroscopy at the Liquid-Solid Interface: Decomposition of Organic Molecules on Polycrystalline Platinum Substrates, Catal. Lett. 96 (2004) 5.
14. R. B. Rankin and D. S. Sholl, Structure of Enantiopure and Racemic Alanine Adlayers on Cu(110). Surf. Sci. 574 (2005) L1.
15. T. Zheng, D. Stacchiola, D. K. Saldin, J. James, D. S. Sholl and W. T. Tysoe, The Structure of Formate Species on Pd(111) Calculated by Density Functional Theory and Determined using Low Energy Electron Diffraction, Surf. Sci. 574 (2005) 166.
16. Z. Ma and F. Zaera, The Role of the Solvent in the Adsorption-Desorption Equilibrium of Cinchona Alkaloids between Solution and a Platinum Surface: Correlations among Solvent Polarity, Cinchona Solubility, and Catalytic Performance, J. Phys. Chem. B, 109 (2005) 406.

Session D:

Oxide Structures and Oxide-Oxide Superstructures under Reaction

Surface Science Investigations of Titanium Dioxide: Relevant for Photocatalysis?

Ulrike Diebold
Department of Physics
Tulane University, New Orleans, Louisiana 70118

Annabella Selloni
Department of Chemistry
Princeton University, Princeton, New Jersey 08544

In ultrahigh-vacuum (UHV) based fundamental surface science studies much attention has been focused on TiO_2 surfaces, in particular on rutile (110), over the last fifteen years [1]. The surface structure, defects, as well as the adsorption of different test molecules have been investigated with a variety of spectroscopic and imaging techniques, and first-principles calculations have provided many insights into surface properties and processes. In this talk, we give an overview of the main lessons learned from experimental and computational studies of this material. We discuss the surface properties of TiO_2 anatase [2], the much less-understood, but technologically more relevant phase, as well as the structure/reactivity relationship of rutile (011)-1x2 [3], which is quite unique amongst all known single-crystalline TiO_2 surfaces.

Its outstanding stability, non-toxicity, and high oxidative power make TiO_2 the most suitable semiconductor photocatalyst for environmental remediation and energy conversion purposes. However, TiO_2-based photocatalysis is often inefficient. We discuss the promise and limitations of direct, atomic-scale observations to obtain detailed, reliable insights into processes important for the overall photo-oxidation reactions.

[1] U. Diebold "The Surface Science of Titanium Dioxide" Surface Science Reports 48/5-8 (2003) 53 - 229.
[2] U. Diebold, N. Ruzycki, G.S. Herman, and A. Selloni "One Step Towards Bridging the Materials Gap: Surface Studies of TiO_2 Anatase" Catalysis Today, 85 (2003) 93-100.
[3] . T.J. Beck, A. Klust, M. Batzill, U. Diebold, C. di Valentin, A. Selloni "Surface Structure of TiO_2(011)-(1x2)" Physical Review Letters 93 (3) (2004) 036104

Early Transition Metal Oxides as Catalysts: Crossing Scales from Clusters to Single Crystals to Functioning Materials

Dr. David. A. Dixon[1], Co-Principal Investigator (Co-PI), Dr. Zdenek Dohnalek[2], Investigator, Dr. Maciej Gutowski[2], Investigator, Dr. Jianzhi Hu[2], Investigator, Dr. Enrique Iglesia[3], Co-PI, Dr. Bruce D. Kay[2], Co-PI, Dr. Jun Liu[4], Co-PI, Dr. Charles H. F. Peden[2], Co-PI and Project Director, Dr. Lai-Sheng Wang[5], Co-PI, Dr. Yong Wang[2], Investigator, Dr. John M. White[6], Co-PI.

Postdocs: [6]O.A. Bondarchuk, [4]H.-Y. Fan, [2]J.E. Herrera, [5]X. Huang, [2]J. Kim, [2]J.-H. Kwak, [3]T. Stuchinskaya, [5]H.J. Zhai.
Students: [1]C. Chisolm, [3]J. Macht.

[1]University of Alabama, [2]Pacific Northwest National Laboratory, [3]University of California, Berkeley, [4]Sandia National Laboratory, [5]Washington State University, [6]University of Texas at Austin

Contact information: C.H.F. Peden, P.O. Box 999, MS K8-93, Pacific Northwest National Laboratory, Richland, WA 99352 chuck.peden@pnl.gov

Goal

We are employing an integrated experimental/theoretical approach to advance our current ability to understand, design, and control the catalytic and surface chemistry of transition metal oxides, specifically for redox and acid-base chemistries. The approach combines novel solid-state inorganic synthesis, surface science, experimental and theoretical/computational chemical physics, and mechanistic organic chemistry to address this complex and important challenge.

DOE Interest

The proportion of chemical industry processes using catalysts exceeds 80%. Current commercial heterogeneous catalysts are structurally and chemically complex and data gathered from them can seldom be interpreted with atomic-level precision. We seek to reduce the complexity of TMO catalysts to levels addressable and controllable at the atomic level, while maintaining intimate linkages with practical catalysis and catalytic materials. The focus of the proposed work is to gain a fundamental understanding of chemical transformations in order to design and construct new catalysts with more precise control of specific chemical reactions. This will enable us to help DOE reach its goals of doing fundamental science to address the energy needs of the country by (1) improving energy conservation by new means of energy conversion and storage; (2) enable direct chemical conversions previously economically unfeasible and produce new routes to novel materials while at the same time minimizing by-products and environmental impact; and (3) protecting the environment

Recent Progress

Selected highlights from the results obtained in the last year are presented in this section.

Materials synthesis and characterization

Dispersion of catalyst particles on high surface area supports and precise control of cluster or particle sizes are critical for developing efficient catalysts and for understanding the fundamental properties of the catalysts. To date, catalysts particles are dispersed on the support using controlled infiltration or controlled surface hydrolysis. Although these methods are widely investigated, they can not be used to precisely control the particle sizes. We recently developed a new approach to achieve such controls. In this approach, high surface area nanoporous silica is first synthesized using the surfactant as the template. A fraction of the silica surface is then covered with long chain alkylsilane molecules. The

spacing between the silane molecules is determined by the relative surface coverage. The catalyst particles are only allowed to be deposited in the vacant area that is not occupied by the silane molecules and are physically confined in these areas. Therefore, the particle sizes are determined by the spacings between the silane molecules. We showed that if the catalyst particles are directly deposited on nanoporous silica, the main driving force is surface hydrolysis and no catalyst particles are observed. Most likely a continuous molecular film is formed. When the nanoporous silica is first modified with a layer of another oxide such as zirconium oxide, a process previously investigated by our collaborators on this project, very small catalyst nanoparticles are formed. However the particle sizes are not uniform, ranging from 1 nm to 4nm. If the surface is first modified with a short chain alkylsilane, the catalysts have significant mobility. The catalyst agglomerates and forms large nanoparticles from 4 nm to 6 nm in size. Only when the surface is first modified with a long chain alkylsilane, the catalyst is confined to the vacant sites and small and uniform nanoparticles are formed (1 nm in diameter). This work demonstrates a completely new approach to rationally control the catalyst particle size and to prepare high surface area, well dispersed catalysts with homogeneous properties.

In other efforts, we have successfully grafted nearly-isolated polyoxometallate and WO_x domains on supports, and probed their dispersion by spectroscopic and site titration methods to determine the effects of supports and of the composition of the oxide domains on reactivity for redox (methanol oxidation) and acid (butanol dehydration) catalysis. $H_3PMo_{12}O_{40}$ Keggin clusters were grafted onto Ca-modified SiO_2 to give catalysts with structure and redox catalytic function independent of site density (0.1-0.7 Keggin units (KU)/nm^2), indicating that nearly isolated clusters, without significant secondary structures, were prevalent in all samples. In contrast, grafting onto unmodified SiO_2 led to a decrease in methanol oxidation rates (per KU) with increasing surface density and to much higher selectivities to acid-catalyzed dimethylether formation. Infrared spectra and titration of acid sites with hindered organic bases suggest the substantial absence of secondary Keggin structures on Ca-SiO_2. Titration and reduction measurements showed that grafting occurs via replacement of H^+ charge-balancing cations by Ca^{2+} in $H_3PMo_{12}O_{40}$. Samples prepared by grafting onto Cl-modified SiO_2 did not lead to single-site materials, because the nucleophilicity of O-atoms in Keggin clusters is insufficient to displace Cl^- ions on SiO_2 surfaces.

The density and type of acid sites and their specific catalytic roles were examined using 2,6-di-*tert*-butyl-pyridine as a titrant during 2-butanol dehydration on supported WO_3 and $H_3PW_{12}O_{40+}$ clusters. 2,6-di-*tert*-butyl-pyridine titrates only protons at external surfaces of secondary structures in $H_3PW_{12}O_{40}$ (HPW) or their acidic Cs salts in the absence of polar 2-butanol reactants. Internal protons are also titrated by pyridine, which because of its polar nature and small size penetrates secondary HPA structures. These methods can be used to detect proton accessibility during catalysis and to determine their intrinsic reactivity in specific catalytic reactions. These studies were carried out in parallel with UV-visible and Raman studies of the stability of supported HPA clusters.

Our initial studies addressed the effects of support identity on the reducibility, Brønsted acid site density, and dehydration turnover rates on WO_x domains supported on ZrO_2, Al_2O_3, SiO_2, and SnO_2. The density of Brønsted acid sites, but not their intrinsic reactivity, depends on the electronic properties of the support. More reducible supports with smaller band gaps (e.g. ZrO_2, SnO_2) led to higher densities of Brønsted acid sites. The parallel increase in extent of reduction and Brønsted acid site density on WO_x/Al_2O_3, also observed for WO_x/ZrO_2, confirms the similar nature of Brønsted acidity in these materials and the requirement for reduced centers to form acidic OH groups. Supports also influenced dehydration regioselectivity by modifying the basicity of O-atoms in WO_x domains. This approach was extended to $H_3PW_{12}O_{40}$-based materials, on which 2-butanol dehydration turnover rates were unaffected by replacing 1 or 2.5 H^+ by Cs^+ cations or by supporting small secondary Keggin structures onto silica. Dehydration rates on $Cs_{2.5}H_{0.5}PW_{12}O_{40}$, isolated HPW on SiO_2, and WO_x domains on various supports respond similar to reactant and product concentrations, but solvation effects mediated by hydrogen bonding led to more complex kinetics on materials with extended secondary structures. These effects previously precluded a rigorous assessment of the effects of composition on intrinsic reactivity; we have removed these obstacles by the successful isolation of Keggin clusters on supports and by systematic interpretation of complex kinetic effects in measured catalytic rates.

NMR

We are exploring the possibility of quantitatively counting the various acid sites on the surface of WOx supported on mesoporous silica by using a combination of pyridine titration and ^{15}N MAS NMR spectroscopy. In general, three peaks, labeled as 1, 2 and 3, can be identified from the spectrum acquired on the sample of WOx/SBA-15 titrated with ^{15}N isotope enriched pyridine (Figure 1B). Based on the spectrum from SBA-15 (Figure 1A) and the cross-polarization experiment (Figure 1C), peak 1 is assigned to the pyridine tightly bonded to the Brønsted acid sites, peak 2 is assigned to the Lewis acid sites and peak 3 to the silanol sites. We have also carried out 2D ^{15}N isotropic-anisotropic correlation experiment and quantum chemistry predictions on both the NMR isotropic and anisotropic chemical shifts to justify these spectral assignments. Excellent agreement between theoretical predictions and experimental results has been obtained. The 2D experiment successfully separates the overlapped peaks corresponding to silanol and Lewis acid sites, where the peak corresponding to the Lewis site exhibits large anisotropy while that corresponding to the silanol sites exhibits very small anisotropy due to fast rotation of the pyridine molecule about its symmetric axis. Since NMR is quantitative by nature, this may offer an alternate way to accurately quantify the various surface acid sites using NMR on this and similar materials.

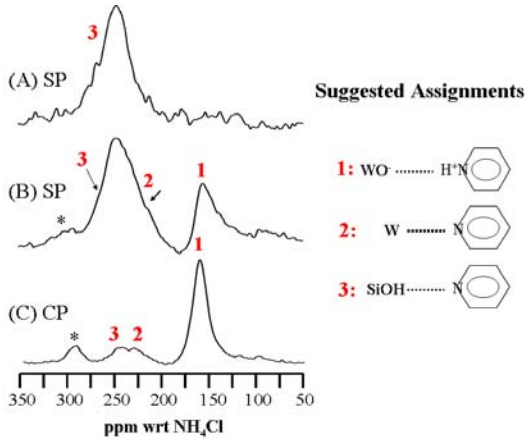

Figure 1. ^{15}N MAS NMR spectra of samples titrated with ^{15}N isotrope enriched pyridine. **(A)** Single pulse (SP) experiment on SBA-15; **(B)** SP on WOx/SBA-15 calcined at 500°C and with 100% silonal surface covered by WOx prior to calcination and **(C)** ^{1}H-^{15}N Cross-polarization experiment on the same sample given in (B). All the spectra were acquired at 11.7T field and at -60C with a sample spinning rate of 6.2kHz. "*" denotes spinning sidebands.

UHV studies of model TMO catalysts

We have studied the structure and catalytic activity of submonolayer amounts of WO_3 deposited on $TiO_2(110)$ under well controlled ultrahigh vacuum conditions. $TiO_2(110)$ was selected as a substrate since its small band gap enables atomically resolved STM imaging. Additionally, the $TiO_2(110)$ surface structure and chemistry has been extensively studied previously [1]. WO_3 was deposited via direct, thermal evaporation from WO_3 powder. This deposition technique provides a reliable, carbon free source of W in the (6+) oxidation state. Using XPS we have determined that WO_3 deposited on $TiO_2(110)$ is thermally stable up to 900K and remains fully oxidized.

Atomically resolved studies of WO_3 deposited at room temperature on $TiO_2(110)$ show only fuzzy, poorly defined features indicating that the clusters are mobile and only weakly bound to the substrate. Subsequent annealing to 600 K results in the formation of bright $(WO_3)_x$ clusters that can be easily imaged. Two different $(WO_3)_x$ coverages are shown in Figure 2. In the case of low WO_3 coverage (Figure 2a), bright rows corresponding to the Ti^{4+} ions on $TiO_2(110)$ are also visible [1]. The images indicate that the majority of clusters have identical size and position with respect to the substrate registry. The amount of deposited WO_3 is determined using a quartz crystal microbalance. Combined with the observed cluster coverage from STM this yields the upper bound of $x \leq 3$ on the number of W atoms in each cluster. Additionally, preferential alignment between $(WO_3)_x$ clusters across the Ti^{4+} rows is observed indicating that the clusters became mobile upon annealing.

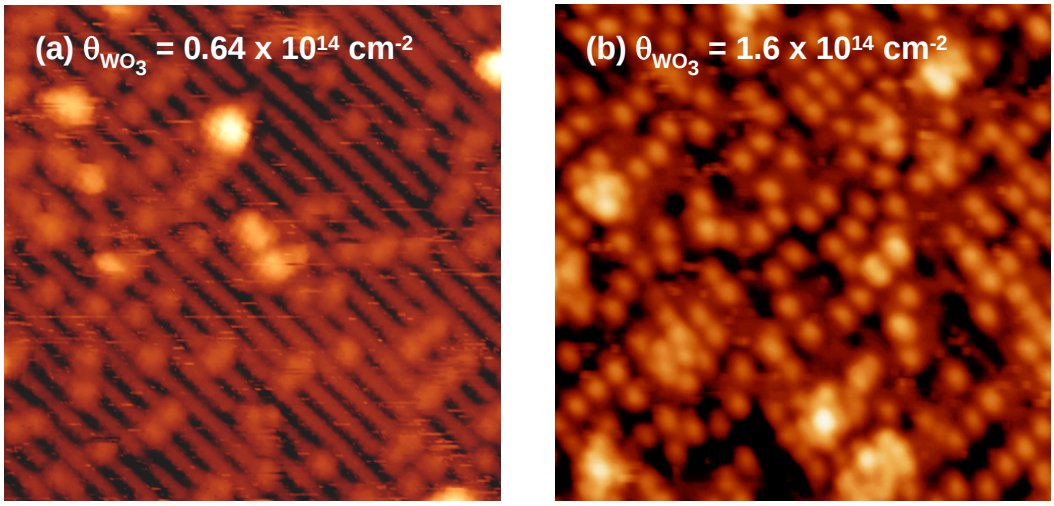

Figure 2: Scanning tunneling images (15×15 nm, 1.8 V, 1 nA) of $(WO_3)_x$ clusters deposited at 300K on TiO_2(110) surface and subsequently annealed to 600K.

The catalytic activity of $(WO_3)_x/TiO_2$(110) system was examined in an ensemble average manner using molecular beam scattering and temperature programmed desorption (TPD) techniques. The TPD of methanol and its potential oxidation products were studied. For methanol no dissociation products were observed in TPD. Our current studies are focusing on partial oxidation of heavier alcohols (e.g. 2-butanol). For formaldehyde adsorption, catalytic polymerization resulting in the formation of trioxane (paraformaldehyde) was observed. We have explored the temperature dependence of trioxane formation and determined that the presence of formaldehyde multilayers is necessary for the trimerization. Submonolayer amounts of formaldehyde result only in monomer desorption. The trimerization yield was measured as a function of $(WO_3)_x$ coverage and formaldehyde exposure. Figure 3 shows that the yield increases linearly with the amount of deposited WO_3 and saturates with formaldehyde dose.

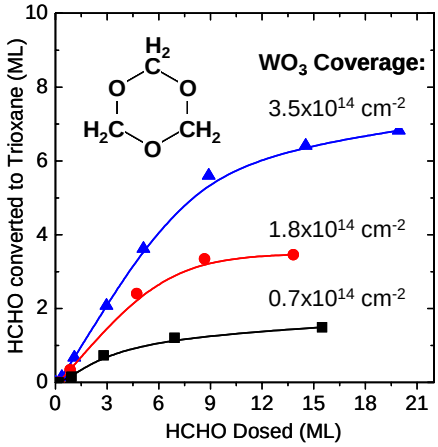

Figure 3: Yield of trioxane from formaldehyde trimerization on $(WO_3)_x/TiO_2$(110).

Photoelectron spectroscopy of $W_xO_y^-$ clusters

The goal of this part of the program is to investigate small oxide clusters and use them as molecular models to obtain insight into properties of bulk catalysts. We have performed a systematic and comprehensive study of the electronic structures and chemical bonding in a series of ditungsten oxide clusters, $W_2O_n^-$ and W_2O_n (n = 1-6), using anion photoelectron spectroscopy and density functional theory (DFT) calculations. Well-resolved photoelectron spectra were obtained at several photon energies and W 5d-based spectral features were clearly observed and distinguished from O 2p-based features.

With increasing oxygen content in $W_2O_n^-$, the photoelectron spectra were observed to shift gradually to higher binding energies, accompanied by a decreasing number of W 5d-derived features. A behavior of sequential oxidation as a result of charge transfers from W to O was clearly observed. A large energy gap (2.8 eV) was observed in the spectrum of $W_2O_6^-$, indicating the high electronic stability of the stoichiometric W_2O_6 molecule.

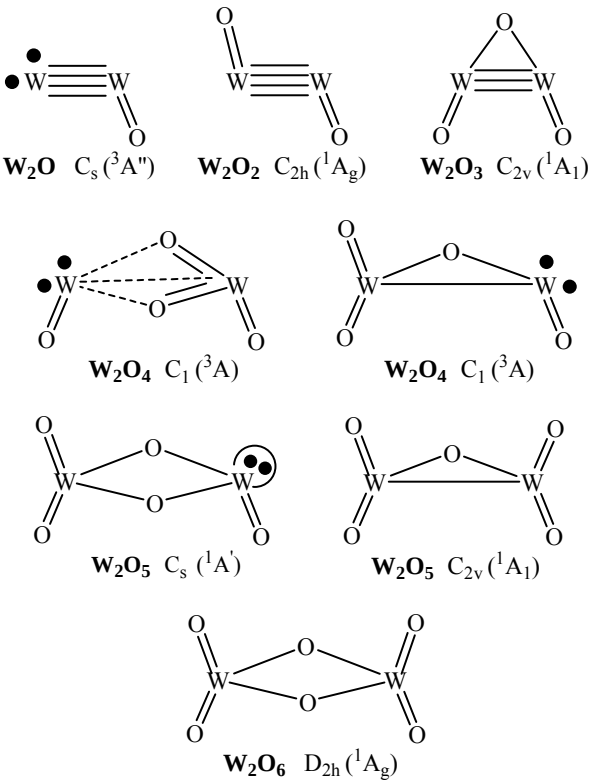

Figure 4. Valence-bond descriptions of W_2O_n (n = 1-6). Bond orders, unpaired electrons, and lone pair are indicated. For W_2O_4 and W_2O_5, two competing structures are shown.

Extensive DFT calculations were carried out to search for the most stable structures of both the anion and neutral clusters. Time-dependent DFT methods were used to compute the vertical detachment energies and compare to the experimental data. Molecular orbitals were used to analyze the chemical bonding in the ditungsten oxide clusters and elucidate their electronic and structural evolution. Figure 4 shows the structures and valence bond descriptions of the W_2O_n (n = 1-6) clusters, displaying how W_2 is oxidized to form the oxide clusters. The energy gap measured for W_2O_6 (2.8 eV) is already very close to the bulk band gap of WO_3. The oxygen deficient clusters possess lone pairs or unpaired electrons on W centers, making them much more reactive. Such defect sites are likely active sites in the bulk oxide or on surfaces. Continued studies of larger W_xO_y clusters may uncover appropriate models for the bulk defect sites and provide insight into their electronic and catalytic properties.

Computational studies of catalyst systems

We have been using density functional theory benchmarked with high level molecular orbital methods to predict the Brönsted acidities, basicities, and Lewis acidities (fluoride affinities) for the molecular clusters $M(=O)_2(OH)_2$, $M(=O)(OH)_4$, $M(OH)_6$, $(OH)M(=O)_2OM(=O)_2(OH)$, $(OH)_3M(=O)OM(=O)(OH)_3$ and $M(OH)_5OM(OH)_5$ for M = Cr, Mo, and W (the Group VIB metals), MO_2, MO_3, and $(MO_3)_6$. The basicities of these compounds are in the range of ammonia. The acidities are quite strong and for $M_6O_{19}H_2$, the acidity is extremely high, ~265 kcal/mol, ~ 45 kcal/mol stronger than that for H_2SO_4 in the gas phase. The structures of the anions provide information on the binding energies of anions to the metal oxides. The fluoride affinities for most of the compounds are on the order of 70 to 80 kcal/mol, relatively modest Lewis acidities. The Lewis acidity of $(WO_3)_6$ is very high, 142 kcal/mol and even that of WO_3 is very high, 138 kcal/mol. These are some of the highest known Lewis acidities for a non borohydride type species. The clustering energies of $(WO_3)_n$ for n = 2, 3, 4, and 6 normalized by n are: 68.2, 91.8, 99.3, and 109.4 kcal/mol. This information has provided us with a new way to view the chemistry of polyoxometallate clusters as nanoclusters of MO_3 with an anionic Lewis acid at the center of the cluster. The proton nmr chemical shifts for many $M_xO_yH_z$, M = Si, W, Mo compounds including hydrogen bonded species have been calculated for comparison with experiment. The electron affinities of some simple MO_x M = W and Mo clusters have been calculated with aug-cc-pVTZ type basis sets at the CCSD(T) and found to be in good agreement with experiment.

The first steps in the reaction of H_2O, CH_3OH, and CH_3OCH_3 have been calculated with a number of transition metal oxide clusters. The potential energy surface for the addition of CH_3OH to WO_3 is exemplary of one of the sets of reaction mechanisms shown below. The reaction proceeds by formation of a Lewis acid complex of the O to the W. The proton transfers with a modest barrier of ~ 20 kcal/mol to form the product $WO_2(OH)(OCH_3)$ where the product formation is highly exothermic. The transfer of the CH_3 group requires a much higher activation energy of ~ 50 kcal/mol.

The second reaction is the acidic reaction of transferring a CH_3 group from a cationic species to CH_3OH leading to formation of the protonated ether as shown below.

$$CH_3OH + CH_3OH_2^+ \rightarrow CH_3OHCH_3^+ + H_2O$$

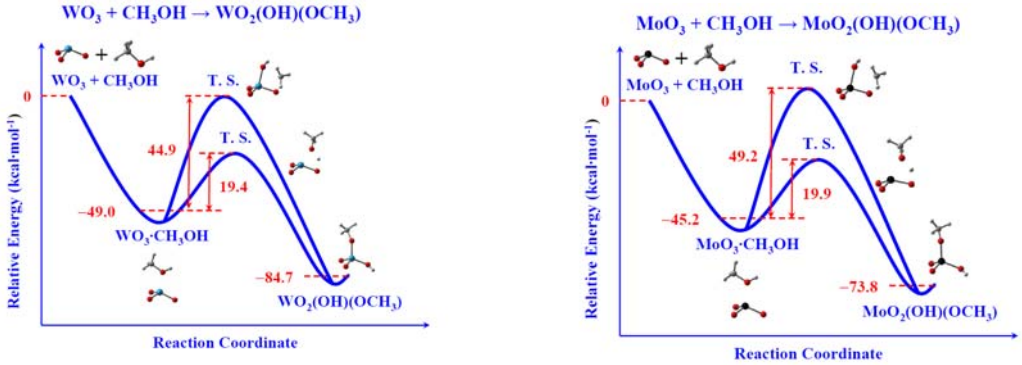

The potential energy surfaces for these two processes are shown for the simple organic reaction and for the one where the ionic species represents a charged metal oxide site. This reaction is exothermic in the gas phase with a low barrier from the initial complex for the organic process. If the alcohol is complexed to a $W(OH)_5^+$ species, the reaction is endothermic and there is a higher barrier between the reactant and pre-product complexes.

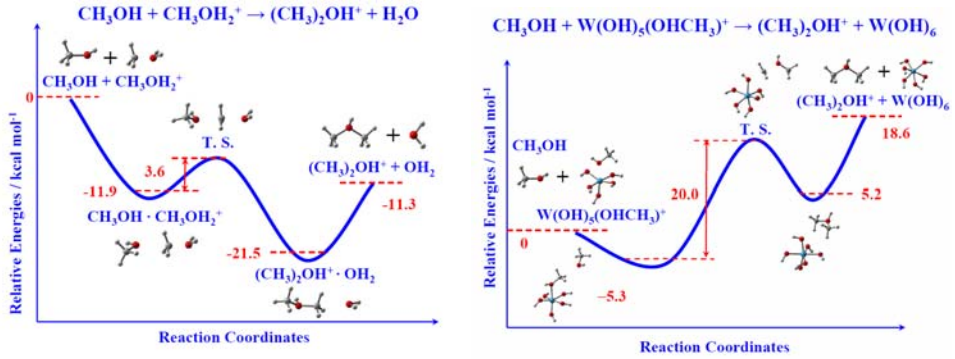

Using a plane-wave implementation of density functional theory (DFT), we characterized different terminations of WO_3 (001). Low temperature bulk WO_3 has a distorted cubic structure with a characteristic tilting of the WO_6 octahedra and alteration of the WO bond lengths, Figure 5. Among different terminations of WO_3 (001), the c(2x2) oxygen terminated surface (see Figure 6) proved to be the most stable, with a calculated surface energy of 1.9×10^{-2} eV/A^2. A comparison of density of states for bulk WO_3 and the c(2x2) slab demonstrates that many surface electronic states are localized in the band gap. The computational results suggest that the surface relaxation is accompanied by a dramatic redistribution of density of states at the Fermi level. This redistribution of states translates into a significant decrease of electronic energy of the slab and may be viewed as a driving force for surface relaxation in WO_3 (001).

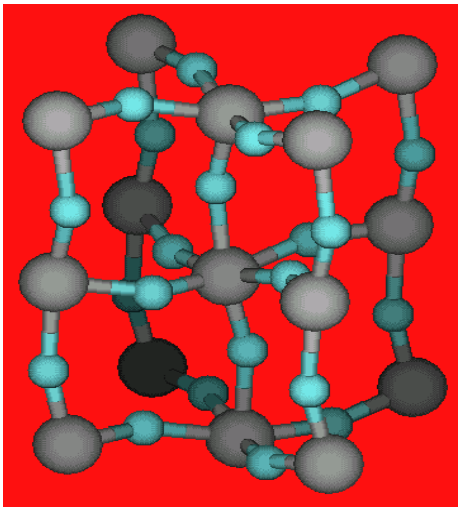

Figure 5. Low temperature monoclinic structure of WO_3. The calculated parameters (a=5.269, b=5.110, c=7.624 Å, α=90 β=92.41, γ=90 deg) agree very well with experimental predictions: a=5.278, b=5.156, c=7.664 Å, α=90 β=91.76, γ=90 deg.

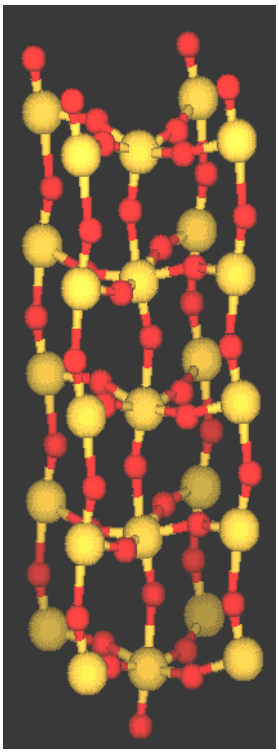

Figure 6. A five-layer WO_3 slab terminated with c(2x2) O-terminated surfaces. The structure is characterized by tilting of the WO_6 octahedra and alternation of the W-O bond lengths.

Physisorption and dissociative adsorption of methanol on regular c(2x2) WO_3(001) have been considered, and the minimum energy structures are presented in Figure 7. The binding energy of physisorbed methanol is 0.73 eV, with the Perdew-Wang 91 exchange-correlation functional. The dissociative adsorption of methanol on a defect-free surface is unfavorable, with the energy 0.16 eV higher than the energy of the WO_3 slab and a methanol molecule in the gas phase.

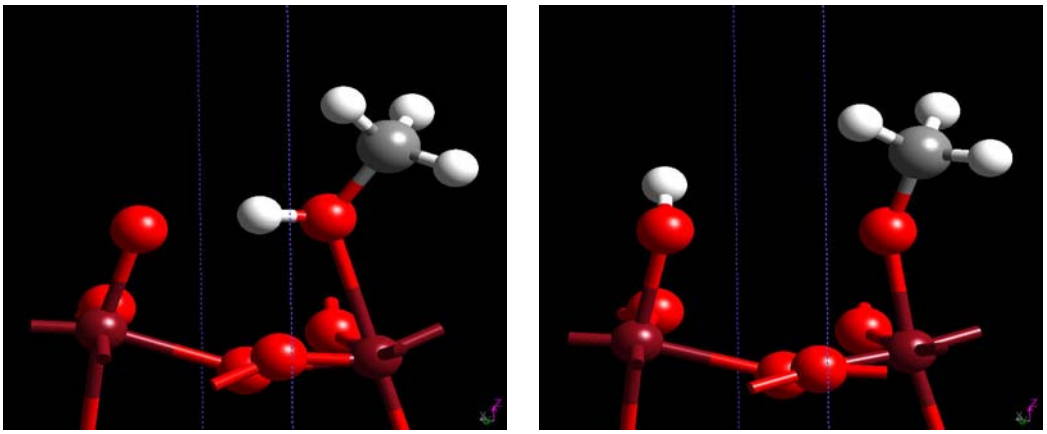

E=-0.73 eV
Methanol physisorbed
with an OH…O bond

E=+0.16 eV
Dissociative adsorption
is not favorable

Figure 7. Methanol on WO_3(001). The zero of energy is set to the energy of the WO_3 slab plus a methanol molecule in the gas phase.

Publications

1. Macht, J.; Baertsch, C.D.; May-Lozano, M.; Soled, S.L.; Wang, Y.; and Iglesia, E. "Support Effects on Brønsted Acid Site Densities and Alcohol Dehydration Turnover Rates on Tungsten Oxide Domains." J. Catal. **227** 479-491 (2004).
2. Zhai, H.-J.; Kiran, B.; Cui, L.-F.; Li, X.; Dixon, D.A.; and Wang, L.-S. "The Electronic Structure and Chemical Bonding in MO_n^- and MO_n Clusters (M = Mo, W; *n* = 3-5): A Photoelectron Spectroscopy and Ab Initio Study." J. Am Chem. Soc. **126** 16134-16141 (2004).
3. Yang, X.; Waters, T.; Wang, X.-B.; O'Hair, R.A.J.; Wedd, A.G.; Dixon, D.A.; Li, J.; and Wang, L.-S. "Photoelectron Spectroscopy of Free Polyoxoanions $Mo_6O_{19}^{2-}$ and $W_6O_{19}^{2-}$ in the Gas Phase." J. Phys. Chem. A **108** 10089-10093 (2004).
4. Hu, J.Z.; Kwak, J.H.; Herrera, J.E.; Wang, Y.; and Peden, C.H.F. "Resolution Enhancement in ^{1}H MAS Spectrum of Mesoporous Silica by Removing Absorbed H_2O Using N_2." Solid State NMR **27** (2005) 200-205.
5. DeVasher, R.B.; Spruell, J.M.; Dixon, D.A.; Broker, G.A.; Griffin, S.T.; Rogers, R.D.; and Shaughnessy, K.H. "Experimental and Computational Study of Steric and Electronic Effects on the Coordination of Bulky, Water-Soluble Alkylphosphines to Palladium under Reducing Conditions: Correlation to Catalytic Activity." Organometallics **24** (2005) 962-971.
6. Sarsani, V.R.; Wang, Y.; and Subramaniam, B. "Toward Stable Solid Acid Catalysts for 1-Butene+Isobutane Alkylation: Investigations of Heteropolyacids in Dense CO_2 Media." Industrial & Engineering Chemistry Research **44** (2005) in press.
7. Zhai, H.-J.; Huang, X.; Cui, L.-F.; Li, X.; Li, J.; and Wang, L.-S. "Electronic and Structural Evolution and Chemical Bonding in Ditungsten Oxide Clusters: $W_2O_n^-$ and W_2O_n (*n* = 1-6)." J. Phys. Chem. A, submitted (March, 2005).
8. Yakovkin, I.N.; Gutowski, M. "Driving Force for the WO_3(001) Surface Relaxation." Surface Science, submitted (February, 2005).

Cited Reference

[1] *The Surface Science of Titanium Dioxide*, U. Diebold, Surf Sci. Rep. **48** (2003) 53.

DE-AC05-76RLO 1830 **Michael A. Henderson,**

Controlling the Thermal and Non-Thermal Reactivities of Metal Oxide Structures Through Nanoscaling

Co-PIs:	Scott A Chambers, Michel Dupuis, Wayne P Hess, Maciej S Gutowski
PNNL staff:	John E Jaffe, Alan G Joly, Igor V Lyubinetsky
Postdocs:	Joshua R Williams, Nedialka I Iordanova, Gang Xiong
Collaborators:	Prof. J. Michael White (University of Texas, Austin), Prof. Hiroshi Onishi (Kobe University, Japan), Prof. James F Groves (University of Virginia, Charlottesville, VA Prof. Ivan N Yakovkin (National Academy of Sciences, Ukraine)
Contact:	**Michael A. Henderson,** Pacific Northwest National Laboratory, PO Box 999, MS K8-93, Richland WA 99352, (509) 376-2192, email: ma.henderson@pnl.gov

Goal

The constrained dimensions in nanoscaled materials produces unique chemical properties that will form the basis for important new technologies. A key scientific challenge is to understand how to tailor materials to generate specific novel properties and functionalities. The wide range of physical and chemical phenomena exhibited by bulk metal oxides suggests that diverse new chemical properties will result from carefully designed nanostructured oxide materials. Currently, remarkably little is known of the chemical behavior of nanoscaled systems based on oxides. We propose an integrated fundamental study of the thermal and non-thermal chemistries of nanoscaled metal oxides. Nanoscale oxide interfaces with well-defined sizes and electronic structures will be synthesized using state-of-the-art oxide film growth techniques. The proposed nanoscale systems will incorporate oxide heterojunctions designed to separate electron/hole pairs generated via non-thermal excitations (photons or energetic electrons). The physical properties of these structures will be examined in a coordinated experimental and theoretical program. In particular, control of the thermal and non-thermal chemistries of the resulting systems will be investigated with the goal of designing nanoscaled structures to optimize the mechanisms of important surface reactions, such as water splitting. The research proposed here will result in the ability to design and grow unique nanoscale oxide structures with predictable chemical reactivities, which will revolutionize the value of oxide materials for energy efficient chemical transformations through the combined application of advanced materials synthesis, chemical reactivity-characterization, and theoretical methods.

We have combined novel synthetic, experimental and theoretical methods that are based on our extensive experience at PNNL in studying the growth and chemical properties of oxide surfaces. Synthetic efforts will focus on the use of molecular beam epitaxy in preparing lattice matched and mismatched nanoscale oxide-oxide heterojunctions. Experimental studies will involve characterizing these structures with a variety of molecular-level probes, and performing photodynamic and photochemical studies exploring the photoreactivity of these nanostructures. Theoretical work will investigate the interfacial charge-separated chemistry in nano-systems using quantum mechanical methods for solid state band structures characterization and embedded cluster localized electronic structure representation.

Recent Progress

- Performed detailed photo-oxidation studies of acetone and trimethyl acetate on a model photocatalyst (rutile TiO_2(110)) concentrating effort on identifying reaction intermediates ejected from or left on the surface. Photodesorption measurement show that radical species (methyl and t-butyl radicals, respectively) are ejected during photolysis. These species likely follow oxidation pathways in media above the surface under more applied conditions.
- Performed calculations based on density functional theory (DFT) with Perdew-Wang 91 (PW91) exchange-correlation functional for corundum structures consisting of α-Cr_2O_3, α-Fe_2O_3 and α-Al_2O_3, along with interfactant layers of various other corundum oxides (e.g., Ti_2O_3) between

these oxides. The calculations show that the band offset properties can be tuned using selected interfactant materials.

- Determined a novel growth mechanism for the Cu_2O nanodots on the $SrTiO_3(100)$ substrate. In contrast to the majority of semiconductor systems, the growth process starts without wetting layer formation with Cu_2O nanodots grow with a little increase in its size but increase in density. After reaching some critical density, growth of scattered, significantly larger islands starts through the coalescence of small nanodots.
- Carried out initial study of photochemical decomposition of trimethyl acetate on heterojunctions and pure surfaces of α-Cr_2O_3 and α-$Fe_2O_3(0001)$. Found interesting photochemistry on α-Cr_2O_3 surfaces at sub-bandgap light energies that appears to be driven by bound exciton formation. This effect likely masks any heterojunction effect that may be present.
- Explored the epitaxial growth of α-Fe_2O_3 on $TiO_2(001)$ rutile as a candidate system for nanodot and type II heterojunction formation, and the associated enhancement of photochemistry due to the simultaneous presence of electrons holes on the surface. High resolution transmission electron microscopy (HRTEM), reflection high energy electron diffraction (RHEED) and x-ray diffraction pole figures confirm that the film is composed of four different in-plane orientations rotated by 90º relative to one another. For a given α-Fe_2O_3 unit cell, the lattice mismatch along the parallel [0001] direction of α-$Fe_2O_3$and the [100] direction of TiO_2 is nominally +67%. However, due to a three-fold repetition of the slightly distorted square symmetry of anion positions within the α-Fe_2O_3 unit cell, there is a coincidental anion alignment along these directions which results in an effective lattice mismatch of only -0.02%. The lattice mismatch is nearly 10% in the orthogonal directions. The film is highly ordered and well registered to the substrate despite a large lattice mismatch in one direction.
- Performed density functional theory (DFT/PW91) calculations of pure and binary corundum structures of α-Cr_2O_3, α-Fe_2O_3 and α-Al_2O_3. The theoretical analysis was shown to be consistent with the band offset description of type II heterojunctions. The experimentally observed strong anisotropy of the electron transport in α-Fe_2O_3 and α-Cr_2O_3, were explained on the basis of a small polaron model computationally characterized via Marcus' theory of electron transfer.
- Charge carrier dynamics of the α-Cr_2O_3/α-Fe_2O_3 heterojunction was examined using ultrafast laser spectroscopy. One laser was used to excite carriers and a second, in a reflection geometry, was used to probe the lifetimes of carriers resulting from the first laser pulse. The wavelength of the first laser was also varied to change the energy of the excited electrons. Starting with a thick α-Fe_2O_3 film (~100nm), we find that charge settling from excitation across the α-Fe_2O_3 band gap occurs on the order of 300 fs. When a large population inversion has been created, a narrowing of the band gap results and persists up to 5 ps after the initial laser pulse. We also find that long lived trap states persist to times well beyond the 10ps.

DOE Interest

The main premise of this project is that nanoscaling the dimensions of a supported semiconducting metal oxide opens new vistas for promoting excited state (non-thermal) and ground state (thermal) chemistries. Effective charge separation in a semiconducting metal oxide as a result of non-thermal excitation (i.e., photons, electrons) can be achieved with careful selection of a host support that results in a type II heterojunction. Utilizing type II heterojunctions to perform new types of chemistry depends critically on the issue of nanoscaling. Potential novel nanostructures are identified, and experimental and theoretical studies addressing their preparation, characterization and photochemistry are performed. These studies will provide new insights into photocatalysis on the nanoscale materials.

Future Plans

- Growth of model films of $TiO_2(101)$ on an wide bandgap oxide (α-$Al_2O_3(112bar0)$) to investigate the depth, as a function of wavelength, from which charge carriers can reach the surface from the bulk.

- Perfect the MBE growth of high-quality epitaxial films of $SrTiO_3$ on Si(001). We are exploring several synthesis routes to achieve maximum film quality, while eliminating substrate oxidation. Subsequent, photochemical studies will be performed on the photodecomposition and photodesorption of methyl halides on this system.
- Compare photodecomposition properties of carboxylic acids on a model surface in which the acid decomposes to give a bidentate carboxylate species (e.g., on TiO_2(110)) versus a monodentate carboxylate species (e.g., on TiO_2(011)). The deciding factor between these two structures depends on the cation-cation distance for available surface sites. The importance of this study lies in determining relative rates for different facet surfaces prevalent on nanoparticles.
- Model the atomic structure of the α-Cr_2O_3/α-Fe_2O_3 heterojunction, followed by calculations of band offset between the two oxides. Next, a cluster model will be designed to study excited electronic states at the heterojunction, i.e., electron-hole pairs. A cluster model approach will be used to determine lifetimes of electron-hole pairs using a semi-classical model of Marcus and Sutin.
- Employing UHV STM will initiate *in-situ* studies of the surface photo- and thermal-chemistry of a model system of small molecules (NO, O_2 and water) on the surface of a typical catalyst (TiO_2(110)). Main focus will be on a characterization of chemical transformations on single active sites.
- TMA photochemistry on model surfaces of α-Cr_2O_3(0001) to explore in more detail the interesting photochemical phenomena observed at sub-bandgap light energies discussed above.
- Efforts are in progress to characterize theoretically the hole transfer at the solid/adsorbate interface and the subsequent elementary steps of reactivity. This is being applied to the system of carboxylates on TiO_2(110).
- PEEM measurements on submicron size Fe_2O_3 particles on an α-Cr_2O_3(0001) substrate. Using two photon ionization schemes and delaying the second pulse time, we will examine the spatial trapping of carriers on and about the Fe_2O_3 particles.

Publications (2004-2005)

Chambers, S. A., T. Droubay, T. C. Kaspar and M. Gutowski (2004). *"Experimental determination of valence band maxima for $SrTiO_3$, TiO_2, and SrO and the associated valence band offsets with Si(001)."* **J. Vac. Sci. Technol. B** 22(4): 2205.

Chambers, S. A., T. Droubay, T. C. Kaspar, M. Gutowski and M. van Schilfgaarde (2004). *"Accurate valence band maximum determination for $SrTiO_3$(001)."* **Surf. Sci.** 554(2-3): 81.

Du, Y., S. Atha, R. Hull, J. F. Groves, I. Lyubinetsky and D. R. Baer (2004). *"Focused-ion-beam directed self-assembly of Cu_2O islands on $SrTiO_3$(100)."* **Appl. Phys. Lett.** 84(25): 5213.

Du, Y., S. Atha, R. Hull, J. F. Groves, I. Lyubinetsky and D. R. Baer (2004). *"Guided control of Cu_2O nanodot self-assembly on $SrTiO_3$(100)."* **Mater. Res. Soc. Symp. Proc**. 811(Integration of Advanced Micro- and Nanoelectronic Devices--Critical Issues and Solutions): 451.

Henderson, M. A. (2004). *"Acetone Chemistry on Oxidized and Reduced TiO_2(110)."* **J. Phys. Chem. B** 108(49): 18932.

Jaffe, J. E., M. Dupuis and M. Gutowski (2004). *"First-principles study of noncommutative band offsets at α-Cr_2O_3/α-Fe_2O_3(0001) interfaces."* **Phys. Rev. B** 69(20): 205106.

Lyubinetsky, I., A. El-Azab, A. S. Lea, S. Thevuthasan and D. R. Baer (2004). *"Initial stages of oxide nanodot heteroepitaxial growth: Cu_2O on $SrTiO_3$(100)."* **Appl. Phys. Lett.** 85(19): 4481.

Rosso, K. M. and M. Dupuis (2004). *"Reorganization energy associated with small polaron mobility in iron oxide."* **J. Chem. Phys**. 120(15): 7050.

Uetsuka, H., H. Onishi, M. A. Henderson and J. M. White (2004). *"Photoinduced Redox Reaction Coupled with Limited Electron Mobility at Metal Oxide Surface."* **J. Phys. Chem. B** 108(30): 10621.

White, J. M., M. A. Henderson, H. Uetsuka and H. Onishi (2004). *"Photoinduced Redox Reaction of Carboxylates on TiO_2(110)."* **Proc. SPIE** 5513 (Physical Chemistry of Interfaces and Nanomaterials III): 66.

White, J. M., J. Szanyi and M. A. Henderson (2004). *"Thermal Chemistry of Trimethyl Acetic Acid on TiO_2(110)."* **J. Phys. Chem. B** 108(11): 3592.
Yakovkin, I. N. and M. Gutowski (2004). *"$SrTiO_3$/Si(001) epitaxial interface: A density functional theory study."* **Phys. Rev. B** 70(16): 165319.

Submitted works

Du, Y., I. Lyubinetsky, D.R. Baer, and J.F. Groves (2005). *"Formation of Controlled Arrays of Oxide Quantum Dots: Cu_2O on $SrTiO_3$ (100)."* **Nano Lett.**, submitted.
Gutowski, M., J.E. Jaffe (2005). *"Effect of a Monolayer M_2O_3 Interfactant (M=Al, Ga, Sc, Ti, Ni) on Electronic and Magnetic Properties of the α-Fe_2O_3/α-Cr_2O_3(0001) Interface."* **Nano Lett.**, submitted.
Henderson, M.A. (2005). *"Photo-oxidation of Acetone on a Model TiO_2 Photocatalyst."* Proceedings of The Ninth International Conference on TiO_2 Photocatalysis: Fundamentals and Applications (TiO_2-9)," San Diego, CA, Oct 2004, in press.
Henderson, M.A. (2005). *"Acetone and Water on TiO_2(110): Competition for Sites."* **Langmuir**, in press.
Henderson, M.A. (2005). *"Photodecomposition of Acetone on TiO_2(110): Conversion to Acetate Via Methyl Radical Ejection."* **J. Phys. Chem. B**, submitted.
Iordanova, N., M. Dupuis and K. Rosso (2005). *"Charge Transport in Metal Oxides: A Theoretical Study of Hematite α-Fe_2O_3."* **J. Chem. Phys.**, in press.
Lyubinetsky, I., A.S. Lea, S. Thevuthasan, and D.R. Baer (2005). *"Formation of Heteroepitaxial Oxide Nanodot on Oxide Substrate: Cu_2O on $SrTiO_3$(100)."* **Surf. Sci.**, submitted.
White, J.M., M.A. Henderson (2005). *"Trimethyl Acetate on TiO_2(110): Preparation and Anaerobic Photolysis."* **J. Phys. Chem. B**, submitted.
Williams, J.R., C. M. Wang, S.A. Chambers (2005). *"Heteroepitaxial Growth and Structural Analysis of Epitaxial α-Fe_2O_3(101bar0) on TiO_2(001)."*, **J. Mat. Res.**, in press.

PIs: Raul F. Lobo and Douglas Doren
Departments of Chemical Engineering and Chemistry and Biochemistry, University of Delaware, Newark DE 19716, lobo@che.udel.edu, doren@udel.edu

Photocatalytic Activity of Microporous Titanium-Silicate ETS-10

Students: Michael Nash (Chemical Engineering) and Anne Marie Zimmerman (Chemistry)

Goals

The goals of this project are to maximize the photocatalytic activity of ETS-10 for the decomposition of VOCs by a combination of synthetic and theoretical methods and to determine the mechanisms and rate determining steps in the decomposition of model compounds (methanol and ethylene) in this photocatalyst.

Background

ETS-10 is a microporous titanium silicate containing chains of TiO_2 octahedra surrounded by a shell of SiO_2. ETS-10 has a three-dimensional pore system with 12-ring pores of ~8 Å in diameter. The chains of TiO_2 behave as nanowires and show an optical bandgap of ~4 eV, higher than anatase (3.2 eV) in part due to the quantum confinement effect of the 1-D nature of the TiO_2 chains. Photocatlytic activity with ETS-10 has been demonstrated by a few groups, but no structure-reactivity relationships have been developed and the effect of dopants on both the bandgap and photocatalytic activity has not been investigated. ETS-10, unlike anatase, is easy to dope with other first-row transition metals.

Recent Progress

Materials Synthesis and Characterization We have prepared pure samples of ETS-10 and doped ETS-10 containing various amounts of Fe, Cr, and V. Figure 1 shows the UV/vis diffuse-reflectance spectra for four different samples and shows that the band edge can change as a function of composition. The change in band edge is clear for V and Fe, but not so for Cr. We will be conducting electronic structure calculations of model structures to elucidate the origin of this qualitative difference between dopants. Below the band edge, doped materials also show additional weaker peaks that are likely related to metal-to-metal transitions

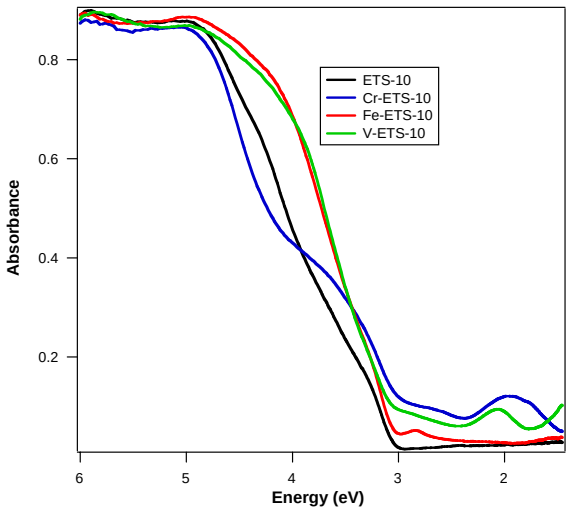

Figure 1 UV/vis diffuse reflectance spectra of ETS-10 and doped samples of ETS-10 (Cr-, Fe- and V-). All samples contain ~10% substitution of Ti by the dopant.

Electron Transfer in ETS-10 One of the contested issues about the photocatalytic activity of ETS-10 is where electron transfer occurs. Can electron transfer between electrons and holes in the TiO_2 chain occur directly from the chain to donors and acceptors in the pores? Or a defect in the chain is needed to allow electron transfer to occur. We have compared these two alternatives by preparing ETS-10 samples containing many defects in the chains (by ammonium chloride exchange and heat treatment) and comparing the formation of silver particles on the samples upon UV irradiation in a silver nitrate solution.

In the case of ETS-10 samples before the treatment, we observe that most of the silver particles are located on the outside of the ETS-10 particles. On the contrary, for the case of highly defective samples, most of the silver appears to be located inside the particles. This difference between the samples provides strong support for end-chain electron transfer processes in the photocatalytic activity of ETS-10.

Electronic Structure Calculations

The models used for our ETS-10 computations are single TiO_2 chains of varying lengths (containing 3-7 Ti atoms) encapsulated in the supporting SiO_2 framework derived from the geometry reported by Anderson et al.[1] Recently, the 2-layer ONIOM method (a hybrid molecular mechanics/molecular orbital method) has been utilized in order to increase the accuracy of our geometry optimizations without greatly increasing the computational cost. The 2-layer ONIOM method allows for a region of interest to be treated with a high level of theory while the remainder of the structure is treated with a much lower level of theory. We have therefore been able to extend our model to include the SiO_2 pores on either side of the TiO_2 chains (Figure 1). The high layer, consisting of the TiO_2 chain and the immediate SiO_2 framework, has been calculated using Density Functional Theory (DFT). In most cases the functional of Perdew, Burke and Ernzerhof was employed with a CEP-121G* basis-set on Na, O, Si and a CEP-121G basis set on Ti and O. The surrounding SiO_2 pores make up the low layer, which has been calculated with the Universal Force Field (UFF) method. For all optimizations the geometry of the low layer region has been fixed while the high layer region has been allowed to relax.

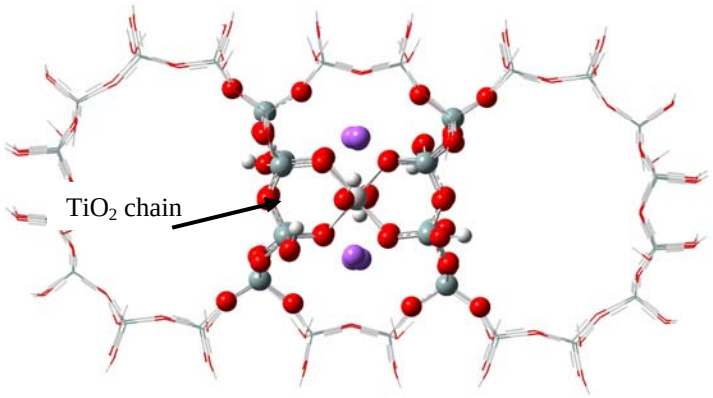

Figure 2. ONIOM model: high level layer shown in ball and stick mode, low level layer shown in sticks only.

Although we are still optimizing our ETS-10 model, our most recent results have produced geometries with one long and one short Ti-O bond length within the TiO_2 chain, consistent with geometries derived using EXAFS data.[2] The Ti-O-Ti, O-Ti-O, and Ti-O-Si bond angles as well as the Ti-O bond lengths perpendicular to the TiO_2 chain are also similar to geometries derived from the EXAFS data. Orbital analysis of our ETS-10 model shows that the main contribution to the HOMO is due to O 2p orbitals within the TiO_2 chain with a minor interaction to the Ti 5d orbitals. The LUMO, however, consists entirely of Ti 5d orbitals (Figure 2). This data is also in agreement with the density of states (DOS) data[3], illustrating that the relatively short TiO_2 chains in our model gives a good representation of the periodic ETS-10 structure.

---

[1] Anderson, M.W.; Terasaki, O.; Ohsuna, T.; Philippou, S.; MacKay, S.P.; Ferreira, A.; Rocha, J.; Lidin, S. *Nature* **1994,** *367*, 347.

[2] Sankar; Bell; Thomas; Anderson; Wright; Rocha *J. Phys. Chem* **1996**, *100*, 449.

[3] Ching; Xu; Gu *Phys. Rev. B* **1996**, *54* (22), 54.

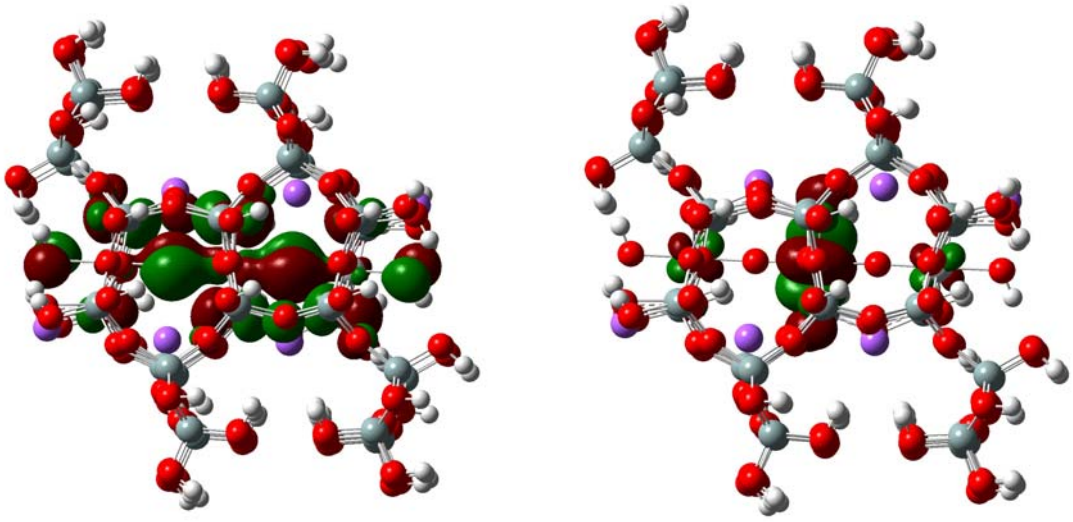

Figure 3. Molecular orbital (MO) diagrams for the HOMO and LUMO of ETS-10 model.

We have also started geometry optimizations where a single Ti atom in the TiO_2 chain has been substituted with V or Cr. Although not in their optimized geometries, preliminary orbital analysis of the doped ETS-10 structures have shown a sizeable decrease in the HOMO-LUMO gap of ~0.5-1 eV when compared to the undoped ETS-10 model. These results are very promising for reducing the overall band gap of 4.03 eV for pure ETS-10.

Future Plans

We have constructed a diffuse-reflectance IR cell that contains a window through which we can shine UV light using fiber optics. In the near future we will study the species that are formed on the surface of ETS-10 upon irradiation with UV light in the presence of electron acceptors and electron donors. Stepwise addition of reactants and oxidants will be used to identify the stable intermediates that are formed inside the crystals during the photocatalytic cycle. Investigations will be conducted using only the initial portion of the bands edge for the pure and doped ETS-10 samples to determine if decreasing the bandgap can be used to increase the activity of ETS-10 with lower energy radiation.

We will be substituting Ti atoms with Fe and Nb as well as employing the time-dependent DFT (TDDFT) method to gain information on the excitation energies and oscillator strengths of important electronic transitions. The combination of TDDFT calculations and analysis of the structural and electronic effects of dopants on ETS-10, will then be used to guide the synthesis of ETS-10 photocatalysts and determine the optimal composition of ETS-10 for photocatalytic activity

DE-FG02-95ER14549 **Robert J. Davis**

Structure and Function of Supported Base Catalysts

Students: Li, Junhui; Siporin, Stacey; Tai, Jianren

Department of Chemical Engineering, University of Virginia, Charlottesville, VA 22904
rjd4f@virginia.edu

Goal

Understand how atomic structure and composition affect the reactivity of surface oxygen atoms on supported basic compounds and transition metals.

Recent Progress

1. Structure and reactivity of zeolite-supported cesium oxide

Earlier work in our lab demonstrated that cesium species supported inside the supercage of a zeolite catalyzes a variety of reactions such as alkylation of toluene with methanol, cyclo-addition of carbon dioxide to ethylene oxide, and double bond isomerization of 1-butene. However, the nature of the occluded alkali has remained elusive.

In an effort to characterize the role of precursor on the final form of zeolite-supported cesium species, cesium-exchanged zeolite X was impregnated with cesium acetate (Cs(Ac)/CsX) or cesium carbonate (Cs_2CO_3/CsX) and subsequently calcined to yield a basic catalyst. The Raman spectra of calcined Cs(Ac)/CsX and Cs_2CO_3/CsX exhibited a new peak at 1036 cm^{-1} associated with the occluded species. No evidence for cesium peroxide or superoxide was observed in the spectra. In addition, chemical titration failed to indicate the presence of peroxide on the samples. The occluded cesium species in both samples is proposed to be an oxycarbonate, which is a metastable intermediate between the cesium carbonate and cesium oxide.

The isomerization of 1-butene to cis and trans-2-butene is catalyzed by cesium-loaded zeolite X. Although CO_2 readily poisoned the active base sites for this reaction, pretreatment of a basic zeolite with O_2 at 373 K did not. Co-feeding O_2 with 1-butene at 373 K, however, completely deactivated the base sites. Analysis of the reactor effluent at 473 K and the IR spectrum of the catalyst indicated the formation of carbon dioxide, which irreversibly adsorbed on the basic sites of the catalyst. Deactivation of basic catalysts by O_2 is proposed to occur through a low temperature oxidation of 1-butene to carbon dioxide, which strongly adsorbs on the active sites. It is quite remarkable that complete combustion of the hydrocarbon is observed at such low temperatures. Exploration of the hydrocarbon oxidation reaction over ion-exchanged zeolites indicates that occluded alkali metal species are responsible for the oxidation activity. The occluded alkali species are not required for the oxidation catalysis.

2. *Influence of Water on the Cs-Catalyzed Condensation of Propionic Acid with Formaldehyde*

We have continued our study of the catalytic conversion of propionic acid and formaldehyde to form methacrylic acid. The reactor system involves the co-feeding of propionic acid and trioxane to a pretreatment reactor, which cracks the trioxane to formaldehyde, and then to a fixed bed reactor containing a basic catalyst. To prevent subsequent reaction of the methacrylic acid, the reactor effluent was quenched rapidly in isopropanol solvent. The reaction was catalyzed with high selectivity by basic materials such as Cs-loaded zeolite, Cs-loaded silica, and Cs-loaded alumina. An attempt to increase the conversion over Cs-loaded zeolite by decreasing the space velocity through the reactor was unsuccessful, presumably because of undesirable side reactions of the product in the zeolite pores which prevent access of reactants to the active sites. Therefore, the Cs-loaded silica and alumina were more effective catalysts than the basic zeolites.

Since water is a product of the condensation reaction, the influence of co-feeding water on the reaction rate was tested. Interestingly, Cs/silica was significantly inhibited by the presence of co-fed water whereas Cs/alumina was only mildly influenced by the extra water. The inhibition observed over Cs/silica was entirely reversible, indicating that water had not permanently altered the catalyst. We are currently exploring the uptake of water and carbon dioxide on these materials to elucidate the surface properties that are responsible for the unusual base catalysis activity in the presence of water.

DOE Interest

The work performed in this program elucidates fundamental principles important in the design of basic and base-promoted catalysts. Solid bases are environmentally benign alternatives to liquid bases.

Future Plans

Low Temperature Oxidation. Our recent work has confirmed that low temperature oxidation occurs on zeolite base catalysts. We plan to determine if the reactivity results from the presence of transition metal impurities in the commercial zeolite or from the unique, high electric field of the zeolite supercages. In addition, we will explore the oxidation of other reactants beyond alkenes and alkanes.

Effect of Water on MAA Synthesis. Our recent work clearly shows a strong influence of the support in stabilizing the active base site in the presence of water. We plan to continue exploring how the local environment affects the reactivity of an active site. In particular, we will examine the hydrolysis of Cs-support bonds in attempt to derive general rules for base catalyst design.

Creation of Base Catalysts for use in Liquid Phase. A major limitation of solid base catalysts for use in condensed phase media is the leaching of the basic sites from the solid into solution. The transesterification of triglycerides with methanol to produce biodiesel fuel is a classic base-catalyzed reaction carried out in liquid phase. Solid bases would provide an excellent alternative to the homogeneous catalysts used in the reaction.

Publications 2003-2005

J. Li and R.J. Davis, “Raman Spectroscopy and Dioxygen Adsorption on Cs-loaded Zeolite Catalysts for Butene Isomerization,” *J. Phys. Chem. B*, (2005) ASAP Web Release March 18, 2005.

J. Tai, Q. Ge, R.J. Davis, and M. Neurock, "Adsorption of CO_2 on Model Surfaces of Cesium Oxides Determined from First Principles," *J. Phys. Chem. B* **108** (2004) 16798-16805.

S.E. Siporin and R.J. Davis "Isotopic Transient Analysis of Ammonia Synthesis over Ru/MgO Catalysts Promoted by Cesium, Barium or Lanthanum," *J. Catal.* 222 (2004) 315-322.

S.E. Siporin, R.J. Davis, W. Raróg-Pilecka, D. Szmigiel, and Z. Kowalczyk, "Isotopic Transient Analysis of Ammonia Synthesis over Ba or Cs-Promoted Ru/Carbon Catalysts" *Catal. Lett.*, 93 (2004) 61-65.

S.E. Siporin, R.J. Davis, "Use of Kinetic Models to Explore the Role of Base Promoters on Ru/MgO Ammonia Synthesis Catalysts," *J. Catal.*, 225 (2004) 359-368.

R.J. Davis, "Basic Nanostructured Catalysts" in *Encyclopedia of Nanoscience and Nanotechnology*, J.A. Schwarz, C.I. Contescu, K. Putyera, Eds., Marcel Dekker, New York, (2004) 225-234.

R.J. Davis, "Bases and Base Catalysis" in *Encyclopedia of Catalysis*, I.T. Horvath, Ed., Wiley: New York, (2003).

S.E. Siporin, B.C. McClaine and R.J. Davis, "Adsorption of N_2 and CO_2 on Zeolite X Exchanged with Potassium, Barium, or Lanthanum," *Langmuir* 19 (2003) 4707-4713.

R.J. Davis, "New Perspectives on Basic Zeolites as Catalysts and Catalyst Supports," *J. Catal.* 216 (2003) 396-405.

J. Li and R.J. Davis, "On the Use of 1-Butene Double Bond Isomerization as a Probe Reaction for Cesium-loaded Zeolite X," *Appl. Catal. A.* 239 (2003) 59-70.

DE-FG03-02ER15368 **C. J. Brinker**

Novel Transport Behaviors of Porous and Composite Nanostructures

PI: C. Jeffrey Brinker (UNM Depts. of Chemical and Nuclear Engineering and Chemistry and Sandia National Laboratories)

Collaborators: Frank van Swol and Hongyou Fan (UNM Dept. of Chemical and Nuclear Engineering and SNL), Nitant Kenkre (UNM Dept. of Physics), Tom Sigmon (UNM Dept. of Electrical and Computer Engineering), Vitaly Vodyanoy (Auburn Dept. of Veterinary Medicine)

Postdocs: Yi Yang (UNM Dept. of Chemical and Nuclear Engineering), George Xomeritakis (UNM Dept. of Chemical and Nuclear Engineering), Seema Singh (UNM Dept. of Chemical and Nuclear Engineering), Ralph Koehn (UNM, Department of Chemical and Nuclear Engineering), Nanguo Liu (UNM Dept. of Chemical and Nuclear Engineering now at Los Alamos National Laboratory)

Graduate Students: Zhu Chen (UNM Dept. of Chemical and Nuclear Engineering), Xingmao Jiang (UNM Dept. of Chemical and Nuclear Engineering)

Undergraduate Student: Adam Hurd (UNM Dept. of Chemistry)

Affiliation: C. Jeffrey Brinker, Department of Chemical and Nuclear Engineering, the University of New Mexico, Albuquerque, NM 87131, 505-272-7627, cjbrink@sandia.gov

Goal - Our goal is the design, synthesis and understanding of materials whose nanocomposite architecture allows tailoring of the motion of molecules, ions, electrons, and electronic excitations. Our research exploits evaporation-induced self-assembly *EISA* to form highly ordered porous thin film silica nanostructures with precisely defined pore size, connectivity, orientation, and surface chemistry. Through introduction of organic monomers or organically-stabilized nanocrystals, organic/inorganic self-assembly during *EISA* results in the formation of nanocomposites in which the polymers or nanocrystals are confined within ordered, monosized cavities or 1-, 2-, or 3-dimensional pore networks bounded by the inorganic host matrix. Importantly the *EISA* process allows us to use simple coating and printing procedures to integrate these porous and composite nanostructures into electronic, fluidic, photonic, and membrane platforms, thereby providing a means to characterize their transport behaviors and functionality.

Our NSET research focuses on two general classes of materials:

- natural (nanoporous-supported) membrane-bound ion channels or synthetic analogues that exhibit ionic or molecular selectivities
- nanocomposite systems that exhibit novel mass, charge, and energy transport characteristics through controlled nanostructuring and nano-confinement effects.

For both classes of materials, our NSET research has provided well-defined and adjustable nanostructures, which are important for establishing structure/property relationships and for future modeling of transport behavior.

Recent Progress

Nanoporous-Supported and Synthetic Ion Channels

Many membrane functions such as regulation of cellular potential, maintenance of ion concentration gradients, selective filtration, and regulation of nutrient and waste movement are regulated by channels that enable active, directional, and preferential transport of ions (across the otherwise impermeable lipid bilayer membrane) in response to a specific stimulus.

Figure 1. Fluorescence images of the FITC doped patterned silica support demonstrating our ability to create porosity, topology and surface energy differences into an otherwise passive uniform surface.

Our NSET research uses the evaporation-induced self-assembly EISA process we developed to create precise, periodic patterns of uniformly-sized pores (see **Figure 1**) in a rapid process completely compatible with silicon-based microelectronics processing. Pore diameter can be controlled over the range 1 – 20-nm, depending on the size of the surfactant or block copolymer pore template. Due to their uniform pore size and hydrophilic nature, these nanoporous films spontaneously fill with water, buffer, and aqueous-based reagents. As depicted schematically in **Fig.1,** we use the nanoporous films as a permanently water-filled ionic reservoir on which to support natural membrane-bound ion channels (nanoporous-supported ion channels) or as a robust totally synthetic ion channel.

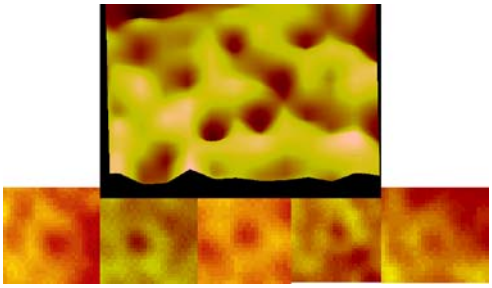

Figure 2. AFM image and montage of individual channels created in a POPC bilayer supported on a smart silica surface.

Recently, we have utilized the underlying porous architecture not only as a passive ionic reservoir, but also as an active smart interface. To achieve this, the underlying silica films were patterned by UV/Ozone exposure causing the exposed area to become porous and condensed by oxidation of organics and thereby creating patterns of varying topology, surface energy, and porosity (**Figure 1**). By immobilizing ion donors/acceptors to these different areas of interest we have better control of the ion transport pathways. Also proton transport across the bilayer and its permeability to ions are being studied using ion sensitive dyes in silica films and lipid bilayers.

Since the bilayer fluidity is dependent on many factors such as lipid and cholesterol composition as well as temperature, we are optimizing the bilayers for facile channel incorporation. **Figure 2** shows AFM images of channels formed in a 1-Palmitoyl-2-Oleoyl-sn-Glycero-3-Phosphocholine (POPC) bilayer supported on a patterned silica surface. Channel formation was initiated *in-situ* by introducing micro molar amounts of AmB in buffer to a preformed bilayer formed on a patterned mesoporous silica surface. We see appearance of channels after a few hours of incubation. A better understanding of the channel formation mechanism, for example, the influence of the porous support on channel formation/reorganization and whether AmB is introduced before or after the bilayer is deposited by vesicle fusion on the porous support is the focus of current research. This information will be used in formation of multi-channel complex architectures with desired ion transport properties.

Synthetic systems exhibiting ion-channel-like behavior

Last year, we reported the synthesis of functional nanoporous silica membranes with positively or negatively charged pore surfaces and controlled charge densities. These synthetic ion channels exhibit properties (such as stochastic sensing and rectification) similar to those of natural ion channels. This year, we tested whether we could record a signal from DNA oligomers as they are translocated through our nanoporous membranes. As shown in **Figure 3** (top), we observed only white noise when a bias of -120 mV was applied to the ion reservoir system. However, after addition of 2.0μM dispersion of DNA oligomer hairpins to the buffer, we observed single-molecular events which may involve the adsorption/desorption or translocation of DNA oligomers (**Figure 3** bottom).

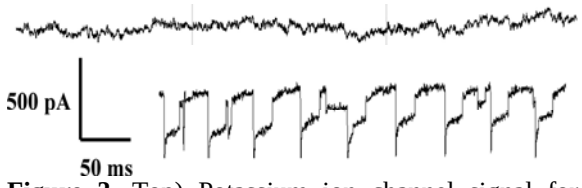

Figure 3. Top) Potassium ion channel signal for ~10^{12} pores; Bottom) Signal measured for 2.0 μM solution of DNA oligomer hairpins.

Tin oxide-based sensors for room-temperature hydrogen sensing

SnO_2-based gas sensors correlate changes in resistance, caused mainly by reduction/oxidation of the crystal surface, to monitor gas concentration. To date elevated temperatures or UV light are required to achieve rapid adsorption/desorption and oxidation/reduction kinetics needed for a practical, rapid, and sensitive detector. Very recently nanocrystalline SnO_2 based sensors showed room temperature sensitivity towards ethanol and carbon monoxide, but they are poor in sensing hydrogen gas.

The sensing process in tin oxides is still not fully understood. It is assumed that the reduction of the tin oxide happens only on the surface of the material and thereby the resistance drops depending on the amount of reduction. It is widely accepted that due to adsorbed oxygen on the surface the resistance increases as the oxygen accepts electrons from the tin oxide conduction band. Upon hydrogen introduction the surface oxygen reacts with the hydrogen to form water and electrons are donated back into the tin oxide valence band decreasing the resistance. Doping of tin oxides with palladium increases the original resistance by reducing the amount of free valence band electrons within the tin oxide surface. In presence of hydrogen the palladium acts as a catalyst increasing the speed of the reduction of the tin oxide on the surface.

This year we developed a surfactant-assisted sol-gel synthesis of a novel nanostructured PdO-SnO_2 sensor that exhibits very high sensitivity for H_2 gas at room temperature. **Figure 4** shows the structure to be composed of crystalline casserite nanocrystals of 4-5 nm diameter. Energy-dispersive X-ray scattering (EDS) confirmed the presence of both Pd and Sn uniformly distributed in the films. The porous structure was further confirmed by nitrogen physisorption measurements using our surface acoustic wave (SAW) based sorption technique. The material exhibits pore sizes in the range of about 5 nm and a BET surface area of ca. 143.5m^2/g which is about ten times more (14.4m^2/g) than that of the same material synthesized without any surfactant.

The resistivity of the thin (~200 nm) PdO-SnO_2 sensor films deposited on quartz substrates are a strong function of the partial pressure of O_2 and H_2 in the atmosphere above the sensor (P_{tot}= 1 atm, T=22ºC). As seen in **Figure 5a**, the resistivity of the sensor decreases from ~150

kOhm at P_{H2}=500 ppm, down to ~1.5 kOhm at P_{H2}=5,000 ppm (balance N_2 in both cases), e.g. by a factor of 100. Note that the resistivity of the sensor in pure air is usually >100 Mohm. **Figure 5b** shows the effect of 10% O_2 introduced in a H_2 process stream (3.5% in N_2), where the sensor undegoes a reversible resistivity change from ~1 kOhm (no O_2) up to 2,000 kOhm (10% O_2), e.g. by a factor of 2000. These unprecedentedly large and fast changes in resistivity with respect to H_2 and O_2 partial pressure arise from the unique nanocrystalline structure and intimate mixing of PdO and SnO_2 in our sensor material. This room temperature sensitivity has its tremendous potential for applications requiring H_2 (and O_2) sensing need as we go to a hydrogen economy.

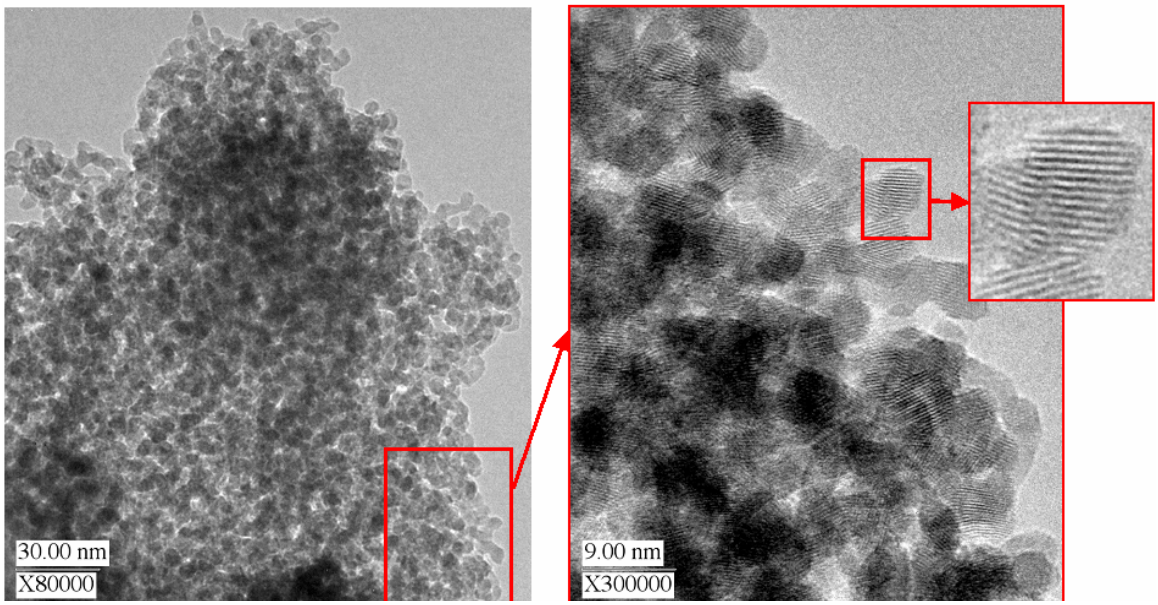

Fig. 4. TEM image of nanostructured Pdo-SnO_2 film prepared by surfactant assisted self-assembly

No evidence of pure palladium nanoclusters was found in SEM and TEM. X ray absorption near edge spectroscopy (XANES) analysis of the material in air and under reducing conditions in 5% hydrogen in nitrogen proving that the palladium is atomically dispersed within the tin oxide. This also explains the high reversibility in the sensing process of hydrogen. The palladium can react as a catalyst in the reduction of the tin oxide surface without changing its localization within the lattice.

DOE Interest - Materials with controlled transport properties are needed in diverse areas of emerging technologies of interest to DOE, including membrane-based separations and sensing, drug delivery, fuel cells, artificial photosynthesis, photovoltaics, catalysis, and molecular electronics.

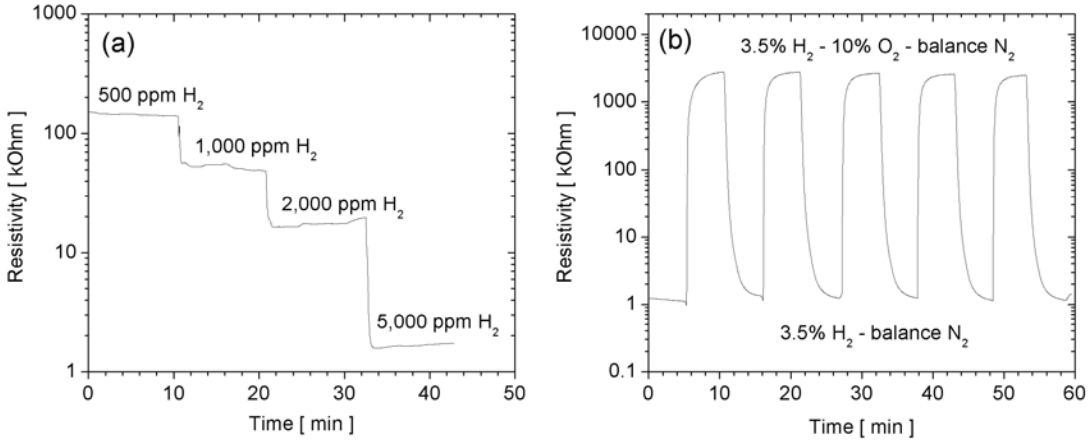

Figure 5. Sensor response at 22ºC to: (a) different partial pressures of H_2 (500-5,000 ppm) in N_2 and (b) O_2 (10% vol.) entering a H_2 process stream (7% vol. in N_2).

Publications (Jan. 2004-present)

1. **Controlled synthesis of 2-D and 3-D dendritic platinum nanostructures**, Song, YJ; Yang, Y; Medforth, CJ; Pereira, E; Singh, AK; Xu, HF; Jiang, YB; Brinker, CJ; van Swol, F; Shelnutt, JA, **J. Am. Chem. Soc**; JAN 21 2004; v.126, no.2, p.635-645
2. **Self-assembly of ordered, robust, three-dimensional gold nanocrystal/silica arrays**, Fan, HY; Yang, K; Boye, DM; Sigmon, T; Malloy, KJ; Xu, HF; Lopez, GP; Brinker, CJ, **Science**; APR 23 2004; v.304, no.5670, p.567-571.
3. **Photoregulation of Mass Transport through a Photoresponsive Azobenzene-Modified Nanoporous Membrane**, Nanguo Liu, Darren R. Dunphy, Plamen Atanassov, Scott D. Bunge, Zhu Chen, Gabriel P. López, Timothy J. Boyle, and C. Jeffrey Brinker, **Nano. Lett**; APR 2004; v.4, no.4, p.551-554.
4. **Unusual hydrocarbon chain packing mode and modification of crystallite growth habit in the self-assembled nanocomposites zinc-aluminum-hydroxide oleate and elaidate (cis- and trans-[Zn2Al(OH)(6)(CH3(CH2)(7)CH=CH(CH2)(7)COO-)] and magnesium analogues**, Xu, ZP; Braterman, PS; Yu, K; Xu, HF; Wang, YF; Brinker, CJ, **Chem. Mater**; JUL 13 2004; v.16, no.14, p.2750-2756
5. **Characterization of self-assembled lamellar thermoresponsive silica-hydrogel nanocomposite films**, Garnweitner, G; Smarsly, B; Assink, R; Dunphy, DR; Scullin, C; Brinker, CJ **Langmuir**; Oct 26 2004; v.20, no.22, p.9811-9820.
6. **A general route to macroscopic hierarchical 3D nanowire networks**, Wang, DH; Luo, HM; Kou, R; Gil, MP; Xiao, SG; Golub, VO; Yang, ZZ; Brinker, CJ; Lu, YF, **Agnew Chemie**, Nov 19 2004; v.43, no.45, p.6169-6173
7. **In situ real-time monitoring of profile evolution during plasma etching of mesoporous low-dielectric-constant SiO_2,** Gerung, H; Brinker, CJ; Brueck, SRJ; Han, SM, **J Vac. Sci. & Tech. A**, March 2005; vol.23, no.2, p.347-54.
8. **Aqueous sol-gel encapsulation of genetically engineered Moraxella spp. cells for the detection of organophosphates**, Yu, D; Volponi, J; Chhabra, S; Brinker, CJ; Mulchandani, A; Singh, AK **Biosensors and Bioelectronics**; Jan 15 2005; v.20, no.7, p.1433-1437.
9. **Microporous sol-gel derived aminosilicate membrane for enhanced carbon dioxide separation** Xomeritakis, G; Tsai, CY; Brinker, CJ, **Sep. and Purif. Tech**; April 2005; v.42, no.3, p.249-257.
10. **Surfactant-Assisted Synthesis of Water-Soluble and Biocompatible Semiconductor Quantum Dot Micelles**, Fan, HY; Leve, EW; Scullin, C; Gabaldon, J; Tallant, D; Bunge, S; Boyle, T; Wilson, MC; Brinker, CJ, **Nano. Lett**. Web Release Date: 01-Mar-2005.
11. **Nanocrystalline mesoporous palladium activated tin oxide thin films as room-temperature hydrogen gas sensors,** De, Goutam; Köhn, Ralf; Xomeritakis, George; Brinker, CJ, submitted to **Nature Mater.**, Fri, Feb 04, 2005. Manuscipt # NM05020184

DE-FG02-86ER13622 **Steven L. Suib**

Microporous and Mesoporous Nanosized Transition Metal Oxides: Preparation, Characterization and Applications

Students: Jason Durand, Sinue Gomez, Josie Villegas, Xiongfei Shen.
Collaborators: Alex Navrotsky, UC Davis; Jon Hanson, Brookhaven National Labs, Bill Reiff, Northeastern University, Thorsten Ressler, Fritz-Habr-Institut der MPG
Contact: Steven L. Suib, Unit 3060, Department of Chemistry, 555 N. Eagleville Rd., University of Connecticut, Storrs, CT 06269-3060; (860)-486-2797, (860)-486-2981 (FAX), E-mail - Steven.Suib@uconn.edu , Website: <http://web.uconn.edu/chemistry/SuibGroup/suibg.html>

Goals

The goals of this project are as follows:

(1) To prepare aqueous colloids of nano-size (10 Å to 1000 Å) porous manganese oxides as precursors for various OMS systems.
(2) To prepare novel doped octahedral molecular sieve (OMS) and octahedral layer (OL) structures via aqueous colloidal routes.
(1) To understand factors that control size and shape of porous nano-size oxides.
(2) To fully characterize physical and chemical properties of the above-mentioned systems.
(3) To use porous metal oxides for selective oxidations, shape selective oxidations, and chiral oxidations.
(4) To explore new potential applications of these systems in secondary non-aqueous rechargeable batteries, and as membranes.

Recent Progress

A systematic way to control these tunnel sizes has recently been demonstrated using hydrated Na^+ ions as inorganic templates/structure directors by hydrothermal treatment of Na-birnessite under different pH conditions as shown in the figure below. Manganese oxides with tunnel sizes of 1×1 (2.3 Å × 2.3 Å), 2×3 (4.6 Å × 6.9 Å), and 2×4 (4.6 Å × 9.2 Å) have been synthesized at pH values of 1.0, 7.0, and 13.0, respectively. During hydrothermal treatment of Na-layer manganese oxide precursors, the strength of the hydration bonding for the interlayer Na^+ ions increases with increasing pH values: thus, more water molecules will be stabilized by association with Na^+ ions. As a result, larger hydrated Na^+ ions are produced as structure directors for templating syntheses of materials with larger tunnel sizes.[20]

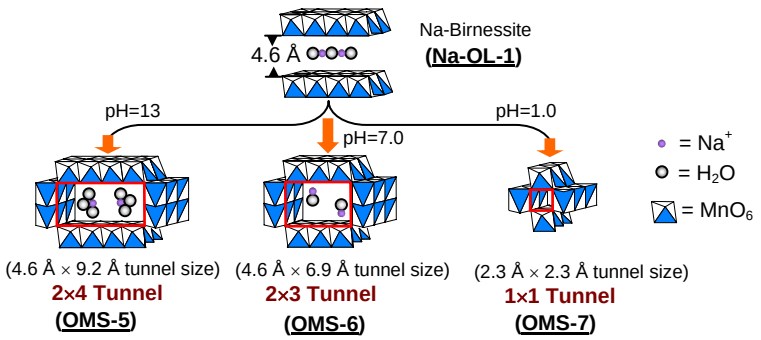

DOE Interest

Fundamental knowledge in the areas of synthesis, new characterization methods, structural analysis, mixed valency, electron transfer, magnetic behavior, conductivity, catalysis, and photocatalysis has been obtained in our studies of OMS and OL materials. The novelty of porous semi-conducting molecular sieves has allowed fundamental studies of effects of electron transfer in such systems. High resolution spectroscopic and microscopic characterization (imaging, surface studies) have led to an excellent understanding of many of the fundamental structural and electronic features of these systems. Catalytic studies have led to correlations of activity/selectivity, shape selectivity, and redox or electron transfer capability. Unique features of our systems include the unusual hollowness of MnO_2 materials; the myriad of morphologies available in these systems (helices, nano-ropes, nano-wires, nano-lines, nano-patterns, nano-spheres); variety of tunnel structures (1x1/1x2, 2x2, 3x3, 2x4, 3x5); excellent conductivity; ease of ion-exchange; transformations to alternate structures while preserving the macro-morphologies of wires, lines, and patterns; outstanding selectivity and activity in selective oxidations; and excellent adsorption properties. Helices or wires with such variation in length and diameter, as well as the uniquely high permeability and porosity are novel. Porous thin films are important for sensors, optical coatings, membranes, and in catalysis. Novel battery and sensor systems have been designed that are functional and low cost. Catalytic oxidations and condensations are the focus of our catalysis studies. The unique combination of availability of many structural types, good electrical properties, high permeability, and high porosity is rare.

Future Plans

Our major efforts continue to be focused on the aerobic catalytic oxidation of alcohols. We have been studying the kinetics of such reactions and finding ways to enhance activity, which in most cases can be as high as 100%. We are also trying to extend this work to chiral alcohols. Catalytic shape selective oxidations (selective, not total) are a major goal of this work.

In the area of synthesis of new materials, we are trying to prepare nanosize manganese oxide layered materials of various morphologies and surface areas to make available a set of catalytic materials for a variety of applications. We are continuing the nano-film work with protein/manganese oxide layers for catalytic studies such as the conversion of styrene to styrene oxide is one such reaction. Framework doping with iron has produced ferromagnetic materials and these are looked at with susceptibility studies.

The colloidal preparations have led to a new family of materials that have unique morphologies and properties. Porous, helices, wires, thin films and nano-patterns of manganese oxide have been synthesized. These systems offer outstanding porosity, versatility for preparation of new materials, and many new applications. We are continuing to prepare such systems and are trying to understand their mechanisms of formation. We have made headway in making similar manganese oxide colloids solely from aqueous solutions and also in the preparation of a variety of transition metal nano-lines and nano-patterns.

Publications, 2003 -2004

1. Giraldo, O.; Durand, J.P.; Ramanan, H.; Laubernds, K.; Suib, S. L.; Tsapatsis, M.; Brock, S. L.; Marquez, M. Dynamic Organization of Inorganic Nanoparticles into Periodic Micrometer-Scale Patterns, *Ang. Chem., Int. Ed*., 2003, **42**, 2905-2909.
2. Yuan, J.; Gomez, S.; Villegas, J.; Laubernds, K.; Suib, S. L. Spontaneous Formation of Inorganic Paper-Like Materials, *Adv. Mat*., 2004, **16**, 1729–1732.
3. Yuan, J.; Laubernds, K.; Zhang, Q.; Suib, S. L. Self-Assembly of Microporous Manganese Oxide Octahedral Molecular Sieve Hexagonal Flakes into Mesoporous Hollow Nanospheres, *J. Am Chem. Soc*., 2003, **125**, 4966-4967.
4. Liu, J.; Son, Y. C.; Cai, J.; Shen, X,; Suib, S. L.; Aindow, M. Size Control, Metal Substitution and Catalytic Application of Cryptomelane Nanomaterials Prepared Using Cross-linking Reagents, *Chem. Mater*., 2004, **16**, 276-285.
5. Polverejan, M.; Suib, S. L. High valebt Substitution in Octahedral Molecular Sieves, *J. Am. Chem. Soc*., 2004, **126**, 7774-7776.
6. Liu, J.; Makwana, V.; Cai, J.; Suib, S. L.; Aindow, M. Effects of Alkalai Metal and Ammonium Cation Templates on Nanofibrous Cryptomelane-type Manganese Oxide Octahedral Molecular Sieves (OMS-2), *J. Phys. Chem*., 2003, **107**; 9185-9194.
7. Garces, L. V.; Hincapie, B.; Makwana, V.; Laubernds, K., Sacco, A. Suib, S. L. Effect of using polyvinyl alcohol and polyvinyl pyrrolidone in the synthesis of octahedral molecular sieves, *Micropor. And Mesopor. Mater*., 2003, **63**, 11-20.
8. Gao, Q.; Suib, S. L.; Thomson, M.; Bowden, W. Unusual nanometer-sized nsutite from Mn(ClO4)2.6H2O-(C2H5)4NOH-CsMnO4-H2O basic systems, *J. Chem. Eng. Jap*., 2003, **36**, 1222-1226.
9. Liu, J.; Durand, J. P.; Espinal, L.; Garces, L. J.; Gomez, S.; Son, Y. C.; Villegas, J.; Suib, S. L. Layered Manganese oxides: Synthesis, Properties and Applications, in Handbook of Layered Materials Science and Technology, S. A. Auerbach, K. A. Carrado, P. K. Dutta, Eds., Marcel Dekker, NY, 2003, 475-508.
10. Gomez, S.; Giraldo, O.; Garces, L. J.; Villegas, J.; Suib, S. L. New Synthetic Route for the Incorporation of Manganese Species into the Pores of MCM-48, *Chem. Mater*., 2004, **16**, 2411-2417.
11. Villegas, J.; Giraldo, O. Suib, S. L. New Layered Double Hydroxides Containing Intercalated Manganese Oxide Species: Synthesis and Characterization, *Inorg. Chem*., 2003, 42, 5621-5631.
12. Hincapie, B. O.; Garces, L. J.; Zhang, Q.; Sacco, A.; Suib, S. L. Synthesis of Mordenite Nanocrystals, *Micropor. Mesopor. Mater*., 2003, **67**, 19-26.
13. Espinal, L.; Suib, S. L.; Rusling, J. F. Electrochemical Catalysis of Styrene Epoxidation with Films of MnO_2 Nanoparticles and H_2O_2, *J. Am. Chem. Soc*., 2004, **126**, 7676-7682.
14. Makwana, V.; Garces, L. J.; Liu, J.; Son, Y. C.; Suib, S. L., *Catal Today*., 2003, **85**, 225-233.
15. Ghosh, R.; Son, Y. C.; Suib, S. L. Liquid Phase Epoxidation of Olefins by Manganese Octahedral Molecular Sieves, *J. Catal*., 2004, **224**, 288-296.

16. Ghosh, R.; Garces, L. J.; Hincapie, B. O.; Suib, S. L. Solid Acid Catalyst in the alkylation of benzene, *Stud. Surf. Sci. Catal*., 2004, **149**, 341-353.
17. Garces, J. Suib, S. L. Selective N,N-methylation of Aniline over co-crystallized Zeolites RHO and Zeolite X(FAU) and over Linde Type L(Sr,K-LTL), *J. Catal*., 2003, **217**, 107-116.
18. Shen, X.; Ding, Y.; Liu, J.; Laubernds, K.; Zerger, R. P.; Polverejan, M.; Son, Y. C.; Aindow, M.; Suib, S. L. Synthesis, Characterization, and Catalytic Applications of Manganese Oxide Octahedral Molecular Sieve (OMS) Nanowires with a 2 X 3 Tunnel Structure, *Chem. Mater*., 2004, **16**, 5327-5336.
19. Villegas, J. C.; Garces, L. J.; Gomez, S. Durand, J. P.; Suib, S. L. Particle Size Control of Cryptomelane nanomaterials by use of H_2O_2 in Acidic Conditions, *Chem. Mater*., 2005, in press.
20. Shen, X.; Suib, S. L. Control of Nano-scale Tunnel Sizes of Porous Manganese Oxide Octahedral Molecular Sieve (OMS) Nanomaterials, *Adv. Mater*., 2005, in press.

Patents.

A. Suib, S. L.; Giraldo, O.; Marquez, M.; Brock, S. L. Manganese Oxide Helices, Rings, Strands, and Films and Methods of their Preparation, US Patent 6,503,476, January 7, 2003.
B. Malz, R. E. Jr.; Kumar, R.; Garces, L. J.; Suib, S. L.; Process for preparing ortho substituted phenylamines, US Patent 7,016,244, January 30, 2004.

Session E:

Nanocatalysis and Advanced Instrumentation — University, National Lab, Industry Cooperation

Synthesis, Charge Transfer, Three-Dimensional Structural Characterization, and *ab initio* Simulations of Ligand-Stabilized and Supported Metal Nanoparticles

Principal Investigators: Judith Yang **DE FG02-03ER15475**
Duane Johnson[*], Ralph G. Nuzzo[**] **DE FG02-03ER15476**
Anatoly Frenkel[***] **DE-FG02-03ER15477**

Collaborators: Ray Twesten[*], Royce Murray[****]
Post-doctoral research associates: Huiping Xu, Shangpeng Gao; Joo Kang, Linlin Wang*
Graduate students: Charles Hills, Laurent Menard, Nathan Mack[**]
Undergraduate students: Dana Glasner, Louisette Soussan, Sarah Nemzer, Ilana Pister, Talia Harris***

Department of Materials Science and Engineering, University of Pittsburgh, Pittsburgh, PA 15261
[*] Department of Materials Science and Engineering, University of Illinois Urbana-Champaign, Urbana Il 61801
[**] Department of Chemistry, University of Illinois Urbana-Champaign, Urbana Il 61801
[***] Department of Physics, Yeshiva University, New York, NY, 10016
[****] Department of Chemistry, University of North Carolina – Chapel Hill, Chapel Hill, NC 27514

Goal:

This project involves the characterization of metal nanoparticles with the goal of achieving a fundamental understanding of their dynamical and structural properties and the correlations these have with behavior seen in catalytic chemistry. Nanomaterials prepared via controlled chemical syntheses are characterized using a variety of analytical techniques, highlighted by the complementary use of X-ray absorption spectroscopy and advanced electron microscopy. Theoretical calculations further augment an understanding of structures that are characteristic of the nanometer dimensions of catalyst materials or of the local environment of the catalyst (support, ligands, and reactant molecules).

DOE Interest:

A fundamental understanding of the structure of nanomaterials has far-reaching implications in the development of more efficient catalysts. Our research focus has included identifying crystallographic structures and bimetallic phases that differ from those observed in the analogous bulk materials. Important to our investigation is probing not only how these static structural elements impact catalytic activity but also the evolution of dynamical structure under reactive conditions.

Recent Progress:

This report describes the synthesis, characterization, and properties of the model system used in our x-ray absorption spectroscopy (XAS), electron microscopy, and theoretical studies. The phosphine-to-thiol exchange technique was adapted to produce the monodisperse and compositionally well-defined *icosahedral* gold clusters, $Au_{13}[PPh_3]_4[S(CH_2)_{11}CH_3]_2Cl_2$ and $Au_{13}[PPh_3]_4[S(CH_2)_{11}CH_3]_4$. These clusters were studied and compared to larger, fully-thiolated monolayer-protected clusters (MPCs) that were determined to have *cuboctahedral* structure. These sub-nanometer clusters exhibit molecule-like properties that are strongly influenced by the chemistry of their ligand shells. These clusters were also studied by x-ray absorption near edge structure (XANES) measurements at the phosphorus and sulfur absorption edges, and new information about ligand-specific gold-ligand charge transfer in these clusters was obtained. The in-depth structural characterization of these materials using XAS and advanced electron microscopy is presented. We also report on the synthesis of dodecanethiol-stabilized gold nanoparticles with different Au/thiol ratios and the new method of their size determination by surface stress studies using extended x-ray absorption fine structure (EXAFS). We report on the studies of the TiO_2 (anatase)-supported Au nanoclusters by both EXAFS and TEM and explored different in situ methods of ligand removal. Finally, another supported cluster, [PtRu5]/C was modeled by the application of density-functional methods and the distribution of the first nearest neighbor distances obtained by theory was determined to be in excellent agreement with our experimental analysis by EXAFS, providing insight into the nature of self-organizing structures of supported $[PtRu_5]$-based clusters.

I. Controlled synthesis of Au clusters with mixed-ligand and fully thiolated shells

The partial exchange of dodecanethiol (C12SH) onto phosphine-halide gold clusters was used to produce the monodisperse and compositionally well-defined icosahedral gold clusters, $Au_{13}(PPh_3)_4(SC12)_2Cl_2$ and $Au_{13}(PPh_3)_4(SC12)_4$. These clusters exhibit enhanced stability relative to the phosphine-halide parent clusters and are isolable in 100 mg quantities from a single synthesis. It was possible to isolate a fraction of nanoparticles from these preparations that were larger, fully thiol-protected nanoparticles with a distribution of sizes between 0.8 and 3.2 nm. This fully-thiolated sample was studied for a comparison to the monodisperse icosahedral Au_{13} clusters. It additionally served as a test of the capability of XAS and TEM to provide complementary information on particles with a significant size distribution – a situation more representative of nanoparticle catalysts.

The clusters were characterized by ^{1}H and $^{31}P\{H\}$ NMR, UV-visible spectroscopy, XPS, electrochemical measurements, near-IR luminescence, and liquid chromatography. Properties distinctly different from bulk metals were observed in all nanoclusters. The following sections describe the characterization of these clusters by advanced methods of TEM and EXAFS.

II. TEM characterization

TEM characterization of mixed-ligand and fully thiolated clusters

Transmission electron microscopy of the mixed-ligand clusters identified them as sub-nanometer, highly monodisperse nanoparticles with an average core of 13 atoms. Scanning transmission electron microscopy (STEM) measurements were quantitatively analyzed to obtain the number of gold atoms in individual clusters. This was achieved by collecting the scattered electrons only at high angles (> 100 mrad) where the contribution of Bragg electrons is minimized and the electrons collected are predominantly those that are incoherently scattered. This is referred to as high angle annular dark field (HAADF) STEM or "Z-contrast" microscopy. With careful calibration of the detector efficiency, inner and outer scattering angles of collection, and microscope magnification, the scattering cross-sections of an individual cluster, which is proportional to the absolute scattered intensity, can be calculated. Since the scattering cross-section of a cluster core is simply the sum of the cross-sections of the atoms in the core, the number of atoms in the cluster can be determined using an atomic cross-section calculated from theory.

Figure 1 is a representative HAADF-STEM image of $Au_{13}(PPh_3)_4(SC12)_2Cl_2$ clusters on an ultrathin carbon (~3 nm) coated TEM grid. Figure 2 is a histogram showing the distribution of the number of atoms in individual nanoparticles. The average measured cross-section for the nanoparticles was 0.25 ± 0.06 $Å^2$. The atomic electron scattering cross-section for Au over the collection angles was calculated using partial-wave methods and found to be 0.019 $Å^2$. Thus, the average cluster core was determined to contain 13 gold atoms with a narrow standard deviation of ± 3 atoms for the ~300 particles analyzed.

The structures of both mixed-ligand and fully-thiolated nanoparticles were further investigated using high resolution electron microscopy (HREM). The mixed-ligand Au_{13} clusters (Figure 3) and larger, fully-thiolated MPCs were identified as having icosahedral and cuboctahedral geometries, respectively,

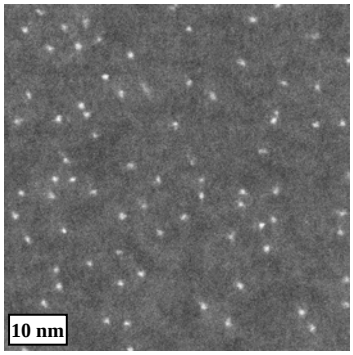

Figure 1. Representative HAADF-STEM image of Au_{13} clusters.

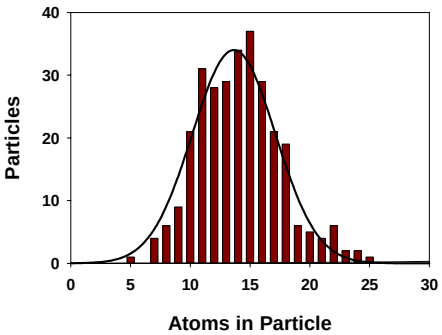

Figure 2. Histogram of quantitative STEM results of Au_{13} clusters. N=295.

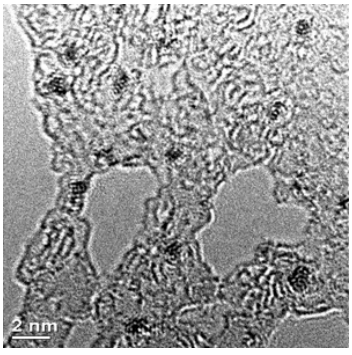

Figure 3. High-resolution electron micrograph of icosahedral Au_{13} clusters.

by analysis of lattice images of high resolution electron microscopy (HREM) performed on a Jeol 2010 FETEM operating at 200kv. Determination of the icosahedral shape of the Au_{13} clusters was achieved by the trace analysis of the particle edges in Figure 3. A d-spacing value of 2.39 ± 0.07 Å was obtained that corresponds to a cubic 111 net plane (d-spacing of 2.36 Å for bulk gold). Similarly, the cuboctahedral shape of gold particles with fully-thiolated shells can be determined from microdiffraction of single particles. The angle between 1-11 or -111 and 002 and d-spacing can be measured to be about 56° and 2.32 ± 0.05 Å, respectively, which agrees closely with those calculated for FCC Au (where a=4.07 Å, c/a=1.155, θ = 54.74°). The Au-Au bond length can be obtained as 2.82 Å, which is in excellent agreement with the Au-Au bond distance (2.81 ± 0.01 Å) obtained by our EXAFS analysis.

Deposition of Au13 onto anatase TiO_2 and exploration of different ligand removal methods

In order to realize high activity for CO oxidation, we explore the deposition of ligand-protected Au_{13} clusters onto anatase TiO_2 followed by treatments to remove the ligands while maintaining small particle size. In addition to this, it is still not clear how the metal oxides substrates affect the presence of Au^0 and Au^1. A comparison of EXAFS data for $Au_{13}(PPh_3)_4(SC_{12})_4$ and $Au_{13}(PPh_3)_4(SC_{12})_4$ deposited on TiO_2 indicates little change in either the Au-Au coordination or the Au-S/Au-P coordination. The EXAFS spectrum for Au_{13} on TiO_2 after thermal desorption of the ligands at 375ºC for 1 hr under He inert atmosphere is qualitatively indistinguishable from that of the gold foil standard, indicating full removal of ligands but also cluster annealing to large particles. Finally, the UV-ozone treated sample shows that the treatment is successful in removing some ligand (evident by a loss of Au-P and Au-S scattering contributions at low R) but does not result in a large increase in Au-Au coordination - either due to the retention of small particle size or to the development of larger gold islands that are raft-like in nature. In order to confirm the EXAFS results above, further TEM examination is needed. Figure 4 shows representative dark field STEM micrographs of heat (Fig. 4a) and UV-ozone (Fig. 4b) treated Au/TiO_2 and next to each micrograph is the representative particle size distribution for each sample. As Figure 4 indicates, average particle size for UV-ozone treated sample is smaller on average and has a narrower range of sizes centered on an average particle dimension of 3.7 ± 1.5 nm, while the average particle size for heat treated Au/TiO_2 is 6.2 ± 3.6 nm. Furthermore, HREM lattice images of UV-ozone treated Au particles on TiO_2 were analyzed. The Fourier transformed images can be uniquely indexed to a simple close-packed face centered cubic (fcc) structure with the zone axis of 110 and 100, consisting of twins, although ligand-protected Au_{13} before deposition and post-treatment exhibits icosahedral shape.

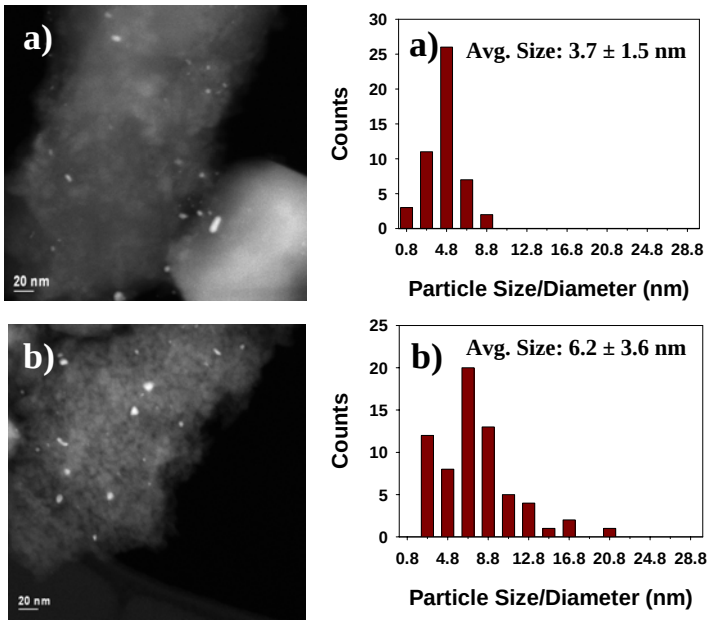

Figure 4. Representative ADF-STEM images of (a) UV-ozone treated and (b) heat treated ligand-protected Au_{13} clusters on TiO_2.

III. EXAFS and XANES characterization of Au nanoclusters

Multiple-scattering EXAFS study of mixed-ligand and fully-thiolated Au nanoclusters

EXAFS data of the mixed-ligand and fully thiolated nanoclusters were collected on beamlines X16C and X11A at the NSLS. Visual observation of the EXAFS data (Figure 5) reveals difference between the local order in the mixed-ligand clusters (Figure 5a,b) and the fully thiolated nanocluster (Figure 5c). The peak between 3 and 4 Å present in the fully – thiolated cluster, is absent in the mixed-

ligand clusters. This peak corresponds to the Au-Au second nearest neighbor distance that is expected to

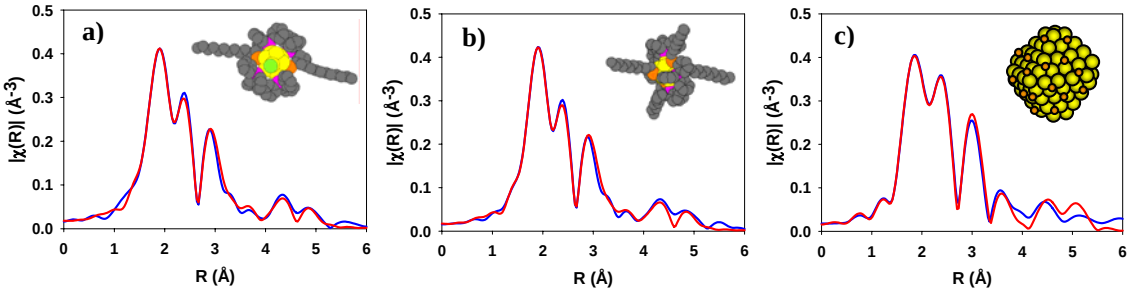

Figure 5. Fourier transformed EXAFS spectra for (a) $Au_{13}(PPh_3)_4(SC12)_2Cl_2$, (b) $Au_{13}(PPh_3)_4(SC12)_4$, and (c) fully-thiolated clusters. The insets show proposed structures for the Au_{13} clusters and a Au_{140} cluster that represents the average size of the fully-thiolated MPCs.

be shorter in the fcc structure (4.08 Å in bulk Au) than in the Ih structure (4.7 Å). Indeed, our quantitative multiple-scattering analysis confirms that the mixed-ligand clusters, $Au_{13}[PPh_3]_4[SC12]_2Cl_2$ and $Au_{13}[PPh_3]_4[SC12]_4$, are 13-atom icosahedra and the fully thiolated cluster has fcc structure and cuboctahedral shape.

Ligand-specific charge transfer studies in mixed-ligand Au nanoclusters by sulfur and phosphorus XANES

Charge transfer from gold to thiol and phosphine ligands was studied by S and P K-edge XANES, respectively, using beamline X15B at the NSLS. Transition states "1" and "3" of P and "2" of S absorption edges regions in references triphenylphosphine (PPh_3) (Fig. 6a) and dodecanethiol (Fig. 6b), respectively, are modified in their complexes with Au nanoparticles. Namely, for the S edge of $Au_{13}[PPh_3]_4[SC12]_2Cl_2$ (Fig. 6b), the XANES region has peaks "1" and "3". In agreement with previous studies of Au-DHLA complexes, we attribute the peak "2" in S XANES of pure thiols (Fig. 6b) to the S 1s electron transitions to the molecular orbitals S-C and S-H. Similar to the published study of Au-DHLA complexes, we interpret the peak "1" in S XANES of $Au_{13}[PPh_3]_4[SC12]_2Cl_2$ nanoparticles as due to the same transitions but shifted by 1.2 eV to lower energy due to the more reduced state of S on the gold cluster relative to that in the free thiol. In agreement with literature, we attribute peak "3" to the S 1s transitions to the unoccupied levels of Au atoms in the nanocluster.

Analysis of Fig. 6a reveals no significant difference in P peak positions and intensities for the two different mixed ligand clusters: $Au_{13}[PPh_3]_4[SC12]_2Cl_2$ and $Au_{13}[PPh_3]_4[SC12]_4$. However, the XANES in the two clusters differ from that of pure PPh3. If we attribute the features "3" in pure PPh3 and "2" in the nanoclusters to the P 1s transition to the P-C molecular orbitals, we observe this transition energy in the nanoclusters shifts ca. 1.0 eV to lower energy, consistent with charge transfer from gold to phosphorus. The peak "4", analogously to Fig. 6b), may be attributed to the P 1s transitions to atomic levels in Au.

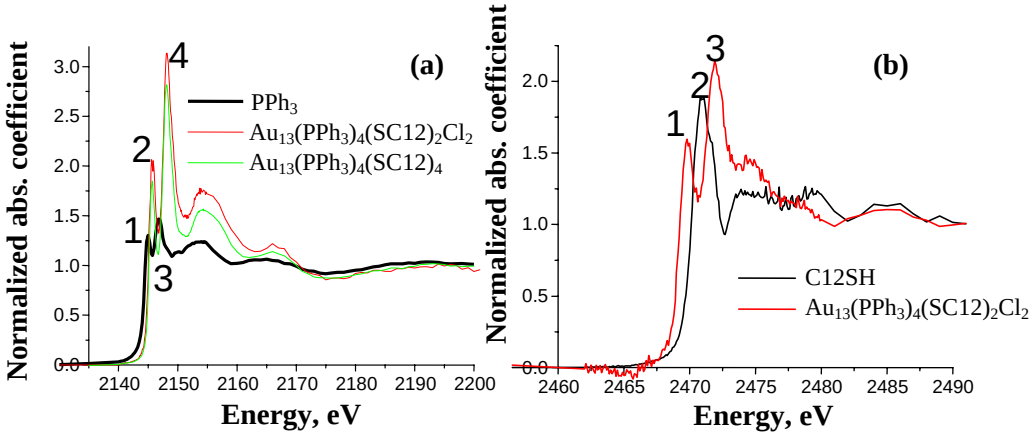

Figure 6. (a) P K-edge and (b) S K-edge of mixed ligand Au_{13} clusters and reference materials.

According to the literature, the oxidation state changes of P and S by 1 cause their XANES peaks shifts by ca. 2 eV and 1.7 eV, respectively. Therefore, our experimental results correspond to the Au-ligand charge transfer of an average of 0.5e per P and 0.7e per S atom, in agreement with the difference in their electronegativies (P: 2.1 and S: 2.5). Thus, the total charge transfer from the Au13 core to the PPh3-SC12 ligands in the $Au_{13}[PPh_3]_4[SC12]_4$ cluster is 4.8e. Our results allow, for the first time, to measure the charge transfer from Au to phosphine and thiol ligands and compare with theoretical predictions.

Size-controlled synthesis and characterization of dodecanethiol-stabilized gold nanoparticles

As discussed in the literature, Au/thiol ratio in alkanethiol-stabilized gold nanoparticles can be used as a parameter controlling the particle size. It is known that at small sizes, most characterization techniques, except HRTEM and EXAFS, do not possess sufficient spatial resolution to reliably determine the size of particles smaller than 10-20 Å. Furthermore, EXAFS is a unique method allowing the study the kinetics of nucleation and growth of nanoparticles *in situ*, under reaction conditions. We have developed reliable and robust methods of nanoparticle size determination by EXAFS analysis, using both the coordination number reduction (CNT) and surface tension (ST) methods. The CNT method uses a model dependent change in the particle coordination number as a function of its diameter. The ST method utilized the equation for the particle diameter $d = 4/3\, f_{rr} K/\alpha$, where f_{rr} and K are the surface stress and compressibility in the bulk, respectively, and $\alpha = \Delta R/R$ is the relative lattice contraction that can be measured by EXAFS.

As a control system, we synthesized and investigated a series of alkanethiol-stabilized nanoparticles by controlling one parameter, the Au/thiol ratio. The dodecanethiol gold nanoparticles were synthesized at Yeshiva University using two methods: (1) a 1-phase method developed by Yee *et al.* and (2) a 2-phase method developed by Brust *et al.* In the 1-phase method, dodecanethiol was added to a solution of $HAuCl_4 \cdot 3H_2O$ in THF followed by reduction with lithium triethylborohydride (THF solution). In the 2-phase method, an aqueous solution of $HAuCl_4 \cdot 3H_2O$ was mixed with a solution of tetraoctylammonium bromide (phase transfer reagent) in toluene. The two-phase mixture was vigorously stirred until all the tetrachloroaurate was transferred into the organic layer. After adding the dodecanethiol, the sodium borohydride reductant was used to reduce the Au^{3+}. The only parameter varied for the both methods was ξ, the Au/thiol molar ratio. The samples were prepared with ξ ranging from 1:6 to 6:1 and the nanoparticle sizes were examined by EXAFS (Figure 7).

As Fig. 7a demonstrates, the particle's Au-S and Au-Au coordination number changed monotonically with ξ. Quantitative analysis of the samples by both the CNT and the ST methods obtained that, for a given value of ξ, the particles prepared using the two-phase synthesis were smaller than those synthesized using the one-phase synthesis (Fig. 7b). In addition, the two methods resulted in very similar values for the particle sizes (Fig. 7c) that reach the minimum size of 14 Å, in excellent agreement with the predicted thermodynamic limit.

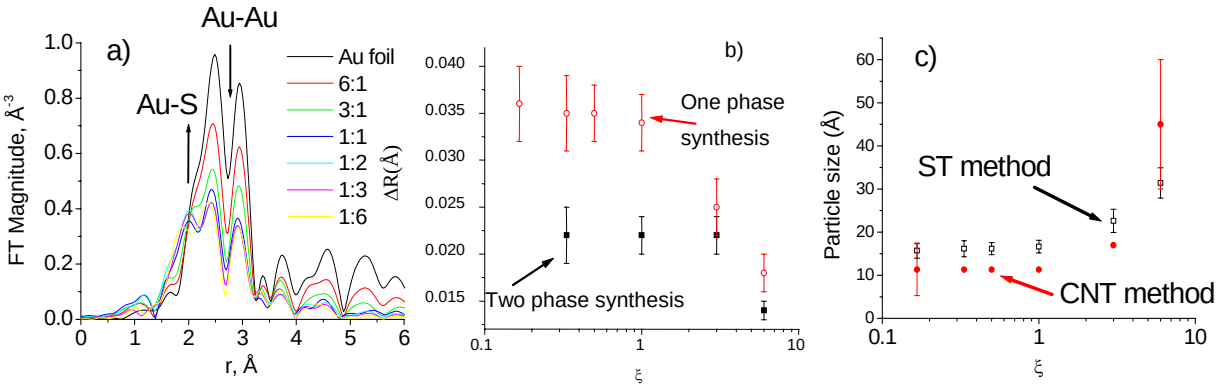

Figure 7. (a) Fourier transform of EXAFS spectra showing the effect of ξ on Au-S and Au-Au coordination. (b) Comparison of particle sizes obtained from one-phase and two-phase syntheses. (c) Particle sizes determined from the ST and CNT methods.

IV. Ab initio theoretical analysis of supported clusters

From careful application of density-functional methods and theoretical analysis, we can explain the observations that supported [$PtRu_5$] metal clusters have fcc(111) cuboctahedral geometry and bulk-like metal-metal bond distances, even for small nanoparticles for which the average coordination number is much smaller than that in the bulk, and, intriguingly, that Pt in the bimetallic clusters segregates to the top (111)-layer of the nanoparticle. For a Pt_6Ru_{31} 37-atom cluster (Fig. 8a), we compare quantitatively to the observed Pt-Pt, Pt-Ru, and Ru-Ru bond distributions versus distance; moreover, we find that the observed *bimodal* frequency distribution of the nearest-neighbor bond lengths in numerous metallic nanoparticles arise from the (111) hexagonal planes being highly anisotropic (Fig. 8b) with six sides successively long and short around the perimeter.

We have provided direct atomic-scale insight into the nature of self-organizing structures of supported [$PtRu_5$]-based clusters that show that the "anomalous" bond distances found in experiment are, in fact, *not* anomalous, but due to structural anisotropy in the nanoparticle mediated by the support, which could not be understood in terms of the isotropic structural model used to simplify the experimental analysis. The computational requirements of supported Pt_6Ru_{31} cluster are equivalent to simulating two interacting rhodopsin proteins, requiring a parallel supercomputer.

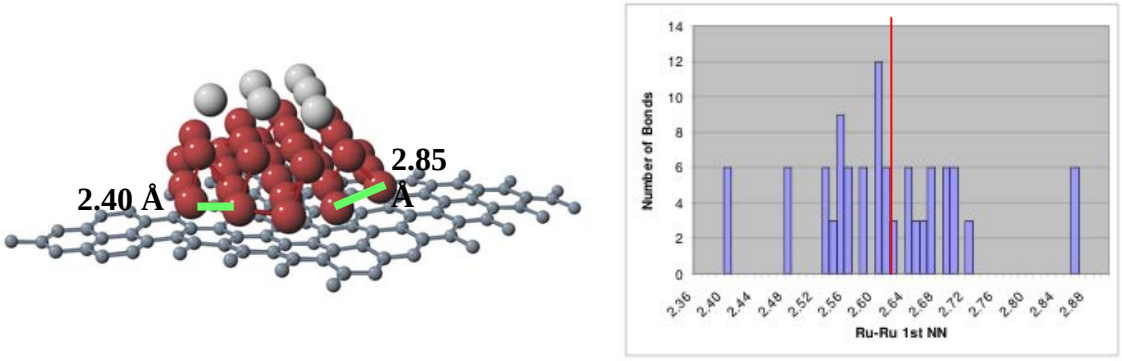

Figure 8. (a) Pt_6Ru_{31} cluster (Ru red, Pt silver) on a carbon support modeled by graphite. The bond distance (in Å) within the (111) hexagonal layer near the support has two distinct values on the perimeter. (b) Frequency of the Ru-Ru nearest-neighbor bond within the cluster, where the average value is 2.63 Å, the minimum value is 2.40 Å, and the maximum value is 2.88 Å. A similar distribution was observed in pure Pt clusters.

Publications

1) H. Xu, S. Gao, L. Menard, A. Frenkel, R. Nuzzo, J. C. Yang , "*Structural determination of supported Au13 nanoparticles* " (in preparation)

2) H. Xu, K. Guy, J. Shapley, J. C. Yang, "*Structural characterization of Pd-Cu bimetallic catalysts for nitrate reduction*" (in preparation)

3) Menard, L. D.; Nuzzo, R. G.; Harper, A. S.; Song, Y.; Wang, G.; Douglas, A. D.; Murray, R. W.; Frenkel, A. I.; Xu, H.; Gao, S.; Yang, J. C.; Twesten, R. D. "*Synthesis and Characterization of Sub-Nanometer Au_{13} Clusters*", **2005**, *in preparation.*

4) Menard, L. D.; Nuzzo, R. G.; Frenkel, A. I.; Xu, H.; Gao, S.; Yang, J. C.; Twesten, R. D.; Harper, A. S.; Song, Y.; Wang, G.; Douglas, A. D.; Murray, R. W. "*Illuminating the Structure of Monodisperse Au_{13} Clusters and Larger Au Nanoparticles with X-Ray Absorption Spectroscopy and Electron Microscopy*", **2005**, *in preparation.*

5) Wang, G.; Huang, T.; Murray, R. W.; Menard, L.; Nuzzo, R. G. "*Near-IR Luminescence of Monolayer-Protected Metal Clusters*", J. Am. Chem. Soc. **2005**, 127, 812.

6) A. I. Frenkel, S. Nemzer, I.Pister, L. Soussan, T. Harris, Y. Sun, M. H. Rafailovich "*Size-Controlled Synthesis and Characterization of Alkanethiol-Stabilized Gold Nanoparticles*", (in preparation)

7) Y. Sun, A. I. Frenkel, N. Chi, N.-L. Yang, M. Rafailovich, J.Sokolov, "*Comparison of Decanethiolate Gold Nanoparticles Synthesized by One-Phase and Two-Phase Routes*" (in preparation)

8) Y. Sun, R. Isseroff, C. Shonbrun, M. Forman, A. I. Frenkel, K. Shin, Ning Chi, N.-L. Yang, T. Koga, O. H. Seeck, M. Rafailovich, J. Sokolov, "*X-Ray Reflectivity and EXAFS Studies of Palladium Nanoparticles*" (in preparation)

9) W. Li, A. I. Frenkel, J. C. Woicik, C. Ni, S. Simat Shah "*Dopant location identification in Nd3+-doped TiO2 nanoparticles* ", Submitted to Physical Review B

10) A. V. Kolobov, P. Fons, J. Tominaga, A. I. Frenkel, A. Ankudinov, S. N. Yannopoulos, K. S. Andrikopoulos, T. Uruga, "*Why phase-change media are fast and stable: a new approach to an old problem"*, Submitted to Jpn. J. Appl. Phys.

11) Q. Qian, T. A. Tyson, M. Deleon, C. -C. Kao, J. Bai, A. I. Frenkel, "*Influence of strain on the local atomic, electronic and magnetic structure of manganite films",* Submitted to Physical Review B

12) A. I. Frenkel, Y. Feldman, V. Lyahovitskaya, E. Wachtel, I. Lubomirsky, *"Microscopic origin of polarity in quasi-amorphous BaTiO3",* Physical Review B **71**, 024116 (2005).

13) A. V. Kolobov, P. Fons, A. I. Frenkel, A. Ankudinov, J. Tominaga, T. Uruga , "*Understanding the phase-change mechanism of rewritable optical media"* Nature Materials, **3**, 703-708 (2004).

14) A. I. Frenkel, D. M. Pease, G. Giniewicz, E. A. Stern, D. L. Brewe, M. Daniel, J. Budnick ,"*Concentration-dependent short range order in relaxor ferroelectric (1-x) Pb(Sc,Ta)O3-xPbTiO3",* Physical Review B **70**, 014106 (2004)

15) X. Wang, J. C. Hanson, A. I. Frenkel, J.-J. Kim, J. A. Rodriguez, "*Time-resolved studies of the mechanism of reduction of copper oxides with carbon monoxide: complex behavior of lattice oxygen and the formation of suboxides,"* J. Phys. Chem. B **108**, 13667 (2004).

16) D. E. Schwarz, A. I. Frenkel, A. Vairavamurthy, R. G. Nuzzo, T. B. Rauchfuss, "*Electrosynthesis of ReS4. XAS analysis of ReS2, Re2S7, and ReS4",* Chem, Mater. **16** , 151-158 (2004).

17) L. Wang, S. Khare, D.D. Johnson, A.A. Rockett, A.I. Frenkel, N.H. Mack, and R.G. Nuzzo, "*Origin of bulk-like structure and bond distributions of Pt6Ru31 nanoclusters on carbon: comparison of theory and experiment*", submitted April 2005.

18) L. Wang and D.D. Johnson, "*Properties of non-metallic Ru and Ru-Pt nanoclusters: failure of DFT and its cause"*, (in preparation).

19) L. Wang and D.D. Johnson, "*Support-mediated changes in structure of Ru- and PtRu5- based nanoclusters*" (in preparation).

20) H. Xu, R. Twesten, L. Menard, A. Frenkel, R. Nuzzo, D. Johnson and J. Yang, "The Effect of Substrates/Ligands on Metal Nanocatalysts Investigated by Quantitative Z-contrast Imaging and High Resolution Electron Microscopy," MRS proceedings (submitted, 2005).

21) H. Xu, L. Menard, A. Frenkel, R. Nuzzo, D. Johnson and J. Yang, "3-Dimensional structural characterization approaches of carbon-supported Au13 nano-clusters," Microscopy & Microanalysis 10 (suppl 2), 454 (2004).

22) H. Xu, K. Guy, J. Shapley, A. Frenkel, D. Johnson, C. Werth and J. C. Yang, "Structural Changes of Bimetallic Pdx/Cu1-x Nanocatalysts Developed for Nitrate Reduction of Drinking Water" MRS proceedings (submitted, 2005)

23) H. Xu, L. Menard, A. Frenkel, R. Nuzzo, D. Johnson and J. C. Yang, "STEM-based mass spectroscopic study of supported metal nanoparticles", a presentation given at the symposium P-Electron Microscopy of Molecular and Atom-scale Mechanical Behavior, Chemistry and Structure, 2004 MRS Fall meeting,, 2004, and the abstract appeared in its Technical Program, pp 401-402

X-ray Facilities – Successful Collaborations

Simon R. Bare, UOP LLC, Des Plaines, IL 60016, USA

Heterogeneous catalysts have, by there very nature, been historically difficult to characterize at the atomic level. It is not surprising then that each time a new technique is developed that it is applied to study catalysts. Such was the case for extended x-ray absorption fine structure (EXAFS). It took only a couple of years after the momentous 1971 publication of Sayers, Stern and Lytle that papers began being published using EXAFS to probe the structure of catalysts. In the intervening 34 years, with the advent of dedicated synchrotron radiation facilities, EXAFS and other X-ray based methods have become somewhat routine tools for probing catalyst structure – but with may innovations along the way. In this talk I will provide some brief background on how synchrotron radiation-based X-ray based methods (with an emphasis on X-ray absorption spectroscopy) have been used to probe catalyst structure. However, the key question is where do we go from here? What is the path forward? How does the catalysis community best utilize these wonderful national resources? Do we need to change anything, or are there better modes of operation and collaboration that would aid the whole catalysis community? I will propose some ideas and concepts - which I hope will lay the framework for some dialogue and discussion of the path forward.

Session F:

Principles of Rational Design of Nanocatalysts

DE-FG02-03ER15466 **W. Nicholas Delgass**

CATALYSIS SCIENCE INITIATIVE: **Catalyst Design by Discovery Informatics**

Co-PIs: J. M. Caruthers, R. G. Cooks, H. W. Hillhouse, F. H. Ribeiro, K. T. Thomson, V. Venkatasubramanian
Postdocs: G. Medvedev, K. Phomphrai, G. Zhu
Students: A. Bhan, L. Bollman, A. Deskins, S.-H Hsu, Y. Joshi, B. Krishnamurthy, G. Krishnamurthy, K. M. Lee, T. Manz, A. Phatak, S. Rai, S. Sharma, A. Tabert
Collaborators: G. Blau, P. Patkar, School of Chemical Engineering; M Abu-Omar, Department of Chemistry; G. Bertoline, L. Arns, Purdue Envision Center for Data Perceptualization; S. Dunlop, D. McKay, M. McLennan, D. Talcott, W. Whitson, L. Zhao, Information Technology at Purdue (ITaP); S. Orcun, S. Nandi, T. Park , e-Enterprise Center, Purdue

Forney Hall of Chemical Engineering
480 Stadium Mall Drive
Purdue University
West Lafayette, IN 47907-2100
765 494 4059, FAX 765 494 0805
Delgass@ecn.purdue.edu

Goal:

Develop and apply an informatics-intensive, model-based approach that extracts knowledge from high throughput data for the design of catalysts, focusing on aromatics production from light alkanes, single-site aryloxide catalysts for polyolefin production, hydrogen production from the water gas shift reaction, and development of parallel mass spectrometry for high throughput analysis of catalysts.

DOE Interest:

Validation of this new design concept has the potential to change the catalysis research landscape by dramatically shortening hypothesis testing and new discovery cycles for virtually any catalyst system. A particular value of the approach is that knowledge archived in the model retains its value for new problems. Over time, overlapping knowledge bases from a variety of problems will accelerate discovery cycles even more. Though the emphasis here is on catalytic applications, the general approach has broad application to materials design and even process improvement. The informatics and data visualization tools developed in this effort also have broad application to knowledge extraction from virtually any large data set.

Research Plan:

The heart of our *Discovery Informatics* approach is the *forward model*, designed to quantitatively connect chemical, structural and higher level descriptors of a catalytic material to its kinetic performance for a specified reaction. The forward model, comprised of a catalytic chemistry component and a microkinetic model, then enables a guided stochastic *inverse search* of the descriptor space to identify trial catalyst materials predicted by the forward model to best satisfy the catalytic performance goals. Discrepancies between the predictions and high throughput evaluation of the trial catalysts can then be used to improve the model. Iteration of this cycle will continue to improve the model until it converges on a set of catalytic materials that meet the design goal. Our research objectives include building the computational, informatics, and experimental infrastructure to support this design algorithm and to further develop the approach through application to three diverse problems.

Aromatization of parafins over zeolites - In this study, we have focused on zeolites because their crystallinity qualifies them as “molecular” heterogeneous catalysts, i.e., ones for which we can compute properties because we have a good starting point for assigning atomic positions. The reaction, conversion

of propane to aromatics has a high level of complexity and thus is a demanding test of the reaction modeling suite.

Aryloxide catalysts for polyolefin production - This homogeneous catalyst system offers the significant advantage of a well-defined, single catalytic site. We are focusing on cationic alkyls of the group 4 metals with cyclopentadienyl and substituted aryloxide ligands. By varying ring substituents and the associated anion, we alter the rate and stereochemistry of the olefin polymerization catalyzed by these cationic compounds. Careful measurements of rates and particularly of reactivity ratios in copolymerizations are a long term objective that will provide a rich data set linking chemical descriptors to reaction performance. We have focused first on the propagation rate for 1-hexene polymerization. This work is closely supported by DFT calculations and is our primary testbed for development of informatics and visualization tools to aid model building and the discovery of appropriate descriptors and for full closure of the discovery informatics cycle.

Hydrogen generation via the water-gas shift (WGS) reaction - For fuel cell applications, the stability of the catalyst against upsets is paramount. To gain robustness, the active, but fragile, Cu/ZnO catalyst must be replaced by appropriately promoted supported metal catalysts. This is a case where the reaction mechanism is relatively simple, but the combinatorial complexity of the catalyst is substantial with choices for support, metal, and multiple promoter oxides. We have started with mechanistic studies of the reaction over single supported metals to establish the Kinetic Model and with construction of a four reactor system that will speed the production of high quality data. That data, together with DFT calculations of the properties of proposed catalyst sites will drive the discovery infomatics process.

Infrastructure – There are two additional research thrusts that support this effort. The first is *parallel mass spectroscopy* for at least semi-quantitative speciation on the timescale of seconds to minutes rather than hours. A four channel device has been designed, is being constructed, and will be used first for parallel characterization of catalysts using temperature programmed methods. The second concerns *informatics*, the hardware, software, and middleware involved in data management, data analysis, model building, data visualization and the extraction of knowledge from data.

Recent Progress:

Aromatization: Reaction kinetic studies of propane conversion to aromatics have been conducted on an HZSM-5 zeolite at a pressure of 1 atmosphere, temperatures in the range 520-550°C and different space times (5-30 gm-cat hr/mol). The rates of production of methane, ethane, ethene, propene, propane, butane, butene, benzene, toluene and xylene have been measured and a kinetic model has been postulated that considers surface species to be neutral alkoxides, reactions of these alkoxide species by carbenium-ion-like transition states and alkane activation by carbonium-ion-like transition states. The associated elementary steps, categorized within the following reaction types: adsorption, desorption, unimolecular protolytic cracking and dehydrogenation, β-scission, oligomerization, hydride transfer, alkylation, dealkylation and cyclization, were parsed into reaction families based on an equal reactivity assumption. 311 reaction steps were grouped in 37 reaction families and the number of unknown parameters was reduced to 25 by using adsorption parameters for n-alkanes and relative rates for β-scission and hydride transfer from the literature. This kinetic model gives a good fit to the reaction behavior over the HZSM-5 catalyst and thus represents the microkinetic model portion of the forward model for this system.

Gallium-modified HZSM-5 has been prepared by incipient wetness impregnation and characterized by XRD, IR and atomic absorption spectroscopy to confirm structure, Ga replacement of proton sites, and Ga content. To model the contribution of the Ga sites, we added 129 elementary reaction steps for the Ga function, including adsorption and desorption, dehydrogenation and hydrogenolysis. The 129 reactions were grouped in 9 reaction families and the number of unknown parameters to represent the Ga function was reduced to 18. These were optimized to fit data obtained at 510-540^{o}C for a catalyst with 10% Ga exchange of the proton sites. When optimizing the parameters of Ga sites, we fixed the parameters for the remaining Bronsted acid sites since we assumed the two sites to behave independently. The fit of the Ga catalyst data is not quite as good as for HZSM-5 alone, but is sufficient at allow predictions of optimal Ga levels for production of aromatics. The predictions are being

tested now. These models validate the ability of our Reaction Modeling Suite software to handle high levels of complexity and provide the first steps toward prediction of the performance of these complex systems.

This work has been strongly supported by DFT computations. Early computations of a lower activation barrier for toluene formation versus benzene are now incorporated into the HZSM-5 model. In recent work, we have extended our DFT analysis in H/GaZSM-5 to incorporate long range interactions of the extended lattice by conducting a two-level ONIOM embedded cluster technique. Through this method we retain DFT-level analyses near reactive sites while adding dispersion/repulsion and Coulombic interactions from the surrounding cage structure by empirical force fields. Applying this method to C_6 diene cyclization, we found that multiple pathways exist depending heavily on whether chemisorption or physisorption of the precursor is preferred, with the lowest activated pathway being 1,6-cyclization rather than 1,5-cyclization followed by ring expansion. Studies of propane activation (dehydrogenation) on GaHZSM-5 suggest that activation energies in line with experiment require Al pair sites, where GaH interacts with two substituted Al sites in the same lattice ring. We found that dehydrogenation activity depends strongly on Al-Al distances in the ring and compute an optimum Al-Al spacing. In an effort to develop lower levels of theory that will be amenable to incorporation into large searches, we have written code that implements the electronegativity equalization method (EEM) for any zeolite structure to yield values for partial charges and local and global softness that can be used as descriptors. Currently, we are tuning the constants for Si, Al, Ga, and O atoms based on high level DFT calculations.

Olefin Polymerizataion: A series of half-sandwich mixed Cp*/aryloxide single site polymerization catalyst precursors [Cp*M(OAr)(CH_3)$_2$] (Cp* = C_5Me_5; M = Ti or Zr; OAr = OC_6H_5, OC_6H_4X-4 (X = F, Cl, Br, I, Ph, OMe, Me, NO_2), $OC_6H_3Me_2$-2,6, $OC_6H_3Et_2$-2,6, $OC_6H_3{}^iPr_2$-2,6, $OC_6H_3Me_2$-2,6-Br-4, $OC_6H_3{}^iPr_2$-2,6-Br-4, and OC_6HPh_4-2,3,5,6) has been synthesized. The titanium dimethyl compounds react with $B(C_6F_5)_3$ and $Ph_3CB(C_6F_5)_4$ to give thermally unstable cationic complexes [Cp*Ti(OAr)CH_3][$H_3CB(C_6F_5)_3$] and [Cp*Ti(OAr)CH_3][$B(C_6F_5)_4$], respectively. The methyl cations generated are active for the polymerization of 1-hexene and styrene in toluene. At 0°C, first-order dependence on the concentration of 1-hexene is observed. The rate of polymerization highly depends on the nature of aryloxide ligands. The polymerization rates decrease with increasing steric hindrance of aryloxides $OC_6H_3R_2$-2,6 in the order R = H > Me > Et > ^{i}Pr. A slow initiation before the propagation was observed for R = Me, Et, and ^{i}Pr leading to higher molecular weight, M_n, and polydispersity, PDI. The introduction of a halogen substituent on the aryloxide ligand at the *para* position decreases the rate of polymerization in the order H > F > Cl > Br. The catalyst activity is significantly enhanced by changing the activator from $B(C_6F_5)_3$ to $Ph_3CB(C_6F_5)_4$. The catalyst activity of 30 g/mmol.h in the polymerization of 1-hexene using Cp*Ti($OC_6H_3Me_2$-2,6)Me_2 is enhanced to 6700 g/mmol.h when activated with $B(C_6F_5)_3$ and $Ph_3CB(C_6F_5)_4$, respectively.

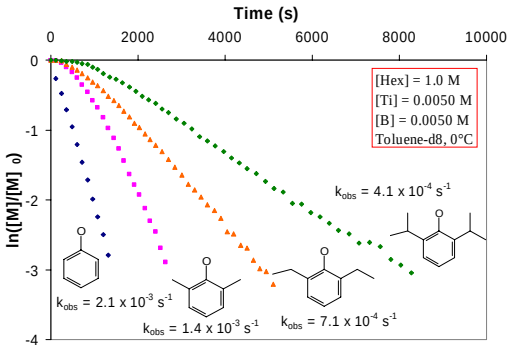

Extraction of the propagation rate constant from the data show above is straightforward, but we are also interested in the chain transfer and termination rate constants. Obtaining the full kinetic description for batch polymerization, requires new models. A population balance method generates thousands of coupled nonlinear differential equations which are solved numerically. From simulation results it has been observed that the molecular weight distribution (MWD) broadens as the polymerization reaction proceeds. Even at the early stage of the reaction there is considerable change in the shape of the MWD. Thus, by measuring the MWD as at a series of early times in the reaction, when the viscosity of the reaction medium is relatively low, the changes in the MWD shape offer the opportunity to obtain the rate constants governing chain length. We anticipate being able to obtain the full kinetic description in

experiments amenable to parallelization. Analysis of the polymer product will be obtained using a multi-detector gel permeation chromatogram (GPC) that combines a differential refractive index detector, a capillary viscometer, a light scattering photometer and a UV/Vis spetrophotometer. Besides the MWD, this combination of data gives the intrinsic viscosity distribution, the Mark-Houwink coefficients and the branching frequency across the polymer distribution.

Using DFT performed in Gaussian 03 using the OLYP/LanL2DZ and B3LYP/6-311++G**// OLYP/LanL2DZ levels of theory, we have computed structural descriptors for approximately 60 different olefin polymerization catalysts of the structure $[Cp'Ti(OAr)Me^{+}]$ $[MeB(C_6F_5)_3^{-}]$ used in this work. In addition, one Zr catalyst is being investigated in order to test descriptors and determine why both experimental and computational studies show the Ti aryloxide catalysts are superior to the Zr catalysts. We have also analyzed the complete reaction mechanism—including transition state geometries, activation energies, and thermochemical analyses—for all of the relevant kinetic steps of the olefin polymerization process for three catalysts. These steps include catalyst activation, chain initiation, chain propagation (frontside and backside), chain transfer (beta hydrogen transfer to monomer), chain termination (beta hydrogen transfer to monomer), and catalyst deactivation (two mechanisms).

In our current efforts to identify descriptors we are considering charge on the metal center, counterion binding energy, metal-counterion distance, cyclopentadienyl and aryloxide ligand cone angles (as measures of ligand steric effects), and metal-carbon distance in the growing polymer chain. We are beginning the construction of the full forward model to correlate these potential descriptors to measured performance.

The Water Gas Shift Reaction: We are currently perfecting the automated operation of our new four-reactor system. Two reactors are now functional in automatic mode. In the kinetic studies, we are measuring WGS rates on various pure metals and fitting the data to various mechanisms to obtain rate constants for all steps. Data as a function of temperature and concentrations of CO, H_2O, CO and CO_2 for supported Cu, Ni, Pd and Pt can all be fit by a single, eight step redox mechanism. At 320°C, the WGS rates order as Cu>>Pt>Pd>Ni. The methanation rate, however, increases in the opposite order. We are seeking to improve the WGS rate and suppress the methanation rate by addition of promoters. Adding calcia to supported Pd, for example, decreases the rate of methanation by two orders of magnitude while enhancing the WGS rate by one order of magnitude. The effect for ZnO is even higher with a rate increase of 30 times and a rate of methanation below our detection limit. We are using both modeling and computation to further understand these effects. We have modeled the doping of ceria with several cations, including Pt, Rh, Pd, Cu and Au using VASP for plane wave calculations. We found the order of stability to be Rh > Pt > Pd > Cu > Au. In addition, we show that cation doping makes formation of oxygen defects more energetically favorable, which could serve to increase reactivity since oxygen defect creation is involved during reaction.

Parallel Mass Spectrometry: The four-channel rectilinear ion trap (RIT) mass spectrometer for high-throughput characterization consists of multiplexed arrays of identical sample introduction capillaries, electron ionization/chemical ionization (EI/CI) sources, ion transfer optics, RIT mass analyzers, and detectors. However, the parallel channels are assembled in a single manifold and have common vacuum pumps and control electronics. The sample, and reagent gas in the case of chemical ionization, are introduced into the ionization volume. Ions enter the RIT axially through a hole in the endcap and, as the RF amplitude is increased linearly, are ejected radially through slits in the x electrodes to impinge upon a dynode/multiplier assembly for detection. Simultaneous data acquisition of the four channels of mass spectra will utilize a National Instruments PCI DAQ card and a custom program written with LabVIEW software. The figure on the left shows the first spectrum for 1,3 dichlorobenzene from one of the four channels. Ability to resolve both the Cl and C isotopes in the m/z

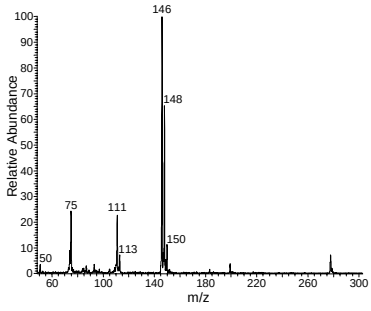

146 region and lower mass sensitivity will be further improved with an increase in RF frequency from 1.325 to ~ 2 MHz.

Informatics Infrastructure: A computer-aided environment that will enable an expert to discover knowledge from high throughput experimental and computational data is the foundation of the discovery informatics approach. The design requirements of the discovery environment have been specified, paying particular attention to allowing the catalyst expert to use language and modes of interaction that are natural rather than computerese. Progress during the past year towards developing a prototype discovery environment includes i) development of an electronic laboratory notebook that both directly archives data and dynamically populates the database that will be used for discovery, ii) enhancing high throughput computation by development of a job sequencer for the management of computational chemistry jobs, including job submission, retrieval, and archiving results and restart of prematurely terminated jobs, iii) expanding the chemistry compiler that allows the specification of chemical reactions and then automatically generates the appropriate differential equations to describe the kinetics to allow the rapid specification of alternative chemical mechanisms followed by appropriate optimization to experimental data and statistical analysis, thereby enabling the critical evaluation, iv) developing nonlinear statistical analysis tools using the maximum likelihood method and eigenanalysis to determine what parameters can be accurately determined from a given set of experimental data, and v) development of code for displaying steroscopic, 3D molecular structures with chemical labels as well as molecular orbitals and development of tools for 2D and 3D graphical representations of data where the points can be represented by symbols with different sizes, shapes, colors or spider graphs or by all or part of the chemical structure. A ring menu structure has been developed to enable the user to easily control the large number of graphics options. All the graphics are being developed using open GL, which will enable scalable graphics from a single monitor PC display to a large tiled wall.

The availability of experimental design/analysis tools which exploit the high speed and parallelizability of computers to sequentially design and analyze experiments to build phenomenologically driven mechanistic models for purposes of scale-up and/or materials design place new demands on handling complex non-linear models. We are developing a Bayesian approach to this problem. The model builder postulates one of more arbitrarily complex mathematical models characterizing his/her belief in the controlling physicochemical phenomena. Experiments are selected and data analyzed using statistical assumption free Markov Chain Monte Carlo (MCMC) methods to generate posterior probability distributions which discriminate these models and estimate model parameters. The results are then presented to the model builder in a graphical format which facilitates the evolution of new/different models which allow him/her to capture missing mechanisms. Additional experiments are then design and analyzed in this fashion until a suitable model is elucidated.. The challenge will be to use state-of-the-art software engineering and high speed computer resources to ensure that data analyses and presentation keep up with HTE.

Publications:

1. Fenwick, A. E., Phomphrai, K., Thorn, M. G., Vilardo, J. S., Trefune, C. A., Hanna, B., Fanwick, P. E., Rothwell, I. P., "Formation of Neutral and Cationic Methyl Derivatives of Titanium Containing Cyclopentadienyl and Aryloxide Ancillary Ligation," Organometallics, *23*, 2146-2156 (2004).

2. Katare, S., Caruthers, J. M., Delgass, W. N., Venkatasubramanian, V., "An Intelligent System for Reaction Kinetic Modeling and Catalyst Design," *Ind. Eng. Chem. Res. and Dev., 43*(14), 3484-3512 (2004).

3. S. Katare, V. Venkatasubramanian, J. M Caruthers and W. N. Delgass, "A Hybrid Genetic Algorithm for Efficient Parameter Estimation of Large Kinetic Models", *Comp and Chem Engg., 28*(12*)*, 2569-2581 (2004).

4. Maddipati, S. V.; Haq, J.; Fenwick, A. E.; Phomphrai, K.; Rothwell, I. P.; Delgass, W. N.; Caruthers, J. M. "Transition from living to chain growth olefin polymerization by a single-site homogeneous group 4 catalyst in a batch reactor." Polymer Preprints (American Chemical Society, Division of Polymer Chemistry) *45(2)*, 541-542 (2004).

5. T.A. Manz, A.E. Fenwick, K. Phomphrai, I.P. Rothwell, K.T. Thomson, "The nature of aryloxide and arylsulfide ligand bonding in dimethyltitanium complexes containing cyclopentadienyl ligation," Dalton Trans., 2005, 668-674.

6. Yogesh Joshi and Kendall T. Thomson, "Embedded Cluster (QM/MM) Investigation of C6 Diene Cyclization in H-ZSM-5," *J. Catal.* 230, 440-463 (2005).

7. Yogesh Joshi and Kendall T. Thomson, Invited Paper: "The Roles of Gallium Hydride and Brønsted Acidity in Light Alkane Dehydrogenation Mechanisms using Ga Exchanged HZSM-5 Catalysts: A DFT Pathway Analysis," *Catalysis Today*, accepted (2005).

8. Bhan, Aditya, Shuo-Huan Hsu, Gary Blau, James M. Caruthers, Venkat Venkatasubramanian, and W. Nicholas Delgass, "Microkinetic Modeling of Propane Aromatization over HZSM-5," *J Catal*, submitted.

DE-FG03-95ER14511 **D. Wayne Goodman**

Toward an Understanding of Catalysis by Supported Metal Nanoclusters

Postdoc: M. S. Chen, Y. F. Han, S. S. Lee, W. T. Wallace

Students: P. Boopalachandran, Y. Cai, K. Gath, D. Kumar, K. Luo, T. Wei, Z. Yan, F. Yang, C. W. Yi

Collaborators: J. Ekerdt, P. Sautet, J. Fackler, R. Crooks

Contact: D. W. Goodman, Dept. of Chem., Texas A&M Univ. College Station, TX 77843;

phone: (979) 845-0214; Email: goodman@mail.chem.tamu.edu

web page: www.chem.tamu.edu/faculty/faculty_detail.php?ID=39

Goal

Develop an atomic-level understanding of catalysis by supported metal nanoclusters.

Recent Progress

Determination of the structure of catalytically active gold on titania: We have successfully determined the active phase of supported gold clusters for CO catalytic oxidation to be a bilayer structure by creating well-ordered gold monolayers [(1x1)] and bilayers [(1x3)] that completely wet (cover) a titanium oxide support grown on a Mo(112) surface (see Figure 1). HREELS and CO adsorption confirm that the Au atoms are bonded to Ti atoms. The wetting of Au on the titanium oxide film was also confirmed by STM, XPS, TPD and LEIS studies. The Au bilayer structure is significantly more active (by more than an order of magnitude) for CO oxidation than the monolayer, and is approximately 45 times more active than the most active high-surface-area Au/TiO_2 catalyst. The specific rates measured for the Au-(1x3) bilayer structure agree closely with the rates reported previously for Au clusters supported on TiO_2(110) where an activity maximum was observed for Au structures two atomic layers in thickness (*M. Valden, X. Lai, D. W. Goodman, Science 281, 1647 (1998).*). The high catalytic activity observed for Au bilayer structures clearly demonstrates that particle thickness, rather than particle size or support effects, is the key parameter in catalysis by Au.

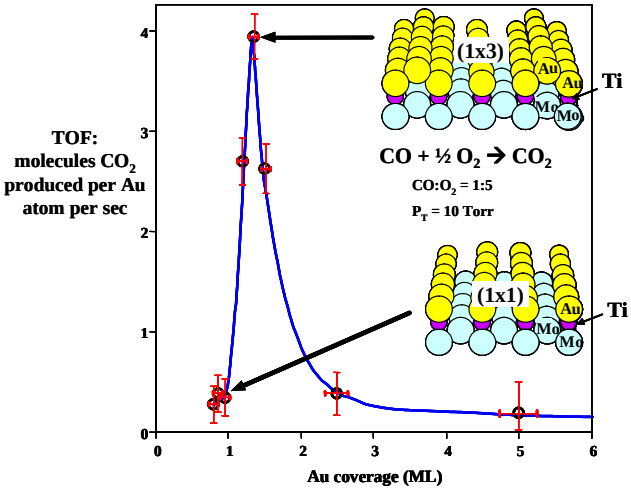

Figure 1. Mono- & bilayer Au on TiO_x

Synthesis of a Sinter Resistant Mixed Oxide Support for Au Nano-Clusters: In order to make highly

active Au catalysts more stable, mixed oxide supports have been developed by substituting Ti atoms in a silica thin film network. Depending on the amount of Ti deposited, the titania-silica surface consists of either atomically implanted Ti atoms or TiOx islands. After depositing Au onto these titania-silica surfaces (under both low and high Ti coverages), it is found that the Ti defects and TiO_x islands act as nucleation sites for Au cluster formation, leading to a marked increase in the cluster density compared to the Ti-free SiO_2 surface. Furthermore, the Au clusters stabilized by the TiO_x islands (Figure 2) do not sinter when exposed to reaction temperatures and pressures.

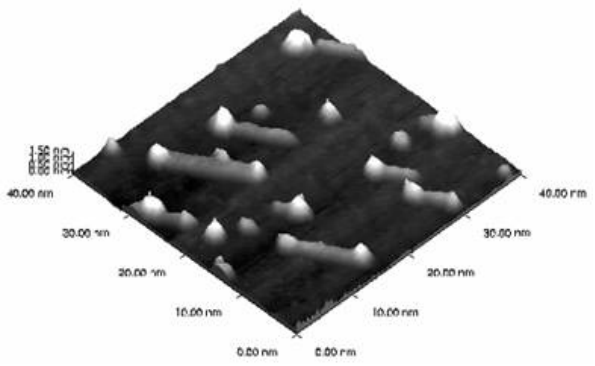

Figure 2. Au clusters on TiO_x islands on SiO_2

Pd-Au bimetal from planar alloy to nano-clusters: The surface composition and properties of Au-Pd bimetals were monitored on ultra-thin Au-Pd films (~ 10 ML) co-deposited onto a refractory substrate. Our results have demonstrated that these model systems can be successfully used to investigate the corresponding bulk alloys. The formation of a surface Pd monomer, Au_6Pd, has been identified on planar Pd-Au and on supported Pd-Au nanoparticles by IRAS of adsorbed CO. This Pd monomer has been identified as an active site for CO oxidation, whereas non-contiguous pairs of Pd monomers are proposed as the active sites for VA synthesis from surface acetate and ethylene species. Au plays an important role in vinyl acetate synthesis on Pd-Au catalysts by enhancing the activity, selectivity and stability.

DOE interest

Supported Au nanoclusters (2~3 nm) exhibit extremely high activities for a number of reactions. In particular, its high activity for the selective oxidation of CO in the presence of hydrogen at room temperature is an important application of Au catalysts in view of the current need for CO-free hydrogen for fuel cells. However, a major obstacle to the commercial utilization of Au catalysts is the rapid sintering of the nanoclusters under reaction condition. Our recent discovery of the active structure of the supported Au catalysts, together with our new strategies for synthesizing singer-resistant supports, promise to accelerate the design of commercial gold nano-structured catalysts for a variety of selective oxidation reactions.

Future plans

We will continue to develop quantitative models for the sintering kinetics of metal nanoclusters. These models will be tested and refined using *in situ* scanning tunneling microscopic measurements with the

ultimate goal of developing sinter resistant supports for nanostructured catalysts. Our efforts will also continue with respect to the synthesis and characterization of well-defined mixed-metal nanoclusters using our newly developed STM shadowing methodology. Our efforts to design supports for nanostructured catalysts that exhibit sinter-resistant properties at realistic reaction conditions will be extended. Finally, the identification of the key reaction intermediates in vinyl acetate synthesis will be addressed *in situ* with PM-IRAS and NVS. In addition to these experimental efforts, a concerted theoretical study in collaboration with Dr. Manos Mavrikakis of the University of Wisconsin will be undertaken with state-of-the-art quantum calculations to understand the special properties of nanosized Pd-Au metal clusters. An understanding regarding the structure of the active centers and the key factors leading to the combustion product (carbon dioxide) will be invaluable in the design of optimum catalysts for this important technical reaction.

Publications 2003-2005

1. "CO Adsorption on Au{110}-(1x2): an Infrared Reflection Absorption Spectroscopy Investigation", D. C. Meier, V. Bukhtiyarov and D. W. Goodman, J. Phys. Chem. B, 107, 12668-12671 (2003).
2. "Non-Oxidative Activation of Methane via its Decomposition", T. V. Choudhary and D. W. Goodman, Catalysis Reviews: Science and Engineering, 45, 151-203 (2003).
3. "Production of COx-free Hydrogen for Fuel Cells via Step-wise Hydrocarbon Reforming and Catalytic Dehydrogenation of Ammonia", T. V. Choudhary, C. Sivadinaryana and D. W. Goodman, Chem. Eng. J., 93, 69-80 (2003).
4. "Size-Dependent Electronic, Structural, and Catalytic Properties of Metal Clusters Supported on Ultra-Thin Oxide Films", A. K. Santra and D. W. Goodman, Catalysis and Electrocatalysis at Nanoparticle Surfaces, Eds. A. Wieckowski, E. R. Savinova, C. G. Vayenas, Marcel Dekker, Inc., NY,. 281-309 (2003).
5. "A combined in situ infrared and kinetic stydy of the catalytic CO + NO reaction on Pd(111) at pressures up to 240 mbar", C. Hess, E. Ozonsoy, D. W. Goodman, J. Phys. Chem. B, 107, 2759 - 2764 (2003).
6. "Catalysis by Supported Gold Nanoclusters", D. W. Goodman, Encyclopedia of Nanoscience and Nanotechnology, Eds. J. A. Schwarz, C. I. Conlescu, K. Putyera, Marcel Dekker, Inc., NY,. 611 - 620 (2004).
7. "Model Catalysts: From Imagining to Imaging a Working Surface", D. W. Goodman, J. Catal., 216, 213-222 (2003).
8. "Surface Characterization Using Metastable Impact Electron Spectroscopy of Adsorbed Xenon", Y. D. Kim, J. Stultz, T. Wei and D. W. Goodman, J. Phys. Chem. B, 107, 592-596 (2003).
9. "The Thermal Stability of Pd Supported on Single Crystalline SiO_2 Thin Films", B. K. Min, A. K. Santra and D. W. Goodman, J. Vac. Sci. Technol. B, 21, 2319-2323 (2003).
10. "Understanding Silica-Supported Noble Metal Catalysis", B. K. Min, A. K. Santra and D. W. Goodman, Catal. Today, 85, 113-124 (2003).
11. "Identification of Defect Sites on Oxide Surfaces by Metastable Impact Electron Spectroscopy", S. Wendt, Y. D. Kim and D. W. Goodman, Progress in Surf. Sci., 74, 141-159 (2003).
12. "The Influence of Metal Cluster Size on Adsorption Energies: CO Adsorbed on Au Clusters Supported on TiO_2", D. C. Meier and D. W. Goodman, J. Am. Chem. Soc., 126, 1892-1899 (2004).
13. "CO Dissociation at Elevated Pressures on Supported Pd Nano-clusters", E. Ozensoy, B. K. Min and D. W. Goodman, J. Phys. Chem. B, 108, 4351-4357 (2004).
14. "The Growth of Ag-Au Bimetallic Nanoparticles on TiO_2(110) ", A. K. Santra, F. Yang and D. W.

Goodman, Surf. Sci., 548, 324-332 (2004).
15. "The Nature of the Surface Species Formed on Au/TiO_2 during the Reaction of H_2 and O_2: An Inelastic Neutron Scattering Study", C. Sivadinarayana, T. V. Choudhary, L. L. Daemen, J. Eckert and D. W. Goodman, J. Am. Chem. Soc., 126, 38-39 (2004).
16. "A Vibrational Spectroscopic Study of the CO + NO Reaction: From Pd Single Crystals at Ultrahigh Vacuum to Pd Clusters Supported on SiO_2 Thin Films at Elevated Pressures", Emrah Ozensoy, Christian Hess, Ashok K. Santra, Byoung Koun Min, D. Wayne Goodman, Proc. of ACS Symposium Series: “Nanotechnology and the Environment”, 225, U965 (2003).
17. "The Formation of PdC_x Over Pd-based Catalysts in Vapor-phase Vinyl Acetate Synthesis: Does a Pd-Au Alloy Catalyst Resist Carbide Formation? ", Y.-F. Han, D. Kumar, C. Sivadinarayana, and D. W. Goodman, Catal. Lett., 94, 131-134 (2004).
18. "The Structure of Thin SiO_2 Films Grown on Mo(112)", M. S. Chen, A. K. Santra and D. W. Goodman, Phys. Rev. B, 69, 155404-1~7 (2004).
19. "Understanding the Catalytic Conversion of Automobile Exhaust Emissions Using Model Catalysts: CO + NO Reaction on Pd(111)", E. Ozensoy, C. Hess and D. W. Goodman, Top. Catal., 6, 3765-3778 (2004).
20. "Kinetics of Ethylene Combustion in the Synthesis of Vinyl Acetate over a Pd/SiO_2 Catalyst", Y.-F. Han, D. Kumar, C. Sivadinarayana and D. W. Goodman, J. Catal., 224, 60-68 (2004).
21. "Synthesis of a Sinter Resistant, Mixed-Oxide Support for Au Nano-Clusters", B. K. Min, W. T. Wallace and D. W. Goodman, J. Phys. Chem. B., 108, 14609-14615 (2004).
22. "Vibrational Spectroscopic Studies on CO Adsorption, NO Adsorption and CO+NO Reaction on Pd Model Catalysts", E. Ozensoy and D. W. Goodman, Phys. Chem. Chem. Phys., 6, 3765-3778 (2004).
23. "The Interaction of Water with Silica Thin Films Grown on Mo(112)", S. Wendt, M. Frerichs, T. Wei, M. S. Chen and D. W. Goodman, Surf. Sci., 565, 107-120 (2004).
24. "The adsorption of Benzene on a Mo(112)-c(2x2)-[SiO_4] Surface", M. S. Chen, A. K. Santra and D. W. Goodman, J. Phys. Chem. B, 108 (2004) 17940-17945.
25. "The Structure of Catalytically Active Gold on Titania", M. S. Chen and D. W. Goodman, Science 306, 252 - 255 (2004).
26. "The Role of Defects in the Nucleation and Growth of Au Nano-Clusters on SiO_2 Thin Films", B. K. Min, W. T. Wallace, A. K. Santra and D. W. Goodman, J. Phys. Chem. B, 108, 16339-16343 (2004).
27. "The Stabilization of Supported Gold Clusters by Surface Defects ", W. T. Wallace, B. K. Min and D. W. Goodman, Proceeding of The Third San Luis Symposium on Surfaces, Interfaces and Catalysis, 228, 3-10 (2005).
28. "An Investigation of the TiO_x-SiO_2/Mo(112) Interface", M.-S. Chen and D. W. Goodman, Surf. Sci., 574, 259-268 (2005).
29. "CO - NO and CO - O_2 Interactions on Cu(100) between 25 and 200 K: Studied with Infrared Reflection Absorption Spectroscopy", C. M. Kim, C.-W. Yi and D. W. Goodman, J. Phys. Chem. B, 109, 1891-1895 (2005).
30. "The Growth of Silver on an Ordered Alumina Surface", K. Luo, C.-W. Yi, K. A. Davis, K. K. Gath and D. W. Goodman, J. Phys. Chem. B, in press.
31. "Titania-Supported PdAu Bimetallic Nanoparticles Prepared from Dendrimer-Encapsulated Nanoparticle Precursors", R. W. J. Scott, C. Sivadinarayana, O. M. Wilson, Z. Yan, D. W. Goodman, R. M. Crooks, J. Am. Chem. Soc., 127, 1380-1381 (2005).
32. "Particle Size Effects in Vinyl Acetate Synthesis over Pd/SiO_2", Y.-F. Han, D. Kumar and D. W. Goodman, J. Catal., 230, 353-358 (2005).
33. "Catalytically Active Au on Titania: Yet Another Example of a Strong Metal Support Interaction (SMSI)?", D. W. Goodman, Catal. Lett., 99, 1-4 (2005).
34. "The Role of F-centers in Catalysis by Au Supported on MgO", Z. Yan, S. Chinta, A. A. Mohamed, J. P. Fackler, Jr., and D. W. Goodman, J. Am. Chem. Soc., 127, 1604-1605 (2005).
35. "Catalytically Active Gold: The Role of Cluster Morphology", T. V. Choudhary and D. W. Goodman,

Appl. Catal. A-Special Issue., in press.
36. "Electronic and Vibrational Properties of Ultrathin SiO_2 Films Grown on Mo(112)", S. Wendt, E. Ozensoy, T. Wei, M. Frerichsr, Y. Cai, M. S. Chen and D. W. Goodman, Phys. Rev. B, in press.
37. "Synthesis of Well-Ordered Ultra-Thin Titanium Oxide Films on Mo(112)", M. S. Chen, W. T. Wallace, D. Kumar, Y. Zhen, K. K. Gath, Y. Cai, Y. Kuroda and D. W. Goodman, Surf. Sci., in press.
38. "MIES and UPS(HeI) studies on reduced TiO_2(110))", S. Krischok, J. Günster, D. W. Goodman, O. Höfft and V. Kempter, Surf. and Interface Anal., 37, 77-82 (2005).
39. "Formation of a High Coverage (3x3) NO Phase on Pd(111) at Elevated Pressures: Interplay Between Kinetic and Thermodynamic Accessibility", E. Ozensoy, C. Hess, D. Loffreda, P. Sautet and D. W. Goodman, J. Phys. Chem. B, in press.
40. "A Kinetic Study of Vinyl Acetate Synthesis Over Pd-Based Catalysts-Kinetics of VA synthesis Over Pd-Au/SiO_2 and Pd/SiO_2 Catalysts", Y.-F. Han, J.-H. Wang, D. Kumar, Z. Yan and D. W. Goodman, J. Catal., in press.
41. "Methane Decomposition: Production of Hydrogen and Carbon Filaments", T. V. Choudhary and D. W. Goodman, Catalysis, RSC, in press.

DE-FG02-03ER15468 **Mark A. Barteau (U. of Delaware)**
DE-FG02-03ER15471 **Richard M. Crooks (TAMU)**
DE-FG02-03ER15469 **Manos Mavrikakis (U. of Wisconsin)**

CATALYSIS SCIENCE INITIATIVE: **From First Principles Design to Realization of Bimetallic Catalysts for Enhanced Selectivity**

Additional PIs: Douglas J. Buttrey, Jingguang G. Chen, Jochen A. Lauterbach, Raul F. Lobo, Dionisios G. Vlachos (Delaware); James A. Dumesic (Wisconsin)
Post-docs: Robert W. J. Scott (TAMU, through 2004)
Students: Adrienne Lukaski, Orest Skoplyak, Amit Goda, Jeff Ludwig, Wei Huang, Ashish Mhadeshwar, Soumitra Deshmukh, Seth Washburn, Joe Dellamorte, William Pyrz (Delaware); Orla Wilson, Heechang Ye (TAMU); George Huber, Jeff Greeley (PhD 2004), Shampa Kandoi, Ed Kunkes (Wisconsin).

Department of Chemical Engineering
University of Delaware
Newark, DE 19716
barteau@che.udel.edu

Department of Chemistry
Texas A&M University
College Station, TX 77842
crooks@tamu.edu

Department of Chemical & Biological Engineering
University of Wisconsin
Madison WI 53706
manos@engr.wisc.edu

Goals:

The goal of this project is to demonstrate a new paradigm for design for catalyst selectivity. Our approach is to enhance selectivity by design via the integration of four research components: Theory and Modeling; Surface Science; Materials Synthesis, Characterization and Scale-up; and Catalyst and Reactor Dynamics and Optimization. This integrative approach is being applied to three important catalytic reactions: selective hydrogenation, selective olefin oxidation and selective reforming of carbohydrates to produce alkane, as well as other chemistries where bimetallic catalysts may be advantageous. We focus on bimetallic catalysts as our principal design targets.

DOE Interest:

"Catalysis by design" has been a dream for decades. To specify the composition and structure of matter to effect a desired catalytic transformation with desired and predicted rate and selectivity remains a monumental challenge, especially in heterogeneous catalysis. Our research thrusts have been chosen not only for their practical and scientific relevance, e.g. for more efficient and sustainable chemicals and fuels production, but also because they provide a foundation for developing and exploring broadly applicable principles and strategies for catalyst design.

Articles highlighting research from this grant:

Chemical & Engineering News, "**Catalysis by the Numbers: Advanced computational methods are revealing mechanistic details and guiding catalyst design**" November 29, 2004, Volume 82, Number 48 pp. 25-28.
Chemical & Engineering News, "**Cheaper Auto Exhaust Catalysts: High-throughput screening reveals promising low-cost Co-Ba catalyst"** January 31, 2005, Volume 83, Number 5 p. 9.

Recent Progress:

Fundamental understanding of bimetallic surface reactivity

During the past year the Mavrikakis group has reported a first-principles-based approach for the identification of Near Surface Alloy (NSA) bimetallic catalysts stable in the presence of hydrogen. Importantly, some of these surfaces bind hydrogen as weakly as the noble metals (Cu, Au), and yet activate H_2 far more easily than the noble metals. The unique combination of weak binding of the dissociation products with the low bond-breaking activation energy barrier opens new possibilities

for the design of highly selective low temperature hydrogen transfer catalysts. The NSA catalyst screening and identification approach developed is quite general, and we are currently working towards identifying bimetallic catalysts that would be promising for a number of catalytic reactions, including water gas shift (WGS). The latter reaction is of central importance for the efficient Aqueous Phase Carbohydrate reforming towards H_2 and alkanes, recently developed by the Dumesic group. This theoretical work complements the ongoing surface science and DFT studies by the Chen and Barteau groups on surface reactions of bimetallics.

Chen and Barteau have shown a near linear correlation between hydrogen binding energy and the surface d-band center for a wide range of bimetallic surfaces. Recent calculations have extended this d-band center correlation to the binding energies of C_2 hydrocarbons and intermediates. Figure 1 shows the binding energy of ethylene vs. the surface d-band center on several bimetallic surfaces. As pointed out by Norskov and coworkers, the extent of interaction between adsorbates and surfaces varies for the 3d, 4d and the 5d metal surfaces, as the 5d orbitals are more extended than the 4d orbitals which are in turn more extended than the 3d orbitals. This effect is not so pronounced in case of simple atomic adsorbates like hydrogen, but must be taken into account when dealing with molecules like ethylene. The results in Figure 1 clearly show that, within each group (3d, 4d or 5d) there is a fairly linear relationship between ethylene binding energy and the position of the d-band center. Overall the trend in Figure 1 shows that the binding energies of ethylene on certain bimetallic surfaces are lower than on the corresponding parent metals, which is consistent with the trend for hydrogen on these surfaces. Furthermore, the DFT predictions on Pt/Ni, Pt/W and Pd/Mo surfaces have been verified experimentally using a combination of TPD and HREELS. Taken together with the results for hydrogen activation from the Mavrikakis group, these results provide a roadmap for the prediction of bimetallic combinations that will be particularly active hydrogenation and dehydrogenation catalysts. Current efforts are directed at understanding the kinetics of key intermediates in these reactions on bimetallic surfaces.

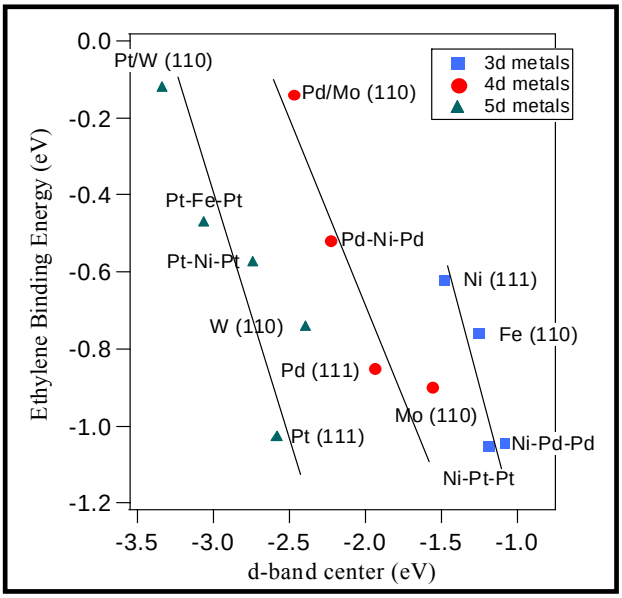

Vlachos' group has been developing a framework for predicting the dynamics of adsorption of reagents on bimetallic surfaces. As a first step we have developed a first-principles potential energy surface (PES) based on a corrugated LEPS potential. The PES was fed into a molecular dynamics (MD) trajectory simulation to compute the dynamics of adsorption of H_2 on Pt(111). Very good agreement with molecular beam experiments was found. Integration of the reactive force field ReaxFF with DFT has been initiated in order to extend these simulations to more complex systems including defects, adsorbates, and bimetallic catalysts.

Applications to new materials and new catalysts

Selective hydrogenation of acetylene in ethylene

The selective hydrogenation of acetylene in excess ethylene is a critical reaction in the polymerization of ethylene. Acetylene poisons the polymerization catalyst and needs to be selectively hydrogenated *without* the hydrogenation of any ethylene. Our attempts to solve this problem involves two parallel approaches: (1) selecting bimetallic catalysts that have different binding energies for acetylene and ethylene based on the computational studies described above and (2) supporting these bimetallic catalysts on zeolites to selectively enhance the adsorption of acetylene. We recently discovered that NiPd bimetallic catalysts, supported on Na^+ β-zeolite**,** show

promising selective hydrogenation activity to acetylene in the presence of excess ethylene. These results have been confirmed both from batch reactor studies using Transmission IR and from flow reactor studies using GC. We are currently expanding our catalyst formulations to include other types of zeolite supports.

Synthesis, structure and catalytic properties of well-defined bimetallic nanoparticles via dendrimer templating

The Crooks' group has investigated electrocatalytic oxygen reduction using dendrimer-encapsulated Pt nanoparticles. Platinum dendrimer-encapsulated nanoparticles (DENs) were prepared within fourth-generation, hydroxyl-terminated, poly(amidoamine) dendrimers and immobilized on glassy carbon electrodes using an electrochemical immobilization strategy (Figure 2). X-ray photoelectron spectroscopy, electron microscopy, and electrochemical experiments confirm that the Pt DENs are about 1.4 nm in diameter and that they remain within the dendrimer following surface immobilization. The resulting Pt DEN films quite robust and are electrocatalytically active for the oxygen reduction reaction.

Figure 2

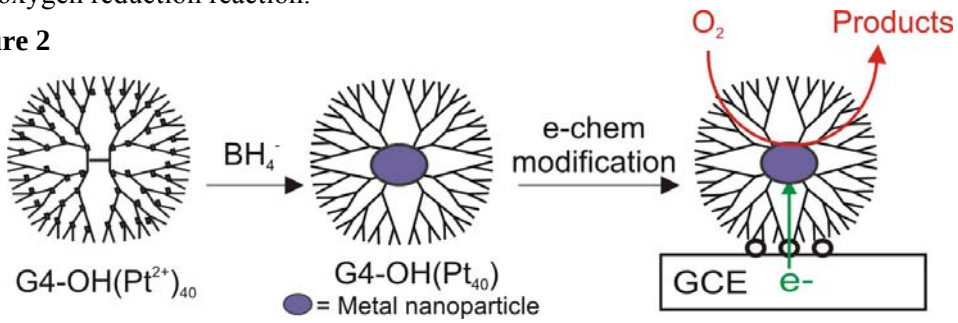

We have also studied the synthesis, characterization, and catalytic activity of titania-supported bimetallic PdAu particles prepared using dendrimer-encapsulated nanoparticle (DEN) precursors (Figure 3). Single-particle energy-dispersive spectroscopy indicated a homogeneous distribution of bimetallic nanoparticles having compositions closely related to the metal-ion ratios used to prepare the DEN precursors. The catalytic activity of the supported PdAu catalysts was compared to that of supported Pd-only and Au-only catalysts; the enhanced CO oxidation activity of the PdAu catalysts (Figure 4) is indicative of a synergetic bimetallic interaction.

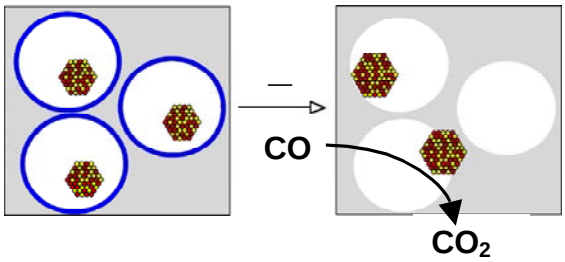

Figure 3. *Schematic representation of DEN-templating of a sol-gel precursor. The dendrimer serves as a template for both the titania matrix and the bimetallic nanoparticles.*

The dendrimer templating approach is an effective route to the synthesis of chemically and structurally well-defined bimetallic catalytic nanoparticles. We envision that these materials will provide excellent experimental models for developing the next generation of catalytic materials emerging from the theoretical and experimental efforts of the PIs.

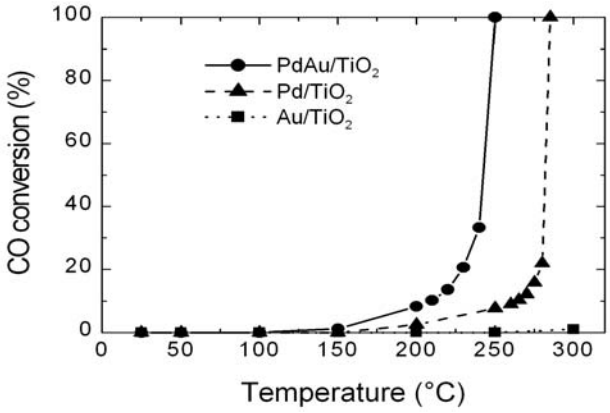

Figure 4. *Percentage CO oxidation as a function of temperature for PdAu, Pd-only, and Au-only catalysts supported on TiO_2. The catalysts were prepared using G4-$NH_2(Pd_{27.5}Au_{27.5})$, G4-$NH_2(Pd_{55})$, and G4-$NH_2(Au_{55})$ DENs, respectively. Catalytic reactions were carried out using a 2:1 ratio of O_2:CO and a gas hourly space velocity of 20,000 $cm^3.g^{-1}.h^{-1}$.*

Synthesis, characterization and catalytic performance of bimetallic nanoclusters produced by reverse micelle methods

The Lauterbach group has synthesized both Pt and Rh monometallic and Pt/Rh bimetallic nanoparticles with the following compositions: 3Pt/1Rh, 1Pt/1Rh and 1Pt/3Rh by weight fraction. All of the nanoparticles have been characterized using transmission electron microscopy and have diameters narrowly distributed around 4.5 nm. These Pt/Rh nanoparticles have been supported on alumina using wet impregnation to create supported nanoparticle catalysts The calcined catalysts were examined with TEM and it was determined that no significant particle sintering occurred during calcinations. Reaction data have been obtained for both CO oxidation and NO reduction with ethylene as a function of temperature. The results show that there may be beneficial size and alloying effects in the nanoparticle catalysts. We have also supported Pt/Rh nanoparticles on barium impregnated alumina (either 7.5Ba or 15Ba) support using wet impregnation to generate nano-NSR (NOx Storage and Reduction) catalysts. Preliminary NOx storage (saturation) studies and short-cycling studies show that the nano-NSR catalysts are active for NOx storage and reduction.

The addition of manganese, iron, and cobalt to NOx storage and reduction (NSR) catalysts containing 1% w/w platinum and 15% w/w barium (1Pt/15Ba) on γ-Al_2O_3 has been studied. Under fuel lean conditions, the addition of Mn or Fe slightly improved the NOx storage, while the addition of Co more than doubled the NOx storage. In addition, a noble metal free 5Co/15Ba catalyst was found to store NOx as efficiently as a 1Pt/15Ba NSR catalyst. This increase in efficiency is associated with the strong oxidizing effect of Co, providing nitric oxide oxidation sites and contact area for NO_2 spillover to the Ba NOx storage sites. By utilizing Co as an oxidizing metal instead of Pt, the storage capacity of NSR catalysts can be improved without the need for an expensive noble metal oxidizing catalyst. The addition of 5% w/w Co to 1%Pt/15%Ba w/w catalysts not only improves the NOx conversion at higher lean fractions but also extends the region of 80-90% NOx conversion to a much larger range of cycle times and lean fractions. These results suggests that Co containing catalysts shift the region of optimum operation to lower cycle times and higher lean fractions which can have a large impact in improving the fuel efficiency of automobile engines.

Catalysts for carbohydrate reforming

During the past year, the Dumesic group has reported a new catalytic process for conversion of biomass-derived carbohydrates to liquid alkanes ranging from n-C_7 to C_{15}, providing a new source of transportation fuel from renewable resources. Liquid alkanes ranging from n-C_7 to C_{15} were selectively produced from biomass-derived oxygenated hydrocarbons by first coupling these latter reactants by aldol-condensation reactions over solid base catalysts, followed by formation of alkanes by aqueous-phase dehydration/hydrogenation (APD/H) reactions over bi-functional catalysts containing acid and metal sites. These liquid alkanes are of the appropriate molecular weight to be used as transportation fuel components, and they contain 90% of the energy of the carbohydrate and H_2 feeds, making the formation of liquid alkanes an attractive option for the effective utilization of renewable biomass resources by existing transportation vehicles.

Very recent results for the production of liquid alkanes by aqueous-phase dehydration/hydrogenation (APD/H) of various biomass-derived feedstocks are shown in Figure 5. Furoin (prepared from furfural by Pinnacol condensation reaction), furfural-acetone (1:1) and furfural-acetone (2:1) (prepared by aldol condensation of furfural and acetone) were converted to alkanes in a APD/H reactor over a Pt/SiO_2-Al_2O_3 catalyst. The main products from furoin were n-C_9 and C_{10} alkanes (Figure 5A). The furfural-acetone (1:1) feed produced mainly n-C_7 and C_8 alkanes in the APD/H process (Figure 5B). Importantly, the furfural-acetone (2:1) feed produced primarily n-C_{11}-C_{13} alkanes from the APD/H reactor (Figure 5B). Crossed aldol-condensation of HMF with acetone was carried out with HMF:acetone molar ratios of 1:1 and 1:10 using mixed Mg-Al-oxide catalyst at room temperature. As shown in Figure 5C, the condensed HMF:acetone products produced mainly C_8 to C_{15} alkanes in the APD/H reactor, depending on the HMF:acetone ratio used in the aldol-condensation step. When the HMF:acetone ratio decreases, the alkane distribution shifts to lighter alkanes (Figure 5C). Another route to make large water-soluble organic compounds is to selectively hydrogenate the C=C bonds of HMF and furfural, producing 5-Hydroxymethyl-tetrahydrofurfural (HMTHFA) and tetrahydrofuran-2 carboxyaldehyde (THF2A), respectively. These species can form carbanion species and undergo self aldol-condensation reactions. The results in Figure 5D show that self aldol-condensation of tetrahydrofuran-3 carboxyaldehyde (THF3A,) and THF2A produced liquid hydrocarbons ranging from C_8-C_{10} from the APD/H reactor. THF2A was produced by dehydrogenation of tetrahydrofurfuryl alcohol in the gas phase over a Cu/SiO_2 catalyst. Bimetallic catalysts are currently being explored.

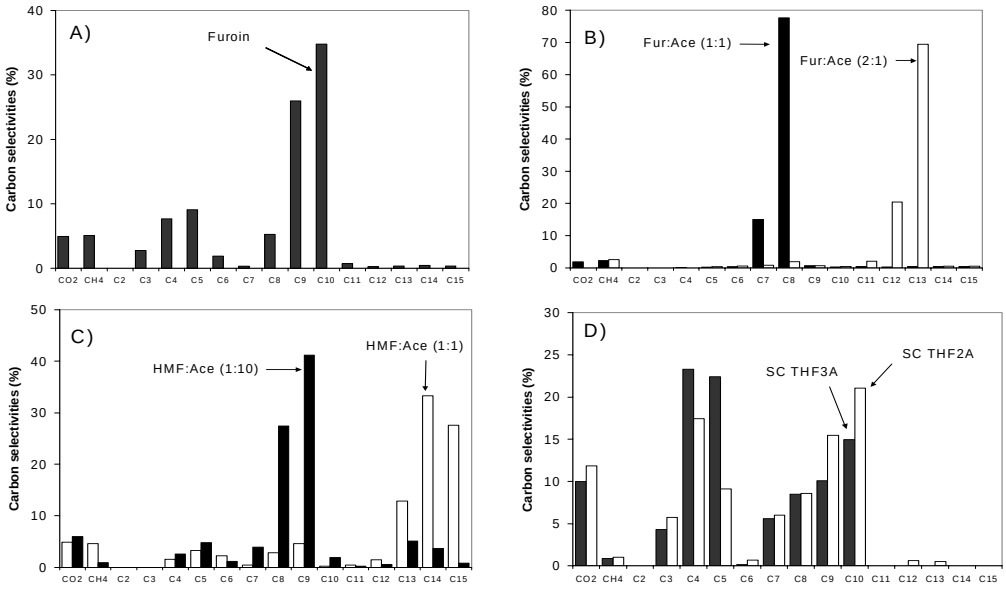

Figure 5. *Carbon selectivities from APD/H processing of various condensed feeds. Figure A: Furoin; Figure B: Fur:Ace (1:1)-1 - black; Fur:Ace (2:1) - white; Figure C: HMF:Ace (1:10) - black, HMF:Ace (1:1)-2 - white; Figure D: SC THF3A - black, SC THF2A - white.*

Future Plans:

A variety of new bimetallic combinations – Ni/Pd for hydrogenation and dehydrogenation; Cu/Ag for olefin epoxidation; Co/Pt for NOx storage and reduction – has begun to emerge from this research. We will continue to search out such synergistic combinations using fundamental surface science and computational tools, while developing synthetic methodologies that allow us to fabricate working catalysts based on these discoveries. We continue to explore the application of bimetallic catalysts to a host of relevant processes for more efficient and cleaner fuels and chemicals production and utilization.

Publications:

1. H. Ye; R. M. Crooks "Electrocatalytic O_2 Reduction at Glassy Carbon Electrodes Modified with Dendrimer-Encapsulated Pt Nanoparticles" *J. Am. Chem. Soc.*, March, **2005** (ASAP).
2. R. W. J. Scott; C. Sivadinarayana; O. M. Wilson; Z. Yan; D. W. Goodman; R. M. Crooks "Titania-Supported PdAu Bimetallic Catalysts Prepared from Dendrimer-Encapsulated Nanoparticle Precursors" *J. Am. Chem. Soc.* **2005**, *127*, 1380-1381.
3. O. M. Wilson; R. W. J. Scott; J. C. Garcia-Martinez; R. M. Crooks "Synthesis, Characterization, and Structure-Selective Extraction of 1-3 nm-Diameter AuAg Dendrimer-Encapsulated Bimetallic Nanoparticles" *J. Am. Chem. Soc.* **2005**, *127*, 1015-1024.
4. R. W. J. Scott; O. M. Wilson; R. M. Crooks "Synthesis, Characterization, and Applications of Dendrimer-Encapsulated Nanoparticles" *J. Phys. Chem. B* **2005**, *109*, 692-704. (Feature Article).
5. R. W. J. Scott; O. M. Wilson; R. M. Crooks "Titania-Supported Au and Pd Composites Synthesized from Dendrimer-Encapsulated Metal Nanoparticle Precursors" *Chem. Mater.* **2004**, *16*, 5682-5688.
6. R. W. J. Scott; O. M. Wilson; S.-K. Oh; E. A. Kenik; R. M. Crooks "Bimetallic Palladium-Gold Dendrimer-Encapsulated Catalysts" *J. Am. Chem. Soc.* **2004**, *126*, 15583-15591.
7. O. M. Wilson; R. W. J. Scott; J. C. Garcia-Martinez; R. M. Crooks "Separation of Dendrimer-Encapsulated Au and Ag Nanoparticles by Selective Extraction" *Chem. Mater.* **2004**, *16*, 4202-4204.
8. Mhadeshwar, A. B. and D. G. Vlachos, "Microkinetic modeling for water-promoted CO oxidation, water-gas shift, and preferential oxidation of CO on Pt" *J. Phys. Chem. B* **108**, 15246-15258 (2004).
9. R. Vijay, R. J. Hendershot, S. M. Rivera-Jiménez, W. B. Rogers, B. J. Feist, C. M. Snively and J. Lauterbach, "Noble metal free NOx storage catalysts using cobalt discovered via high-throughput experimentation" *Catalysis Communications* **2005**, *6*(2), 167.
10. M. B. Zellner, A. M. Goda, O. Skoplyak, M. A. Barteau and J. G. Chen, "Trends in the Adsorption and Decomposition of Hydrogen and Ethylene on Monolayer Metal Films: A Combined DFT and Experimental Study", Surf. Sci. **2005** (in press).
11. Kandoi S., Gokhale A. A., Grabow L., Dumesic J. A., Mavrikakis M., "Why Au and Cu are more selective than Pt for preferential oxidation of CO at low temperature", *Catalysis Letters* **2004**, *93*, 93.
12. Greeley J., Mavrikakis M., "Competitive Paths for Methanol Decomposition on Pt(111)" *J. Am. Chem. Soc.* **2004**, *126*, 3910.
13. Huber G. W., Cortright R. D., Dumesic J. A., "Renewable Alkanes by Aqueous Phase Reforming of Biomass-Derived Oxygenates" *Angewandte Chemie International Edition* **2004**, *43*, 1549.
14. Greeley J., Krekelberg W. P., Mavrikakis M., "Strained-Induced Formation of Subsurface Species in Transition Metals" *Angewandte Chemie International Edition* **2004**, *43*, 4296.
15. Greeley J., Mavrikakis M., "Alloy Catalysts Designed from First-Principles" *Nature Materials* **2004**, *3*, 810.
16. Gokhale A. A., Huber G. W., Dumesic J. A., Mavrikakis M., "Effect of Sn on the reactivity of Cu surfaces" *Journal of Physical Chemistry B* **2004**, *108*, 14062.
17. Gokhale A. A., Kandoi S., Greeley J., Mavrikakis M., Dumesic J. A., "Molecular-level descriptions of surface chemistry in kinetic models using density functional theory" *Chemical Engineering Science* **2004**, *59*, 4679.
18. Schumacher N., Boisen A., Dahl S., Gokhale A. A., Kandoi S., Grabow L., Dumesic J. A., Mavrikakis M., I. Chorkendorff, "Trends in low-temperature water-gas shift reactivity on transition metals" *Journal of Catalysis* **2005**, *229*, 265.
19. Greeley J., Mavrikakis M., "Surface and Subsurface Hydrogen: Adsorption Properties on Transition Metals and Near-Surface Alloys" *Journal of Physical Chemistry B* **2005**, *109*, 3460.

DE-FG02-04ER15501/DE-FG02-00ER15014 **Jingguang G. Chen**

Structure-Property Relationship in Metal Carbides and Bimetallic Alloys

Graduate Students: John Kitchin (graduated in May 2004), Michael Zellner, Luis Murillo, Carl Menning
Collaborators: M.A. Barteau (Univ. Delaware), J.K. Norskov (Technical Univ. Denmark)
Contact: J.G. Chen, Department of Chemical Engineering, University of Delaware, jgchen@udel.edu

Research Goals:

It is well known that the electronic, catalytic and electrocatalytic properties of transition metals can be modified by alloying with carbon or with another metal. The resulting metal carbide or bimetallic alloy often demonstrates properties that are distinctively different from those of the pure parent metal. The objective of the project is to use selected carbides and bimetallic alloys as model systems to unravel the relationship between the electronic/geometric structures and the chemical/catalytic properties for applications in heterogeneous catalysis and in fuel cells.

Research Approaches:

The current research project involves three parallel approaches: (1) Fundamental surface science investigations of the reaction mechanisms of several carefully-chosen probe reactions on carbide and bimetallic surfaces. (2) Correlation of chemical activities of these surfaces with their electronic properties using a combination of experimental measurements and DFT modeling. (3) Reactor or electrochemical evaluation of relevant carbide and bimetallic powders/thin films to bridge the "materials gap" and "pressure gap" between model surface science studies and heterogeneous catalysis/electrocatalysis.

Recent Progress:

A. Correlating Electronic and Catalytic Properties on Carbides and Bimetallic Surfaces

In the past year we have made significant progress in correlating the structure-property relationship by modifying transition metals either with carbon atoms to make carbides, or with metal adlayers to make monolayer bimetallic surfaces (see attached publication list). As shown in the Figure, we have performed DFT modeling to show that the d-band center is significantly modified by the formation of carbides and bimetallic alloys. The DFT results also revealed a near linear correlation between the d-band center and hydrogen binding energy over a wide range of carbide and bimetallic surfaces.

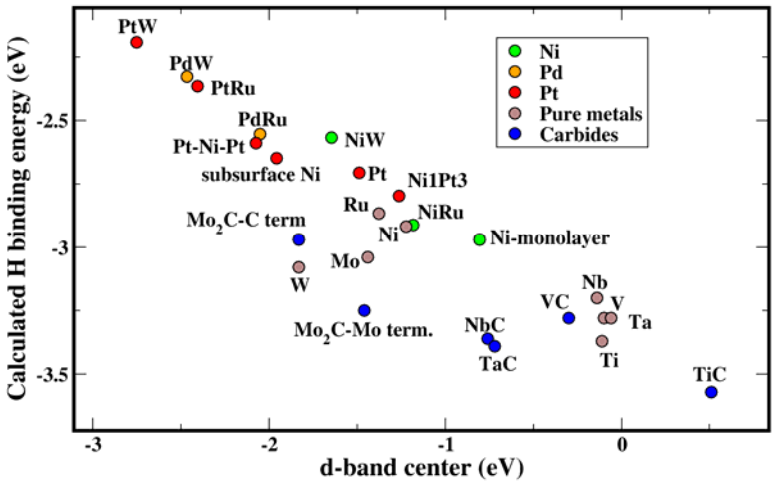

We have confirmed the DFT predictions on several carbide and bimetallic surfaces, including TiC/Ti(0001), Mo_2C/Mo(110), Pd/Mo(110) and Pt/W(110), using experimental techniques such as TPD and HREELS. The combined DFT modeling and experimental measurements clearly indicated that the d-band center can be used as a useful parameter to predict the chemical properties of carbide and bimetallic surfaces. We are currently performing experimental studies on selected carbide and bimetallic systems to determine whether the weakly-bonded hydrogen will lead to the selective hydrogenation pathways, such as the selective hydrogenation of the C=O bond in acrolein (CH_2=CH-CH=O).

B. Carbides and Bimetallic Alloys as Alternative Electrocatalysts for Fuel Cells

Another potential application of carbides and bimetallic alloys is in electrocatalysis for hydrogen and methanol fuel cells. For example, the current anode catalysts in hydrogen and methanol fuel cells are Pt and Pt/Ru, which are very expensive and are susceptible to poison due to strong chemisorption of CO. We are exploring the possibility of using metal carbides, such as Mo and W carbides, as potential alternative electrocatalysts to replace the Pt-group metals. We have performed surface science studies on single crystal carbide surfaces, as well as electrochemical (cyclic voltammetry) measurements of polycrystalline carbide films under fuel cell operating conditions. Our combined surface science and electrochemical results indicate that Mo and W carbides are active toward the electrooxidation of hydrogen and methanol. Equally important, our preliminary results reveal that Mo and W carbides are stable under electrochemical environment.

Future Plans:

In the next year we will use several probe reactions to further investigate the potential applications of carbides and bimetallic alloys in heterogeneous catalysis and in electrocatalysis: (1) We will investigate the hydrogenation mechanisms of acrolein on several carbide and bimetallic surfaces, including TiC/Ti(0001), Mo_2C/Mo(110), Pd/Mo(110) and Pt/W(110), to determine the correlation between the selective hydrogenation activity with the d-band center of these surfaces. (2) We will perform follow up studies to determine the electrocatalytic activity and stability of WC and Mo_2C under *in-situ* conditions. (3) We will start exploratory studies of the design of Pt-based bimetallic catalysts as cathode electrocatalysts for the reduction of oxygen; our main focus in these studies will be to determine the stability of the Pt-based bimetallic structures under *in-situ* fuel cell conditions and to identify ways to improve their electrochemical stability using a combination of UHV surface science, DFT modeling, and *in-situ* electrochemical measurements.

DOE Interest:

The overall goal of the current research is to demonstrate the possibility to predict and design materials with desirable catalytic properties. We believe that carbides and bimetallic alloys are excellent model systems to directly correlate the relationship between electronic/geometric structures and chemical/catalytic properties. Such structure-property relationship, to be determined using a combination of surface science experiments, DFT modeling, and catalytic studies, should help in predicting and controlling the catalytic and electrocatalytic properties of transition metals in general and carbide/bimetallic catalysts in particular.

Publications Sponsored by Current DOE Grant (2004-2005):

1. H.H. Hwu, J.G. Chen, "Surface Chemistry of Transition Metal Carbides", *Chemical Reviews*, 105 (2005) 185-212.
2. M.B. Zellner and J.G. Chen, "Surface Science and Electrochemical Studies of WC and W_2C PVD Films as Electrocatalysts", *Catalysis Today*, 99 (2005) 299-307.
3. H.H. Hwu, M.B. Zellner, and J.G. Chen, "Effect of Oxygen Modification on Electronic and Chemical Properties of C/Mo(110)", *Journal of Catalysis*, 229 (2005) 35-49.
4. J.R. Kitchin, J.K. Norskov, M.A. Barteau and J.G. Chen, "Trend in the Chemical Properties of Early Transition Metal Carbide Surfaces: A Density Functional Study", *Catalysis Today*, (2005) accepted.
5. M.B. Zellner and J.G. Chen, "Potential Application of Tungsten Carbides as Electrocatalysts: Synergistic Effect of Pt-Modification on the Reactions of Methanol, Water, and CO on C/W(110)", *Journal of Electrochemical Society*, (2005) accepted.
6. L.E. Murillo, N.A. Khan and J.G. Chen, The Effect of Hydrocarbon Structure and Chain Length on the Low-Temperature Hydrogenation Activity on Ni/Pt(111) Bimetallic Surfaces", *Surface Science*, (2005) accepted.
7. M.B. Zellner, A.M. Goda, O. Skoplyak, M.A. Barteau and J.G. Chen, "Novel Chemistry of Hydrogen and Ethylene on Monolayer Metal Films: A Combined DFT and Experimental Study", *Surface Science*, (2005) accepted.
8. M.B. Zellner and J.G. Chen, "Supporting Monolayer Pt on W(110) and C/W(110): Modification Effects on the Reaction Pathways of Cyclohexene", *Journal of Catalysis*, submitted (March 2005).
9. J.R. Kitchin, J.K. Norskov, M.A. Barteau and J.G. Chen, "The Role of Strain and Ligand Effects in the Modification of the Electronic and Chemical Properties of Bimetallic Surfaces", *Physical Review Letters*, 93 (2004) 156801.
10. N.A. Khan, L.E. Murillo and J.G. Chen, "Observation of Novel Low-Temperature Hydrogenation Activity on Co/Pt(111), *Journal of Physical Chemistry* B. 108 (2004) 15748-15754.
11. M.B. Zellner and J.G. Chen, "Synthesis, Characterization and Surface Science Study of Tungsten Carbide (WC) PVD Films", *Surface Science*, 569 (2004) 89-98.
12. N.A. Khan, M.B. Zellner, L.E. Murillo and J.G. Chen, "Comparison of Different Activities of Pt/Ni(111) and Ni/Pt(111)", *Catalysis Letters*, 95 (2004) 1-6.
13. N.A. Khan, M.B. Zellner and J.G. Chen, "Cyclohexene as a Probe for the Low-Temperature Hydrogenation Activity of Pt/Ni(111) Bimetallic Surfaces", *Surface Science*, 556 (2004) 87-100.
14. H.H. Hwu and J.G. Chen, "Chemical Properties of Carbon-Modified Titanium: Reaction Pathways of Cyclohexene and Ethylene over Ti(0001) and C/Ti(0001), *Surface Science*, 557 (2004) 144-158.
15. N.A. Khan and J.G. Chen, "Low-Temperature HDS of Thiophene on Monolayer Ni Films Deposited on W(110) and Ru(0001)", *Journal of Molecular Catalysis* A, 208 (2004) 225-232.
16. J.R. Kitchin, J.K. Norskov, M.A. Barteau and J.G. Chen, "Modification of the Surface Electronic and Chemical Properties of Pt(111) by Subsurface 3d Transition Metals", *Journal of Chemical Physics*, 120 (2004) 10240-10246.
17. H.H. Hwu, B. Fruhberger and J.G. Chen, "Different Modification Effects of Carbidic and Graphitic Carbon on Ni Surfaces", *Journal of Catalysis*, 221 (2004) 170-177.

DE-FG02-84ER13183 **James A. Dumesic**

Fundamental Studies of the Reforming of Oxygenated Compounds over Supported Metal Catalysts

Students: Dante Simonetti, Rupali Davda, John Shabaker, Steve Evans
Collaborators: Won Bae Kim (Gwangju Institute of Science and Technology), Randy Cortright (Virent Energy Systems), Manos Mavrikakis (University of Wisconsin)
Contact: James A. Dumesic, Department of Chemical and Biological Engineering, University of Wisconsin, Madison, WI 53706; phone: (608) 262-1095; E-mail: dumesic@engr.wisc.edu
Web page: http://www.engr.wisc.edu/che/faculty/dumesic_james.html

Goal

The goal of this project is to elucidate the fundamental surface chemistry involved in the catalytic conversion of renewable biomass resources to produce energy. The primary focus of this work has been the catalytic production of hydrogen by aqueous-phase reforming of biomass-derived oxygenated hydrocarbons over supported metal catalysts. More recent work has involved the production of energy by oxidation of CO using aqueous solutions of polyoxometalate compounds over gold nano-tubes and nano-particles.

Recent Progress

Production of Hydrogen by Aqueous-phase Reforming: We have shown how biomass-derived oxygenated hydrocarbons such as carbohydrates and polyols (e.g., methanol, ethylene glycol, glycerol, sorbitol, glucose) can be efficiently converted with water in the aqueous phase over heterogeneous catalysts at temperatures near 500 K to produce primarily H_2 and CO_2. We have elucidated how the selectivity for production of hydrogen can be controlled by altering the catalytically active metal and by choice of catalyst support. For example, we have shown that various bimetallic catalyst systems (such as PtFe and PdFe alloys) show high catalytic activity, selectivity, and stability versus time-on-stream for the production of hydrogen, provided that these metal particles are deposited on high surface area supports (such as alumina, titania, zirconia) that do not promote dehydration processes over acidic sites. In addition, we have demonstrated that the desirable catalytic properties of precious-metal-based materials for aqueous-phase reforming can also be achieved by modifying the catalytic properties of nickel. In particular, whereas nickel-based catalysts lead to the production of methane during aqueous-phase reforming of oxygenated hydrocarbons, we have found that addition of tin to nickel suppresses that rate of methanation, such that Ni_3Sn-based catalysts show excellent catalytic activity and selectivity for production of hydrogen. Importantly, we have demonstrated that these Ni_3Sn-based catalysts show good stability versus time-on-stream for aqueous feed streams containing high concentrations of oxygenated hydrocarbons (e.g., 30 wt% organics). We have also determined how the APR processes can be conducted to achieve low levels of CO in the gaseous effluent (e.g., lower than 100 ppm).

Oxidation of CO over Gold Nano-tubes and Nano-particles: We have recently shown that it is possible to study the catalytic properties of metallic gold, without interference from a catalyst support, using nanotubes of gold in polycarbonate membranes. Gold

nanotubes of uniform size were prepared via a template synthesis method by electroless deposition of gold within the pores of a 10 μm-thick, track-etched polycarbonate membrane containing 220 nm-diameter pores. These nanotubes exhibit catalytic activity for oxidation of carbon monoxide by O_2 at room temperature, and this activity is enhanced by liquid water, especially at high pH. These rates are comparable with rates over heterogeneous catalysts comprised of gold nanoparticles on oxide supports, suggesting that the high activity of these latter catalysts may be related to promotional effects of hydroxyl groups. Based on our work dealing with CO oxidation in the presence of liquid water, we have recently reported a process for oxidation and utilization of CO over gold nanotubes or nanoparticles involving the reaction of CO and liquid water with a reducible polyoxometalate (POM) compound, such as $H_3PMo_{12}O_{40}$, that serves as a strong oxidizing agent for CO and as an energy storage agent for electrons and protons. In our process, CO is oxidized to CO_2, thereby forming an aqueous solution of reduced POM species according to the representative reaction:

$$CO_{(g)}+H_2O_{(l)}+PMo_{12}O_{40}{}^{3-}{}_{(aq)} \rightarrow CO_{2(g)}+2H^{+}{}_{(aq)}+PMo_{12}O_{40}{}^{5-}{}_{(aq)}$$

This solution contains stored energy in the form of protons and electrons associated with reduced metal cations that can be re-oxidized readily at a fuel cell anode, by transfer of electrons from the POM to the electrode and transport of protons through a proton-exchange membrane to the cathode. In this way, the reducible POM compound facilitates the CO oxidation step by undergoing reduction and the reduced POM then serves as a fuel for the electrical energy generation step by undergoing oxidation at a fuel cell anode.

DOE Interest

Environmental and political problems created by our dependence on fossil fuels, such as global warming and national security, combined with diminishing petroleum resources are causing our society to search for new renewable sources of energy and chemicals. In addition, fuel cells have emerged as promising devices for meeting future global energy needs, and the full environmental benefit of generating power from hydrogen fuel cells is achieved when hydrogen is produced from renewable sources. Accordingly, renewable biomass resources are promising options for the sustainable production of hydrogen in an age of diminishing fossil fuel reserves.

Future Plans

We plan to conduct fundamental studies to elucidate details of the reaction pathways for the production of hydrogen and alkanes from the reforming of oxygenated hydrocarbons, and we plan to conduct *in situ* characterization studies of the catalytic materials for these reforming reactions. An important goal of these studies will be to compare the surface catalytic chemistry for reforming reactions in the vapor phase versus in the liquid phase. Our future research to elucidate the differences in the fundamental surface chemistry for liquid versus vapor-phase reforming of oxygenated hydrocarbons will involve reaction kinetics studies, *in situ* ATR-IR measurements, and *in situ* Mössbauer spectroscopic studies of Fe- and Sn-containing catalysts. In addition, we would like to extend our work to consider the oxidation of CO by reducible polyoxometalate compounds, such as $H_3PMo_{12}O_{40}$, in liquid water over various supported metal catalysts, e.g., Au, Pt, Pd, Ir, and Rh. In these studies, we are particularly interested in determining the factors that control the rate of CO oxidation and the selectivity for the oxidation of CO versus the oxidation of H_2 in $CO{:}H_2$ gas mixtures.

Publications for the past 2 years:

R. R. Davda, R. Alcala, J. W. Shabaker, G. W. Huber, R. D. Cortright, M. Mavrikakis, and J. A. Dumesic, DFT and Experimental Studies of C-C and C-O Bond Cleavage in Ethanol and Ethylene Glycol on Pt Catalysts, in Science and Technology in Catalysis 2002 (M. Anpo, M. Onaka, H. Yamashita, eds.), Elsevier, Amsterdam, 2003, pg. 79.

R. R. Davda, J. W. Shabaker, G. W. Huber, R. D. Cortright, and J. A. Dumesic, Aqueous-phase Reforming of Ethylene Glycol on Silica-supported Metal Catalysts, Applied Catalysis B **43**, 13 (2003).

J. W. Shabaker, R. R. Davda, G. W. Huber, R. D. Cortright, and J. A. Dumesic, Aqueous-Phase Reforming of Methanol and Ethylene Glycol Over Alumina-Supported Platinum Catalysts, Journal of Catalysis **215**, 344 (2003).

R. Alcalá, M. Mavrikakis, and J. A. Dumesic, DFT Studies for Cleavage of C-C and C-O Bonds in Surface Species Derived from Ethanol on Pt(111), Journal of Catalysis **218**, 178 (2003).

J. W. Shabaker, G. W. Huber, R. R. Davda, R. D. Cortright, and J. A. Dumesic, Aqueous-Phase Reforming of Ethylene Glycol Over Supported Platinum Catalysts, Catalysis Letters **88**, 1 (2003).

R. R. Davda and J. A. Dumesic, Catalytic Reforming of Oxygenated Hydrocarbons for Hydrogen with Low Levels of Carbon Monoxide, Angewandte Chemie International Edition **42,** 4068 (2003).

G. W. Huber, J. W. Shabaker, and J. A. Dumesic, Raney Ni-Sn catalyst for H_2 Production from Biomass-derived Hydrocarbons, Science **300**, 2075 (2003).

J. W. Shabaker, G. W. Huber, and J. A. Dumesic, Aqueous-Phase Reforming of Oxygenated Hydrocarbons Over Sn-Modified Ni Catalysts, Journal of Catalysis **222**, 180 (2004).

R. R. Davda and J. A. Dumesic, Renewable Hydrogen by Aqueous-phase Reforming of Glucose, Chemical Communications, 36 - 37, (2004)..

M. A. Sanchez-Castillo, C. Couto, W. B. Kim, and J. A. Dumesic, Gold Nanotube Membranes for Oxidation of CO at Gas-Water Interfaces, Angewandte Chemie International Edition **43**, 1140 (2004).

J. W. Shabaker and J. A. Dumesic, Kinetics of Aqueous-Phase Reforming of Oxygenated Hydrocarbons: Pt/Al_2O_3 and Sn-Modified Ni Catalysts, Industrial and Engineering Chemisty Research **43**, 3105 (2004).

W. B. Kim, T. Voitl, G. J. Rodriguez-Rivera, and J. A. Dumesic, Powering Fuel Cells with CO via Aqueous Polyoxometalates and Gold Catalysts, Science **305**, 1280 (2004).

Won Bae Kim, T. Voitl, G. J. Rodriguez-Rivera, S. T. Evans, and J. A. Dumesic, Preferential Oxidation of CO in H_2 by Aqueous Polyoxometalates over Metal Catalysts, Angewandte Chemie International Edition **44**, 778 (2005).

J. W. Shabaker, D. A. Simonetti, and J. A. Dumesic, Sn-Modified Ni Catalysts for Aqueous-Phase Reforming: Characterization and Deactivation Studies, Journal of Catalysis **231**, 67 (2005).

R. R Davda, J. W. Shabaker, G. W. Huber, R. D. Cortright, and J. A. Dumesic, A Review of Catalytic Issues and Process Conditions for Renewable Hydrogen and Alkanes by Aqueous-phase Reforming of Oxygenated Hydrocarbons over Supported Metal Catalysts, Applied Catalysis B **56**, 171 (2005).

KC-03-04-01 **Peter C. Stair (NU/ANL)**
KC-03-04-01 **Michael J. Pellin (Argonne National Lab)**
KC-03-04-01 **Larry A. Curtiss (Argonne National Lab)**

***CATALYSIS SCIENCE INITIATIVE*: Nanostructured Membrane Catalysis**

Additonal PIs: Jeff Elam, Peter Zapol, Hau Wang, (Argonne National Lab)
Postdocs: G. Xiong (Argonne National Lab)
Students: H. Feng, A. Whitney (Northwestern University)

Department of Chemistry
Northwestern University
Evanston, IL 60208
pstair@northwestern.edu

Chemistry Division
Argonne National Lab
Argonne, IL 60439
curtiss@anl.gov

Materials Science Div
Argonne National Lab
Argonne, IL 60439
pellin@anl.gov

Goals

The goal of this project is to significantly advance the molecular-level understanding and control of pathways for selective catalytic oxidation of hydrocarbon molecules by exploiting a new and unique architecture for ultra-uniform catalysts. The research plan involves nanostructured membranes, fabricated by a combination of anodic aluminum oxidation and atomic layer deposition that possess most, if not all, the features of the ideal support for ultra-uniform catalytic systems. Novel approaches are used for the introduction of metal, metalo-oxo, and organometallic catalysts into the membrane pores resulting in custom-designed catalysts for systematic studies of oxidation reactions. In principle, this approach can produce catalytic systems with exquisite control over reagent delivery, product removal, catalyst aging, reactive site sequencing, etc. We use a variety of state-of-the-art characterization techniques to investigate the catalysts and reactions to achieve a mechanistic understanding of oxidative catalytic chemistry at the level of individual elementary reactions. Computational simulations are an important complement to the experimental investigations in this project by providing fundamental theoretical insight at the atomistic level of the catalytic properties of the nanostructured membranes.

DOE interest

The understanding and control of reactions catalyzed on solid surfaces *at the molecular-level* is a "grand challenge" for 21st Century catalysis science. We expect that the fundamental results of this research will provide structure-function relationships between catalytically active sites and the chemical reactions they catalyze that are at the heart of this challenge. This project brings together a team of university and national laboratory researchers who develop methods for the design and synthesis of active catalytic sites at the atomic scale and tailored support structures at the nanometer scale, diverse spectroscopy, microscopy, and x-ray scattering techniques for detailed characterization (both ex-situ and in-situ) of catalyst structure and dynamics, elucidation of catalytic reaction mechanisms, and theory applied to catalytic processes.

Research plan

Mesoporous and microporous catalytic material syntheses are often approached in a "one step" process. In this work we are using a new approach based on two steps: production of a stable mesoporous scaffold and then carefully controlled modification of the scaffold, where each step can be optimized independently. Our work involves gas phase deposition allowing directed control of the pore wall composition and diameter. The scaffold that is used is anodized aluminum oxide (AAO) and the deposition method is atomic layer deposition (ALD).

AAO membranes are an ideal scaffold with highly-aligned, parallel pores and narrow pore diameter distributions.[1] Electrochemical conditions can be arranged to produce most probable pore diameters in the range 20 to 400 nm and membrane thicknesses in the range 0.5 to >250 μm. Prior catalytic studies using AAO showed interesting yield enhancements, but were limited to unreleased (pore blocked) films.[2] Moreover, as-grown AAO membranes suffer from poorly defined pore wall morphology and composition with significant (5%) amounts of incorporated electrolyte anions.

ALD is a growth technique that uses alternating, saturating reactions between gaseous precursor molecules and a substrate to deposit films in a layer-by-layer fashion.[3] By repeating the binary reaction sequence in an ABAB… fashion, films of micrometer thickness can be deposited with atomic layer precision. Current viscous flow reactor designs allow this monolayer by monolayer growth to proceed very rapidly, resulting in growth rates as high as 0.1 micron/hour.} Binary reaction sequences have been developed to deposit a wide variety of materials including oxides, nitrides, sulfides and metals. ALD composite oxides can also be formed by depositing alternating layers ("nanolaminates") or partial layers of the component oxides at a specific ratio that controls the composition of the composite layer. Because gas transport into mesoporous and microporous materials is diffusion-limited; surfaces at the entrance to the AAO membrane will receive reactant exposures that are ~10^3 larger than interior surface. Despite this, ALD has a demonstrated ability to coat mesoporous materials including AAO. The key to fabricating uniform nanoporous membranes from AAO templates is the "self-limiting" nature of the ALD binary reaction scheme.

The second part of this project utilizes state-of-the-art chemical, materials, and reaction characterization techniques along with advanced computing methodologies to systematically investigate catalytic reaction selectivity in prototypical selective oxidation reactions. In the first experiments membranes with catalytic phases deposited by conventional impregnation and novel ALD methods are compared in order to make a connection with the extensive catalytic literature. Later, single catalytic particles will be deposited in each nanopore and reaction experiments performed to elucidate how elementary, catalytic reaction steps depend on the catalyst structure and composition at the atomic level. Membranes with a programmed series of catalytic particles in each pore will be used to study sequences of catalytic reactions. In collaboration with experiments, theoretical modeling at the ab initio and phenomenological level will be used to elucidate fundamental catalytic mechanisms.

Recent Progress

We have synthesized ultra-uniform inorganic catalytic membranes using a combination of anodic aluminum oxidation (AAO)[1] and atomic layer deposition (ALD)[3] and have found that they have distinct catalytic properties.

For this work we have synthesized extremely uniform AAO membranes. These are highly-ordered, 70 μm thick AAO scaffolds produced in oxalic acid.[4] A typical plan view Secondary Electron Micrograph (SEM) of a scaffold is displayed in **Figure 1A.** The hexagonal arrangement of pores (dark features) is clearly evident on this length scale; over longer distances the registry is less well defined. ALD was used to precisely control the chemical composition and diameter of the AAO scaffold pores.

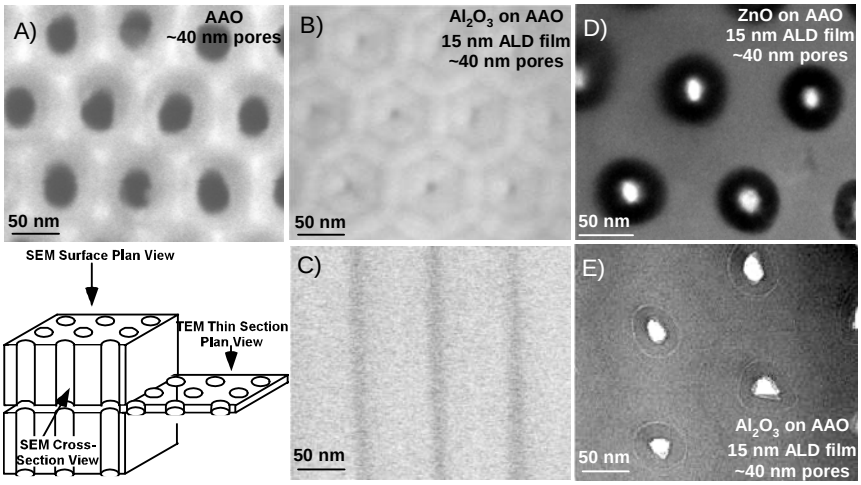

Figure 1. A) Plan view SEM image of surface of the original 40 nm AAO material. B) Plan view SEM image of the surface of the 40 nm AAO material coated with 15 nm of alumina. C) Cross sectional view of 40 nm AAO material coated with 15 nm of alumina taken from the center of the AAO membrane (note that the coating is uniform despite the high aspect ratio) D) Plan view TEM thin section image taken from the center of a 40 nm AAO membrane coated with 15 nm of ZnO. E) Plan view TEM thin section image taken from the center of a 40 nm AAO membrane coated with 15 nm of Al_2O_3 (note that the ALD coating conformally coats pores with eccentric pore shapes).

Subsequently we applied highly conformal ALD coatings with atomic layer precision to the AAO membranes using a wide variety of materials (Al_2O_3, TiO_2, ZnO, V_2O_5, and Pd) to narrow the pore diameters from 38 nm to 5 nm and deposit catalytically active layers. **Figure 1B** and **1C** demonstrate a membrane with 10 nm pores produced by depositing 15 nm of ALD Al_2O_3 on an AAO scaffold with an initial pore diameter of 40 nm. **Figure 1C** is a cross sectional SEM demonstrating that the pores have been narrowed uniformly throughout their entire pore length. **Figure 1D** demonstrates that the ALD coating technology can be extended to ZnO. The darkened circles in this Transmission Electron Micrograph (TEM) are the ZnO coating while the AAO pores are the bright central regions. Note that the highly conformal ALD coating exaggerates the ellipticity of pores that are initially non-circular. EDAX images (not shown) reveal that the Zn is uniform throughout the membrane. The TEM in **Figure 1E** shows a region of

an ALD Al_2O_3 coated AAO membrane having many irregular pores and again illustrates the superb conformality of ALD.

To test their catalytic behavior, two ALD coated membranes, with a 1 nm and a 15 nm Al_2O_3 ALD coating and thus 38 nm and 10 nm pore diameters respectively, were tested and compared to both an uncoated AAO membrane and a conventional high surface area γ-alumina powder catalyst (180 m^2g^{-1}). The membranes had approximately one monolayer of vanadium oxide added as the active species by standard impregnation with ammonia metavanadate to a loading of 12 μmol V^{5+}/m^2 followed by drying at 150°C for 3 hrs and calcination at 500°C for 5 hrs. The alumina powder was impregnated at 20 wt.% V_2O_5/Al_2O_3 to obtain a comparable conversion efficiency to the membrane catalyst. It should be noted that both the ALD and incipient wetness coatings cover the pore walls *and* the AAO membrane front and back surfaces. However, the pore wall to surface area ratio is 111 and 874 for the 10nm and the 38 nm membranes respectively, so that the catalytic performance should be dominated by reactions on the pore walls.

The well-studied oxidative dehydrogenation (ODH) of cyclohexane was chosen to test the membrane catalytic performance because it can probe selectivity. ODH has the potential to convert short chain alkanes to alkenes, exothermically. ODH of cyclohexane can, for instance, produce both cyclohexene and cyclohexadiene (generally produced at low yield) -- both useful intermediates for polyadditions. Further oxidation leads to the useless products benzene (because cyclohexane is mostly produced by hydrogenation of benzene) and carbon oxides (CO and CO_2).

Table 1 compares the selectivity to individual products (molar fraction of converted cyclohexane to that product) for vanadia coated AAO membranes (with two pore diameters) to more conventional alumina catalysts at similar conversion efficiencies. The vanadia-coated AAO membranes exhibited higher selectivity for the partial oxidation product, cyclohexene, than vanadia supported on γ-Al_2O_3 catalysts. The lower selectivity for the conventional catalyst is not a consequence of different conversions; since its cyclohexane conversion was lower, and conversion efficiency and selectivity are often inversely correlated. Instead, this appears to reflect a limiting of secondary oxidation reactions by a contact time of the reagents which is 10^3-10^5 times shorter in the membrane channels than in the conventional catalyst bed (1 s compared to 10^{-5} s). Among the membranes, the vanadia-coated AAO supported ALD membranes showed higher selectivity, especially the one with 10 nm channels. This may result from the uniformity of the Al_2O_3 ALD coating, reagent gas flow dynamics, or other factors. While the conversion percentages for O_2 and C_6H_{12} are lower for the 10 nm membrane than its larger pore cousins, the conversion per mole of vanadate is significantly higher. Since the mean free paths of molecules are 10-40 nm under the reaction conditions, the molecular flux in the larger channels will be a combination of convective and diffusive (Knudsen) flow. The velocity profile of convective flow would be laminar in which the flow in the center is proportionately over-collected when sampling at the exit. Essentially, this portion of the sample bypasses the reactor without contact with the catalyst on the wall. There is also a significant and repeatable difference in selectivity between 10 nm ALD pores and 38 nm pores. As one might expect as the temperature is raised to increase conversion rates the specificity of the membranes decrease. In all cases the membranes outperform conventional supported alumina catalysts.

Table 1: Conversion and Selectivity of γ-alumina and AAO supported V_2O_5 catalysts for the oxidative dehydrogenation of cyclohexane. The reaction was carried out in a quartz flow reactor with a feed mixture of He, O_2 and cyclohexane at a ratio of 94.6:3.5:1. Reaction temperature was 450°C. The carbon balance is within 2 %. All AAO membranes have an AAO framework with 40 nm pores through a 70 micron membrane. V_2O_5/Al_2O_3/AAO membranes have been coated with 15 nm and 1 nm thickness of ALD Al_2O_3. The V_2O_5 /AAO membrane had no ALD coat. All catalysts have ~ 1 monolayer of vanadium oxide produced using incipient wetness.

		V_2O_5/ Al_2O_3/ AAO (10 nm)	V_2O_5/ Al_2O_3/ AAO (38 nm)	V_2O_5/ AAO (40 nm)	V_2O_5/ γ Al_2O_3
Conversion (%)	O_2	5.1	9.9	3.7	6.6
	C_6H_{12}	3.0	4.2	4.0	4.4
Selectivity (%)	C_6H_{10}	29.8	8.5	6.9	3.1
	C_6H_6	14.5	28.9	19.0	33.3
	CO	13.7	19.1	23.5	20.1
	CO_2	41.9	43.5	50.5	43.5

Our initial theoretical studies in this project have focused on oxidative dehydrogenation of propane on bulk and supported vanadium oxide. Experimental studies of the ODH propane reaction with supported vanadia catalysts have generally envisioned the reaction occurring in three steps. (1) The catalyst donates an oxygen atom to the propane molecule, which then binds to the catalyst surface. (2) The surface-bound propane forms propene and releases a water molecule. (3) An oxygen molecule present in the feed stream returns an oxygen atom to the catalyst to fill the vacancy left in the first step. Although this mechanism is consistent with most experimental studies, three important questions remain to be answered. First, which oxygen atom is removed from the catalyst surface? Does it come from the vertical V=O vanadyl bond, or one of the bridging oxygen linkages? Secondly, what is the rate-limiting step for the ODH reaction? Thirdly, how does propane interact with the catalyst oxygen atom to form propene and water? There is strong evidence that step (3) is not rate-limiting, and the observed dependence of catalyst reactivity on the support material suggests that the V-O-S linkage may be involved in the reaction, but the details are not well understood because of the complexity of the catalyst surfaces.

We have carried out a density functional study (B3LYP, B3PW91) of dissociative adsorption of propane on the (010) surface of V_2O_5 as well as on a $V_2O_7H_4$ cluster on a TiO_2 substrate. The bulk surface serves as a model system for this reaction and it is known that it is not reactive for propane oxidative dehydrogenation. Calculations are being done on both cluster models and periodic models. The calculations on periodic models of the surface were used to determine the size of cluster needed to obtain reliable

potential energy surfaces for the reaction mechanism. Most of the calculations were done at the B3LYP/6-31G* level of calculation, but we also examined some energies at higher levels of theory to check its accuracy. In both the bulk and supported systems we have examined the reaction of propane with the vanadyl (V=O) and bridging oxygen.

In the case of the clean V_2O_5 surface we have calculated both equilibrium structures and transition states involved in the propane reaction with these sites. The steps along the pathway are all endothermic and the triplet state pathway is found to be favored over the singlet state pathway by 10-30 kcal/mol. The results for the (010) surface indicate that dissociative propane reaction with bridging sites to form propoxide + OH is more favorable than reaction with the vanadyl oxygen site by about 5-10 kcal/mol, but both are endothermic. The barrier to formation of propoxide + OH involves a singlet/triplet curve crossing for both the bridging and vanadyl sites and is about 55 kcal/mol in both cases. Thus, in terms of rates either site may participate, but the subsequent hydrogen rearrangement leads to oxygen removal from a bridging site via H_2O formation. The barrier for elimination of propane and water from the surface is about 75-80 kcal/mol and results in an oxygen vacancy at a bridging site. Thus, the dissociative adsorption of propane is not the rate limiting step, rather it is water desorption to form an oxygen vacancy site. The regeneration of the vanadium oxide surface via O_2 has not been studied, although this is likely to be downhill energetically.

In preliminary results on the supported cluster, we have found the dissociative adsorption on a vanadyl oxygen is endothermic, similar to the bulk surface. However, the bridging oxygen between the $V_2O_7H_4$ cluster and the TiO_2 surface is found to be much more reactive towards propane than the vanadyl oxygen.

References:

1. V. P. Menon, C. R. Martin, Anal. Chem. 67 (1995) 1920.
2. G. Patermarakis, C. Pavlidou, J. Catal. 147 (1994) 140.
3. J. W. Elam, S. M. George, Chem. Mater. 15 (2003) 1020.
4. C. Y. Han, Z. L. Xiao, H. H. Wang, G. A. Willing, U. Geiser, U. Welp, W. K. Kwok, S. D. Bader, G. W. Crabtree, ATB Metallurgie 43 (2003) 123.

Publications:

1. Elam, J. W., A. Zinovev, et al. (2005). "Atomic Layer Deposition of Palladium Films on Al_2O_3 Surfaces." *Thin Solid Films* **submitted**.
2. Pellin, M. J., P. C. Stair, et al. (2005). "Mesoporous Catalytic Membranes: Synthetic Control of Pore Size and Wall Composition." *Catalysis Letters* **Submitted**.
3. Redfern, P. C., P. Zapol, et al. (2005). "Quantum Chemical Study of the Potential Energy Surface for Propane Adsorption on the (010) Surface of V_2O_5." *J. Phys. Chem. B.* **submitted**.
4. Xiong, G., J. W. Elam, et al. (2005). "Effect of atomic layer deposition coatings on the surface structure of anodic aluminum oxide membranes." *J. Phys. Chem. B.* **Submitted**.
5. Xiong, G., H. Feng, J. W. Elam, S. P. Adiga, L. E. Iton, H.-H. Wang, P. Zapol, L. A. Curtiss, M. J. Pellin, M. Kung, H. Kung, P. C. Stair (2005) "Oxidative Dehydrogenation of Cyclohexane over Vanadium Oxide Catalyst Supported on Nanoporous Alumina Membranes" *J. Catal.* **in preparation.**

Poster Presentations

In Situ UV-Raman and FTIR Spectroscopies: Studies of 3-D nanostructured catalysts

J. W. Ager III, Y. Borodko, and G. A. Somorjai

Chemical Sciences and Materials Sciences Divisions, Lawrence Berkeley National Laboratory, Berkeley, CA 94720

Deep ultraviolet (UV) Raman and infrared spectroscopy techniques are developed in order to perform *in-situ* studies of 3-D nanostructured catalysts. For Raman spectroscopy, use of excitation at 244 nm avoids fluorescence interference and can enhance some spectral features due to resonance effects. For infrared spectroscopy, use of a hybrid absorption/reflection technique is shown to reduce effects due to self-absorption and produce transmission-like vibrational spectra. These techniques were applied to study the vibrational properties of mesoporous silica (SBA-15) with and without the presence of platinum nanoparticles in the mesopores that were incorporated by sonication. Raman and IR spectral line assignments were made by comparison to amorphous silicas

The incorporation of Pt nanoparticles strongly decreases the Raman peak (D_2) associated with 3-membered siloxane rings at the surface. At loadings above 2 wt. %, a peak is observed at between 530 and 580 cm^{-1} in the UV-Raman spectrum that is attributed to a Pt-O stretching motion. This mode shifts to lower frequency with increasing Pt loading, suggesting an increase in the interaction of the Pt nanoparticles with the oxide support. Exposure to reducing conditions causes the peak to disappear, suggesting that it is due to a very thin layer of oxide on the nanoparticles surface. Other metal oxides can be observed with the UV-Raman technique. For example, a RhO_x feature at 540 cm^{-1} is observed in SBA-15 with a 0.6% wt. loading of Rh nanoparticles.

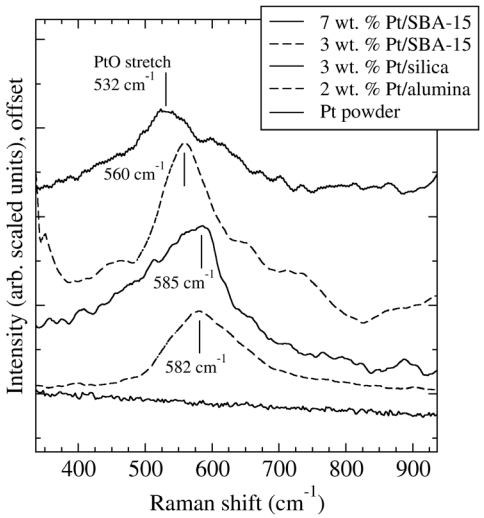

Comparison of UV-Raman spectra in the Pt-O stretch region for SBA-15 with two loadings of Pt nanoparticles, 3 wt. % Pt dispersed on amorphous silica, and 2 wt. % Pt dispersed on alumina. The data are obtained by subtracting the spectrum of the unloaded support in each case. The position of the PtO_x stretch feature is indicated.

Changes in internal surfaces of SBA-15 were studied with *in-situ* FTIR. The formation of 2-membered siloxane surface rings (peak at 890 cm^{-1}) and a decrease in the free silanol feature were observed in Pt/SBA-15 under low-temperature oxidizing conditions (O_2 flow at 450°C). The surface changes are reversible; under reducing conditions (H_2 flow at 450°C) the Si-OH intensity is restored and the strained siloxane peak disappears. This reversible reaction does not occur in silica at this temperature or in SBA-15 without Pt nanoparticles.

Nanostructured Metal Oxide Catalysts via Building Block Syntheses

Students:
Jason Clark, Geoffrey Eldridge, Ming-Yung Lee, Richard Mayes, Dustin Collier
PI Contact Information:
Department of Chemistry
University of Tennessee
Knoxville, TN 37996-1600
Office: 865 974 3446
Email: cebarnes@utk.edu

I. Overall Research Goals:

The primary goal of this research project is to develop a general methodology with which to prepare nanostructured mixed metal oxide materials in which the composition and surface structure may be tailored to enhance catalytic activity. Ultimately we seek to prepare, by design, single site, site isolated supported catalysts with defined catalytic sites and to relate these sites to specific catalytic activities. In this manner we will connect the nanostructuring of a specific site environment with its reactivity in catalysis.

II. Recent Progress

Synthesis of Nanostructured Metal Oxide Catalysts: We now have a reasonably well developed understanding of how to link together Si_8O_{20} spherosilicate building blocks with a variety of high valent metals such as vanadium and titanium (Figure 1). The reaction involves a fast initial coupling of the first metal chloride to a corner of the silicate cube to form a capping Si-O-MCl_x group. We have been able to prepare a number of octasilyl chloride cubes by slow addition of the octatin cube to excess silyl chlorides such as $SiCl_4$ (e.g. $Si_8O_{12}(OSiCl_3)_8$). These new silylchloride capped spherosilicates actually form a complimentary set of building blocks which will be investigated in the future.

Figure 1 Building block materials based on the Si_8O_{20} cube

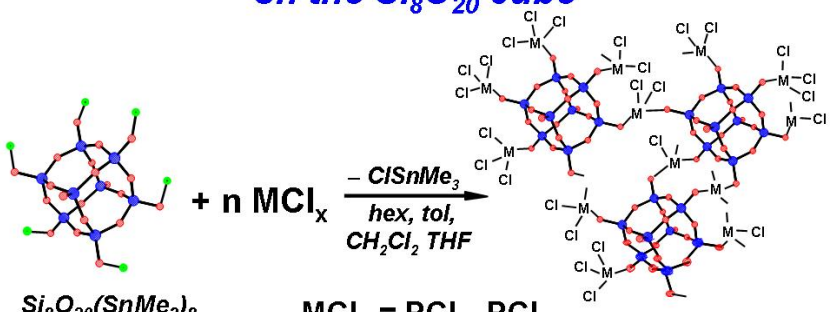

Metal oxide synthesis under mild, nonaqueous conditions

Growth and cross-linking of the matrix can be controlled simply by sequential slow addition of metal chloride linkers. By first linking with limiting amounts of metal chlorides such as titanium and vanadium and then cross-linking the small

oligomers that develop with $SiCl_4$ we have been able to prepare Ti and V that are three- and four-connected to Si_8O_{20} building blocks. Reversing the sequence of cross-linking agents ($SiCl_4$ followed by $TiCl_4$ or $VOCl_3$) we can also produce Ti- or V-silicate catalysts that have the metals in exclusively surface (one-connected) positions. We have also extended this methodology to aluminosilicate solid acids using $AlCl_3$ as a linker.

Catalysis Studies: The atomically dispersed metals and aluminum in silicate building block matrices may be used as catalysts of a number of reactions including selective oxidation reactions (epoxidation by either Ti or V on bb-SiO_2) and solid acid reactions such as transesterification (Ti and Al on bb-SiO_2). Transesterification reactions are being studied in collaboration with Goodwin's group in the Chemical Engineering Department at Clemson University in conjunction with his interest in developing acid catalysts for the production of biodiesel fuels from renewable feed stocks such as waste vegetable oils and fatty residues.

Finally we are currently constructing our own combination TPD-microcatalysis gas phase reactor. The system will consist of mass flow controlled carrier gas and substrate feed lines leading to a multiport valve and U-tube reactor in a furnace. Analysis of the product mixture will be conducted via mass spec probes both before and after GC separation of the product mixture.

III. DOE Interest

The development of general methodologies for the preparation of heterogeneous catalysts in which the surface catalyst sites are isolated, well defined and homogeneous has been a goal of catalysis science for many years. As indicated in recent Technology 2020 reports, a critical need in the development of next generation "ultraselective" catalysts is the development of new approaches for the preparation of new, single site heterogeneous catalysts. We are focusing on developing building block syntheses of mixed metal-silicate materials where the immediate environments around every active metal site can be tailored at will but all remain identical and robust. We anticipate that this degree of controlled nanostructuring of surface sites will lead to higher selectivity and activity without sacrificing broad applicability.

IV: Future Plans

We now seek to relate the nature sites with different characteristics (e.g. embedded versus surface) to their catalytic activities. Although applicable to many areas of catalysis, we are currently investigating selective oxidation chemistry (epoxidation of functionalized olefins) and solid acid catalysts related to the development of new biodiesel feed stocks. In the coming year we will finish the construction of our TPD-microcatalysis reactor. This will be used to conduct initial surveys of solid acid strength and epoxidation reactions using titanium and vanadium catalysts. These studies will parallel batch reactions to determine long term stability of the catalysts.

Publications:

- Narendra N. Ghosh, Jason C. Clark, Geoffrey T. Eldridge and Craig E. Barnes "Building Block Synthesis of Site-isolated Vanadyl Groups in Silicate Oxides." *Chemical Communications* 2004, (7), 856-857.
- Cheri W. Clavier, David L. Rodman, Joseph F. Sinski, Leonardo R. Allain; Hee-Jung Im; Yihui Yang; Jason C. Clark; Ziling Xue; "A Method for the Preparation of Transparent Mesoporous Silica Sol-Gel Monoliths Containing Grafted Organic Functional Groups" *J. Mater. Chem*., accepted for publication.
- Jason C. Clark, Suree Saengkerdsub, Geoff T. Eldridge, Chuck Campana, Craig E. Barnes "Synthesis and Structure of Stanylated Spherosilicate Building Block Molecules for Materials Synthesis" in preparation
- Jason C. Clark, Craig E. Barnes "The Reaction of $Si_8O_{20}(SnMe_3)_8$ Building Block with Silyl Chlorides: A new Synthetic Methodology for Preparing Building Block Solids" in preparation
- Jason C. Clark, Dora E. Lopez, David A. Bruce, James G. Goodwin, Jr., Craig E. Barnes "Synthesis of Novel Aluminun and Titanium Based Solid Acid Catalysts for Biodiesel applications using Building Block Methods" in preparation

Electrocatalytic Microsensors for Separate Monitoring of Nitric Oxide and Peroxynitrite on NOS-modified Electrodes

Pubudu Peiris, Serban F. Peteu, Jean A. Boutros, Mekki Bayachou

Abstract (2 Posters):

The biocatalytic synthesis of nitric oxide (NO) takes place *in vivo* on enzymatic machineries called Nitric Oxide Synthases (NOS). The NO synthesis pathway is very complex and its uncoupling can lead to the formation of peroxynitrite (ONO_2^-). To gain mechanistic and kinetic insights into the NOS reaction as carried on NOS-modified electrodes, it is crucial to quantify NO as the ultimate product, and ONO_2^- generated from an uncoupled "leak pathway" within the overall catalytic reaction. Methods currently available to measure these products in real time are relatively complex, and their sensitivity and selectivity is not suitable for our project, which addresses the NOS reaction on NOS-modified electrodes. We thus set out to develop sensitive electrocatalytic microfiber-based sensors for selective quantification of NO and ONO_2^- *in situ*. Catalyst-modified microfibers have been prepared and characterized by field emission scanning electron microscopy (SEM) with elemental analysis, and by Auger electron and energy dispersive X-ray spectroscopies (AES abd EDS). Electrocatalytic oxidations of the NO and ONO_2^- were assessed by cyclic voltammetry, amperometry in standing solutions, and in flow injection analysis. The modified microfiber sensors showed typical electrocatalytic behavior, with a sensitivity of about ten times higher than the unmodified fiber, and a limit of detection in the nanomolar range in the case of nitric oxide. The performance of these sensors is exploited to quantify electro-chemically driven NO biosynthesis with potential ONO_2^- generation on NOS-modified electrodes. This leads to a better understanding of the NOS catalysis, in general, and enzymatic reactions in confined environments in particular.

Development of a Computer-Aided Discovery Environment for Catalysis Design

L. Delgass,[2] D. Whittenhill,[2] L. Arns,,[2] S-H. Hsu,[1] B. Krishanmurthy,[1] M. McLennan,[2] S. Orcun,[3] N. Sumantra,[3] S. Dunlop,[2] D. Talcott,[2] B. Whitson,[2] T-Z. Park,[2] L.Zhao,[2] G. Medvedev,[1] T. Manz,[1] G. Blau,[1] W.N. Delgass[1] and V. Venkatsubramanian,[1] and J.M. Caruthers[1]

[1]School of Chemical Engineering
[2]Information Technology at Purdue (ITaP)
[3]e-Enterprise Center, Discovery Park
Purdue University
West Lafayette, IN 47907
caruther@ecn.purdue.edu

A computer aided discovery environment is being developed to assist catalyst researchers in developing new understanding about catalysts and the fundamental mechanisms that control their catalytic activity. The objective of the discovery environment is to enable the catalysis researcher to (i) manage the vast amounts of data that are being generated via high throughput experimentation, (ii) efficiently submit/retrieve the data from ensemble quantum chemistry simulations, (iii) rapidly build models that can describe the complex reactions that are occurring, (iv) analyze the data with appropriate non-linear statistics, (v) rapidly postulate and evaluate potential relationships between descriptors of the catalyst and experimentally measured rate constants and (vi) visualize and interact with this information using state-of-the-art display technology. A key feature of the system is that the data storage, computations and visualization are scaleable from a single user PC, to a work-station with a multi-head display, to a computational cluster, with an enterprise-class database and a large tiled wall. We will show a prototype of the system, including how the system can be used in determining knowledge for catalytic systems.

From First Principles Design to Realization of Bimetallic Catalysts for Ultrahigh Selectivity

Personnel at Texas A&M University

- Richard M. Crooks (PI)
- Robert W. J. Scott (postdoc through December, 2004; now an assistant professor at the University of Saskatchewon)
- Orla M. Wilson (current graduate student)
- Heechang Ye (current graduate student)

Department of Chemistry
Texas A&M University
P.O. Box 30012
College Station, TX 77842-3012
979-845-5629
crooks@tamu.edu

Goal

Synthesize and characterize structurally well-defined bimetallic nanoparticles using a dendrimer templating approach, and then evaluate their homogeneous and heterogeneous catalytic properties, as well as their electrocatalytic efficiency for the oxygen reduction reaction, as a function of size, composition, and structure.

Recent Progress

Electrocatalytic oxygen reduction using dendrimer-encapsulated Pt nanoparticles

Platinum dendrimer-encapsulated nanoparticles (DENs) were prepared within fourth-generation, hydroxyl-terminated, poly(amidoamine) dendrimers and immobilized on glassy carbon electrodes using an electrochemical immobilization strategy (Figure 1). X-ray photoelectron spectroscopy, electron microscopy, and electrochemical experiments confirm that the Pt DENs are about 1.4 nm in diameter and that they remain within the dendrimer following surface immobilization. The resulting Pt DEN films are electrocatalytically active for the oxygen reduction reaction (Figure 2). The films are also robust, surviving up to 50 consecutive cyclic voltammograms and sonication.

Figure 1

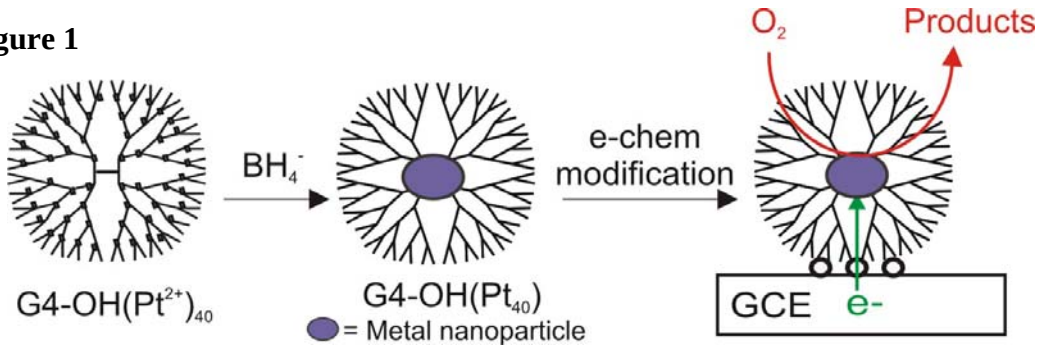

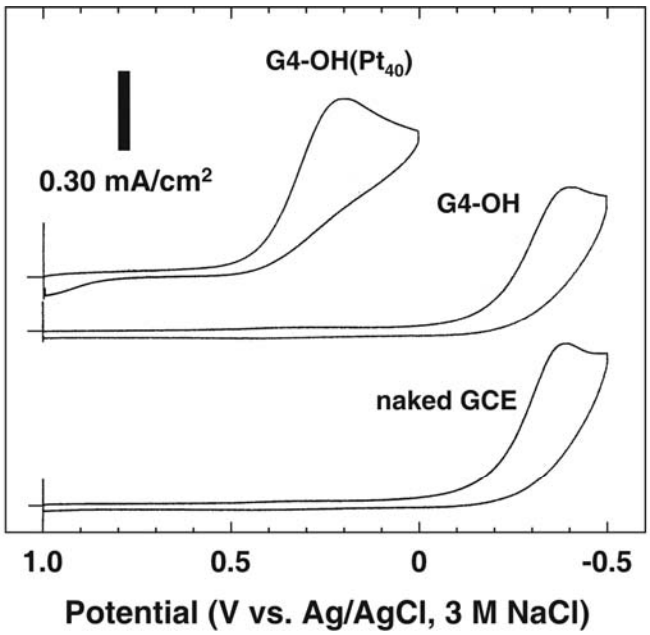

Figure 2. *Cyclic voltammograms for the reduction of O_2 using (top to bottom) a glassy carbon electrode (GCE) modified with generation 4 PAMAM dendrimers containing 40-atom Pt nanoparticles (G4-OH(Pt_{40})); a GCE modified with Pt-free G4-OH dendrimers, and a naked GCE. The data were obtained in an aqueous 0.5 M H_2SO_4 electrolyte solution saturated with O_2. The scan rate was 50 mV/s. The positive shift in the peak potential for the top voltammogram confirms the electrocatalytic properties of the dendrimer-*

Titania-Supported PdAu Bimetallic Catalysts

We studied the synthesis, characterization, and catalytic activity of titania-supported bimetallic PdAu particles prepared using dendrimer-encapsulated nanoparticle (DEN) precursors (Figure 3). Single-particle energy-dispersive spectroscopy indicated a homogeneous distribution of bimetallic nanoparticles having compositions closely related to the metal-ion ratios used to prepare the DEN precursors. The catalytic activity of the supported PdAu catalysts was compared to that of supported Pd-only and Au-only catalysts; the enhanced CO oxidation activity of the PdAu catalysts (Figure 4) is indicative of a synergetic bimetallic interaction.

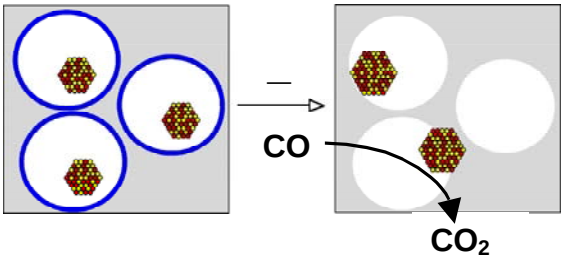

Figure 3. *Schematic representation of DEN-templating of a sol-gel precursor. The dendrimer serves as a template for both the titania matrix and the bimetallic nanoparticles*

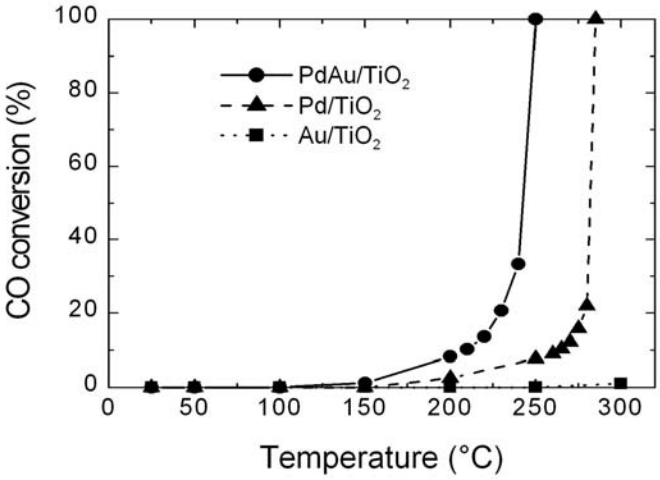

Figure 4. *Percentage CO oxidation as a function of temperature for PdAu, Pd-only, and Au-only catalysts supported on TiO_2. The catalysts were prepared using G4-NH_2($Pd_{27.5}Au_{27.5}$), G4-NH_2(Pd_{55}), and G4-NH_2(Au_{55}) DENs, respectively. Catalytic reactions were carried out using a 2:1 ratio of O_2:CO and a gas hourly space*

DOE Interest

The dendrimer templating approach is an effective route to the synthesis of chemically and structurally well-defined bimetallic catalytic nanoparticles. We envision that these materials will provide excellent experimental models for developing the next generation of catalytic materials. The partnership with the University of Delaware and University of Wisconsin groups allows us to guide future development of highly selective bimetallic catalysts according to theoretical models and study their catalytic properties in depth.

Future Plans

Current investigations are focused on two aspects of this project. First, we are examining the effect of the bimetallic nanoparticle size (in the range of 1 to 3 nm), composition, and structure (alloy vs. core/shell) on homogeneous catalytic reactions. For example, we are determining if there are quantum-size effects on the rates of chemical reactions (hydrogenations and carbon coupling reactions) catalyzed by monometallic and bimetallic nanoparticles. Likewise, we want to know if there are synergistic effects arising from the presence of the two metals and if so why. Second, we have discovered that dendrimer-encapsulated Pt nanoparticles catalyze

the reduction of oxygen, and this opens the door to the study of bimetallic DENs for fuel cell applications. In particular, we are interested in finding metal combinations of metals that could substitute for Pt, and we wish to know if there are particle-size effects on the catalytic efficiency of the oxygen reduction reaction.

During the coming year we will be collaborating with Dr. Randall Winans (Argonne National Lab) to study the structure of bimetallic DENs using the Advanced Photon Source to carry out ASAX and EXAFS studies. We are also collaborating with the Delaware and Wisconsin groups to better understand the theoretical and structural properties of DENs.

Publications (2004-2005)

1. H. Ye; R. M. Crooks "Electrocatalytic O_2 Reduction at Glassy Carbon Electrodes Modified with Dendrimer-Encapsulated Pt Nanoparticles" *J. Am. Chem. Soc.,* March, **2005** (ASAP).
2. R. W. J. Scott; C. Sivadinarayana; O. M. Wilson; Z. Yan; D. W. Goodman; R. M. Crooks "Titania-Supported PdAu Bimetallic Catalysts Prepared from Dendrimer-Encapsulated Nanoparticle Precursors" *J. Am. Chem. Soc.* **2005**, *127,* 1380-1381.
3. O. M. Wilson; R. W. J. Scott; J. C. Garcia-Martinez; R. M. Crooks "Synthesis, Characterization, and Structure-Selective Extraction of 1-3 nm-Diameter AuAg Dendrimer-Encapsulated Bimetallic Nanoparticles " *J. Am. Chem. Soc.* **2005**, *127,* 1015-1024.
4. R. W. J. Scott; O. M. Wilson; R. M. Crooks "Synthesis, Characterization, and Applications of Dendrimer-Encapsulated Nanoparticles" *J. Phys. Chem. B* **2005**, *109,* 692-704. (Feature Article).
5. R. W. J. Scott; O. M. Wilson; R. M. Crooks "Titania-Supported Au and Pd Composites Synthesized from Dendrimer-Encapsulated Metal Nanoparticle Precursors" *Chem. Mater.* **2004**, *16,* 5682-5688.
6. R. W. J. Scott; O. M. Wilson; S.-K. Oh; E. A. Kenik; R. M. Crooks "Bimetallic Palladium-Gold Dendrimer-Encapsulated Catalysts" *J. Am. Chem. Soc.* **2004**, *126,* 15583-15591.
7. O. M. Wilson; R. W. J. Scott; J. C. Garcia-Martinez; R. M. Crooks "Separation of Dendrimer-Encapsulated Au and Ag Nanoparticles by Selective Extraction" *Chem. Mater.* **2004**, *16,* 4202-4204.

KC-03-04-01. **Larry A. Curtiss**

Quantum Chemical Study of Mechanisms for Oxidative Dehydrogenation of Propane on Vanadium Oxide

Collaborators: P. Stair (Northwestern), P. Zapol (ANL), S. Zygmunt (Valparaiso), P. Redfern (ANL), S. Adiga (ANL), M. Sternberg (ANL)
Contact: L. Curtiss, Argonne National Laboratory, Argonne, IL 60515; Phone: (630)252-7380; Email: curtiss@anl.gov

Abstract

We have carried out a density functional study of mechanisms for oxidative dehydrogenation of propane on the (010) surface of V_2O_5. The surface was modeled using both vanadium oxide cluster and a periodic representation of the surface. We have considered adsorption of the propane at both the vanadyl oxygen and bridging oxygen sites followed by desorption of a water molecule and subsequent adsorption of an oxygen molecule to complete the reaction. The results are presented and implications for the catalytic reactions involving vanadium oxide are discussed.

Synthesis of Au catalysts on Nanostructured Supports

Sheng Dai*, Wenfu Yan, Shannon M. Mahurin, Haoguo Zhu, and Steven H. Overbury
Chemical Sciences Division, Oak Ridge National Laboratory, Oak Ridge, TN 37831-6201
*dais@ornl.gov

Surface sol-gel process (SSP) and atomic layer deposition (ALD) are two key synthesis methodologies recently developed for the layer-by-layer functionalization of planar substrates with a monolayer precision.[1-2] These novel technologies enable a molecular-scale control of film thickness over a large two-dimensional substrate area. Compared with conventional deposition methods, these two surface techniques offer the advantage of producing ultrathin conformal films, with control of the thickness and composition of the films possible at the atomic level. The general techniques consist of two half reactions: (a) condensation of metal-alkoxide precursor molecules with surface hydroxyl groups and (b) hydrolysis of the adsorbed metal-alkoxide species to regenerate surface hydroxyls. The iteration of the above sequential condensation and hydrolysis reactions allows the layer-by-layer coating of a selected metal oxide on a hydroxyl-terminated surface. We have been interested in the development of layer-by-layer functionalization techniques to tailor the surfaces of mesoporous materials for catalysis applications.[3-5] Here, we summarize our recent work on the rational application of SSP and ADL in the modification of silica mesopore surfaces and the tuning of mesopore diameters for the preparation of highly active and stable gold nanocatalysts for CO and other oxidation reactions.

1. Ichinose, I.; Senzu, H.; Kunitake, T. *Chem. Mater*. 9, 1296 (1997**)**.
2. Leskela, M.; Ritala, M. *Angew. Chem., Int. Ed*. 42, 5548 (2003).
3. Yan, W. F.; Mahurin, S. M.; Overbury, S. H., Dai, S. *Chem. Mater*.17, 1923 (2005).
4. Yan, W. F.; Chen, B.; Mahurin, S. M.; Hagaman, E. W.; Dai, S.; Overbury, S. H. *J. Phys. Chem. B*, 108, 2793 (2004**).**
5. Yan, W. F.; Chen, B.; Mahurin, S. M.; Dai, S.; Overbury, S. H. *Chem. Comm.* 1918 (2004)
6. Haruta, M. *Catal. Today* 36, 153 (1997).

Catalyst Design by Discovery Informatics

W. N. Delgass[1], J. M. Caruthers[1], R. G. Cooks[2], H. W. Hillhouse[1], F. H. Ribeiro[1], K. T. Thomson[1], V. Venkatasubramanian[1], G. Medvedev[1], K. Phomphrai[2], G. Zhu[1], A. Bhan[1], L. Bollman[1], A. Deskins[1], S.-H Hsu[1], Y. Joshi[1], B. Krishnamurthy[1], G. Krishnamurthy[1], K. M. Lee[1], T. Manz[1], A. Phatak[1], S. Rai[1], S. Sharma[2], A. Tabert[2], G. Blau[1], P. Patkar[1], M Abu-Omar[2], G. Bertoline[3], L. Arns[3], S. Dunlop[4], D. McKay[4], M. McLennan[4], D. Talcott[4], W. Whitson[4], L. Zhao[4], S. Orcun[5], S. Nandi[5], T. Park[5]

[1]School of Chemical Engineering, [2]Department of Chemistry, [3]Envision Center for Data Perceptualization, [4]Information Technology at Purdue (ITaP), [5]e-Enterprise Center, Discovery Park
Purdue University
West Lafayette, IN 47907
Delgass@ecn.purdue.edu

The goal of this work is to develop and apply an informatics-intensive, model-based approach that extracts knowledge from high throughput data for the design of catalysts.

In the study of *aromatization of propane over HZSM-5*, we have achieved a good fit of the data with a model which includes adsorption, desorption, unimolecular protolytic cracking and dehydrogenation, β-scission, oligomerization, hydride transfer, alkylation, dealkylation and cyclization. The 311 reaction steps were grouped into 37 reaction families governed by 25 parameters. For Ga-HZSM-5, we have assumed that each Ga replaces one proton, but the remaining protons retain their original activity. For the Ga activity, 129 reactions, grouped in 9 reaction families and governed by 18 kinetic parameters, were added. The fit to data for a single Ga loading is good, but is being refined with data from catalysts with other loadings and matching of the optimum Ga loading found experimentally. The success of this complex microkinetic model is a validation of the computer software developed to make modeling of such complex systems possible. The complexity and non-linearity of this system has also led us to reformulate parameter estimation and analysis of error. This work is strongly supported by DFT computations of adsorption of alkanes and alkenes, relative rates of ring closure, and the role of Ga.

We are currently perfecting the automated operation of our new four-reactor system for study of the *water gas shift reaction* (WGS). We have fit data as a function of temperature and concentrations of CO, H_2O, CO and CO_2 for supported Cu, Ni, Pd and Pt and determined apparent activation energies and reaction orders. An eight step redox mechanism fit to the data for Cu and Pt is adequate for Cu but does not give the correct surface concentrations for Pt. We are refining the fitting and evaluating alternative models. We are also focusing on the dramatic suppression of methanation and enhancement of WGS caused by addition of oxide promoters. ZnO shows the strongest effect with a rate increase of 30 times and suppression of methanation by three orders of magnitude. Characterization of the many new catalysts anticipated in the study of the fundamentals and optimization of these promoters will be aided by the 4 parallel channel mass spectrometer just now showing its first spectra. This new tool will be used first in temperature programmed desorption and reaction studies of these catalysts.

We have come closest to closure of the *discovery informatics* cycle in our studies of *olefin polymerization.* We have measured propagation rate constants and computed a variety of energies for an extended series of half-sandwich mixed Cp*/aryloxide Ti single site polymerization catalysts activated with $B(C_6F_5)_3$ or $Ph_3CB(C_6F_5)_4$. These homogeneous catalysts show the expected electronic and steric effects associated with the electron withdrawing/donating character or bulkiness of the substituents on the aryloxide ring, but descriptors such as ligand cone angles and the counter ion binding energy have pointed to an unexpectedly high activity associated with the 2,3,5,6-tetraphenylphenoxide ligand. The 2-phenylphenoxide ligand, predicted by this analysis to have high activity because of its low counter ion binding energy, has proved to be our most active catalyst yet. The forward model used to predict performance is still in crude form, but we take its success as an early validation of the discovery informatics approach and encouragement to continue to enrich the experimental and computational database that is the resource for more detailed model building and knowledge extraction for these single site catalysts.

The role of oxygen composition on the surface functionality of SnO_2(101)

Matthias Batzill, Ulrike Diebold,
Department of Physics, Tulane University, New Orleans, LA 70118, USA

The structure, composition, and functionality of surfaces of multi-valent oxides may depend on the oxidation potential of the gas phase. The variation of the surface-oxygen concentration is an important mechanism for understanding the chemical and physical properties of these materials. In the case of dual-valent Sn, we show that surfaces of SnO_2(101) can be prepared with surface tin-atoms in either a Sn(IV) or Sn(II) oxidation state, i.e. with or without bridging oxygen, respectively [1, 2]. On the reduced, i.e. Sn(II), surface, surface states associated with Sn-5s lone pair electrons are identified by angle resolved photoemission spectroscopy [3]. These surface states are lying deep in the band gap. Furthermore, the work function decreases by 1 eV upon reduction of the surface to Sn(II). This is important for tuning band alignment at the interface to SnO_2 in the use of this material as a transparent electrode in optoelectronics applications. Benzene adsorption has been used to probe the alignment of molecular orbitals with respect to the SnO_2 valence band for the two surface compositions [4]. Differences in the surface reactivity have been measured by water adsorption experiments. Surfaces with missing bridging oxygen are found to be unreactive towards dissociative adsorption, while stoichiometric (Sn(IV)) surfaces adsorb water dissociatively. In addition downward band bending of ~0.35 eV is observed for dissociative water adsorption that translates in a strong change of surface conductivity of the SnO_2 sample. Thus the changed chemical functionality can be measured in a conductivity response [5]. Lastly, metal adsorption was investigated by scanning tunneling microscopy on the SnO_2(101)-Sn(II) surface. Surprisingly, Pd wets the surface and grows in pseudo-1D islands of uniform width (1nm) and tens of nanometers in length. This is the first example of the growth of self-organized1D-metal nanostructures on a wide band gap oxide support.

[1] M. Batzill, A. M. Chaka, U. Diebold, ***Europhys. Lett. 65***, 61 (2004).

[2] M. Batzill, K. Katsiev, A. M. Chaka, U. Diebold, submitted to ***Phys. Rev. B***

[3] M. Batzill, J. Burst, A. M. Chaka, B. Delley, U. Diebold, submitted to ***Phys. Rev. B***

[4] M. Batzill, Kh. Katsiev, U. Diebold, ***Appl. Phys. Lett.* 85,** 5766 (2004).

[5] M. Batzill, W. Bergermayer, I. Tanaka, U. Diebold, submitted to ***Phys. Rev. Lett.***

Theoretical Characterization of Charge Transport in Metal Oxides

Nedialka Iordanova, Michel Dupuis, and Kevin M. Rosso
Pacific Northwest National Laboratory, Chemical Sciences Division, Richland WA 99354

Mobility and transport of electrons and holes are critical factors in the control and manipulation of photocatalytic reactivity of metal oxides through nanoscaling. We report here the application for the first time of Marcus theory to the characterization of electron-hole mobility in semiconductor metal oxides. Transport of conduction electrons and holes in hematite (α-Fe_2O_3) and chromia (α-Cr_2O_3) was modeled as a valence alternation of metal cations. In the context of a small polaron model, we used the ab initio cluster approach to compute the quantities that determine the mobility of electrons and holes, i.e. the reorganization energy and the electronic coupling matrix element that enter Marcus' theory using the Generalized Mulliken-Hush approach and the quasi-diabatic method. Calculated electron mobility is in excellent accord with the experimentally observed strong anisotropy between basal and 'c' directions. Holes display mobility similar to electrons. These later findings are in contrast to past classical arguments.

DE-FG02-03ER15453 **Richard G. Finke**

Nanocluster Catalysts Formation and Stabilization Fundamental Studies

Students: Starkey, L.; Finney, E.; Besson, C.

Contact: Department of Chemistry, Colorado State University,
Ft. Collins, CO 80523
phone: (970)-491-2541; Email: Rfinke@lamar.colostate.edu
web page: http://www.chm.colostate.edu/rgf/index.html

Goals

One primary goal of our DOE-funded program is to determine which stabilizers and other factors are best for the formation, stabilization and catalytic activity of transition-metal nanoclusters. A second goal is to continue our mechanistic studies of the nucleation, growth and agglomeration of transition-metal nanoclusters. A third goal is to exploit nanoclusters in interesting catalytic reactions. Each of these goals is central to the rational advancement of nanoclusters in catalysis.

Recent Progress

(1)Nanocluster Stabilization Fundamental Studies. Our paper detailing a tridentate, C_3 symmetry lattice size-matching model for the binding of nanocluster stabilizers to {111} surfaces of transition-metal nanoclusters appeared in 2004.[1] This is important as it provides the first molecular insights into how preferred, tridentate stabilizers can bind to transition-metal nanocluster catalysts.[1] A prediction of that work is that HPO_4^{2-} would be a superior, previously unknown stabilizer of transition-metal nanoclusters. That prediction was tested and found to be true via synthesis and conversion into nanoclusters of the new precursor, $\{[Bu_4N][(1,5\text{-}COD)Ir{\bullet}HPO_4]\}_n$.[2] In very recent work we were able to solve at least part of the mystery of why ionic liquids (ILs) are (unexpectedly) such good stabilizers of transition-metal nanoclusters: they form surface *N*-heterocyclic carbenes via oxidative addition of the imidazolium component of the IL, something that we detected via D_2 plus ^2H NMR studies as shown in Figure 1.[3]

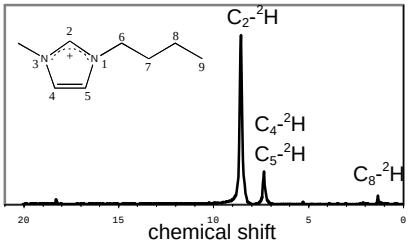

Figure 1. ^2H NMR spectroscopy showing deuterium incorporation from D_2 in the 2, 4, 5, and 8 positions of the imidazolium cation shown above. The rate of D incorporation is faster for the 2, 4, and 5 positions vs the 8 position, as one might expect if a surface *N*-heterocyclic carbene is required for D-incorporation into the 8 position.

(2) Fundamental Studies of NanoclusterFormation and Agglomeration. In an exciting development that promises to have very broad ramifications, we recently published three full papers[4,5,6] that detail the first complete mechanism for transition-metal nanocluster nucleation,

growth (autocatalytic surface growth), bimolecular agglomeration and now also the novel step of autocatalytic agglomeration between smaller nanoclusters and larger bulk metal particles. Another key insight from these studies,[5,6] an insight which promises to have a broad impact on the nanocluster area, is the size-sensitive nature of metal-ligand bond dissociation energies of small nanoclusters: they appear to be up to 2-fold stronger than those for bulk metal!

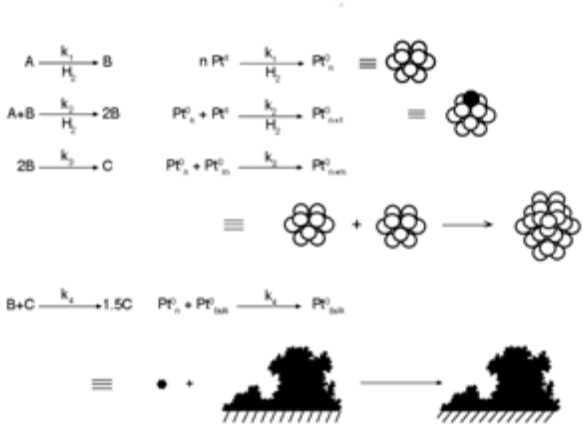

(3) Nanocluster Catalysis Studies: Iridium(0) Nanocluster, Acid-Assisted Catalysis of Neat Acetone Hydrogenation at Room Temperature: Exceptional Activity, Catalyst Lifetime and Selectivity at Complete Conversion. We discovered that simply placing $[(1,5\text{-COD})IrCl]_2$ under H_2 cleanly yields $Ir(0)_n$ nanoclusters plus HCl, the best current catalyst for the *room temperature, high activity, and highly selective* hydrogenation of acetone at 22 °C and 40 psig H_2 pressure to give 95% 2-propanol and 5% diisopropyl ether, all at 100% conversion with 16,400 demonstrated total catalytic turnovers.[7] Catalysis of this seemingly simple reaction is of broader interest since the reversible conversion between acetone and 2-propanol is of interest for use in chemical heat pumps, fuel cells, and other H_2 storage and use applications.

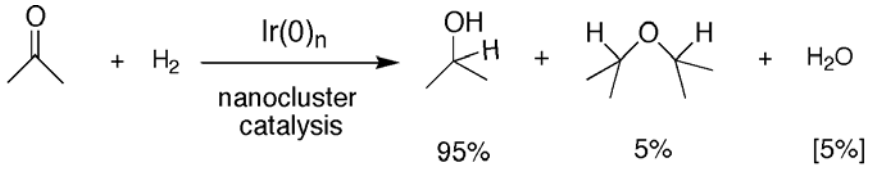

DOE Interest

Nanoclusters are metal particle catalysts closely analogous to the supported-metal particles in the most commonly used commercial catalysts, heterogeneous catalysts. However, nanoclusters have the advantage of being soluble; *hence, they can be made and studied by powerful solution synthesis, spectroscopic characterization and kinetic methods.* Well-defined nanoparticle catalysts promise to be important in the development of the concepts and technical advances en route to achieving the "Holy Grail" of heterogeneous catalysis, namely single-site, high selectivity, and high activity metal-particle catalysts. Nanoparticles are also expected to have their own, unique reactivity as seen in the above acetone hydrogenation reaction with its high activity and selectivity.

Future Plans

In the coming year we will strive to complete for publication our remaining studies of the factors and additives (solvents, polymers, dendrimers, halides, tetradentate polyoxoanions, or ionic liquids) that best allow the formation and stabilization of catalytically active transition-metal nanoclusters. We also plan to complete additional kinetic and mechanistic studies of our new, double autocatalytic step mechanism[5,6] of nanocluster formation and agglomeration to see how general it is and to learn what factors turn on this mechanism. These studies—all of a fundamental nature—are possible only due to our DOE grant support, funding for which we remain most grateful.

Publications 2004-2005

1. "Molecular Insights for How Preferred Oxoanions Bind to and Stabilize Transition-Metal Nanoclusters: A Tridentate, C_3 Symmetry, Lattice Size-Matching Binding Model", Özkar, S.; Finke, R. G. *Coord. Chem. Rev.* **2004**, *248*(1-2), 135-146.
2. "The Hydrogenphosphate Complex of (1,5-cyclooctadiene)Iridium(I), $\{[Bu_4N][(1,5\text{-}COD)Ir{\bullet}HPO_4]\}_n$: Synthesis, Spectroscopic Characterization, and ES-MS of a New, Preferred Precursor to HPO_4^{2-} and Bu_4N^+ Stabilized $Ir(0)_n$ Nanoclusters", Özkar, S.; Finke, R. G. *J. Organomet. Chem.* **2004**, *689(3)*, 493-501.
3. "Nanoclusters in Ionic Liquids: *N*-Heterocyclic Carbene Formation from Imidazolium-Based Ionic Liquids Detected by ^2H NMR", Starkey Ott, L.; Cline, M. L.; Deetlefs, M.; Seddon, K. R.; Finke, R. G. *J. Am. Chem. Soc.*, **2005**, in press.
4. "Transition-Metal Nanocluster Kinetic and Mechanistic Studies Emphasizing Nanocluster Agglomeration: Demonstration of a Kinetic Method That Allows Monitoring All Three Phases of Nanocluster Formation and Aging", Hornstein, B. J.; Finke, R. G., *Chem. Mater.*, **2004**, *16*, 139-150.
5. "A Mechanism for Transition-Metal Nanoparticle Self-Assembly", Besson, C.; Finney, E. E.; Finke, R. G. *J. Am. Chem. Soc.*, **2005**, accepted for publication.
6. "Nanocluster Nucleation, Growth and Then Agglomeration Kinetic and Mechanistic Studies: A More General, Four-Step Mechanism Involving Double Autocatalysis", Besson, C.; Finney, E. E.; Finke, R. G. *Chem. Mater*. **2005**, accepted for publication.
7. "Iridium(0) Nanocluster, Acid-Assisted Catalysis of Neat Acetone Hydrogenation at Room Temperature: Exceptional Activity, Catalyst Lifetime and Selectivity at Complete Conversion", Özkar, S.; Finke, R. G. *J. Am. Chem. Soc.*, **2005**, *127*, 4800-4808.

Catalyst Characterization through Time-Resolved FT-IR Monitoring under Reaction Conditions

Heinz Frei

Physical Biosciences Division, Lawrence Berkeley National Laboratory, Berkeley, CA 94720

Understanding of elementary reaction steps is an important vehicle for optimizing the design of 3-D catalyst supports and metal nanoparticle arrangement for achieving high product selectivity. In particular, detecting transient surface intermediates and learning how they relate kinetically to final product formation under reaction conditions will furnish crucial insights on the catalyst properties that steer the intermediates to the desired products.

Using the prototype ethylene hydrogenation as an example, we have directly observed the conversion of transient surface ethyl intermediate to gas phase ethane on Pt particles under reaction conditions (323 K, 1 atm, 9 L min^{-1} H_2/N_2 flow). An industrial catalyst (Exxon) with finely divided Pt particles on Al_2O_3 support was used. 25 ms time-resolution of the catalysis was achieved by synchronizing the forward motion of the interferometer mirror with the opening of a fast mechanical valve for release of a millisecond pulse of ethylene gas. Surface ethyl species were detected at 2870 and 1200 cm^{-1}, gas phase ethane product at 2954 and 2893 cm^{-1}. The CH_3CH_2Pt growth was instantaneous on the time scale of 25 ms under all experimental conditions. At 323 K, the decay time of surface ethyl (122 ± 10 ms) coincides with the rise time of C_2H_6 (144 ± 14 ms). This establishes direct kinetic evidence for surface ethyl as the rate limiting reaction intermediate. Such a link between the temporal behavior of an unstable surface intermediate and the final product in a heterogeneous catalytic system has not been demonstrated before. A fraction (10 percent) of the asymptotic ethane growth at 323 K is prompt, indicating that there are surface ethyl species that react much faster than the majority of the CH_3CH_2Pt intermediates. The dispersive kinetics is attributed to the varying strength of interaction of the ethyl species with the Pt surface caused by heterogeneity of the surface environment. At 473 K, the majority of ethyl intermediates are hydrogenated prior to the recording of the first time slice (24 ms), and a correspondingly large prompt growth of ethane is observed.

We have observed the same temporal behavior of ethane growth when conducting ethylene hydrogenation on Pt nanoparticles occluded in SBA-15 mesoporous silica (2.7% (wt) loading). The result shows that ethylene uptake and ethane release from the pores is not rate limiting. In parallel, time-resolved ethane hydrogenolysis and cyclohexane hydrogenation/dehydrogenation over Pt catalysts are being studied, and latest results will be presented.

EXAFS and XANES studies of 3D structure and metal-ligand charge transfer of ligand-stabilized and supported metal nanoparticles

Anatoly Frenkel (Yeshiva University), ***DE-FG02- 03ER15477***
Laurent Menard, Ralph Nuzzo (UIUC) ***DE-FG02- 03ER15476***

We developed reliable and robust methods of EXAFS analysis of ligand-stabilized nanoclusters that include multiple-scattering contributions from metal atoms and metal-S contributions due to sulfur adsorbtion. We tested our methods on the two systems of mixed ligand Au13 clusters: 1) $Au_{13}(PPh_3)_4(SC_{12})_4$ and 2) $Au_{13}[PPh_3]_4[S(CH_2)_{11}CH_3]_2Cl_2$ and on the somewhat larger, fully thiolated cluster. All samples were highly monodisperce, as ascertained by high resolution electron microscopy measurements. We obtained that the first two clusters were icosahedral, and the third one – cuboctahedral, in agreement with HR TEM, and quantified the bond lengths, structural disorder, and the thiol binding sites in the both types of clusters. In order to realize high activity for CO oxidation, we explored the deposition of ligands protected Au13 clusters onto anatase TiO_2 and optimum thermal treatment methods to remove ligands by *in situ* EXAFS.

Using S and P K-edge XANES, we studied charge transfer from gold to thiol and to phosphine ligands, respectively, by analyzing the shifts in the P and S edge positions in the nanoparticles compared to their respective references (phosphines and thiols). Our experimental results correspond to the Au-ligand charge transfer of the average of 0.5e per P and 0.7e per S atom, in agreement with the difference in their electronegativies (P: 2.1 and S: 2.5).

Finally, we have developed reliable and robust methods of nanoparticle size determination by EXAFS analysis, using both the coordination number reduction (CNT) and surface tension (ST) methods. The CNT method uses model dependent change in the particle coordination number as a function of its diameter. The ST method utilized the equation for the particle diameter $d = 4/3\, f_{rr} K/\alpha$, where f_{rr} and K are the surface stress and compressibility in the bulk, and $\alpha = \Delta R/R$ is the relative lattice contraction that can be measured by EXAFS. As a control system, we synthesized and investigated a series of alkanethiol-stabilized nanoparticles by controlling one parameter, the Au/thiol ratio. Our results for the particle size as obtained by the two different methods were in very good agreement. We also obtained that the particle size stabilizes at ca. 15 Å when Au/thiol ratio is 1:2 and does not decrease any further when the Au/thiol ratio decreases. This size is in excellent agreement with the predicted minimum size of 14 Å of gold nanoparticles that are thermodynamically stabilized by thiols.

Templated Chiral Surfaces for Enantioselective Adsorption

Andrew J. Gellman, Dept. Chem. Eng., Carnegie Mellon University
Pittsburgh, PA 15213-3890

Templated chiral Cu surfaces are being prepared for enantioselective adsorption and separations. One such set of surfaces are Cu(100) single crystals that are being modified by adsorption of chiral 2-butanols and adsorption of chiral amino acids. The second type of chiral surface is based on Cu powders packed into a chromatography column. These chiral surfaces are to be used for study of enantioselective adsorption and desorption of chiral adsorbates under UHV conditions and enantioselective separations within a gas chromatograph.

Cu(100) surfaces modified by the adsorption of chiral 2-butanoxy groups ($CH_3CH(O\text{-})C_2H_5$) are being prepared by first oxidizing the Cu(100) surface and then exposing the surface to chiral 2-butanols. During heating to 300 K the 2-butanols are deprotonated by the oxygen to form 2-butanoxy groups bound to the Cu(100) surface. The water generated by the deprotonation reaction desorbs from the surface. The coverage of the 2-butanoxy groups is dictated by the initial coverage of oxygen on the Cu(100) surface. These 2-butanoxy groups are stable on the Cu(100) to temperatures of ~ 370 K at which point they decompose by β-hydride elimination to form methyl-ethyl ketone (Figure 1). Cu(100) surfaces templated with varying coverages of R- and S-2-butanoxy groups have been prepared. The important point about templating the Cu(100) surfaces with chiral 2-butanoxy groups is that chiral probes such as R- and S-propylene oxide can be reversibly adsorbed and then desorbed from the surface without disturbing the 2-butanoxy template layer. Enantioselective adsorption and desorption can then be studied by comparing adsorption of the two enantiomers of the propylene oxide probe on the same 2-butanoxy template overlayer.

Adsorption and desorption of R- and S-propylene oxide from the clean Cu(100) surface and the Cu(100) surface with an adsorbed layer of 0.15 ML of 2-butanoxy groups has been shown to be reversible. On the clean Cu(100) surface the propylene oxide desorbs at ~230 K. Enantioselectivity is expected when comparing the desorption R- and S-propylene oxide from the Cu(100) surface templated with R-butanoxy groups. Similarly, enantioselectivity is expected when comparing the adsorption of R-propylene oxide on the Cu(100) surfaces templated with R-2-butanoxy and S-2-butanoxy. Enantioselectivity can be observed as differences in the desorption kinetics or in the coverages of propylene oxide adsorbed at a given exposure.

Our measurements of propylene oxide desorption at coverages of 0.15 ML of the 2-butanoxy template have not revealed enantioselectivity. This is consistent with the measurements of Tysoe *et al*. made on the Pd(111) surface. Based on those prior measurements we expect to observe enantioselective adsorption of propylene oxide at higher coverages of 2-butanoxy. Adsorption and desorption of R- and S-propylene oxide on the Cu(100) surfaces with coverages of the 2-butanoxy template in the range 0.15 – 1 ML are currently being made.

Modification of the chromatography apparatus with a column based on Cu powder is nearly complete. This system has been design to allow in-situ treatment of the Cu powder to clean its surfaces by oxidation in O_2 and reduction in H_2 followed by treatment

with low pressures of amino acid vapors in flowing He. STM measurements on the Cu(100) surface have shown that adsorption of *l*-lysine followed by appropriate heating results in the faceting of the Cu(100) plane into naturally chiral Cu(3,1,17) planes. The chirality of the lysine dictates the handedness of the {3,1,17} facets exposed at the surface. Similar treatment of the Cu powder surface will be performed to create homochiral facets. Subsequently, the Cu powder in the column will be tested as a stationary phase for separation of racemic mixtures.

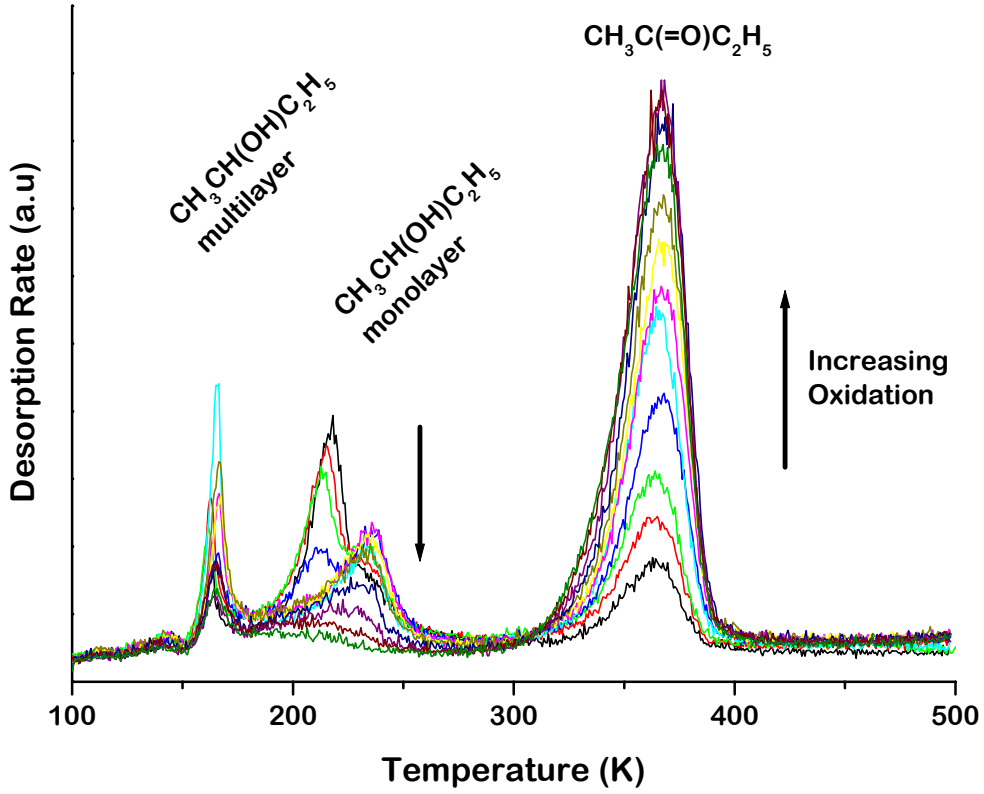

Figure 1. Temperature programmed desorption spectra of R-2-butanol on preoxidized Cu(100) surfaces. Increasing the amount of pre-oxidation increases the amount of R-2-butanoxy on the surface. This desorbs by decomposing to methylethyl ketone at 370 K. Oxidation of the surface reduces the fraction of R-2-butanol that desorbs molecularly at 220 and 240 K.

V. Gogonea

Electrostatic coupling Hamiltonian for hybrid quantum mechanical molecular mechanics calculations

Pradip Biswas,[1] J. Shy,[1] Kiran Tatapudi,[1] Jiansen Niu,[1] Mekki Bayachou, Valentin Gogonea[1,2]*

[1]*Department of Chemistry, Cleveland State University, 2121 Euclid Avenue, Cleveland, OH 44115*
[2]*Department of Immunology, Lerner Research Institute, Cleveland Clinic Foundation, 9500 Euclid Avenue, Cleveland, OH 44195*

Abstract
Studying the reactivity of Nitric Oxide Synthase (NOS) by exploring the potential energy surface (PES) of heme-mediated ariginine oxidation in NOS environment requires the use of a quantum mechanical (QM) - molecular mechanics (MM) methodology. After a careful examination of the QM/MM capable computational programs available in the computational chemistry community, we decided the create an interface between two well known and freely distributed computational software: the QM code CPMD (Car-Parrinello molecular dynamics (ref)) and the MM-molecular dynamics code Gromacs (Groningen Machine for Chemical Simulations (ref)). During this development phase we tried to address some difficulties that most of QM/MM methods share, that is, the treatment of electrostatic interactions between the QM and MM regions. Thus, we propose a renormalized electrostatic coupling Hamiltonian for a hybrid quantum mechanical (QM) molecular mechanical (MM) calculation. To remedy the divergent QM/MM Coulomb interaction at short-range arising from a point charge description of the MM-atom, we employ a localized Slater-function charge distribution for the point charge, extended over the covalent radius, r_c, of the atom. The resulting potential describes that, at short distances, large scale cancellation of Coulomb interaction arises *intrinsically* from the spatial distribution of the charge, and the potential self consistently reduces to $1/r_c$ providing a *renormalization* to the Coulomb potential near r_c. This effectively deters the electronic density of the QM system from unphysical polarization around MM charges. Employing this renormalized Hamiltonian, we perform QM/MM calculations on water dimer, imidazole carbon monoxide (CO) compound, and heme-CO compound with a thiolate group interacting with an imidazole. This development is crucial for performing QM/MM calculations on NOS enzyme.

Structure-function relationships in Pd-Au catalysts

K. Luo, C.-W. Yi, T. Wei, D. Kumar, M.-S. Chen, Z. Yan, Y. Cai, and D. W. Goodman
Department of Chemistry
Texas A&M University
College Station, TX 77842- 3012

Model mixed-metal catalysts consisting of Pd alloyed with Au as bulk films on refractory metal single crystals and as nanoparticles supported on oxides have been characterized using an array of surface techniques including X-ray photoemission spectroscopy (XPS), low energy ion scattering spectroscopy (LEIS), Auger electron spectroscopy (AES), low energy electron diffraction (LEED), infrared reflection absorption spectroscopy (IRAS), metastable impact electron spectroscopy (MIES), scanning tunneling microscopy (STM), temperature programmed desorption (TPD), and reaction kinetics. The surface sensitivity of LEIS and IRAS has been exploited for elucidating atomic composition of the outermost surface layer. Of special interest is the composition of the surface compared to the overall composition, particularly in transitioning from planar surfaces to nanoparticles, in the presence and absence of adsorbates. The mechanistic details of the vinyl acetate synthesis reaction, used to probe the structure-function relationship of these alloy surfaces, will also be discussed.

NMR and Computational Studies of Solid Acidity
DOE Grant Number

Collaborator: John B. Nicholas (Neurionpharma, Pasadena, CA)

Students: Saifudin Abubakar (Graduate), Philip Kletnieks (Graduate), Ching-Yeh Chen (Graduate), David Marcus (Graduate), Miranda Hayman (Graduate), Mark Wildman (Undergraduate), Kelly McLauchlan (Undergraduate), Yoni Blau (Undergraduate)

Department of Chemistry, University of Southern California, Los Angeles, CA 90089, (213) 740-1022, jhaw@usc.edu

Goal

This project has focused very strongly on the further elucidation of the mechanisms of reactions on solid acid catalysts, especially zeolites. Such reactions include methanol-to-hydrocarbon catalysis, both methanol-to-olefin (MTO) and methanol-to-gasoline (MTG), but the emphasis is moving toward simpler (ideally elementary) reactions that are better suited to decisive theoretical modeling. The modification of zeolite catalysts with well-defined nano-scale materials possessing Lewis acidity or other interesting properties (e.g. metal oxides) that will significantly alter the catalytic properties of the materials is another central focus of the project.

Recent Progress

Elementary Steps in Acid Catalysis: The most simple reaction with an observable effect on product distribution is H/D exchange. In certain cases H/D exchange on solid acids clearly takes place as a single elementary step. In superficially straightforward cases that we have examined recently H/D exchange has proven to involve multiple and even variable numbers of elementary steps that vary in importance with partial pressure, temperature, and solid acid catalyst. Consider the case of propene undergoing going fairly simple acid catalyzed reactions. Figure 1a shows mass spectra of the H/D exchange product obtained from 1 μL pulses of propene on D[Al]ZSM-5, D[B]ZSM-5, and DSAPO-34, respectively, all with a catalyst bed temperature of 573 K. Comparing these mass spectra, one notes that all six protons on propene underwent extensive H/D exchange on D[Al]ZSM-5, but exactly five (and not six) underwent H/D exchange on the boron analog of the zeolite, D[B]ZSM-5. On the silico-aluminophosphate catalyst DSAPO-34, an intermediate result was obtained. Figure 1c explores the temperature dependence of propene H/D exchange on the DSAPO-34 catalyst using 1 μL pulses to approximate the limit of very low propene partial pressure under transient conditions. One notes that at the lowest temperature studied, 473 K, H/D exchange was clearly incomplete for the contact time used, and a distribution between d_0 and d_5 resulted. At 523 K the product was almost entirely propene-d_5, and the molecular ion of this molecule, at m/e 47, can loose either a proton to yield m/e 46 or a deuteron to yield m/e 45. Increasing the catalyst bed temperature increases the rate of propene-d_6 formation.

Metal Oxide Functionalized Acidic Catalyst: Figure 2 is an illustrative example of one of the promising routes that we are realizing in the synthesis of new zeolite catalysts with controlled properties and novel sites. Atoms of a normally divalent metal are introduced in the gas phase to a zeolite material with a low (controlled) acid site density such that it is initially captured as an M^{1+} complex with the framework base site. Controlled oxidation (with water, for example) regenerated the acid site but leaves the metal

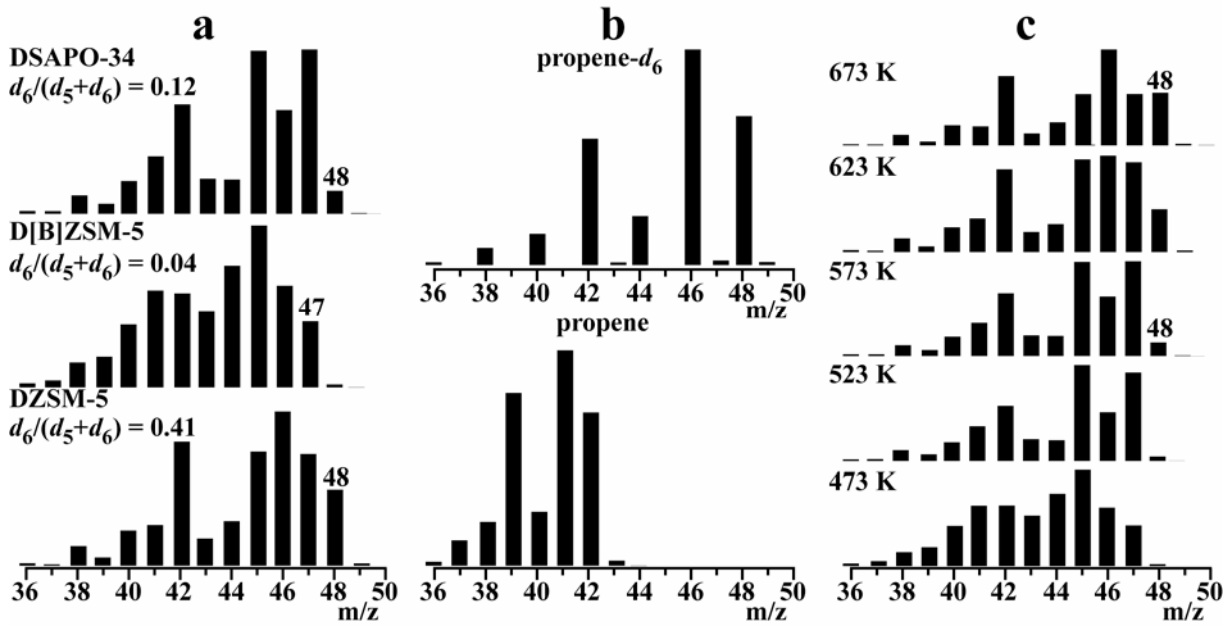

Figure 1. **(a)** Ion mass distributions of propene deuterated over DZSM-5, D[B]ZSM-5, and DSAPO-34 at 573 K and a loading of 1.0 µL propene on 200 mg deuterated catalyst beds. DZSM-5 gave the highest degree of deuteration, with ca. 41 % of the propene that has at least five deuteriums going all the way to propene-d_6. In contrast, on D[B]ZSM-5, only ca. 4 % of the propene that is at least d_5 is propene-d_6. Unlike DZSM-5, or even DSAPO-34, much of the propene is not even deuterated to d_5. On DSAPO-34, ca. 12% of the propene that is at least propene-d_5 went all the way to propene-d_6. **(b)** For comparison, the ion mass distributions of propene and propene-d_6. **(c)** Ion mass distributions of propene deuterated over a range of temperature at a loading of 1.0 µL propene per pulse on a 200 mg DSAPO-34 catalyst bed. There is a clear trend toward deuteration of the final proton position of propene-d_5 (m/z = 47) to propene-d_6 (m/z = 48) with increased temperature.

entrained as a highly dispersed species, ideally monomeric MO. The new catalyst has multiple functions, including the original Brønsted acidity, but also (potentially) Lewis acidity, basicicity, and steric modification by reduction in the dimensions of the cage or channel intersection in the vicinity of the original acid site. Examples of this catalyst type have been realized synthetically, and provocative catalytic results have been obtained in early testing.

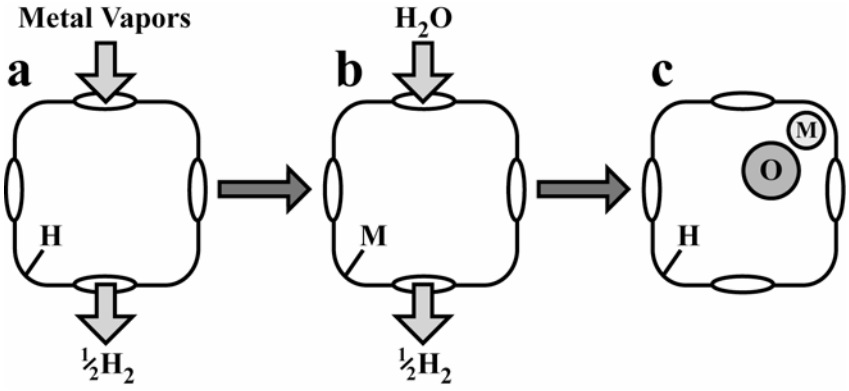

Figure 2. Schematic of controlled functionalization of acidic catalyst with metal oxides. **(a)** Unfunctionalized acidic catalyst cage i.e. HSAPO-34. **(b)** Modification of the acidic catalyst cage with volatile divalent metal vapors, e.g. cadmium, zinc, magnesium; to form univalent metal cation. **(c)** Controlled adsorption of water to regenerate the catalytic acid sites and form metal oxides in the catalyst cage.

DOE Interest

Fundamental study of catalytic reaction mechanism and the discovery of new catalysts and processes are central to progress in catalysis. Recent progress in methanol conversion catalysis has provided a clearer, molecular-level, understanding of zeolite (and zeotype) catalysis than has usually been possible in the past. In addition, the development and application of methodologies such as novel reactors, in situ spectroscopy, and theoretical study verified by experiment is useful in enabling other research.

Future Plans

As stated before, the emphasis is moving in the direction of fundamental studies of steps in acid catalysis that are amenable to theoretical modeling, and a renewal proposal emphasizing this work is in preparation.

Publications 2003 - 2005.

- Haw, J. F.; Marcus, D. M., "Well-Defomed (Supra)Molecular Structures in Zeolite Methanol-to-Olefin Catalysis", *Topics in Catalysis* **2005**, *34*, in press.
- Song, W.; Marcus, D. M.; Abubakar, S. M.; Jani, E.; Haw, J. F., "Trimethylsilylation of Framework Brønsted Acid Sites in Microporous Zeolites and Silico-aluminophosphates", *J. Am. Chem. Soc.* **2003**, *125*, 13964-13965.
- Chua, Y. T; Stair, P. C.; Nicholas, J. B.; Song, W.; Haw, J. F., "UV Raman Spectrum of 1,3-dimethylcyclopentenyl Cation Adsorbed in Zeolite H-MFI", *J. Am. Chem. Soc.* **2003**, *125*, 866-867.
- Song, W.; Haw J. F., Highlighted Communication: "Improved Methanol-to-Olefin Catalyst with Nanocages Functionalized through Ship-in-a-Bottle Synthesis from PH_3", *Angew. Chemie* **2003**, 42, 891-894.
- Haw, J. F.; Song, W.; Marcus, D. M.; Nicholas, J. B., "The Mechanism of Methanol to Olefin Catalysis", *Acc. Chem. Res.* **2003**, *36*, 317-326.
- Haw, J. F., Invited Feature Article: "Zeolite Acid Strength and Reaction Mechanisms in Catalysis", *Phys. Chem. Chem. Phys*., **2002**, *4*, 5431 - 5441.
- Song, W.; Nicholas, J. B.; Sassi, A.; Haw, J. F., "Synthesis of the Heptamethylbenzenium Cation in Zeolite Beta: *In Situ* NMR and Theory", *Catal. Lett.* **2002,** *81*, 49-53.
- Sassi, A.; Wildman, M. A.; Haw, J. F., "Reactions of Butylbenzene Isomers on Zeolite HBeta: Methanol-to-Olefins Hydrocarbon Pool Chemistry and Secondary Reactions of Olefins", *J. Phys. Chem. B.* **2002**, *106*, 8768-8773.
- Sassi, A.; Song, W.; Wildman, M. A.; Haw, J. F. "Methanol to Hydrocarbon Catalysis on Sulfated Zirconia Proceeds Through a Hydrocarbon-Pool Mechanism, *Catal. Lett.* **2002**, *81*, 25-31.
- Haw, J. F., Invited Feature Article: "Zeolite Acid Strength and Reaction Mechanisms in Catalysis", *Phys. Chem. Chem. Phys*., **2002**, *4*, 5431 - 5441.
- Marcus, D. M.; Song, W.; Ng, L. L.; Haw, J. F., "Aromatic Hydrocarbon Formation in HSAPO-18 Catalysts: Cage Topology and Acid Site Density", *Langmuir* **2002**, *18*, 8386-8391.
- Fu, H.; Song, W.; Marcus, D. M.; Haw, J. F., "Ship-in-a-Bottle Synthesis of Methylphenols in HSAPO-34 Cages From Methanol and Air", *J. Phys. Chem. B.* **2002**, *106*, 5648-5652.
- Song, W.; Marcus, D. M.; Fu, H.; Ehresmann, J. O.; Haw, J. F., "An Oft-Studied Reaction That Never Was: Direct Conversion of Methanol or Dimethyl Ether to Hydrocarbons on the Solid Acids HZSM-5 or HSAPO-34", *J. Am. Chem. Soc.* **2002**, *124*, 3844-3845.
- Sassi, A.; Song, W.; Wildman, M. A.; Ahn, H. J.; Prasad, P.; Nicholas, J. B.; Haw, J. F., "Methylbenzene Chemistry on Zeolite HBeta: Multiple Insights into Methanol to Olefin Catalysis", *J. Phys. Chem. B.* **2002**, *106*, 2294-2303.

Photocatalysis on a Model TiO_2 surface: Acetone on Rutile TiO_2(110)

Michael A. Henderson
Pacific Northwest National Laboratory, Richland, WA 99352

Although acetone is commonly used to evaluate the performance of oxide photocatalysts, little is known about the mechanistic details of its photo-oxidation. This study provides insights into the photodecomposition of adsorbed acetone using the (110) face of rutile TiO2 as a model photocatalyst. In the absence of UV light, acetone desorbs from the clean TiO2(110) surface without decomposition, exhibiting strong coverage-dependence in its temperature programmed desorption (TPD) peak that shifts from 350 K to below 250 K as the monolayer is populated. Acetone molecules desorbing at 350 K constitute about 0.25 ML and exhibit H/D exchange with surface hydroxyl groups. On the other hand, coadsorbed water displaces about 0.75 ML of the acetone monolayer into physisorbed states, but does not influence the remaining 0.25 ML that constitutes the 350 K TPD peak. These strongly bound acetone molecules are not associated with oxygen vacancies. Virtually no photodecomposition is observed in the absence of surface preoxidation or gas phase O2. Exposure to UV light in gas phase O2 results in conversion of acetone to acetate via cleavage of a carbonyl-methyl bond. Photodesorption measurements reveal that the methyl group is ejected from the surface, and reacts on the chamber walls to make formaldehyde. The acetone photodecomposition cross section increases with increasing acetone coverage, but decreases with coadsorbed water.

Density Functional Studies of Metcar Nanoparticles as Hydrodesulfurization Catalysts

Ping Liu, José A. Rodriguez and James T. Muckerman

Department of Chemistry, Brookhaven National Laboratory, Bldg. 555, Upton, NY 11973, USA

The destruction of S-containing molecules is a very important issue in the chemical industry and the control of environmental pollution. Elementary reaction steps and barriers for thiophene hydrodesulfurization (HDS) on metcar nanoparticles were investigated using density functional theory. It is found that that despite its high carbon concentration, metcars display a superior catalytic potential for hydrodesulfurization over the bulk carbides. Compared to the industrial catalysts, the hydrogen dissociation and C-S bond cleavage on metcars are more facile, and the removal of sulfur is energetically comparable. Our results also show that the catalytic activity of metcars can be associated with its unique structure that is quite different from that of bulk metal carbides.

Molecular Modeling of Inorganic and Polymer Supports for Molecular Catalysts

Chandrashekhar G. Sonwane, Andrew Swann, Peter J. Ludovice
School of Chemical & Biomolecular Engineering
Georgia Institute of Technology

In order to predict the effect of the support structure on the catalytic behavior of supported homogeneous catalysts, an accurate model of the support must exist. A poor model of the support will not allow the accurate prediction of the interaction of the molecular catalyst site with the substrate. This is particularly difficult when the structure of the supports is complex and contains various types of structural order. This is the case with the mesoporous silicates and polymers we have chosen to use as supports.

Mesoporous silicates such as SBA-15 have been chosen because they contain reproducible pores with a high surface area. While the mesopores are structurally regular the structure of the pore surface is complicated by the pseudo-amorphous structure of the interstitial silicates between the pores and the presence of micropores in the walls. By systematically manipulating the structural order in the interstitial silicate and the presence of micropores we have produced models that accurately reproduce diffraction and gas adsorption experiments on such materials. Using these models, we are now investigating the interaction of the catalyst sites with the pore walls to investigate the optimal structure of the supported catalyst system. We are also investigating the structure of poly(norbornene) produced by Ring Opening Metathesis Polymerization (ROMP) as a substrate. This polymer was chosen as a support because it is relatively ease with which catalyst sites can be bonded to it. Based on the polymer structure, we hypothesize that it adopts a conformation intermediate between the random coil and a rigid rod. The accessibility of catalyst sites tethered to this polymer would be very sensitive to such conformational behavior. Recent efforts have produced a symplectic MD code and force field to accurately reproduce the dynamics of this polymer. We are now investigating how this conformational behavior and hence catalyst site accessbility varies with the cis-trans ratio of the double bond in the polymer backbone.

Guest Exchange in a Nanoporous Fe-Ag System

Yixun Zhang, Banglin Chen, Frank R. Fronczek, and Andrew W. Maverick
Department of Chemistry, Louisiana State University, Baton Rouge, LA 70803

Reaction of the trigonal-planar node $Fe(Pyac)_3$ with $AgNO_3$ yields three types of crystalline product. With excess Ag, a ladder-type crystal with Fe:Ag = 2:3 is produced; its pores are filled with organic solvent/guest molecules. These guests can be exchanged in *single-crystal-to-single-crystal transformations* when the crystals are immersed in different solvents. Use of equimolar reactants yields a porous 1:1 "honeycomb" structure, or a less porous, interpenetrated 3D structure, depending on the polarity of the solvent mixture.

DE-FG02-01ER15267 **Andrew W. Maverick**

Inorganic-Organic Molecules and Solids with Nanometer-Sized Pores

Postdoc: Chandi Pariya
Graduate students: Christopher Sparrow, Yixun Zhang, and James Kakoullis Jr.

Contact: A. W. Maverick, Department of Chemistry, Louisiana State University, Baton Rouge LA 70803-1804; phone (225)578-4415;
email maverick@lsu.edu
website http://www.chem.lsu.edu/htdocs/people/awmaverick/research.htm

Goal

We are constructing porous inorganic-organic hybrid molecules and solids that contain coordinatively unsaturated metal centers.

Recent Progress

We have prepared extended-solid and molecular porous materials based on multifunctional β-diketone ligands, and studied their host-guest chemistry.

(a) Extended solids

These materials are constructed by using $M(Pyac)_2$ (see Figure 1) or $M(Pyac)_3$ as building block. We previously reported the chemistry of the rod-shaped building block $Cu(Pyac)_2$ with other metals: with Cd^{2+}, 1D and 2D porous materials are produced.

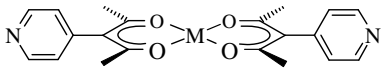

Figure 1. The"rod"-shaped molecule $M(Pyac)_2$.

As an alternative "building block" we have used the iron(III) complex $Fe(Pyac)_3$. Its three pyridine N atoms are in an approximately trigonal arrangement around the Fe atom. Although this species is coordinatively saturated, it can still be used to construct porous materials. Reaction with $AgNO_3$ produces two nanoporous bimetallic crystalline solids: a 1:1 "honeycomb" structure (**AgFe**, Figure 2), and a 2:3 structure containing 1-D "ladders", $[Fe(Pyac)_3]_2[AgNO_3]_3(solvent)_x$ (**Ag_3Fe_2**$(solvent)_x$, Figure 3, next page). The crystal structure of the 1,2-dichlorobenzene adduct is shown; the guests can be replaced by several other aromatic guests *without disruption of the crystal structure*.

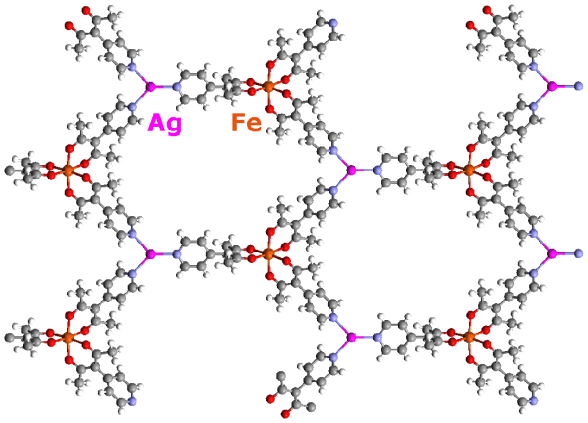

Figure 2. Structure of the 2D honeycomb M′MOF "**AgFe**".

(b) Molecular materials

We chose the *m*-phenylenebis(β-diketones shown in Figure 4, because they appeared to be well suited for the preparation of hexanuclear metal complexes. However, the only isolable product on reaction with Cu^{2+} is the molecular square! We attribute this unexpected product to entropic factors: as long as it is not too highly strained, the smaller oligomer is favored.

These new molecular square complexes react with various organic guests. The structure of the C_{60} adduct is shown. Binding of C_{60} results in a slight decrease in the Cu···Cu distances compared to the "empty" molecular square. We are now studying the effects of greater flexibility in ligands (R = Et etc.) on the solubility of the metal complexes, and the host-guest chemistry when other metals are used (e.g. Zn, Co).

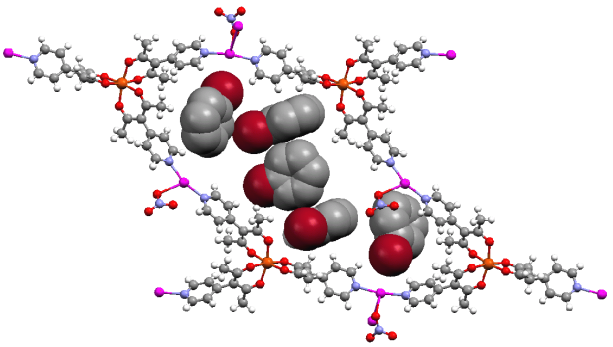

Figure 3. Structure of the 1D porous ladder M′MOF "Ag_3Fe_2", with C_6H_5Br guest molecules.

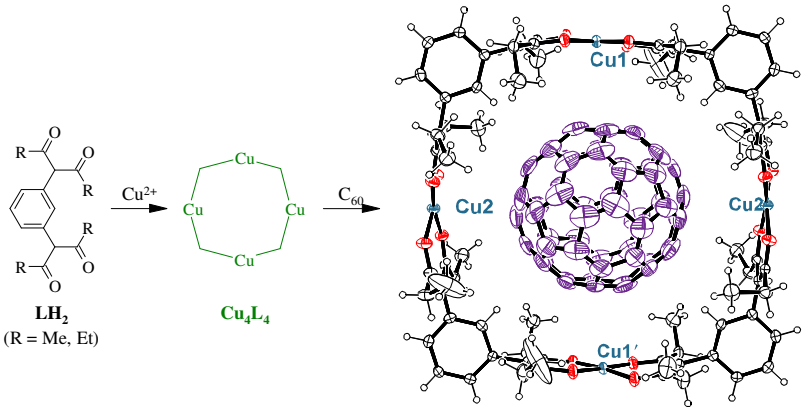

Figure 4. The *m*-disubstituted ligands L form *molecular-square* complexes Cu_4L_4 with Cu^{2+}. These bind organic guests including C_{60} (see ORTEP drawing at right; Cu···Cu 14.1 Å).

(c) New multifunctional ligands

We have recently synthesized the new multidentate β-diketone ligands shown in Figure 5, and we are now preparing their metal complexes. The tris- and tetrakis(β-diketones) are expected to yield polyhedral and network-solid metal complexes. The phosphine-β-diketone $Pphac_3H_3$ is of special interest because its P atom is expected to bind to noble metals (e.g. Rh) while its O atoms coordinate to harder metals. The result should be supramolecular structures that contain embedded Rh sites, for application as sterically selective catalysts.

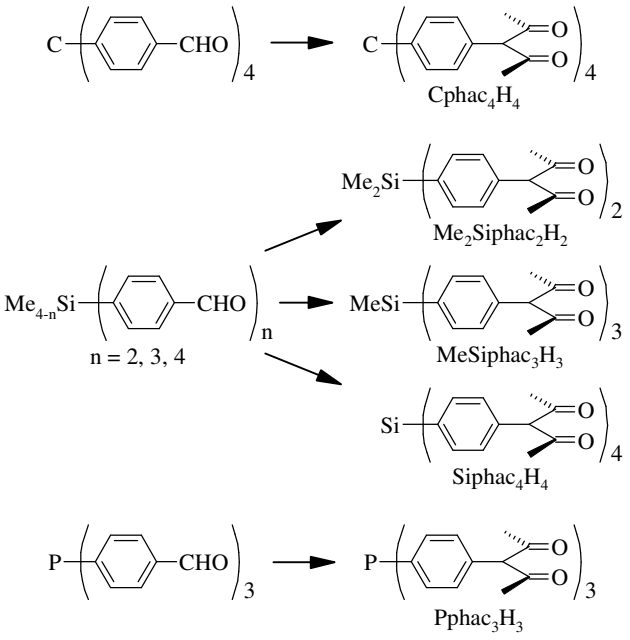

Figure 5. Newly prepared bis-, tris-, and tetrakis(β-diketones.

DOE Interest

We expect to use the approaches outlined here to prepare new porous molecules and solids that expose reactive metal sites to the interiors of enclosed cavities and channels. Possible applications of the resulting materials include sensors, thin-film membranes for separations, and catalysts, all of which may derive improved selectivity from the placement of the active metal sites inside the cavities.

Future Plans

For the expended-solid species, we are now working toward porous materials that have both exposed M sites and the ability to exchange guest molecules while maintaining structural integrity. We are also exploring new techniques for preparing and interconverting our supramolecular materials, and approaches for incorporating catalytic sites into the structures.

Publications

"Solvent-dependent 4^4 square grid and $6^4.8^2$ NbO frameworks formed by $Cu(Pyac)_2$ (bis[3-(4-pyridyl)pentane-2,4-dionato]copper(II))"; Chen, B.; Fronczek, F. R.; Maverick, A. W. *Chem. Commun.* **2003**, 2166-2167.

"3-(4-Cyanophenyl)pentane-2,4-dione and its copper(II) complex"; Chen, B.; Fronczek, F. R.; Maverick, A. W. *Acta Crystallogr., Sect. C*, **2004**, *C60*, m147-m149.

"Porous Cu-Cd mixed-metal-organic frameworks constructed from $Cu(Pyac)_2$ (bis[3-(4-pyridyl)pentane-2,4-dionato]copper(II))"; Chen, B.; Fronczek, F. R.; Maverick, A. W. *Inorg. Chem.* **2004**, *43*, 8209-8211.

"Flexible cofacial binuclear metal complexes derived from α,α′-bis(salicylimino)-*m*-xylene"; Maverick, A. W.; Laxman, R. K.; Hawkins, M. A.; Martone, D. P.; Fronczek, F. R. *Dalton Trans.* **2005**, 200-206.

(Two others in preparation)

Alloy Catalysts Designed from First-Principles

Manos Mavrikakis
Dept. Chem. Eng., University of Wisconsin – Madison
Madison, WI 53706-1691

The rational design of pure and alloy metal catalysts from fundamental principles has the potential to yield catalysts of greatly improved activity and selectivity. A promising research area in this field concerns the role that Near-Surface Alloys (NSAs) can play in endowing surfaces with novel catalytic properties. NSAs are defined as alloys wherein a solute metal is present near the surface of a host metal in concentrations different from the bulk; here, we use Density Functional Theory to introduce a new class of these alloys that can yield superior catalytic behavior for hydrogen-related reactions. Certain of the NSA's bind atomic hydrogen (H) as weakly as the noble metals (Cu, Au) while, at the same time, dissociating H_2 much more easily. This unique set of properties may permit these alloys to serve as low-temperature, highly selective catalysts for pharmaceuticals production and as robust fuel cell anodes.

First-Principles Study of Ti-Catalyzed Hydrogen Chemisorption on an Al Surface: A Critical First Step for Reversible Hydrogen Storage in $NaAlH_4$

Santanu Chaudhuri and James T. Muckerman

Complex metal hydrides are perhaps the most promising hydrogen storage materials for a gradual transformation to a hydrogen-based economy. We have used a computational approach to aid the ongoing experimental effort to understand the reversible hydrogen storage in Ti-doped $NaAlH_4$ and propose a plausible first step in the rehydrogenation mechanism. The study provides insight into the catalytic role played by the Ti atoms on an Al surface in the chemisorption of molecular hydrogen and identifies the local arrangement of the Ti atoms responsible for the process. Our results can potentially lead to ways of making other similar metal hydrides reversible.

Surface Chemistry Related to Heterogeneous Catalysis

Co-Investigators: Steven H. Overbury, Jun Xu
Post Docs: Shannon Mahurin, Jing Zhou

Chemical Sciences Division, Oak Ridge National Laboratory, Oak Ridge, TN 37831-6201
mullinsdr@ornl.gov

Goal

The long-range goal of this program is to develop a detailed understanding of how the interactions between a reducible oxide support and supported metals control the mechanisms of reactions they catalyze. The focus is on well-characterized model surfaces and on particular redox reactions (e.g. CO, ethylene or ammonia reacting with O_2, NO or NO_2,) which are likely to involve oxygen exchange with the oxide support. Detailed reaction mechanisms are determined by spectroscopy of surface species and mass spectral analysis of products.

Recent Progress

During the past year we have focused on how a related series of molecules interact directly with a cerium oxide surface and then how the presence of Rh nanoparticles on the ceria alters that interaction. We have examined H_2O, CH_3OH, H_2S and CH_3SH. By breaking an O-H or S-H bond, these molecules can interact with the ceria increasing their adsorption energy and forming new reaction products.

Interactions of –OH and –SH Groups with Cerium Oxide: The adsorption and reaction of CH_3OH, CH_3SH and H_2S on oxidized and reduced cerium oxide films was studied by temperature programmed desorption (TPD), soft x-ray photoelectron spectroscopy (SXPS) and near-edge x-ray absorption fine structure (NEXAFS). CH_3OH was a very effective reductant producing H_2O and CH_2O. H_2S also removed lattice O by producing H_2O but it left the S behind. CH_3SH did not interact strongly with the oxidized film. The formation of H_2O at 200 K, and the similarity of the O 1s spectra for CH_3OH, H_2O and H_2S on CeO_2 suggest that water may adsorb dissociatively on CeO_2 and then recombine at low temperature.

All of the molecules reacted with a reduced surface by breaking an OH or SH bond and forming a stable species on the surface. CH_3O decomposed to form CO and H_2 at elevated temperatures while CH_3S reacted with surface hydroxyls to form CH_4. The decomposition of CH_3SH on reduced CeO_X is much more selective than its decomposition on metal surfaces.

Adsorption of Formaldehyde on CeO_X: Adsorption of CH_2O on CeO_x was studied by TPD, SXPS and NEXAFS. The adsorption states, reactions pathways and intermediates were identified. These experiments were a critical complement to the CH_3OH work since CH_2O is a product from the oxidation of methanol on CeO_2 and the two adsorbates may have common intermediates during reaction. The surface spectrocopies clearly demonstrated that CH_3O was the principal intermediate formed from methanol and CH_2O_2 (dioxymethylene) was the

principal intermediate formed from formaldehyde. On a reduced CeO_X surface some of the dioxymethylene intermediates disproportionate to form formate and methoxy on the surface. These species decompose between 500 K – 600 K to produce CO and H_2.

Adsorption of Alcohol on Rh/ CeO_X: Adsorption of CH_3OH on CeO_2 was studied by reflection absorption reflection-absorption infra-red spectroscopy (RAIRS), TPD, SXPS and NEXAFS. The pathways of decomposition and desorption were determined as a function of temperature for reduced and fully oxidized cerium oxide both with and without Rh particles deposited on the surface. When Rh is present on CeO_2 the methoxy intermediates on the ceria produce CO and H_2 rather than CH_2O as occurs in the absence of Rh. On reduced CeO_X the presence of Rh results in a lower temperature decomposition of methoxy than on the Rh-free surface. The results indicate that Rh promotes the non-selective decomposition of CH_3O at the Rh-CeO_X interface. The decomposition appears to be the rate determining step and diffusion of methoxy on ceria to the Rh interface is rapid.

DOE Interest

A detailed understanding of the interactions between adsorbates, supported metals and oxide supports is related to many catalytic processes relevant to energy utilization including emission control, lean burn catalysis, and catalysts for fuel cells and hydrogen utilization.

Future Plans

Reaction Mechanisms and Rates on Rh / Ceria: Redox reactions will be studied by mixed gas exposures in UHV using the methodology of King and Wells. Products evolved during exposure will be analyzed as a function of surface temperature and incident gas ratio. Initially, experiments will focus on the CO+NO reaction. The reaction products and rates will be compared at low (10^{-5} torr) and high (1 torr) pressures. Reactions of model supported Rh/cerium oxide catalysts will be benchmarked to high surface area catalysts prepared using wet impregnation upon sol-gel prepared cerium oxide supports.

The end station for SXPS will be modified to permit simultaneous monitoring of surface species during the co-exposure in UHV. Results of co-exposure reactions will be combined with results of individual reactions in order to formulate a complete microkinetic model of the reaction mechanisms. Eventually other reductants such as ammonia and ethylene will be substituted for CO.

The Role of Lattice Oxygen in Reactions on Ceria: Reaction mechanisms on CeO_X will be studied by growing ceria thin films using isotopically labeled $^{18}O_2$. Ceria is a readily reducible oxide and its oxygen may be incorporated into reaction products occurring on its surface. The initial experiments will examine CH_3OH on CeO_X and Rh / CeO_X. Incorporation of ^{18}O into CH_2O or CO reaction products will indicate whether surface intermediates involving the lattice oxygen are involved in the reaction mechanism. This methodology will be incorporated into future experiments such as the redox experiments described above to differentiate the oxygen in the CO, NO and ceria in the reaction mechanism.

Correlation between Surface Structure and Chemical Activity: Scanning probe microscopy (SPM) will be used to examine the geometric and electronic structure of

metal particles deposited on cerium oxide supports. The effect of reduction of the cerium oxide support upon the structure of deposited Rh or Pt particles will be studied. This is of interest because previously it was shown that the reduction state of the ceria support affects dissociation reactions occurring on the metal particles, and SPM may be able to distinguish whether this is an effect of changes in geometric structure or of electronic modification of the metal particles. It is anticipated that it may be possible to image oxygen vacancies on oxidized and reduced CeO_2, and the location of the vacancies relative to metal particles will be examined. The effect of reductants such as methanol and ethylene which are known to lead to reduction of cerium oxide will be examined to determine whether vacancies cluster near metal particles. This is of interest to learn the process by which metals mediate reduction of the support and to look for encapsulation or structural rearrangements resulting from the reduction process.

First Principals Investigation of Adsorption and Reaction on Ceria: Computational studies will be initiated to study the chemistry of defective cerium oxide surfaces. Interactions of molecules (water and alcohol) and of molecular fragments (e.g. hydroxyls, methoxy) with structural defects on a CeO_2(111) surface will be examined. Rh clusters will then be added to study interactions between the two phases and learn how molecular adsorbates bond on the surfaces and interfaces of these two phases. The long range goal is to build computational capabilities to study reaction pathways such as those measured experimentally.

Publications (2003-4)

1. Xu, J and S. H. Overbury, "H_2 Reduction of CeO_2(111) Surfaces via Boundary Rh-O Mediation," Journal of Catalysis, 222 (2004) 167.
2. D. R. Mullins, "Adsorption of CO and C_2H_4 on Rh-Loaded Thin-Film Praseodymium Oxide", Surface Science, 556 (2004) 159.
3. W. T. Tysoe and D. R. Mullins, "Substituted Hydrocarbons on Metal Surfaces" in *Physics of Covered Solid Surfaces*, Vol. III / 42A3, H. P. Bonzel, ed., Landolt-Bornstein, pub., New York, 2003.
4. H. Piao, K. Adib, Z. Chang, H. Hrbek, M. Enever, M. A. Barteau and D. R. Mullins, "Multi-step reaction processes in epoxide formation from 1-chloro-2-methyl-2-propanol on Ag(110) revealed by TPXPS and TPD experiments", J. Phys. Chem. B, **107** (2003) 13976.
5. K. Adib, D. R. Mullins, G. Totir, N. Camillone III, J. P. Fitts, K. T. Rim, G. W. Flynn and R. M. Osgood, Jr., "Dissociative Adsorption of CCl_4 on the Fe_2O_3(111)-(2x2) Selvedge of alpha-Fe2O3(0001)", Surface Science, **524** (2003) 113.
6. M. H. Zhang, H. H. Hwu, M. T. Buelow, J. G. Chen, T. H. Ballinger, P. J. Andersen and D. R. Mullins, "Decomposition Pathways of NO on Clean and Oxycarbide-Modified W(111) Surfaces", Surface Science, **522** (2003) 112.

Probing the Effects of Surface Oxygen on Al_2O_3-Supported Platinum Nanoparticles

Laurent Menard, Joo Kang, Ralph Nuzzo *(University of Illinois at Urbana-Champaign)*

Using *in situ* x-ray absorption spectroscopy (XAS), we have studied the adsorption of molecular oxygen on Pt nanoparticles supported on γ-alumina. The purpose of these investigations was to probe the effects of adsorbate perturbations on the structure of the supported nanoparticles. Specifically, the effect on Pt-Pt bond lengths and disorder in the nanoparticles was investigated with extended x-ray absorption fine structure (EXAFS) measurements. Oxidation at room temperature and at 350°C resulted in significant changes in the Pt-Pt coordination shells for samples of 0.5 wt%, 1 wt%, and 5 wt% Pt on γ-Al_2O_3. Interestingly, the behavior observed under these conditions differed greatly depending on the sample examined. Quantitative EXAFS fitting and electron microscopy studies were performed to ascertain the origin of these differences and understand the implications of cluster size and structure on adsorption processes.

Additional studies were performed on 1 wt% Pt on Al_2O_3 samples that further varied the oxidation temperature to include a range of reactive conditions in which oxygen was chemisorbed on the platinum surface in varying amounts up to temperatures driving the formation of surface Pt oxide species. EXAFS measurements were made at a number of temperatures over which these phases were stable to analyze the contributions of static and thermal disorder to the Debye-Waller disorder parameter. These measurements establish metal nanoparticles as systems that interact dynamically with adsorbates not only in the formation of metal-adsorbate bonds but also in the effects that such interactions have on the metal-metal coordination, bond lengths, and disorder of the nanoparticles.

On factors influencing diffusion and reaction of molecules on nanostructured surfaces

Talat S. Rahman
Kansas State University
DE-FG03-03ER15465

With the long term DOE interest in understanding, modeling, and controlling chemical reactivity and energy transfer processes on surfaces for energy-related applications in mind, we are carrying out systematic studies of factors that are expected to control diffusion and reaction of molecules on nanostructured surfaces. These calculations are based on density function theory with the general gradient approximation for the exchange correlation term. In this presentation the impact of four factors on selected chemical reactions will be considered: undercoordinated sites on oxide surfaces, alkali coadsorption, presence of steps, and the nature of the elemental metal.

Oxide surface: Experiments suggest that while $RuO_2(110)$ is a highly reactive surface for CO oxidation, the same is not the case for NO adsorbed on this surface. Our results confirm that NO like CO sits on-top of Ru-cus for 1 ML coverage, but while CO oxidizes easily on this surface because of an attractive interaction with O on the neighboring bridge site, NO experiences a repulsive interaction with this O atom and does not form NO_2. Detailed analysis of the coverage dependent surface electronic structure, including the activation energy barriers, charge transfer, charge density distribution and local electronic density of states together with its hybridization will be presented to compare and contrast the energetics, diffusion and vibrational dynamics of CO and NO on $RuO_2(110)$.

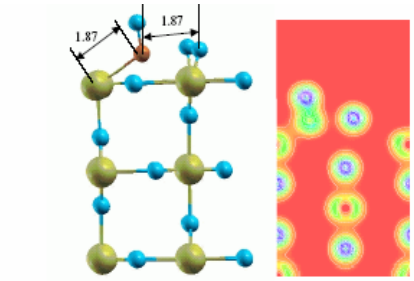

Ball and stick model accompanied with charged density plot showing the interaction of NO with O (bridge) on $RuO_2(110)$. *Repulsive* interaction found between NO and O^{bridge} at bond lengths d(N-O) = 1.16 Å, $d(N\text{-}O^{bridge})$ = 1.87 Å.

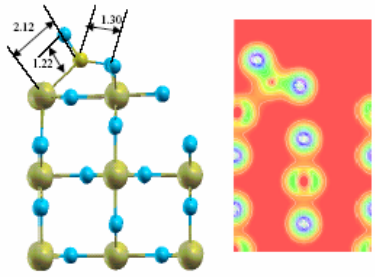

Ball and stick model accompanied with charged density plot showing the oxidation of CO with O (bridge) on $RuO_2(110)$. Attractive interaction found between CO and O^{bridge} at bond lengths d(C-O) = 1.22 Å and $d(C\text{-}O^{bridge})$ = 1.30 Å.

Alkali coadsorption: In efforts to understand and predict factors that may enhance and/or channel the diffusion and reactivity of molecules on metal surfaces, we have carried out *ab initio* electronic structure calculations of the dynamics of CO and O_2 on Cu(111) and Pd(111) in the presence of alkali co-adsorbates. A large softening in the vibrational frequencies of these molecules is found as they approach the metal surface and even before adsorption, as a result of strong enhancement of electronic polarizability induced by the alkali atoms. Related calculations of the changes in the diffusion barriers for CO on Cu(111) in the presence of K were performed to motivate experiments by Bartels and Heinz groups on the system. The dependence of the results on adsorbate coverage will also be examined.

As a step towards understanding the relative role of *steps* and *elemental metal* in a specific chemical reaction, we have calculated adsorption energies (E_{ad}), diffusion barriers and the first dissociation barriers (E_1) for NH_3 on the Ni(111), Pd(111), Ni(211) and Pd(211). The top sites are found to be

preferred for NH_3 adsorption on Ni(111) and Pd(111) and the diffusion barrier is substantially higher for Pd(111) than for Ni(111). We also find that during the first dissociation step (NH_3 => NH_2 +H) on Ni(111), NH_2 moves from the top site to the nearest hollow site, while on Ni(211) it moves from the initial top site at the step edge to the bridge site on the same step chain. H is found to occupy the hollow sites for both surfaces. For the reaction on Ni(111), the adsorption energy is found to be lower that the dissociation energy by 0.23 eV, while at the step of Ni(211), E_1 and E_{ad} are almost equal to each other. This suggests that the molecule will rather desorb than dissociate on Ni terrace, but dissociate at the step. Further, the NH_3 => NH_2 + H dissociation barrier at the step of Pd(211) is found to be higher (by 0.6 eV) than the NH_3 desorption energy and also the dissociation barrier on Ni(211). These differences in the barriers may explain why the NH_3 decomposition rate on Pd is much lower than on Ni.

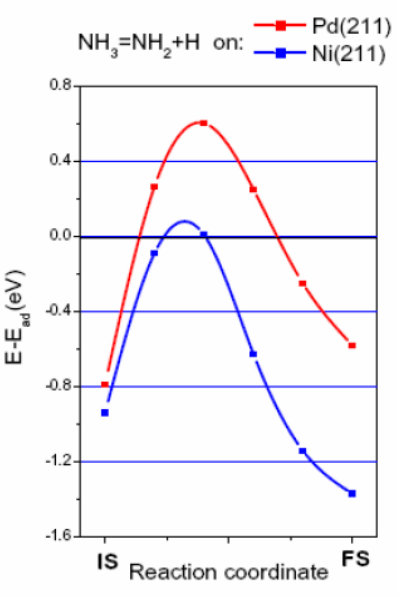

Although the last stage of the NH_3 decomposition (nitrogen recombinative desorption 2N => N_2(gas)) has very high activation barrier (1-2 eV) and hence has been proposed to be a rate limiting stage, our findings show the importance of the NH_3 => NH_2 + H reaction step.

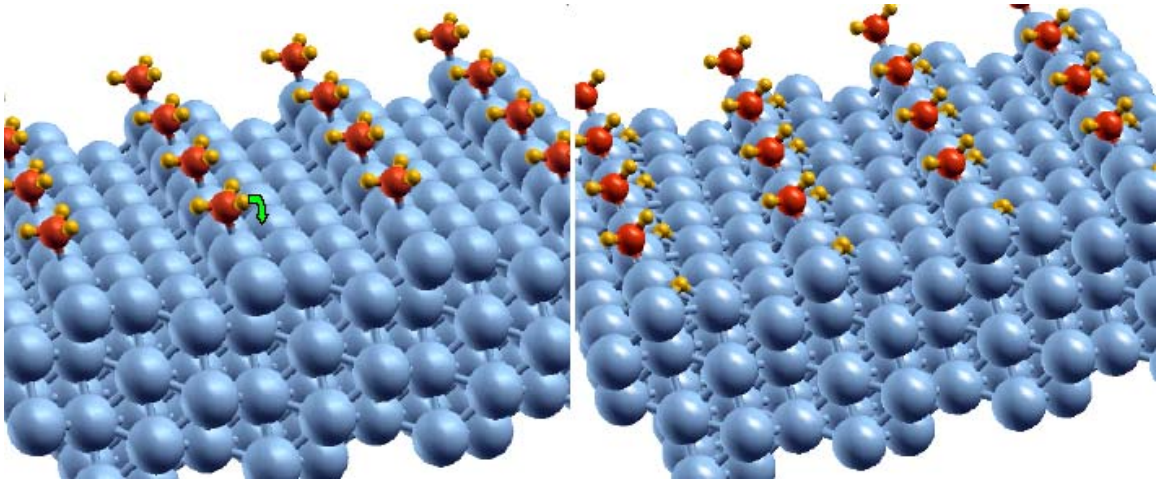

Initial and final states for the NH_3 => NH_2+H dissociation on the step of Ni(211).

Towards an Understanding of the Re/alumina Catalysts: Theory, Simulations, and X-ray Spectroscopy Experiment

F. Vila[1], J. J. Rehr[1], and S. R. Bare[2]
[1] *Department of Physics, University of Washington, Seattle, WA 98195*
[2] *UOP LLC, Des Plaines, IL 60017*

We discuss an approach toward the understanding of Re/g-Al2O3 catalysts based on a combination of ab initio theory and simulations and modern x-ray spectroscopy experiments. We carry out density functional theoretic (DFT) calculations to determine the structure of isolated Re Clusters and the preferred interaction sites for single Re atoms on g-Al2O3. From this we determine the preferred Re interaction sites on g-Al2O3. With this theoretical structure information we investigate the predicted variation of the XANES spectra of Re clusters, interacting with the Al2O3 surface, using the ab initio FEFF8 code. The results are compared with experimental results for the structure, based on x-ray absorption spectra. These yield the local atomic structure of an oxidized Re catalyst and the local atomic structure of a reduced Re catalyst. We also study the variation of the atomic structure with experimental conditions. Finally details of the electronic structure of the catalysts are interpreted using theoretical results from the FEFF8 code.

In situ Time-resolved Characterization of Cu-CeO_2 Nanocatalysts during the Water Gas Shift Reaction

José A. Rodriguez[1*], Xianqin Wang[1], Jonathan C. Hanson[1], Daniel Gamarra[2], Arturo Martínez-Arias[2] and Marcos Fernández-García[2]
[1]*Chemistry Department, Brookhaven National Laboratory, Upton, NY, 11973 (USA)*
[2]*Instituto de Catálisis y Petroleoquímica, CSIC, Campus Cantoblanco, 28049 Madrid (Spain)*
*rodrigez@bnl.gov

Introduction

A big challenge within the world demand for energy is the need to protect our environment by increasing energy efficiency and through the development of "clean" energy sources. Hydrogen is a potential answer to satisfying many of our energy needs while reducing (and eventually eliminating) carbon dioxide and other greenhouse gas emissions. The water–gas shift (WGS) reaction ($CO + H_2O = CO_2 + H_2$) is used in industrial hydrogen production as well as in fuel processing for fuel cell applications. CeO_2-based nanocatalysts have been reported to be very promising for the WGS reaction. Among these materials, the two most studied systems currently are Cu- and Pt-based catalysts[1]. It is anticipated that, with proper development, metal promoted ceria nanocatalysts should realize much higher CO conversions than even commercial CuZnO catalysts. However, the roles played by ceria and the metal in the WGS reaction are still a matter of debate. The redox properties and oxygen storage capacity of ceria is usually claimed, while the metal plays a direct role in the mechanism of the WGS reaction [2]. In order to clarify the debate, *in situ* time-resolved characterizations of the nanocatalysts under operational conditions are critical. To the best of our knowledge, no systematic studies have been reported examining the structural and chemical properties of Cu-CeO_2 nanocatalysts during the WGS reaction. In this work, synchrotron-based *in situ* time-resolved X-ray diffraction (TR-XRD) and time-resolved X-ray absorption fine structure (TR-XAFS) are employed to study the WGS reaction over Cu-CeO_2 catalytic systems.

Materials and Characterization Methods

The reference CuO, Cu_2O and Cu bulk samples used in this work were obtained from commercial sources (>99.99% purity). Two types of Cu-CeO_2 nanocatalysts were studied in this work: Cu impregnated ceria labeled as A% Cu/CeO_2 (A=1, 3, and 5; representing Cu weight loading amount per gram catalyst) and Cu doped ceria labeled as $Cu_xCe_{1-x}O_2$ (x= 0.05, 0.1 and 0.2; representing the Cu molecular amount). The Cu impregnated ceria samples were prepared by impregnation of the nano CeO_2 support with an aqueous solution of $Cu(NO_3)_2{\cdot}3H_2O$ (Merck, 99.5% purity), while the Cu doped ceria samples and the nano ceria support for the impregnated samples were prepared with a modified reverse microemulsion method [3].

The *in situ* time-resolved X-ray diffraction experiments were carried out on beam line X7B of the National Synchrotron Light Source (NSLS) at Brookhaven National Laboratory. A MAR345 detector was used to record X-ray patterns. The WGS reaction was carried out isothermally with a 5% CO and 95% He gas mixture at a flow rate of ~10 ml/min. Diffraction patterns were collected over the catalysts during the WGS reaction. The relative ratio of water vapor pressure to CO in the gas mixture was ~ 0.35. Cu K absorption edge XAFS spectra were collected *in situ* at beamline X18B with a similar condition to the experiments at X7B. The X-ray absorption spectra were taken repeatedly in the "fluorescence-yield mode" using a pips detector cooled with circulating water. The products from both TR-XRD and TR-XAFS experiments were measured with a 0-100 amu quadruple mass spectrometer (QMS, Stanford Research Systems).

Results and Discussion

Figure 1 indicates that copper in the impregnated samples underwent an oxidation state change from CuO to metallic Cu during the WGS reaction when the temperature increased from 200 to 300°C. Figure 2 shows the relative hydrogen concentrations in the products at different temperatures as a function of time for the samples of 5%Cu/CeO_2 and $Cu_{0.2}Ce_{0.8}O_2$, as well as the reference compound, CuO. The data were obtained while the TR-XRD patterns were collected at the same time. By comparison of the TR-XRD data in Figure 1 and the green curve in Figure 2 for 5% Cu/CeO_2 sample, it is clear to conclude that the activity of the catalysts was closely related to the formation of the metallic Cu. No activity was observed for all the samples when there was not a metallic Cu phase at low temperature (200°C). However, the high activity could not be obtained only on metallic copper as indicated from the CuO result in Figure 2. The ceria support played a role in the WGS reaction. The lower activity at 500°C than at 400°C for 5% Cu/CeO_2 in Figure 2 is possibly due to the sintering of ceria as indicated in Figure 1.

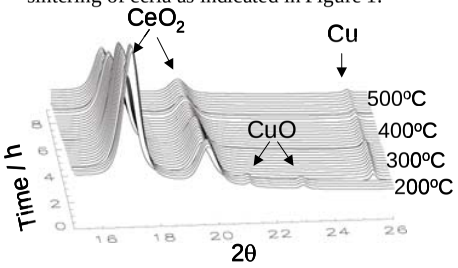

Figure 1. TR-XRD patterns for 5%Cu/CeO_2 catalysts during the WGS reaction.(λ=0.921Å)

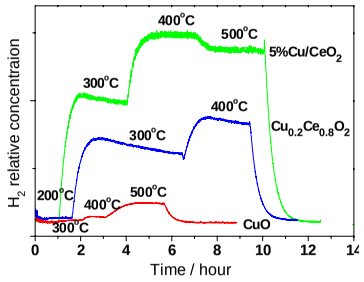

Figure 2. Relative H_2 concentrations in the products.

Significance

The *in situ* time-resolved studies for the Cu-CeO_2 nanocatalysts clarified the metallic Cu role and the ceria support function during the WGS reactions. We were able to determine the oxidation states of Cu under different reaction conditions.

References

1. Li, K., Fu, Q., Flytzani-Slephanopoulos, M., *Appl. Catal. B: Environmental*, 27(3), 179(2000)
2. Jacobs, G., Chenu, E., Patterson, P. M., Williams, L., Sparks, D., Thomas, G.; Davis, B. H., *Appl. Catal. A: General* 258(2), 203(2004)
3. Martínez-Arias, A., Fernández-García, M., Gálvez, O., Coronado, J. M., Anderson, J. A., Conesa, J. C., Soria, J., Munuera, G., *J. Catal.*, 195, 207(2000).

Theoretical Investigations in Transition-Metal Catalysis

John S. Sears and C. David Sherrill*

Center for Computational Molecular Science and Technology
School of Chemistry and Biochemistry
Georgia Institute of Technology

As part of a multi-disciplinary team of chemists and chemical engineers (including also the Jones, Weck, and Ludovice groups at Georgia Tech and the Davis group at Virginia), we are using electronic structure theory to shed light on previously unanswered questions in transition-metal catalysis. Over the last decade, metallated pincer systems have seen extensive interest for molecular catalysis due to their high catalytic activity and reportedly high stability at reaction temperatures. Together with our experimental collaborators, we have been able to demonstrate the instability of two common Pd-pincer systems. We have proposed a mechanism for the decomposition pathway and have used density functional theory to compute the reaction path for the initial steps of the decomposition. The calculations confirm that at reaction temperatures, the pincer arms can undergo ligand exchange with the amine base. Upon coordination of the metal by the base, the proposed decomposition mechanism involves β-hydrogen elimination from the amine to the metal center. The calculated barriers to exchange show the Pd-P bond to be much stronger than the Pd-S bond and are consistent with the relative stabilities of these two systems, although neither system is stable at reaction temperatures. In separate work, we are using high-level *ab initio* techniques to explore several questions surrounding the Mn(salen) catalytic systems that have seen such extensive experimental and theoretical investigation over the past few years. We have performed the first stability analysis on the Hartree-Fock wavefunctions for this system, and we find that some of them are *unstable* and *artifactual*, giving a possible explanation for the great discrepancies seen in previous theoretical work. We have also carried out computations using several popular density functionals, such as BP86 and B3LYP. Although the DFT approaches do not seem to suffer from the wavefunction instability problems of Hartree-Fock theory, each of the functionals gives a qualitatively different ordering for the spin-states of this system. This is shown to be dependent almost exclusively to the exchange treatment of the various functionals. We compare results from each of the employed functionals with high-level results from both single- and multi-reference methods. We have also investigated previously-unexplored low-lying excited states of this system which may have an impact on its catalytic activity.

DE-FG02-01ER15258 **Lawrence R. Sita**

Ferrocene-Based Nanoelectronics

Postdoctoral Associates Denis A. Kissounko, Laura Picraux
Graduate Students Chaiwat Engtrakul, Lixin Wang,
Collaborators Michael Fuhrer, Stephanie Getty, Harold Baranger

Department of Chemistry and Biochemistry, University of Maryland, College Park, MD 20742
lsita@umd.edu

Goal

Synthesize and investigate the conduction physics of a variety of proposed ferrocene diode / transistor designs in order to address the fundamental question; can electron transport within nm-length scale molecular structures be modulated in a controlled and reversible fashion?

Recent Progress

There remains considerable interest in the development of theories that can be used to qualitatively and quantitatively describe 'molecular conduction' through metal lead / molecule / metal lead (LML) heterojunctions. This talk will focus on the results of a collaboration arising from the fields of chemistry and physics to pursue the primary objective of experimentally recording the conduction physics of LML heterojunctions constructed from extended organometallic frameworks, and to successfully correlate the results of these studies with theoretical models of electronic structure as derived from state of art computational methodologies. Extended mono- and polynuclear organometallic frameworks incorporating transition metals as key structural units are chosen for study in order to test new design paradigms for achieving high transmission via transport through metal-centered low lying electronic states of the molecular bridge. Success has now been achieved for a monoferrocene incorporated into an electromigrated metal nanogap test structure (see Figure 1) where single-molecule transport measurements establish that conductance can exceed 70% of the quantum value, G_o (≈ 77 μS). Calculations using density functional theory (DFT) coupled with a nonequilibrium Green function (NEGF) provide theoretical support for the conclusion that the symmetrically disposed conductance resonances, and the unprecedented level of single-molecule conductance, originate with a low-lying molecular state of the system that can be brought into resonance by applying either a forward or reverse bias; in accordance with Landauer theory. Lineshape analysis (green line in Figure 1) was further used to establish that this high on-resonance conductance is associated with strong, symmetric molecule electrode coupling.

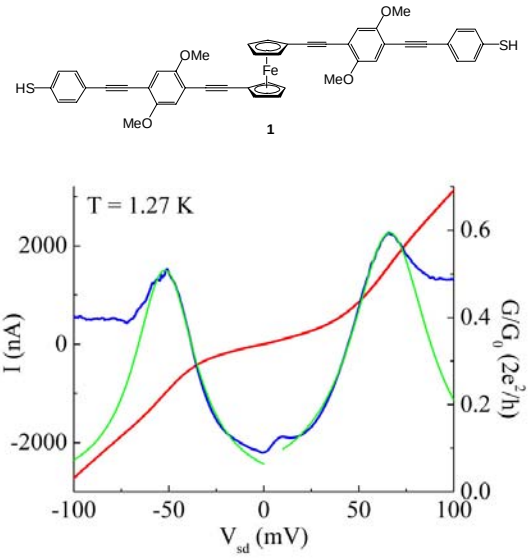

Figure 1. Single molecule conductance measurements for metal / molecule / metal heterojunctions derived from adsorbate **1**. Legend: (—) I / V, (—) G / V, (—) Lorentzian fit.

DE-FG02-ER15373-A000 **Larry G. Sneddon**

New Chemical Routes to Nanostructured Advanced Ceramic Materials via Metal Catalyzed Syntheses and Polymerization Reactions of Alkenylpolyboranes

Graduate Students: X. Wei, K. Forsthoefel, U. Kusari, J. Clapper, R. Butterick, Y. Li, C. Yoon

Department of Chemistry, University of Pennsylvania, Philadelphia, Pennsylvania 19104-6323, lsneddon@sas.upenn.edu

Goal. Develop new metal-catalyzed routes to single-source precursors to technologically important solid-state materials.

Recent Progress

Metal-Catalyzed Routes to Organodecaborane Polymers and Functional Polyboranes. As a part of our interest in the design of new polymeric precursors to non-oxide ceramics, we have been investigating the development of new general metal-catalyzed methods for the synthesis of polyborane polymers. We have shown that ruthenium-catalyzed ring opening metathesis polymerization (ROMP) of organodecaboranes containing cyclic-olefin substituents provides a new efficient route to poly(organodecaborane) polymers.

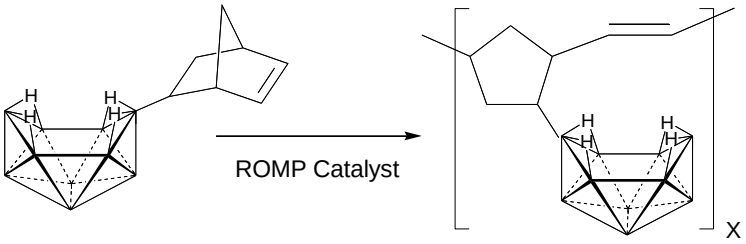

Other studies in our laboratory have also shown that the homometathesis and cross-metathesis of alkenylboranes catalyzed by Grubbs-type catalysts are efficient high yield methods for the synthesis of functional organopolyboranes.

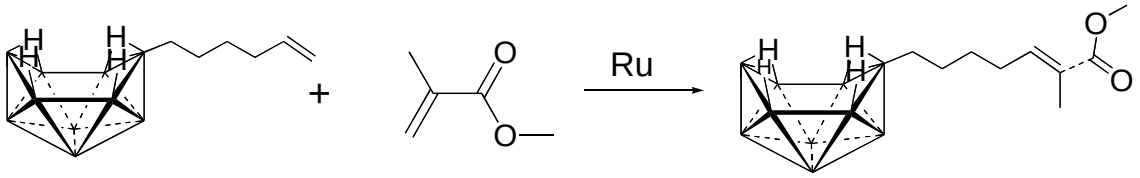

Organodecaborane Polymeric Precursors to Nanostructured Ceramics. Nanostructured ceramics have a number of potential applications, including uses as electronic and optical devices, structural reinforcements, and ceramic membranes for catalyst supports or gas separations. Achieving such ceramic structures requires the parallel development of both new, efficient precursors and new methods for the formation of materials on the nanoscale. We have now demonstrated that the new organodecaborane polymers described above are high yield processable precursor to boron carbide ceramics in processed forms.

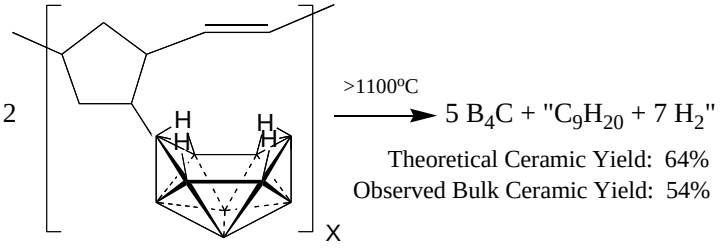

Likewise, we have shown that the formation of nonoxide ceramic nanofibers and nanocylinders can be achieved using organodecaborane polymers in conjunction with nanoporous alumina templating methods.

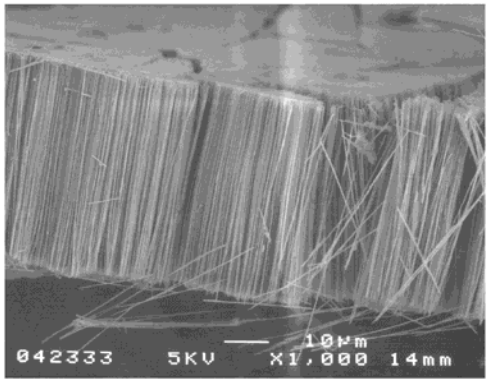

Boron Carbide Nanofibers

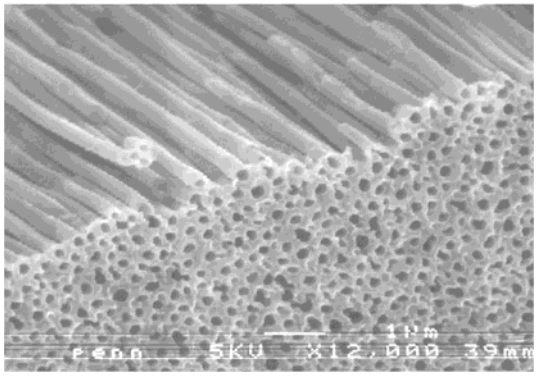

Boron Carbide Nanocylinders

Alumina templating methods are limited to small-scales and larger scale methods are needed if such materials are to be used in real applications. In collaboration with Harry Allcock's group at Penn State University, we have been investigating the use of electrostatic spinning as a method of producing non-oxide ceramics nanofibers on much larger scales. Electrostatic spinning, followed by pyrolysis, has already been shown to be an efficient and simple method to prepare fine fibers of carbon, silica, alumina-borate, titania, alumina, niobium oxide, and some composite fibers, but there has been no previous use of this technique to prepare nonoxide ceramic fibers.

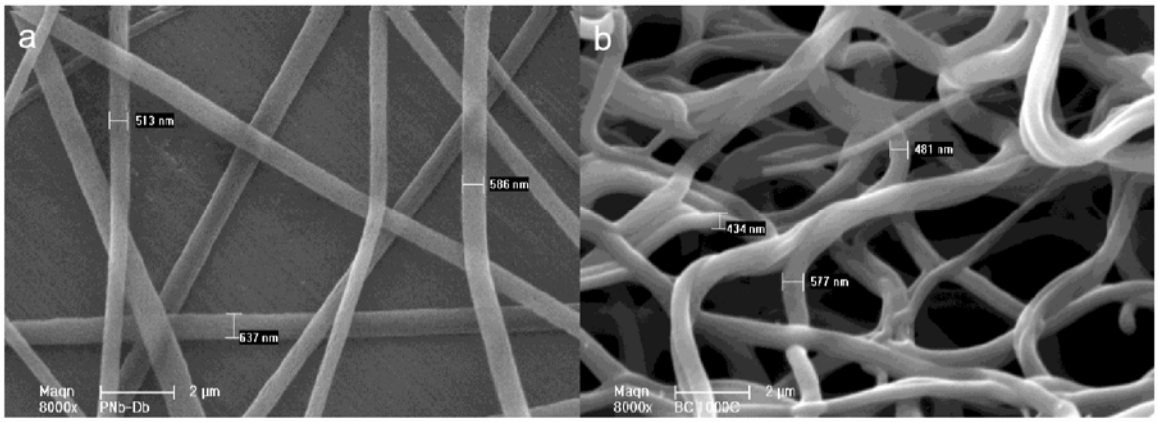

*SEM images of electrospun PND (**A**) and boron carbide (**B**) fibers obtained upon 1000°C pyrolysis.*

As shown in the SEM images in the above Figure, we have now found that solutions of the new poly(norbornenyldecaborane) (PND) polymer can be electrostatically spun to give non-woven mats of fine polymer fibers. Uniform cylindrical fibers with diameters from 500 to 650 nm were obtained from a 13 wt. % PND solution (**Figure A**). Subsequent pyrolysis of the PND polymer fibers then provided an efficient, large-scale route to non-woven mats of boron carbide nanoscale ceramic fibers (**Figure B**) with narrow size distributions. Both XRD and DRIFT analysis of these fibers showed the characteristic boron carbide patterns.

Future Studies. The results presented above clearly demonstrate that metal-catalyzed reactions are important new methods for the systematic formation of polyborane polymers. We will now explore the use of these reactions to produce more complex poly(organopolyborane) polymers and copolymers than possible with our previously developed methods. Due to the versatility of electrostatic spinning technique, this approach should now also prove useful with polymer blends to fabricate composite ceramic fibers with various compositions and thus allow the fabrication of ceramics tailored for specific applications.

Impact on Science and Technologies of Relevance to DOE. The development of efficient methods for the production of complex structural and electronic materials in usable forms with controlled structures, orders and porosities ranging over different length scales is one of the most challenging and important problems of modern solid-state chemistry and materials science. This research program is focused on the design, syntheses and applications of new processible chemical precursors to non-oxide ceramics, including boron carbide, silicon carbide and boron-carbide/silicon-carbide composites, that will allow the formation of these technologically important materials in forms, such as films, fibers and nanostructures, that have been unattainable with conventional methods.

Recent DOE Sponsored Publications (2002-present)

1. Interrante, L.V.; Moraes, K.; Liu, Q.; Lu,N.; Puerta, A. R.; Sneddon, L.G. "Si-Based Ceramics from Polymer Precursors" *Pure and Applied Chem.* **2002**, *74*, 2111-2117.
2. Puerta, A.R.; Remsen, E.E.; Bradley, M.G.; Sherwood, W.; Sneddon, L.G. "Synthesis and Ceramic Conversion Reactions of 9-BBN-Modified Allylhydridopolycarbosilane: A New Single-Source Precursor to Boron-Modified Silicon Carbide" *Chem. Mater.* **2003**, *15*, 478-485.
3. Moraes, K.; Vosburg, J.; Wark, D.; Interrante, L.V.; Puerta, A.R.; Sneddon, L.G.; Narisawa, M. "The Microstructure and Indentation Fracture of SiC-BN Composites Derived from Blended Precursors of AHPCS and Polyborazylene" *Chem. Mater.* **2004**, *16*, 125-132.
4. Wei, X.; Carroll, P.J.; Sneddon, L.G. "New Routes to Organodecaborane Polymers via Ruthenium-Catalyzed Ring Opening Metathesis Polymerization" *Organometallics* **2004**, *23*, 163-5.
5. Kusari, U.; Li, Y.; Bradley, M.G.; Sneddon, L.G. "Polyborane Reactions in Ionic Liquids. New routes to Functionalized Decaborane and *ortho*-Carborane Clusters" *J. Am. Chem. Soc.* **2004**, *126*, 8662-8663.
6. Sneddon, L.G.; Pender, M.; Forsthoefel, K.; Kusari. U.; Wei, X. "Design, synthesis and applications of chemical precursors to advanced ceramic materials in nanostructured forms" J. Eur. Ceram. Soc. **2004**, *25*, 91-97.
7. Welma, D.; Allcock, H.; Wei, X.; Sneddon, L.G. "Preparation of Boron Carbide Nanofibers from a Poly(norbornenyldecaborane) Single-Source Precursor via Electrostatic Spinning" *Adv. Mater.* **2005**, accepted.
8. Welna, D.T.; Wei, X.; Bender, J.D.; Krogman, N.R.; Sneddon, L.G.; Allcock, H.R. "Electrostatic Spinning, Pyrolysis, Characterization of Boron Carbide Nanofibers Prepared from Poly(norbornenyldecaborane)–A Polymeric Ceramic Precursor" *Mater. Res. Soc. Proc.* **2005**, accepted.
9. Wei, X.; Welna, D.T.; Bender, J.D.; Sneddon, L.G.; Allcock, H.R. "Design and synthesis of boron carbide and boron-carbide/silicon-carbide ceramics from poly(norbornenyldecaborane)" *Mater. Res. Soc. Proc.* **2005**, accepted.

Atomic Level Control of Nanostructured Membranes for Catalysis

M. J. Pellin, L. A. Curtiss, A. F. Wagner, J. W. Elam, L. E. Iton, H.-H. Wang and R. E. Winans
Argonne National Laboratory

P. Stair, H. Kung, and M. Kung
Northwestern University

Selective catalytic oxidation remains one of the most desirable and elusive technologies for chemicals and fuels processing and environmental protection. The goal of this effort is to advance the understanding and control of the pathway(s) by which hydrocarbon molecules are transformed by catalytic oxidation. We are exploiting the control of catalytic site synthesis made possible using a new type of nanoporous membrane combined with advanced characterization techniques to develop a predictive, atomic-level understanding of catalytic chemistry. This project utilizes electrochemically-produced Anodic Aluminum Oxide (AAO) to form organized arrays of channels with pore diameters as small as 20 nm, pore densities exceeding $10^{11}cm^{-2}$ and lengths from 10's to 100's of microns. The pores can be coated layer-by-layer with a wide variety of pure or mixed-metal oxide (including alumina), carbide, nitride or metallic films along a controllable percentage of the pore length (including 100%) using Atomic Layer Deposition techniques (ALD) to produce uniform pores of arbitrary diameter and composition. Remarkably, AAO pore diameters can be narrowed from their starting diameter of 40 to 200 nm to dimensions as small as ~1 nm. This size range encompasses much of the most interesting catalytic dimensionality. We have made significant progress in building controlled, nanostructured membrane catalysts and have determined that the membranes are active and stable in the catalytic reaction environment, and extremely flexible in their chemical content and dimensions at the nanoscale. These are unique catalytic materials. Indeed, initial catalytic experiments on the oxidation of cyclohexane using AAO supported V_2O_5 have demonstrated remarkably high selectivity for oxidative dehydrogenation to produce cyclohexene. By comparison, conventional V_2O_5/Al_2O_3 catalysts produce some benzene but very little cyclohexene.

Microporous and Mesoporous Nanosized Transition Metal Oxides: Preparation, Characterization and Applications

Students: Jason Durand, Sinue Gomez, Josie Villegas, Xiongfei Shen.
Collaborators: Alex Navrotsky, UC Davis; Jon Hanson, Brookhaven National Labs, Bill Reiff, Northeastern University, Thorsten Ressler, Fritz-Habr-Institut der MPG
Contact: Steven L. Suib, Unit 3060, Department of Chemistry, 555 N. Eagleville Rd., University of Connecticut, Storrs, CT 06269-3060; (860)-486-2797, (860)-486-2981 (FAX), E-mail - Steven.Suib@uconn.edu , Website: <http://web.uconn.edu/chemistry/SuibGroup/suibg.html>

Goals

The goals of this project are as follows:

(1) To prepare aqueous colloids of nano-size (10 Å to 1000 Å) porous manganese oxides as precursors for various OMS systems.
(2) To prepare novel doped octahedral molecular sieve (OMS) and octahedral layer (OL) structures via aqueous colloidal routes.
(1) To understand factors that control size and shape of porous nano-size oxides.
(2) To fully characterize physical and chemical properties of the above-mentioned systems.
(3) To use porous metal oxides for selective oxidations, shape selective oxidations, and chiral oxidations.
(4) To explore new potential applications of these systems in secondary non-aqueous rechargeable batteries, and as membranes.

Recent Progress

A systematic way to control these tunnel sizes has recently been demonstrated using hydrated Na^+ ions as inorganic templates/structure directors by hydrothermal treatment of Na-birnessite under different pH conditions as shown in the figure below. Manganese oxides with tunnel sizes of 1×1 (2.3 Å × 2.3 Å), 2×3 (4.6 Å × 6.9 Å), and 2×4 (4.6 Å × 9.2 Å) have been synthesized at pH values of 1.0, 7.0, and 13.0, respectively. During hydrothermal treatment of Na-layer manganese oxide precursors, the strength of the hydration bonding for the interlayer Na^+ ions increases with increasing pH values: thus, more water molecules will be stabilized by association with Na^+ ions. As a result, larger hydrated Na^+ ions are produced as structure directors for templating syntheses of materials with larger tunnel sizes.[20]

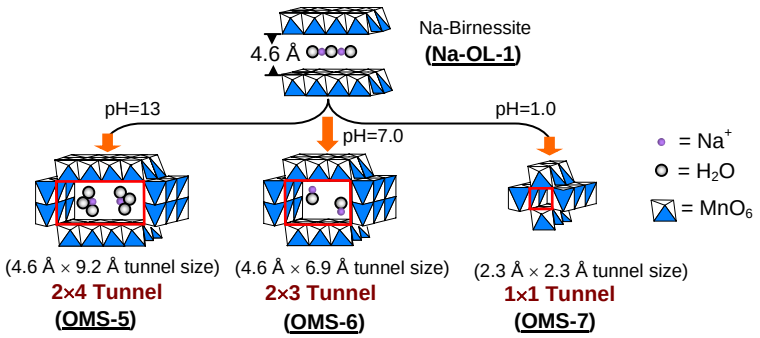

DOE Interest

Fundamental knowledge in the areas of synthesis, new characterization methods, structural analysis, mixed valency, electron transfer, magnetic behavior, conductivity, catalysis, and photocatalysis has been obtained in our studies of OMS and OL materials. The novelty of porous semi-conducting molecular sieves has allowed fundamental studies of effects of electron transfer in such systems. High resolution spectroscopic and microscopic characterization (imaging, surface studies) have led to an excellent understanding of many of the fundamental structural and electronic features of these systems. Catalytic studies have led to correlations of activity/selectivity, shape selectivity, and redox or electron transfer capability. Unique features of our systems include the unusual hollowness of MnO_2 materials; the myriad of morphologies available in these systems (helices, nano-ropes, nano-wires, nano-lines, nano-patterns, nano-spheres); variety of tunnel structures (1x1/1x2, 2x2, 3x3, 2x4, 3x5); excellent conductivity; ease of ion-exchange; transformations to alternate structures while preserving the macro-morphologies of wires, lines, and patterns; outstanding selectivity and activity in selective oxidations; and excellent adsorption properties. Helices or wires with such variation in length and diameter, as well as the uniquely high permeability and porosity are novel. Porous thin films are important for sensors, optical coatings, membranes, and in catalysis. Novel battery and sensor systems have been designed that are functional and low cost. Catalytic oxidations and condensations are the focus of our catalysis studies. The unique combination of availability of many structural types, good electrical properties, high permeability, and high porosity is rare.

Future Plans

Our major efforts continue to be focused on the aerobic catalytic oxidation of alcohols. We have been studying the kinetics of such reactions and finding ways to enhance activity, which in most cases can be as high as 100%. We are also trying to extend this work to chiral alcohols. Catalytic shape selective oxidations (selective, not total) are a major goal of this work.

In the area of synthesis of new materials, we are trying to prepare nanosize manganese oxide layered materials of various morphologies and surface areas to make available a set of catalytic materials for a variety of applications. We are continuing the nano-film work with protein/manganese oxide layers for catalytic studies such as the conversion of styrene to styrene oxide is one such reaction. Framework doping with iron has produced ferromagnetic materials and these are looked at with susceptibility studies.

The colloidal preparations have led to a new family of materials that have unique morphologies and properties. Porous, helices, wires, thin films and nano-patterns of manganese oxide have been synthesized. These systems offer outstanding porosity, versatility for preparation of new materials, and many new applications. We are continuing to prepare such systems and are trying to understand their mechanisms of formation. We have made headway in making similar manganese oxide colloids solely from aqueous solutions and also in the preparation of a variety of transition metal nano-lines and nano-patterns.

Publications, 2003 -2004

1. Giraldo, O.; Durand, J.P.; Ramanan, H.; Laubernds, K.; Suib, S. L.; Tsapatsis, M.; Brock, S. L.; Marquez, M. Dynamic Organization of Inorganic Nanoparticles into Periodic Micrometer-Scale Patterns, *Ang. Chem., Int. Ed*., 2003, **42**, 2905-2909.
2. Yuan, J.; Gomez, S.; Villegas, J.; Laubernds, K.; Suib, S. L. Spontaneous Formation of Inorganic Paper-Like Materials, *Adv. Mat*., 2004, **16**, 1729–1732.
3. Yuan, J.; Laubernds, K.; Zhang, Q.; Suib, S. L. Self-Assembly of Microporous Manganese Oxide Octahedral Molecular Sieve Hexagonal Flakes into Mesoporous Hollow Nanospheres, *J. Am Chem. Soc*., 2003, **125**, 4966-4967.
4. Liu, J.; Son, Y. C.; Cai, J.; Shen, X,; Suib, S. L.; Aindow, M. Size Control, Metal Substitution and Catalytic Application of Cryptomelane Nanomaterials Prepared Using Cross-linking Reagents, *Chem. Mater*., 2004, **16**, 276-285.
5. Polverejan, M.; Suib, S. L. High valebt Substitution in Octahedral Molecular Sieves, *J. Am. Chem. Soc*., 2004, **126**, 7774-7776.
6. Liu, J.; Makwana, V.; Cai, J.; Suib, S. L.; Aindow, M. Effects of Alkalai Metal and Ammonium Cation Templates on Nanofibrous Cryptomelane-type Manganese Oxide Octahedral Molecular Sieves (OMS-2), *J. Phys. Chem*., 2003, **107**; 9185-9194.
7. Garces, L. V.; Hincapie, B.; Makwana, V.; Laubernds, K., Sacco, A. Suib, S. L. Effect of using polyvinyl alcohol and polyvinyl pyrrolidone in the synthesis of octahedral molecular sieves, *Micropor. And Mesopor. Mater*., 2003, **63**, 11-20.
8. Gao, Q.; Suib, S. L.; Thomson, M.; Bowden, W. Unusual nanometer-sized nsutite from Mn(ClO4)2.6H2O-(C2H5)4NOH-CsMnO4-H2O basic systems, *J. Chem. Eng. Jap*., 2003, **36**, 1222-1226.
9. Liu, J.; Durand, J. P.; Espinal, L.; Garces, L. J.; Gomez, S.; Son, Y. C.; Villegas, J.; Suib, S. L. Layered Manganese oxides: Synthesis, Properties and Applications, in Handbook of Layered Materials Science and Technology, S. A. Auerbach, K. A. Carrado, P. K. Dutta, Eds., Marcel Dekker, NY, 2003, 475-508.
10. Gomez, S.; Giraldo, O.; Garces, L. J.; Villegas, J.; Suib, S. L. New Synthetic Route for the Incorporation of Manganese Species into the Pores of MCM-48, *Chem. Mater*., 2004, **16**, 2411-2417.
11. Villegas, J.; Giraldo, O. Suib, S. L. New Layered Double Hydroxides Containing Intercalated Manganese Oxide Species: Synthesis and Characterization, *Inorg. Chem*., 2003, 42, 5621-5631.
12. Hincapie, B. O.; Garces, L. J.; Zhang, Q.; Sacco, A.; Suib, S. L. Synthesis of Mordenite Nanocrystals, *Micropor. Mesopor. Mater*., 2003, **67**, 19-26.
13. Espinal, L.; Suib, S. L.; Rusling, J. F. Electrochemical Catalysis of Styrene Epoxidation with Films of MnO_2 Nanoparticles and H_2O_2, *J. Am. Chem. Soc*., 2004, **126**, 7676-7682.
14. Makwana, V.; Garces, L. J.; Liu, J.; Son, Y. C.; Suib, S. L., *Catal Today*., 2003, **85**, 225-233.
15. Ghosh, R.; Son, Y. C.; Suib, S. L. Liquid Phase Epoxidation of Olefins by Manganese Octahedral Molecular Sieves, *J. Catal*., 2004, **224**, 288-296.

16. Ghosh, R.; Garces, L. J.; Hincapie, B. O.; Suib, S. L. Solid Acid Catalyst in the alkylation of benzene, *Stud. Surf. Sci. Catal*., 2004, **149**, 341-353.
17. Garces, J. Suib, S. L. Selective N,N-methylation of Aniline over co-crystallized Zeolites RHO and Zeolite X(FAU) and over Linde Type L(Sr,K-LTL), *J. Catal*., 2003, **217**, 107-116.
18. Shen, X.; Ding, Y.; Liu, J.; Laubernds, K.; Zerger, R. P.; Polverejan, M.; Son, Y. C.; Aindow, M.; Suib, S. L. Synthesis, Characterization, and Catalytic Applications of Manganese Oxide Octahedral Molecular Sieve (OMS) Nanowires with a 2 X 3 Tunnel Structure, *Chem. Mater*., 2004, **16**, 5327-5336.
19. Villegas, J. C.; Garces, L. J.; Gomez, S. Durand, J. P.; Suib, S. L. Particle Size Control of Cryptomelane nanomaterials by use of H_2O_2 in Acidic Conditions, *Chem. Mater*., 2005, in press.
20. Shen, X.; Suib, S. L. Control of Nano-scale Tunnel Sizes of Porous Manganese Oxide Octahedral Molecular Sieve (OMS) Nanomaterials, *Adv. Mater*., 2005, in press.

Patents.

A. Suib, S. L.; Giraldo, O.; Marquez, M.; Brock, S. L. Manganese Oxide Helices, Rings, Strands, and Films and Methods of their Preparation, US Patent 6,503,476, January 7, 2003.
B. Malz, R. E. Jr.; Kumar, R.; Garces, L. J.; Suib, S. L.; Process for preparing ortho substituted phenylamines, US Patent 7,016,244, January 30, 2004.

Enantioselective Chemisorption on Chirally Patterned Surfaces in Ultrahigh Vacuum

W.T. Tysoe, D.J. Stacchiola and L. Burkholder

Department of Chemistry and Biochemistry, and Laboratory for Surface Studies, University of Wisconsin-Milwaukee, Milwaukee, WI 53211

The enantioselective chemisorption of S-and R- propylene oxide has been measured in ultrahigh vacuum on a Pd(111) surface chirally patterned using S- and R-2-butoxide species on Pd(111). It is found that the coverage of R-propylene oxide adsorbing on an R-2-butoxide modified surface, ratioed to that on one covered by S-2-butoxide, reaches a maximum value of ~2. Heating a 2-butoxide-covered surface to ~150 K leads to the formation of a ketone with concomitant loss in chirality. However, when the surface is patterned using 2-methyl butanoic acid, where the chiral center is identical to that in 2-butanol but is now anchored to the surface by a carboxylate group, the enantioselectivity is completely lost. It is restored when using 2-amino butanoic acid (an amino acid) as a modifier, and the loss of enantioselectivity for the carboxylic acid is ascribed to a loss of rigidity of the chiral center, which allows it to azimuthally rotate. The enantioselectivity of a Pd(111) surface modified by a series of amino acid was explored, where it is found that the enantioselectivity decreases slightly with increasing alkyl chain length, but decreases to zero for branched alkyl chains. In all cases, the enantioselectivity varies with modifier coverage showing a peak enantioselectivity at ~50% of saturation coverage. Preliminary work has been carried out using low-energy electron diffraction and density functional theory to determine the structures of amino acids on Pd(111). Experiments were also carried out using 1-(naphthyl) ethylamine (NEA) as a modifier and propylene oxide as a probe, where no enantioselectivity was found. Enantioselectivity was restored when 2-butanol was used as a probe, an effect that is ascribed to a stronger direct interaction between NEA and 2-butanol. In this case, the enantioselectivity reaches a maximum when flat-lying NEA saturates the surface, and decreases as the adsorbed NEA tilts.

Design, Synthesis, and Catalytic Activity of Polymer Supported Metallated Salen Catalysts

Postdoctoral Fellows: Holbach, M.; Zhang X.
Students: Sears, J.; Sommer, W.
Collaborators: Davis, R.; Jones, C.; Sherrill, D.

School of Chemistry and Biochemistry and School of Chemical & Biomolecular Engineering, Georgia Institute of Technology, Atlanta, GA 30332
Department of Chemical Engineering, University of Virginia, Charlottesville, VA 22904
marcus.weck@chemistry.gatech.edu

Goal

To develop a fundamental understanding of the interactions between soluble catalyst supports such as polymers and soluble nanoparticles and well-defined transition metal catalysts, in particular catalysts for organic transformations such as carbon-carbon bond formations, epoxidations, and hydrolytic kinetic resolutions.

Recent Progress

This project is part of a larger DOE funded initiative to elucidate the basic design principles that govern the interactions between well-defined transition metal catalysts and supports ranging from polymers to porous silica. Over the past twelve months, we focused our efforts on the synthesis of polymer supported metallated salen complexes and studied their catalytic activity and selectivity.

Epoxidations with Supported Mn-Salen Complexes: Metallated salen complexes are among the most important catalyst systems in asymmetric catalysis since Jacobsen's and Katsuki's introduction of chiral manganese salen complexes as catalysts for epoxidations of unfunctionalized olefins in 1990. Over the last decade, several attempts have been reported to produce equally active and selective supported analogues. Despite the high number of reports, the success was severely limited and a highly active and selective recyclable supported salen system has not been fully realized to date. In most studies, the activities and selectivities of the supported catalysts were significantly lower than their homogeneous counterparts. These deficiencies clearly demonstrate the need for novel strategies towards the synthesis of supported salen complexes.

We have developed a novel strategy that is based on the monofunctionalization of salen ligands using carbon-carbon bonds without the introduction of any heteroatoms thereby preventing oxidation of the supported species, the most common degradation pathway. Furthermore, we are using norbornene as monomer which can be polymerized via ring-opening metathesis polymerization (ROMP). Due to the living nature of ROMP, this polymerization method will give us the highest degree of control over the polymer properties and allows for the synthesis of copolymers. The synthesis of our norbornene-functionalized monomers is outlined below:

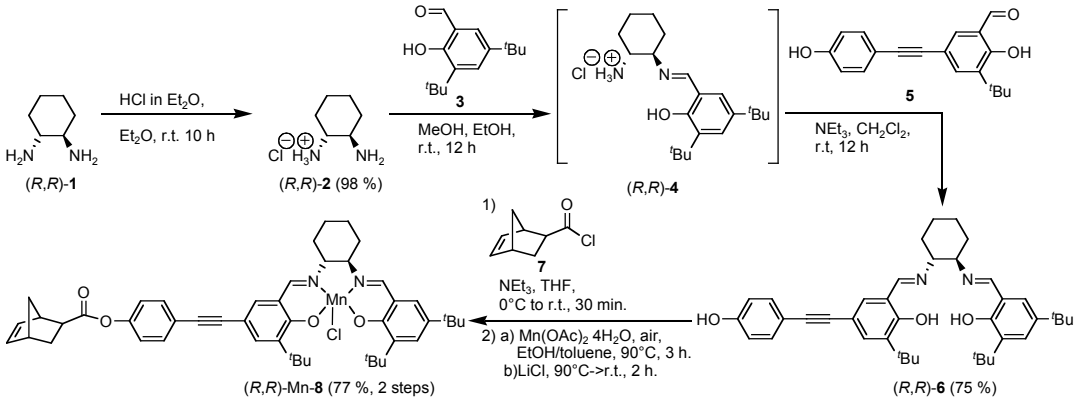

Homo and co-polymerizations with a spacer monomer of monomer **8** can be carried out using Grubbs' first generation ruthenium catalyst. For studying the catalytic properties of the polymeric Mn-salen complexes for the asymmetric epoxidation of unfunctionalized olefins, we dissolved the polymeric catalysts, N-methl-morpholino-N-oxide (NMO), styrene (STY) or 1,2-dihydro-naphthalene (DHN), and dodecane as an internal standard in methylene chloride, cooled the solutions to –20 °C and added *meta*-chloroperoxybenzoic acid (*m*-CPBA) in three equal portions over a period of two minutes. The catalytic activities and selectivities were characterized by GC and NMR. Our novel polymer supported catalysts are as active and selective as their non-supported Jacobsen counterpart. The Figure below displays the activities of various copolymers in comparison to the Jacobsen catalyst for the epoxidation of styrene. As can be seen, the activities are comparable.

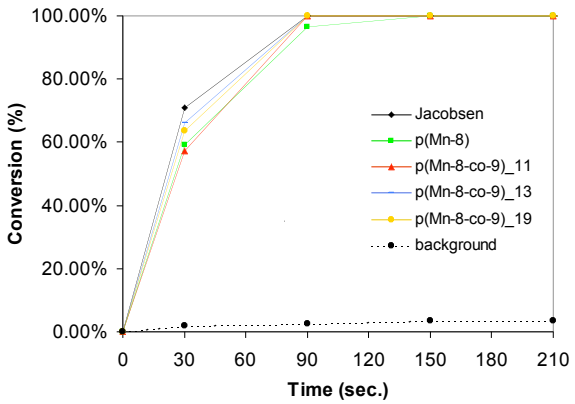

The selectivities of the supported catalysts in comparison to the Jacobsen system are displayed below. In all cases, the enantioselectivities are comparable to the non-supported Jacobsen system.

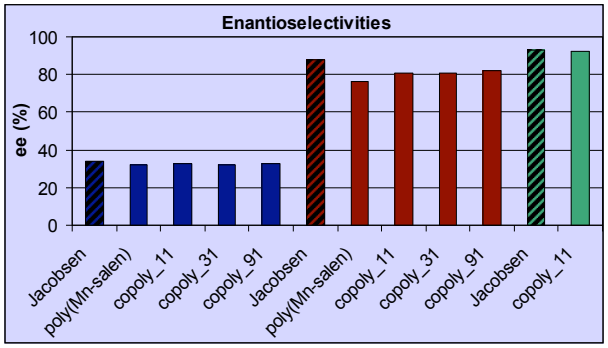

These results clearly demonstrate the outstanding activities and selectivities of our poly(norbornene) system. Current efforts are focused towards investigating if these polymers can be recycled and reused.

Hydrolytic Kinetic Resolutions of Supported Co-Salen Complexes: Compound **6** was also metallated with Co after attachment to **7** and ROMPed. The resulting homopolymers and copolymers were employed as catalyst for the hydrolytic kinetic resolution of epoxides such as epi-chlorohydrin. Again, our polymers are as selective and active as their non-supported analogous. Furthermore, in very preliminary investigations, we were able to recycle and reuse these polymers several times. One example, the hydrolytic kinetic resolution of epi-chlorohydrine with our co-polymers before and after recycling is shown below:

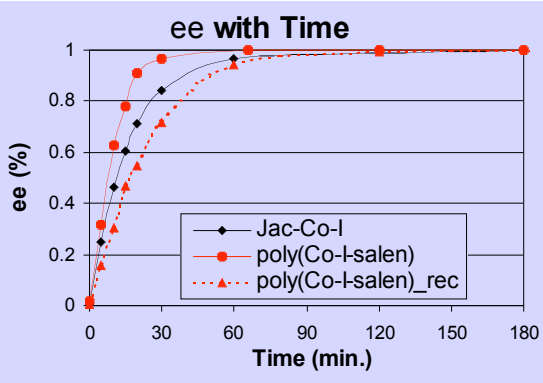

Finally, we have also synthesized soluble and in-soluble poly(styrene) analogs of these Co-salen poly(norbornene)s. Again, the catalytic activities and selectivities of these poly(styrene) supported Co-salen complexes are outstanding. Current efforts are targeted towards the synthesis of silica-supported analogs and to systematically vary the linker that connects the salen complex to the support. Furthermore, the development of computational methods to describe such complex polymer supported salen complexes are being carried out.

DOE Interest

A detailed understanding of the underlying design principles that dictate the interactions between a supported catalyst and its support are of utmost importance in catalysis. This research will improve the rational design of reusable and recyclable supported catalysts that are able to use the current basic carbon-hydrogen feedstock to create complex molecules and important precursors for drugs and polymers and it is therefore of general interest to the DOE.

Publications (May 2004-present)

Tow manuscripts are in preparation and will be submitted before the DOE contractors meeting in May.

1. "Synthesis and Application of Poly(norbornene)-Supported Monofunctionalized Salen Complexes" M. Holbach and M. Weck, *Journal of the American Chemical Society*.

2. "Recoverable, Recycleable Immobilized Co-Salen for the Hydrolytic Kinetic Resolution of Racemic Epoxide" X. Zheng, M. Holbach, C. W. Jones, and M. Weck, *Journal of the American Chemical Society*.

Characterization and reactivity of molybdenum carbide nanoparticles formed on Au(111) using Reactive-Layer Assisted Deposition

Jillian M. Horn,[1] Denis Potapenko[2] and Michael G. White[1,2] (presenter)

[1] Department of Chemistry, SUNY Stony Brook, Stony Brook NY 11794
[2] Chemistry Department, Brookhaven National Laboratory, Upton, NY 11973

We have developed a novel method for the synthesis of transition metal compound nanoparticles on an inert support. Specifically, molybdenum carbide nanoparticles have been prepared by depositing Mo by physical vapor deposition (PVD) on a reactive layer of ethylene, which was physisorbed on a Au(111) substrate at low temperatures (85-100 K). STM imaging shows that the resulting MoC_x particles have a narrow size distribution and preferentially nucleate near the "elbow" sites on the reconstructed $(22 \times \sqrt{3})$-Au(111) surface. Auger and XPS indicate that the MoC_x particles are near stoichiometric ($x \approx 1$) with an electronic structure similar to carburized Mo metal and $Mo_2C(0001)$ surfaces. Initial reactivity results for the dehydrogenation of cyclohexene on MoC_x/Au(111) surfaces will also be presented. This work was supported by the U.S. Department of Energy, Office of Basic Energy Sciences, Division of Chemical Sciences under contract No. DE-AC02--98CH10886

Reactivity of Size-Selected Gas-Phase Transition Metal Carbide and Sulfide Clusters

James M. Lightstone,[1] Melissa J. Patterson,[1] Michael G. White[1, 2] (presenter)

[1]Department of Chemistry, Stony Brook University, Stony Brook, NY 11974
[2] Chemistry Department, Brookhaven National Laboratory, Upton, NY 11973

We have recently constructed a cluster deposition apparatus which employs a magnetron sputtering source for generating gas-phase cation clusters of pure metals and metallic compounds. The focus is on generating clusters of the early transition metal compounds (carbide and sulfides), which are known in their bulk form to be active catalysts for a wide range of heterogeneous reactions. In many cases, metal carbides offer distinct advantages over the parent metal in selectivity and resistance to poisoning, and for certain reactions their catalytic behavior is similar to that of the Group 8-10 noble metals. The work reported here examines the gas-phase reactivity of small transition metal carbide and sulfide clusters as a first step towards investigations of model catalysts prepared by size-selected deposition. Results will be presented for the adduct formation and reactions of the $Ti_8C_{12}^+$ Met-Car with a variety of sulfur containing molecules (OCS, CS_2, SO_2, CH_3SH, C_4H_4S). In addition, we will also present results on the reactivity and proposed structures of $Mo_xS_y^+$ and $W_xS_y^+$ clusters and future plans for size-selected cluster deposition. This work was supported by the U.S. Department of Energy, Office of Basic Energy Sciences, Division of Chemical Sciences under contract No. DE-AC02--98CH10886

DE-FG02-04ER15611 **Ruqian Wu**

First Principles Investigations and Simulations for Catalytic Properties of Au Nonoclusters on Oxide Surface

Post Doctor: Jisang Hong
Collaborators: D.W Goodman (Texas A&M University)

Contact: Ruqian Wu, Department of Physics and Astronomy, University of California, Irvine, CA 92697-4575
Phone: 949-824-7640
Email: wur@uci.edu

Research Goals:

Catalysis of "nanostructured" metal particles supported on oxide substrates is a fascinating and challenging phenomenon. This theoretical research project focus on three main directions for Au_n (n=1-20) nanoclusters on MgO(001), TiO_2(110) and SiO_2(111): (i) simulations for the onset of growth and nucleation on defected sites; (ii) studies of size, shape, and substrate dependence of their electronic properties; and (iii) reaction simulations for CO oxidation on Au_n. Theoretical research will describe the fundamentals of Au/oxide catalysts, and will furthermore develop and apply novel theoretical approaches including the time dependent density functional theory and a generalized version of the full potential linearized augmented plane wave (FLAPW) method.

Research Approaches:

We use DMol and plane-wave codes to scan over possible structures and transition states. The highly-precise all-electron relativistic FLAPW method approach is used for the key configurations (1) to safeguard the validity of energies and atomic structure optimizations, and (2) to determine physical properties. The time dependent DFT under development is an ultimate solution for the correct determination of XAS. We are developing and will apply the Kinetic Monte Carlo approach to explore temperature and dynamics effects.

Progress in the last 8 months:

A. Growth of SiO_2 on Mo(112)

We recently studied the evolvement of band gap of SiO_2 thin films on Mo(110). The calculations include studies for Mo(112) surface, free SiO_2 layers and the combined systems. The atomic structures are fully relaxed according to an energy minimization approach guided by calculated atomic forces. We found that a monolayer SiO_2 already displays a sizeable band gap (>3 eV), although the atomic geometry is quite different from the quartz structure. We analyzed other physical properties of SiO_2/Mo(110) surface, including the interfacial interaction, charge redistribution, and core level shift, in light of recent experimental results of Goodman's group.

B. Chemical Properties of Pd/Au bimetallic nanoclusters

It was found recently that Pd-Au/SiO_2 is excellent for vinyl acetate synthesis. Furthermore, the Pd dimers on the surface are found to be crucial. Using DMol and FLAPW approaches, we examined the formation energies of Pd dimers on Au surface and nanoclusters. We found that Pd atoms tend to stay close to each other, especially at the edge of nano clusters (by 0.4 eV lower in energy compared to the dimers on flat Au(001) surfaces). The Pd atoms relax to a much lower position compared to surrounding Au surface atoms. The chemical properties of Pd monomer and dimer on Au(111) and Au(001) are significantly different from those of Pd(001), reflected in plots of density of states and charge densities.

We also studied CO adsorption on Pd monomer and Pd dimer to compare with the TPD, XPS and EELS data. The adsorption energies and stretch frequencies agree well with the experimental data available. This validates our calculations and furthermore the insights disclosed through DFT approaches.

Future Plans:

In the next year we will conduct more calculations to investigate the chemical properties of Au and Pd+Au clusters on TiO_2 and SiO_2. We will explore the effects of surface charge on the geometries of the clusters, using defected and reduced substrates. We will introduce $CO+O_2$, C_2H_4 and CH_3COOH molecules to simulate chemical reactions, along with experimental efforts of collaborators. Some of these calculations are under way. We will finish TD-DFT implementation for the determination of the final state effect in XAS calculations, which will allow us to provide more accurate results for core level shifts.

DOE Interest:

Through collaborations with experimentalists, our DFT simulations demonstrate a capability that theoretical/computational approaches can clearly explain a wide spectrum of physical properties and may eventually play an essential role in the optimization of constituents, atomistic arrangements, and conditions of synthesis of novel catalysts. This is extremely important in nanocatalysts where changes even in individual atom may alter the performance.

Publications Sponsored by Current DOE Grant:

1. Z.X. Yang and R.Q. Wu, *"Origin of the Positive Core Level Shifts in Observed Sparse Au Clusters on Oxides"*, Phys. Rev. B **67**, 081403(R) (2003).
2. J.S. Hong, and R.Q. Wu, *"Chemical Properties of SiO2 monolayer on Mo(112)"*, Phys. Rev. B, submitted.
3. R.Q. Wu *"Distribution and Chemical Properties of Pd dimers on Au Surface and Clusters"*, J. Phys. Chem, to be submitted.
4. R.Q. Wu *"CO adsorption on Pd doped Au Surface and Clusters"*, in preparation.

DE-FG02-96ER45439 **Judith Yang**

Electron Microscopy Studies of Supported Au Nanoparticles

Huiping Xu, Shangpeng Gao, Judith C. Yang
Materials Science and Engineering, University of Pittsburgh, Pittsburgh, PA

Abstract

Two popular and powerful methods for charactering supported nanoparticles used in heterogeneous catalysis, is transmission electron microscopy (TEM) and X-ray spectroscopy, such as X-ray absorption fine structure (XAFS). Here we present the applications of quantitative Z-contrast imaging and high-resolution electron microscopy (HREM) techniques as a complementary tool to XAFS, to gain insights into the 3-dimensional structure of supported Au_{13} nano-clusters. Of particular usefulness is the quantification of the absolute intensity of the Z-contrast image that provides the number of atoms per nanocluster.

We chose Au_{13} clusters on carbon as a model system, because a 13-atom Au cluster is a ligand-stablized one with a full-shell "Magic Number" against aggregation into larger particles. A 13-atom gold cluster often exists in the form of either regular icosahedrons or cubo-octahedron geometry. Our studies revealed that both shapes are produced depending on the synthesis conditions, i.e. with mixed-ligand and fully thiolated shell. The Au_{13} produced with a fully thiolated shell were uniform in size distribution, and icosahedral in shape. The Au_{13} produced with mixed ligands were cuboctahedron that were larger, on average, than the Au_{13} produced with a fully thiolated shell, We are currently investigating Au_{13} nanoclusters on carbon and TiO_2 supports.

The HAADF experiments were performed on a VG-HB501 STEM at the Materials Research Laboratory, University of Illinois at Urbana Champaign. The Philips 200CM FEG is at Carnegie Mellon University and the assistance of Noel T. Nuhfer is gratefully acknowledged.

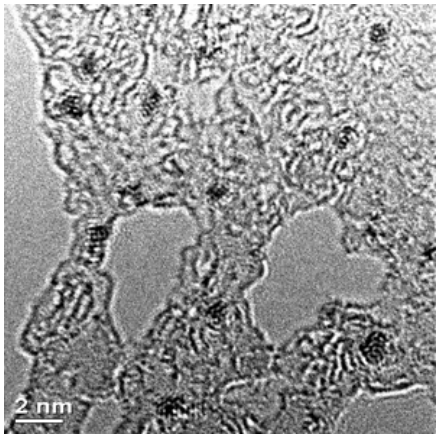

Figure 1. HREM image of Au_{13} dispersed onto an ultra-thin carbon, where the diameter of these particles are ~8Å.

Cinchona Alkaloids as Chiral Modifiers for Imparting Chirality to Platinum Hydrogenation Catalysts

L. Mink, Z. Ma, J. Kubota and F. Zaera
Department of Chemistry, University of California, Riverside, CA 92521

As part of the overall DOE-funded project entitled "Molecular Level Design of Chiral Heterogeneous Catalysts", we at Riverside have been investigated the physical properties of cinchona alkaloids that make them ideal modifiers for imparting chirality to metal surfaces. It is believed that these cinchona affect the catalytic properties of platinum and palladium based catalysts towards the hydrogenation of α-keto esters by forming a 1:1 modifier:reactant complex. Here, infrared spectroscopy has been used to characterize the adsorption of cinchonidine and other related modifiers in situ on platinum surfaces. In general, it was determined that the chiral properties of the catalyst are defined by the nature of the adsorption of the chiral modifier, and that those in turn are influenced by the details of the cinchona/Pt system, by parameters such as the concentration of the modifier in solution, the type of solvent used, and the nature of the gasses dissolved in the liquid phase.

Vibrational assignments for the cinchonidine were first made using a combination of experimental spectroscopic measurements and ab initio computational methods. Several bands in both the IR and Raman spectra were identified as useful in providing information regarding the mode of adsorption of cinchonidine on metal surfaces. It was then determined that the adsorption of the cinchona chiral template on Pt is very sensitive to the concentration in solution: while at low and intermediate concentrations the cinchonidine is bonded with the quinoline ring parallel to the surface, at high concentrations the ring is tilted away from the surface. Optimum catalytic enantioselectivity is seen under conditions that are consistent with a template adsorption geometry having the quinoline ring parallel to the surface.

The influence of different dissolved gases on the adsorption of cinchonidine from CCl_4 solutions onto polycrystalline platinum surfaces was characterized next. It was observed that most of the gases studied, which included Ar, N_2, O_2, air, and CO_2, neither enhance the adsorption of cinchonidine nor damage the cinchonidine adlayers once they have formed on the surface. On the other hand, H_2 was seen to play a unique role, initially facilitating the uptake of cinchonidine, but later removing some of the resulting adsorbed cinchonidine from the platinum surface. The solvent was also determined to have a strong influence on the adsorption of the chiral modifier on the surface of the catalysts. In particular, the polarity of the solvent was found to influence the kinetics of cinchonidine desorption into solution in a manner that correlates well with its influence on the enantioselectivity of the templated catalyst. It appears that cinchonidine adsorbs irreversibly on platinum from non-polar solutions such as cyclohexane, but can be easily removed by more polar solvents such as dichloromethane. The evolution of the adsorbed cinchona overlayer upon flushing with different solvents is illustrated in Figure 1. The behavior observed in our studies correlates well both with the solubility of cinchonidine and with the performance of the cinchona/platinum catalyst as a function of the nature of the solvent.

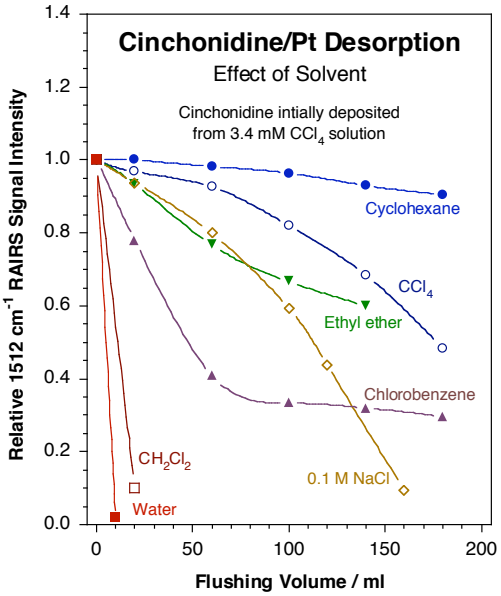

Figure 1. Desorption of cinchonidine adsorbed on a platinum surface as a function of rinsing volume for different solvents. In these experiments the cinchonidine was first adsorbed from a carbon tetrachloride saturated solution onto a polished polycrystalline platinum disk, and then flushed with sequential 20 ml aliquotes of the stated solvents. The remaining coverage of the adsorbate was determined in-situ by following the infrared absorption signal at 1512 cm^{-1}, which corresponds to an in-plane deformation of the quinoline ring. It is clearly seen here that the reversibility of the desorption is severely affected by the nature of the solvent, going from fast desorption in water and dichloromethane, to virtually irreversible adsorption in cyclohexane and other alkanes. This trend correlates well with the ability of cinchonidine to impart chirality to platinum catalysts for enantioselective hydrogenation.

More recent work has been directed at probing the parameters that control the adsorption geometry of the cinchona modifiers, and with that their efficiency in imparting enantioselectivity to catalytic processes. A comparative study was carried out using cinchonine, cinchonidine, quinine, quinidine, and the dihydro analogs of those four molecules. Significant differences were observed not only in their adsorption properties on the platinum surface, but also in their solubilities in a variety of solvents (Figure 2). Those differences were deemed to be due to intrinsic molecular properties associated with their structure. Both experimental NMR and theoretical DFT data suggest that the most stable configuration of each molecule may be determined by the steric effects exerted by the groups (vinyl, methoxy) bonded to the outside molecular frame, and that those may be different in each case. This behavior may account for the differences in catalytic enantioselectivity obtained with cinchonine vs. cinchonidine.

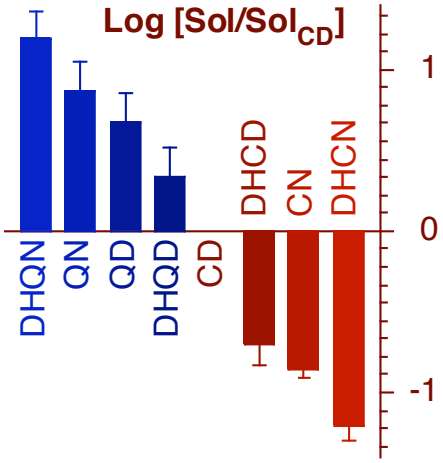

Figure 2. Solubilities of different cinchona relative to those of cinchonidine (CD). The numbers reported here are averages over the values measured in more than 30 solvents, and the error bars correspond to 95% confidence intervals. No significant variations were observed as a function of the nature of the solvent, implying that the changes in solubility observed are intrinsic to the structure of the cinchona. 2-D NMR experiments allowed us to track those changes to variations in the configurations allowed for each structure, which are in turn affected by the groups attached to the ends of the quinuclidine and quinoline rings.

Participant List

Participant List

Last Name	First Name	Organization	Phone	Email
Ager	Joel	Lawrence Berkeley National Laboratory	510-486-6715	JWAger@lbl.gov
Angelici	Robert	Ames Laboratory	515-294-2603	angelici@iastate.edu
Arns	Laura	Purdue University	765-494-4069	larns@purdue.edu
Bakac	Andreja	Ames Laboratory	515-294-3544	bakac@ameslab.gov
Bare	Simon	UOP LLC	847-391-3171	simon.bare@uop.com
Barnes	Craig	University of Tennessee, Knoxville	865-974-3141	cebarnes@utk.edu
Barteau	Mark	University of Delaware	302-831-8905	barteau@che.udel.edu
Bartels	Ludwig	University of California at Riverside	951-827-2041	ludwig.bartels@ucr.edu
Bayachou	Mekki	Cleveland State University	216-875-9716	m.bayachou@csuohio.edu
Brinker	C. Jeffrey	Sandia National Laboratories	505-272-7627	cjbrink@sandia.gov
Brown	Seth	University of Notre Dame	574-631-4659	brown.114@nd.edu
Caruthers	James	Purdue University	765-494-6625	caruther@ecn.purdue.edu
Chen	Jingguang	University of Delaware	302-831-0642	jgchen@udel.edu
Crooks	Richard	Texas A&M University	979-845-5629	crooks@tamu.edu
Curtiss	Larry	Argonne National Laboratory	630-252-7380	curtiss@anl.gov
Dai	Sheng	Oak Ridge National Laboratory	865-576-7307	dais@ornl.gov
Davis	Robert	University of Virginia	434-924-6284	rjd4f@virginia.edu
Delgass	Nick	Purdue University	765-494-4059	delgass@purdue.edu
Delgass	Leif	Purdue University	765-494-4069	ldelgass@purdue.edu
Delmau	Lætitia	Oak Ridge National Laboratory	865-576-2093	delmaulh@ornl.gov
Diebold	Ulrike	Tulane University	504-862-8279	diebold@tulane.edu
Dixon	David	University of Alabama	205-348-8441	dadixon@bama.ua.edu
Dohnalek	Zdenek	Pacific Northwest National Laboratory	509-376-3726	Zdenek.Dohnalek@pnl.gov
Dumesic	James	University of Wisconsin	608-262-1095	dumesic@engr.wisc.edu
Dupuis	Michel	Pacific Northwest National Laboratory	509-375-2617	michel.dupuis@pnl.gov
Elam	Jeffrey	Argonne National Laboratory	630-252-7979	jelam@anl.gov
Finke	Richard	Colorado State University	970-491-2541	rfinke@lamar.colostate.edu
Francis	Matt	University of California, Berkeley	510-643-9915	francis@cchem.berkeley.edu
Frei	Heinz	Lawrence Berkeley National Laboratory	510-486 4325	HMFrei@lbl.gov
Frenkel	Anatoly	Yeshiva University	212-340-7827	frenkel@bnl.gov
Gates	Bruce	University of California Davis	530-752-3953	bcgates@ucdavis.edu
Gellman	Andrew	Carnegie Mellon University	412-268-3848	gellman@cmu.edu
Gogonea	Valentin	Cleveland State University	216-875-9717	v.gogonea@csuohio.edu
Goodman	David	Texas A&M University	979-845-0214	goodman@mail.chem.tamu.edu
Gordon	John	Los Alamos National Laboratory	301-903-2153	john.gordon@science.doe.gov
Gutowski	Maciej	Pacific Northwest National Laboratory	509-375-4387	maciej.gutowski@pnl.gov
Haller	Gary	Yale University	203-432-0356	gary.haller@yale.edu

Participant List

Last Name	First Name	Organization	Phone	Email
Harris	Alex	Brookhaven National Laboratory	631-344-4301	alexh@bnl.gov
Haw	James	University of Southern California	213-740-1022	jhaw@usc.edu
Heinz	Tony	Columbia University	212-854-6564	tony.heinz@columbia.edu
Henderson	Michael	Pacific Northwest National Laboratory	509-376-2192	ma.henderson@pnl.gov
Hess	Wayne	Pacific Northwest National Laboratory	509-376-9907	wayne.hess@pnl.gov
Hill	Craig	Emory University	404-727-6611	chill@emory.edu
Hwang	Robert	CFN - Brookhaven National Laboratory	631-344-3322	hwangr@bnl.gov
Iglesia	Enrique	University of California, Berkeley	510-642-9673	iglesia@cchem.berkeley.edu
Johnson	Duane	University of Illinois Urbana-Champaign	217-265-0319	duanej@uiuc.edu
Jones	Christopher	Georgia Institute of Technology	404-385-1683	cjones@chbe.gatech.edu
Kay	Bruce	Pacific Northwest National Laboratory	509-376-0028	bruce.kay@pnl.gov
Kimmel	Greg	Pacific Northwest National Laboratory	509-376-2501	gregory.kimmel@pnl.gov
Lin	Victor	Iowa State University and Ames Laboratory	515-294-3135	vsylin@iastate.edu
Liu	Jun	Sandia National Laboratories	505-845-9135	jliu@sandia.gov
Liu	Ping	Brookhaven National Laboratory	631-344-5970	pingliu3@bnl.gov
Long	Jeffrey	University of California, Berkeley	510-642-0860	jrlong@berkeley.edu
Ludovice	Peter	Georgia Institute of Technology	404-894-1835	pete.ludovice@chbe.gatech.edu
Marceau	Diane	US DOE Office of Basic Energy Sciences	301-903-0235	diane.marceau@science.doe.gov
Maupin	Paul	US DOE Office of Basic Energy Sciences	301-903-4355	paul.maupin@science.doe.gov
Maverick	Andrew	Louisiana State University	225-578-4415	maverick@lsu.edu
Mavrikakis	Manos	University of Wisconsin, Madison	608-262-9053	manos@engr.wisc.edu
Menard	Laurent	University of Illinois at Urbana-Champaign	217-244-7440	LMENARD@UIUC.EDU
Miller	John	US DOE Office of Basic Energy Sciences	301-903-5806	john.miller@science.doe.gov
Miranda	Raul	US DOE Office of Basic Energy Sciences	301-903-8014	raul.miranda@science.doe.gov
Muckerman	James	Brookhaven National Laboratory	631-344-4368	muckerma@bnl.gov
Mullins	David	Oak Ridge National Laboratory	865-574-2796	mullinsdr@ornl.gov
Mullins	Charles	University of Texas at Austin	512-471-5817	mullins@che.utexas.edu
Musaev	Djamaladdin	Emory University	404-727-2382	dmusaev@emory.edu
Nuckolls	Colin	Columbia University	212-854-6289	cn37@columbia.edu
O'Brien	Stephen	Columbia University	212-854-9478	so188@columbia.edu
Overbury	Steven H.	Oak Ridge National Laboratory	865-574-5040	overburysh@ornl.gov
Peden	Charles	Pacific Northwest National Laboratory	509-376-1689	chuck.peden@pnl.gov
Pruski	Marek	Ames Laboratory	515-294-2017	mpruski@iastate.edu
Quirk	David	Cleveland State University	216-687-2243	djquirk7@yahoo.com
Rahman	Talat	Kansas State University	785-532-1611	rahman@phys.ksu.edu
Rehr	John	University of Washington	206-543 8593	jjr@phys.washington.edu
Resasco	Daniel	University of Oklahoma	405-325-4370	resasco@ou.edu

Participant List

Last Name	First Name	Organization	Phone	Email
Ribeiro	Fabio	Purdue University	765-494-4069	fabio@purdue.edu
Rodriguez	Jose	Brookhaven National Laboratory	631-344-2246	rodrigez@bnl.gov
Schneider	Bill	University of Notre Dame	574 631 8754	wschneider@nd.edu
Schwartz	Viviane	Oak Ridge National Laboratory	865-576-6749	schwartzv@ornl.gov
Scott	Susannah	University of California, Santa Barbara	805-893-5606	sscott@engineering.ucsb.edu
Shelnutt	John	University of Georgia/Sandia National Laboratories	505-272-7160	jasheln@unm.edu
Sherrill	David	Georgia Institute of Technology	404-894-4037	sherrill@chemistry.gatech.edu
Simonson	J. M.	Oak Ridge National Laboratory	865-547-4986	simonsonjm@ornl.gov
Sita	Lawrence	University of Maryland	301-405-5753	lsita@umd.edu
Sneddon	Larry	University of Pennsylvania	215-898-8632	lsneddon@sas.upenn.edu
Somorjai	Gabor	University of California, Berkeley and Lawrence Berkeley National Laboratory	510-642-4053	Somorjai@berkeley.edu
Stair	Peter	Northwestern University/Argonne National Laboratory	847-491-5266, 630-252-6499	pstair@northwestern.edu
Suib	Steve	University of Connecticut	860-486-2797	Steven.Suib@uconn.edu
Tillotson	Jenett	Purdue University	765-494-4069	jalayne@purdue.edu
Tysoe	Wilfred	University of Wisconsin Milwaukee	414-229-5222	wtt@uwm.edu
Vlachos	Dion	University of Delaware	302-831-2830	vlachos@che.udel.edu
Wang	Lai-Sheng	Washington State University	509-376-8709	ls.wang@pnl.gov
Wang	Yong	Pacific Northwest National Laboratory	509-376-5117	yongwang@pnl.gov
Weck	Marcus	Georgia Institute of Technology	404 385-1796	marcus.weck@chemistry.gatech.edu
White	John	University of Texas / Pacific Northwest National Laboratory	509-376-5500	jm.white@pnl.gov
White	Michael	Brookhaven National Laboratory	631-344-4345	mgwhite@bnl.gov
Wu	Ruqian	University of California, Irvine	949-824-7640	wur@uci.edu
Yang	Judith	University of Pittsburgh	412- 624-8613	jyang@engr.pitt.edu
Zaera	Francisco	University of California, Riverside	951-827-5498	zaera@ucr.edu
Zhou	Aimin	Cleveland State University	216-687-2416	a.zhou@csuohio.edu